

IMPROVED OIL RECOVERY FROM UPPER JURASSIC SMACKOVER  
CARBONATES THROUGH THE APPLICATION OF ADVANCED  
TECHNOLOGIES AT WOMACK HILL OIL FIELD, CHOCTAW AND  
CLARKE COUNTIES, EASTERN GULF COASTAL PLAIN

Annual Report  
May 1, 2001-April 30, 2002

By:

Ernest A. Mancini	Brian Panetta
Charles Hayes	William Tedesco
Joe Benson	Tiffany Hopkins
David Hilton	Juan Avila
David Cate	Ekene Chijuka
Thomas Blasingame	Ammi Tan
Wayne Ahr	Leo Lynch
Rosalind Archer	Todd French
R.P. Major	Karen Thompson
Lewis Brown	Magan Green
Alex Vadie	John Sorrell
Wayne Stafford	

Date Published: November 2002

Work Performed Under Contract No. DE-FC26-00BC15129

University of Alabama  
Tuscaloosa, Alabama



**National Energy Technology Laboratory  
National Petroleum Technology Office  
U.S. DEPARTMENT OF ENERGY  
Tulsa, Oklahoma**

## **DISCLAIMER**

This report was prepared as an account of work sponsored by an agency of the United States Government. Neither the United States Government nor any agency thereof, nor any of their employees, makes any warranty, expressed or implied, or assumes any legal liability or responsibility for the accuracy, completeness, or usefulness of any information, apparatus, product, or process disclosed, or represents that its use would not infringe privately owned rights. Reference herein to any specific commercial product, process, or service by trade name, trademark, manufacturer, or otherwise does not necessarily constitute or imply its endorsement, recommendation, or favoring by the United States Government or any agency thereof. The views and opinions of authors expressed herein do not necessarily state or reflect those of the United States Government.

This report has been reproduced directly from the best available copy.

Improved Oil Recovery from Upper Jurassic Smackover Carbonates  
through the Application of Advanced Technologies at Womack Hill Oil  
Field, Choctaw and Clarke Counties, Eastern Gulf Coastal Plain

By  
Ernest A. Mancini  
Charles Hayes  
Joe Benson  
David Hilton  
David Cate  
Thomas Blasingame  
Wayne Ahr  
Rosalind Archer  
R.P. Major  
Lewis Brown  
Alex Vadie  
Wayne Stafford  
Brian Panetta  
William Tedesco  
Tiffany Hopkins  
Juan Avila  
Ekene Chijuka  
Ammi Tan  
Leo Lynch  
Todd French  
Karen Thompson  
Magan Green  
John Sorrell

November 2002

Work Performed Under DE-FC26-00BC15129

Prepared for  
U.S. Department of Energy  
Assistant Secretary for Fossil Energy

Gary Walker, Project Manager  
National Energy Technology Laboratory  
National Petroleum Technology Office  
One West Third Street, Suite 1400  
Tulsa, OK 74103

Prepared by  
Department of Geological Sciences  
Box 870338  
202 Bevill Building  
University of Alabama  
Tuscaloosa, AL 35487-0338

## TABLE OF CONTENTS

	Page
Disclaimer	
Title Page	
Abstract .....	v
Table of Contents .....	iii
Introduction .....	1
Executive Summary .....	8
Experimental .....	13
Work Accomplished in Year 2 .....	13
Work Planned in Year 3 .....	142
Results and Discussion .....	150
Conclusions .....	157
References .....	161



## **ABSTRACT**

Pruet Production Co. and the Center for Sedimentary Basin Studies at the University of Alabama, in cooperation with Texas A&M University, Mississippi State University, University of Mississippi, and Wayne Stafford and Associates are undertaking a focused, comprehensive, integrated and multidisciplinary study of Upper Jurassic Smackover carbonates (Class II Reservoir), involving reservoir characterization and 3-D modeling and an integrated field demonstration project at Womack Hill Oil Field Unit, Choctaw and Clarke Counties, Alabama, Eastern Gulf Coastal Plain.

The principal objectives of the project are: increasing the productivity and profitability of the Womack Hill Field Unit, thereby extending the economic life of this Class II Reservoir and transferring effectively and in a timely manner the knowledge gained and technology developed from this project to producers who are operating other domestic fields with Class II Reservoirs.

The principal research efforts for Year 2 of the project have been reservoir characterization, which has included three (3) primary tasks: geoscientific reservoir characterization, petrophysical and engineering property characterization, and microbial characterization and recovery technology analysis, which has included 3-D geologic modeling. In the second year, the research focus has primarily been on completion of the geoscientific reservoir characterization and 3-D geologic modeling tasks. This work was scheduled for completion in Year 2.

Overall, the project work is on schedule. Geoscientific Reservoir Characterization has been completed. Petrophysical and Engineering Characterization and Microbial Characterization are essentially on schedule with minor problems with well downhole pressure testing and the acquisition of whole core material. 3-D Geologic Modeling has been completed.



## INTRODUCTION

Pruet Production Co. and the Center for Sedimentary Basin Studies at the University of Alabama, in cooperation with Texas A&M University, Mississippi State University, University of Mississippi, and Wayne Stafford and Associates are undertaking a focused, comprehensive, integrated and multidisciplinary study of Upper Jurassic Smackover carbonates (Class II Reservoir), involving reservoir characterization and 3-D modeling and an integrated field demonstration project at Womack Hill Oil Field Unit, Choctaw and Clarke Counties, Alabama, Eastern Gulf Coastal Plain (Fig. 1).

Estimated reserves for Womack Hill Field are 119 million barrels of oil. During the production history of the field, which began in 1970, 30 million barrels of oil have been produced. Conservatively (additional 10-20 percent), another 12 to 24 million barrels of oil remains to be recovered through the application of advanced technologies in optimizing field management and production. Womack Hill Field is one of 57 Smackover fields in the regional peripheral fault trend play of the eastern Gulf Coastal Plain. To date, 674 million barrels of oil have been produced from these fields. The fields in this play have a common petroleum trapping mechanism (faulted salt anticlines), petroleum reservoir (ooid grainstone and dolograins shoal deposits), petroleum seal (anhydrite), petroleum source (microbial carbonate mudstones), overburden section, and timing of trap formation and oil migration. Therefore, the proposed work at Womack Hill Field is directly applicable to these 57 fields and can be transferred to Smackover fields located along this fault trend from Florida to Texas.

Phase I (3.0 years) of the proposed research involves characterization of the shoal reservoir at Womack Hill Field to determine reservoir architecture, heterogeneity and producibility in order to increase field productivity and profitability. This work includes core and well log analysis; sequence stratigraphic, depositional history and structure study; petrographic and diagenetic study; and pore system analysis. This information will be integrated with 2-D seismic data and probably 3-D seismic data to produce an integrated 3-D stratigraphic and structural model of the reservoir at Womack Hill Field. The results of the reservoir characterization and modeling will be integrated

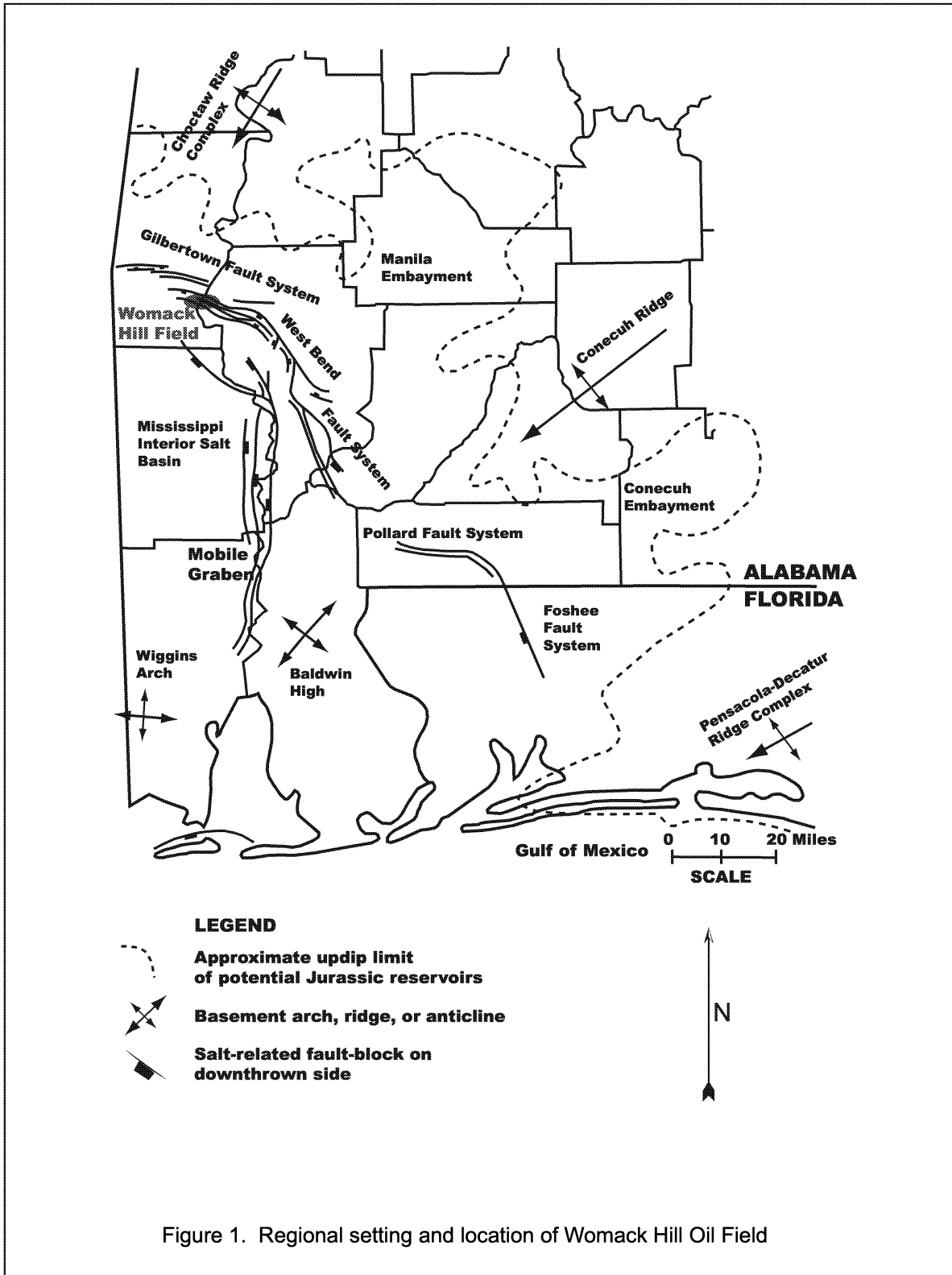


Figure 1. Regional setting and location of Womack Hill Oil Field

with petrophysical and engineering data and pressure communication analysis to perform a 3-D reservoir simulation of the field reservoir. The results from the reservoir characterization and modeling will also be used in determining whether undrained oil remains at the crest of the Womack Hill structure (attic oil), in assessing whether it would be economical to conduct strategic infill drilling in the field, and in determining whether the acquisition of 3-D seismic data for the field area would improve recovery from the field and is justified by the financial investment. Parallel to this work, engineers are characterizing the petrophysical and engineering properties of the reservoir, analyzing the drive mechanism and pressure communication (through well performance data), and developing a 3-D reservoir simulation model. Further, the engineering team members will determine what, if any, modifications should be made to the current pressure maintenance program, as well as assess what, if any, other potential advanced oil recovery technologies are applicable to this reservoir to extend the life of the field by increasing and maintaining productivity and profitability. Also, in this phase, researchers are studying the ability of *in-situ* micro-organisms to produce a single by-product (acid) in the laboratory to determine the feasibility of initiating an immobilized enzyme technology project at Womack Hill Field Unit.

Phase II (2.5 years) of the proposed research will proceed along three lines if the results from Phase I justify the continuance of this work. Line 1 involves the integration of the 3-D seismic imaging of the structure and reservoir into the 3-D geologic model to assess the merits of conducting a strategic infill drilling program in the field, including drilling in the interwell area and a crestal well, and if new well(s) are drilled assess by using fracture identification log technology whether a lateral-multilateral completion for these wells would be successful. Line 2 involves integrating the data obtained from the 3-D seismic imaging, petrophysical and engineering data acquired from drilling new wells using lateral-multilateral well completions, and the results of the analysis of the well performance data (field/well pressure and rate histories). These integrated data will be used to refine the 3-D reservoir simulation model, implement modifications to the pressure maintenance program, and initiate any additional activities, such as further infill drilling and/or advanced oil technology applications to improve recovery. Line 3 involves confirming the ability of

*in-situ* micro-organisms to produce a single by-product (acid) and injecting nutrients into the field reservoir to sustain the cells rather than to support cell proliferation for initiation of the immobilized enzyme technology project .

Phase III (0.5 year) of the proposed project involves monitoring the enhanced pressure maintenance program and advanced technology application project, and evaluating the viability of entering existing field wells for lateral-multilateral well completions to improve field productivity and profitability. Also, the immobilized enzyme technology project will be monitored to evaluate the impact of this technique on overall oil recovery from the field.

The objectives of this project are as follows:

1. Increase the productivity and profitability of the Womack Hill Field Unit, thereby extending the economic life of this Class II Reservoir and enhancing National economic and energy security.
2. Demonstrate the feasibility of transferring the knowledge gained and technology developed from previous studies of Class II Reservoirs to the analysis of the Womack Hill shallow shelf (ramp) carbonate reservoir.
3. Demonstrate to producers in the Eastern Gulf Region the significance and procedures for developing an integrated reservoir approach based on geological, geophysical, petrophysical, and well performance data, highlighting reservoir characterization activities and utilizing 3-D reservoir simulation as mechanisms for making decisions regarding field operations, such as selecting well locations for strategic infill drilling, identifying wells for recompletion (and/or simulation), as well as for constructing and implementing programs of reservoir surveillance.
4. Demonstrate to producers in the Eastern Gulf Region the value of 3-D reservoir simulation in the design, implementation, and maximizing of a pressure maintenance program, including optimization of injection wells, well locations, and injection-production balancing, and the value of chemistry and chemical agents that can be used to improve injection conformance and increase oil recovery.

5. Demonstrate the usefulness of 3-D seismic imaging in defining the productive limits of the reservoir.
6. Demonstrate the value and utility of strategically targeted infill drilling to improve the productivity and profitability of heterogeneous carbonate reservoirs, including drilling wells that are optimal in the sense of location, well completion components, and well stimulation.
7. Demonstrate the usefulness of lateral-multilateral well completions in naturally fractured carbonate reservoirs to increase reservoir producibility.
8. Demonstrate the utility of an immobilized enzyme technology project to increase oil recovery effectiveness and efficiency.
9. Transfer the knowledge gained, technology developed and successes and failures of this project to producers who are operating other fields with Class II Reservoirs through technology workshops, presentations at professional meetings, and publications in scientific and trade journals.
10. Contribute to the knowledge base on carbonate sequence stratigraphy, depositional systems, lithofacies analysis, diagenesis, and pore systems and to the understanding of carbonate reservoir architecture, heterogeneity and producibility, carbonate petroleum systems, fluid-rock interactions, petrophysical properties of carbonates, reservoir drive mechanisms and pressure communication in carbonates, immobilized enzyme recovery process, 3-D seismic imaging in carbonates, lateral-multilateral well completions in fractured carbonate reservoirs, and the dynamics of effective and balanced pressure maintenance in heterogeneous grainstone and dolograins reservoirs.

The principal problem at Womack Hill Field is productivity and profitability. With time, there has been a decrease in oil production from the field, while operating costs in the field continue to increase. In order to maintain pressure in the reservoir, increasing amounts of water must be injected annually. These problems are related to cost-effective, field-scale reservoir management, to reservoir connectivity due to carbonate rock architecture and heterogeneity, to pressure

communication due to carbonate petrophysical and engineering properties, and to cost-effective operations associated with the oil recovery process.

Improved reservoir producibility will lead to an increase in productivity and profitability. To increase reservoir producibility, a field-scale reservoir management strategy based on a better understanding of reservoir architecture and heterogeneity, of reservoir drive and communication and of the geological, geophysical, petrophysical and engineering properties of the reservoir is required. Also, an increased understanding of these reservoir properties should provide insight into operational problems, such as why the reservoir is requiring increasing amounts of freshwater to maintain the desired reservoir pressure, why the reservoir drive and oil-water contact vary across the field, how the multiple pay zones in the field are vertically and laterally connected and the nature of the communication within a pay zone.

Several potential opportunities have been identified which could lead to increased reservoir productivity. First, the drilling of the Dungan Estate Unit 14-5 well in Sec. 14, T.10N., R.2W. suggests that undrained oil (attic) may be present on the crest of the Womack Hill Field structure. The 14-5 well encountered oil in the Norphlet and Smackover at a horizon that previously was not productive in the field. These productive zones were structurally higher in this well than encountered in any of the field wells prior to the drilling of the 14-5 well.

Second, field scale heterogeneity affects the producibility of the reservoir. A major barrier to flow separates the field reservoir into a western portion and an eastern portion and results in structural compartmentalization in Womack Hill Field. This flow barrier dramatically impacts production strategy in the field. Only the western portion of the field has been unitized and only this part of the reservoir is experiencing pressure maintenance. The reservoir drive mechanism in the eastern portion of the field is a strong bottom-up water drive, while the drive mechanism in the western portion of the field is primarily solution gas. This flow barrier has been interpreted to be a major fault (megascopic heterogeneity) or change in permeability. If the barrier to flow is a result of lower permeability, the reduction in permeability could be due to a change in mesoscopic heterogeneity (depositional facies change), a change in microscopic heterogeneity (diagenetic

change), or a combination of the two processes. Also, there are multiple shoal lithofacies in the field. The nature of the communication among and within these multiple pay zones is unclear at this time. Carbonate depositional systems involve the complex interaction of biological, chemical and physical processes. Further, the susceptibility of carbonates to alteration by early to late diagenetic processes dramatically impacts reservoir heterogeneity. Diagenesis is the fundamental influence in determining which carbonate deposits will become seals, which will become reservoirs, and what the nature of the reservoir quality and producibility will be. Reservoir characterization and the study of heterogeneity, therefore, becomes a major task because of the physiochemical and biological origins of carbonates and because of the masking of the depositional rock fabric and reservoir architecture principally due to dolomitization. Thus, greater lithofacies and/or diagenetic variability (greater reservoir heterogeneity) translates into more difficulty in predicting between wells (interwell areas) at any spacing but particularly at Womack Hill Field where the well spacing is as great as 120 acres.

Third, prior investigations have suggested that Smackover carbonate reservoirs should be naturally fractured at depths of 11,000 ft. Therefore, well completions, such as lateral-multilateral completions, that utilize the fractured nature of these carbonates should lead to increased producibility of the field.

Fourth, understanding and accurately predicting the flow units and barriers to flow in this heterogeneous reservoir is vital to improving producibility. An enhanced pressure maintenance program, advanced oil recovery application, and/or immobilized enzyme technology project that accounts for inherent properties of this heterogeneous reservoir, multiple pay zones, and the nature of the variable drive mechanisms and oil-water contacts in the field should result in increased producibility of Womack Hill Field. The improved connectivity in this compartmentalized reservoir should result in the production of more incremental oil.

The project will build on the experiences and lessons learned from the previous Class II Reservoir studies. Techniques, methods and technologies utilized in previous studies will be applied and modified accordingly for application to the Womack Hill reservoir. These technologies and techniques include reservoir characterization and modeling, reservoir simulation, 3-D seismic

imaging, infill drilling, horizontal/lateral drilling, and waterflood design for Class II reservoirs. The particular advanced technologies applied will include developing an integrated geoscientific and engineering digital database for Womack Hill Field, characterizing the Smackover reservoir and modeling (in 3-dimensions) these heterogeneous carbonates for cost-effective management of the reservoir on a fieldwide scale and for making decisions regarding field operations. These data and this modeling will be integrated with petrophysical properties of the reservoir, field pressure and production data, and other engineering information and used in 3-D reservoir simulation to evaluate the effectiveness of the existing pressure maintenance program and to assess the viability of initiating other advanced oil recovery applications in the field. These data and 3-D geologic modeling will also be utilized in developing an infill drilling strategy for this heterogeneous reservoir.

The project results will be vigorously transferred to producers through five technology workshops in project Years 4, 5 and 6. The first workshop (Year 4) will focus on the results of Phase I of the project and will include carbonate reservoir characterization, data integration, carbonate reservoir modeling, and 3-D reservoir simulation. The second workshop (Year 5) will focus on aspects of the integrated field demonstration project and will include the results of the 3-D seismic imaging and the new wells drilled in the field. Workshops 3, 4 and 5 (Year 6) will focus on the results of using lateral-multilateral well completions in the field, results of the enhanced pressure maintenance program and advanced oil recovery application project, and the results of the immobilized enzyme technology project. These workshops will be conducted in cooperation with the Eastern Gulf Region (EGR) of the Petroleum Technology Transfer Council (PTTC).

## **EXECUTIVE SUMMARY**

Pruet Production Co. and the Center for Sedimentary Basin Studies at the University of Alabama, in cooperation with Texas A&M University, Mississippi State University, University of Mississippi, and Wayne Stafford and Associates are undertaking a focused, comprehensive, integrated and multidisciplinary study of Upper Jurassic Smackover carbonates (Class II Reservoir), involving reservoir characterization and 3-D modeling and an integrated field

demonstration project at Womack Hill Oil Field Unit, Choctaw and Clarke Counties, Alabama, Eastern Gulf Coastal Plain.

Phase I (3.0 years) of the proposed research involves characterization of the shoal reservoir at Womack Hill Field to determine reservoir architecture, heterogeneity and producibility in order to increase field productivity and profitability. This work includes core and well log analysis; sequence stratigraphic, depositional history and structure study; petrographic and diagenetic study; and pore system analysis. This information will be integrated with 2-D seismic data and probably 3-D seismic data to produce an integrated 3-D stratigraphic and structural model of the reservoir at Womack Hill Field. The results of the reservoir characterization and modeling will be integrated with petrophysical and engineering data and pressure communication analysis to perform a 3-D reservoir simulation of the field reservoir. The results from the reservoir characterization and modeling will also be used in determining whether undrained oil remains at the crest of the Womack Hill structure (attic oil), in assessing whether it would be economical to conduct strategic infill drilling in the field, and in determining whether the acquisition of 3-D seismic data for the field area would improve recovery from the field and is justified by the financial investment. Parallel to this work, engineers are characterizing the petrophysical and engineering properties of the reservoir, analyzing the drive mechanism and pressure communication (through well performance data), and developing a 3-D reservoir simulation model. Further, the engineering team members will determine what, if any, modifications should be made to the current pressure maintenance program, as well as assess what, if any, other potential advanced oil recovery technologies are applicable to this reservoir to extend the life of the field by increasing and maintaining productivity and profitability. Also, in this phase, researchers are studying the ability of *in-situ* micro-organisms to produce a single by-product (acid) in the laboratory to determine the feasibility of initiating an immobilized enzyme technology project at Womack Hill Field Unit.

The principal problem at Womack Hill Field is productivity and profitability. With time, there has been a decrease in oil production from the field, while operating costs in the field continue to increase. In order to maintain pressure in the reservoir, increasing amounts of water must be

injected annually. These problems are related to cost-effective, field-scale reservoir management, to reservoir connectivity due to carbonate rock architecture and heterogeneity, to pressure communication due to carbonate petrophysical and engineering properties, and to cost-effective operations associated with the oil recovery process.

Improved reservoir producibility will lead to an increase in productivity and profitability. To increase reservoir producibility, a field-scale reservoir management strategy based on a better understanding of reservoir architecture and heterogeneity, of reservoir drive and communication and of the geological, geophysical, petrophysical and engineering properties of the reservoir is required. Also, an increased understanding of these reservoir properties should provide insight into operational problems, such as why the reservoir is requiring increasing amounts of freshwater to maintain the desired reservoir pressure, why the reservoir drive and oil-water contact vary across the field, how the multiple pay zones in the field are vertically and laterally connected and the nature of the communication within a pay zone.

The principal research efforts for Year 2 of the project have been reservoir characterization, which has included three (3) primary tasks: geoscientific reservoir characterization, petrophysical and engineering property characterization, and microbial characterization and recovery technology analysis, which has included 3-D geologic modeling. In the second year, the research focus has primarily been on completion of the geoscientific reservoir characterization and 3-D geologic modeling tasks. This work was scheduled for completion in Year 2.

Geoscientific Reservoir Characterization has been completed. The upper part of the Smackover Formation is productive from carbonate shoal complex reservoirs that occur in vertically stacked heterogeneous porosity cycles (A, B, and C). The cycles typically consist of carbonate mudstone/wackestone at the base and ooid and oncoidal grainstone at the top. The carbonate mudstone/wackestone lithofacies has been interpreted as restricted bay and lagoon sediments, and the grainstone lithofacies has been described as beach shoreface and shoal deposits. Porosity has been enhanced through dissolution and dolomitization. The grainstone associated with Cycle A is dolomitized (upper dolomitized zone) in much of the field area. Although Cycle A is present across

the field, its reservoir quality varies laterally. Dolomitization (lower dolomitized zone) can be pervasive in Cycle B, Cycle C and the interval immediately below Cycle C. Cycle B and Cycle C occur across the field, but they are heterogeneous in depositional texture and diagenetic fabric laterally. Porosity is chiefly solution-enlarged interparticle, grain moldic and dolomite intercrystalline pores with some intraparticle and vuggy pores. Pore systems dominated by intercrystalline pores have the highest porosities. Median pore throat aperture tends to increase with increasing porosity. Probe permeability strongly correlates with median pore throat aperture, and tortuosity increases with increasing median pore throat aperture. Larger tortuosity and median pore throat aperture values are associated with pore systems dominated by intercrystalline pores.

Petrophysical and Engineering Characterization is on schedule except for a delay in well downhole pressure testing. Extensive efforts have been made to integrate and correlate the core and well log data for the field. Reservoir permeability has been correlated with core porosity, gamma ray well log response, and resistivity well log response. The petrophysical data have been segregated into flow units prescribed by the geological data, and for the data in these flow units a histogram of core porosity and the logarithm of core permeability were prepared. These histograms yield statistical measures, such as the mean and median values, which will be used to develop spatial distributions and to provide data for the numerical simulation model. Evaluation of production, injection and shut-in bottomhole pressure data for the field have been interpreted and analyzed using appropriate mechanisms, such as decline type curve analysis and estimated ultimate recovery analysis. The volumetric results are relevant as virtually every well yielded an appropriate signature for decline type curve analysis. However, a discrepancy in the estimate of total compressibility for this system has arisen, and the absolute volumetric results will need to be revised. The estimation of flow properties, such as permeability and skin factor has emerged as a problematic issue because little early time data, which are required for this analysis, are available. Therefore, the results of these analyses should be considered qualitative. The correlation of estimated ultimate recovery and the  $N_{c+}$ - product is consistent suggesting that a strong relationship exists between contacted oil-in-place and recovery.

Microbial Characterization is on schedule with the recent acquisition of Smackover core material from south Alabama. Initially water samples and core samples taken from wells in the Womack Hill Field yielded no micro-organisms capable of growing at 90°C. This result was due to a combination of factors, including the fact that the core samples were exposed to air for decades and the equipment necessary to maintain an anaerobic environment was inadequate. Well cuttings from the Smackover Formation acquired from a field near Womack Hill Field were analyzed for micro-organisms. Growth of micro-organisms was evident in the samples prepared from these well cuttings in association with oil from the Womack Hill Field. These organisms consumed ethanol and are presumed to produce carbon dioxide or the gas was derived from organic acids produced from the oil reacting with carbonate. These findings suggest that micro-organisms capable of producing acetic acid from ethanol have a high probability of being present in Womack Hill Field and of being induced to grow and be metabolically active at the subsurface temperature in the reservoir.

A 3-D Geologic Model has been constructed for the Womack Hill Field structure and reservoir(s). The 3-D geologic modeling shows that the petroleum trap is more complex than originally interpreted. The geologic modeling indicates that the trap in the western part of the field is a fault trap with closure to the south against the fault, and that the trap in the central and eastern parts of the field is a faulted anticline trap with four-way dip closure. The pressure difference between wells in the western and central parts of the field and wells in the eastern part of the field may be attributed to a flow barrier due to the presence of a north-south trending fault in the field area. The modeling shows that the Smackover reservoirs are heterogeneous. Four reservoir intervals are identified in the field area: Cycle A, Cycle B, Cycle C, and the interval immediately below Cycle C. A permeability barrier to flow is present potentially between the western and eastern parts of the field.

## **EXPERIMENTAL**

### **Overview**

The principal research efforts for Year 2 of the project have been reservoir characterization, which has included three (3) primary tasks: geoscientific reservoir characterization, petrophysical and engineering property characterization, and microbial characterization and recovery technology analysis, which has included 3-D geologic modeling. In the second year, the research focus has primarily been on completion of the geoscientific reservoir characterization and 3-D geologic modeling tasks (Table 1). This work was scheduled for completion in Year 2.

### **Work Accomplished in Year 2**

#### ***Task RC-1. Geoscientific Reservoir Characterization***

**Description of Work.**--This task is designed to characterize reservoir architecture, pore systems and heterogeneity based on geological and geophysical properties (Tables 1 and 2).

**Rationale.** Reservoir characterization is fundamental to determining reservoir architecture, pore systems, and heterogeneity. It is critical in the design of a cost-effective fieldwide reservoir management strategy and for making sound operational decisions. Deformational (structural), depositional, and diagenetic processes exert the major influences on reservoir quality and evolution and produce heterogeneities at various scales. To predict accurately changes in reservoir quality, heterogeneity, and producibility in interwell areas, it is crucial to characterize and understand the processes that produce carbonate rock textures and the diagenetic fluid-rock interactions that have altered the primary rock fabric and pore system.

This task has been completed and the data and results from this work have been presented in the Year 1 Report for this project and are presented herein.

**Core Description.**--Reservoir characterization begins with core description and analysis. Six slabbed cores from Womack Hill field were described following the methodology of Bebout and Loucks (1984). Graphic logs were constructed for each of the cores (Figs. 2 through 7). One hundred eighteen thin sections were cut from the cores, with care taken to sample all diagenetic and stratigraphic changes. In addition, 66 thin sections were available from the Alabama State Oil and



**Table 2  
Milestone Chart—Year 2**

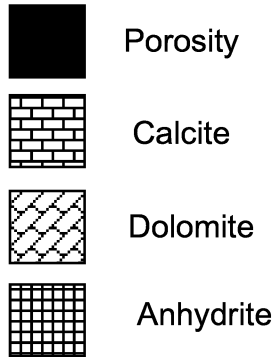
Tasks (Phase I)	M	J	J	A	S	O	N	D	J	F	M	A
Reservoir Characterization												
Geoscientific												
Petrophysical and Engineering												
Microbial												
Data Integration												
Recovery Technology Analysis												
3-D Geologic Model												

Work Planned   
 Work Accomplished xx

Depth (ft.)	Pore Type	Mineral Composition (Incl. Porosity)			Structures	Texture	Fabric	Grain Size (mm)	Color	Cement	Comments		
		0%	50%	100%									
11460	BC					Peloidal	WS	.004 - .25	B	D	Anhydrite laths Very fossiliferous: algae, pelecypods, gastropods, echinoids, crinoids		
	WP BP M V					Oolitic	GS	.004 - 4.0	G	C			
	WP BP M V					Oolitic Peloidal	GS	.004 - 4.0	B	C		Anhydrite healed pores Echinoids and pelecypods	
11470	No Recovery				Oolitic Peloidal	PS WS	.004 - 1.0	B	C	Interbedded Packstone and Wackestone Wackestone lamina seem more dolomitized			
	WP BP M V	M BP											
11480	M BP					Oolitic Peloidal	WS	.004 - .5	DG	C	Pelecypod shell frags.		
	M BP					Shale Partings	Peloidal	WS	.004 - .125	DG	C	Anhydrite along shale partings	
	BP												
	BP												
11490	No Recovery				Peloidal	WS	.004 - .25	G	C	Anhydrite filled molds			
	M BP												
	M BP												
	M BP												
11500	BC					Peloidal	MS	.004 .062	B	C	Silty Large anhydrite healed molds of oncoids & pelecypods		
	BC												
	BC												
	BC												
11510	No Recovery				Peloidal	MS	.004 .062	LB	C	Anhydrite laths common			
	V M BP												
	V M BP												
11520	V M BP				Vague Bedding	Oncoidal Peloidal	WS	.004 - 1.0	LB	C	Algae & Pelecypods		
	No Recovery												
	BC											Shale Partings	Micritic
BC M													
11530	BC M					Oncolitic	WS	.004 - 1.0	LG	C	Numerous oncoids		
	BC M												
	No Recovery												
11540	BC					Peloidal	MS	.004 - 1.0	LG	C	Anhydrite vugs and pelecypod shell frags Selective dolomitization of rare grains		
	BC												

# KEY

## Mineral Composition



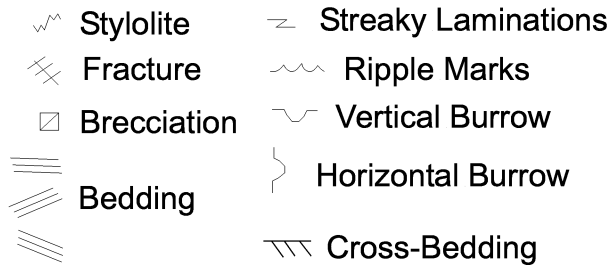
## Pore Types

BP - Interparticle  
WP - Intraparticle  
BC - Intercrystalline  
M - Moldic  
F - Fenestral  
FR - Fracture  
V - Vuggy

## Carbonate Fabrics

MS - Micrite  
WS - Wackestone  
PS - Packstone  
GS - Grainstone

## Structures



## Cements

C - Calcite  
D - Dolomite  
A - Anhydrite

## Colors

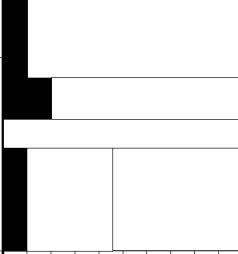
G - Gray  
B - Brown  
W - White

## Color Modifiers

L - Light  
D - Dark  
M - Mottled  
VD - Very Dark

Depth (ft.)	Pore Type	Mineral Composition (Incl. Porosity)			Structures	Texture	Fabric	Grain Size (mm)	Color	Cement	Comments
		0%	50%	100%							
11402	WP, M				 Shale Partings	Peloidal	WS	.004 - .25	LG	D	Anhydrite filled vugs
	WP BC				 Shale Partings				B		
	WP BC										
11412	WP BC				 Cloudy Shale Partings	Peloidal Pelletal	WS	.004 - .125	MGB	D	
	WP BC				 Shale Partings						
11422	BC WP M					Ooid Pelletal Peloidal	WS	.004 - .25	B	D	
	BC				Vague Laminations 	Peloidal	MS	.004 - .062	DG	D	
11432	BC				 Shale Partings						Anhydrite healed vugs
	BP				 Shale Partings	Cloudy					
	BC				 Shale Partings	Ooid Pelletal Peloidal	WS	.004 - .125	MG	C	
11442	BC	No Recovery			 Shale Partings						
	WP BC				 Shale Partings				DG		
	WP				 Shale Partings	Ooid Peloidal	PS	.004 - .25	DG	C	
11452	WP				 Shale Partings						
	BC V				 Cloudy	Pelletal	WS	.004 - .125	B	D	Shaley
	BC V				 Shale Partings	Peloidal	MS	.004 - .031	VDG	D	Poor Recovery
	BC				 Shale Partings						
11462	BC				 Shale Partings	Peloidal	WS	.004 - .062	LB	D	Poor recovery through bottom of core segment (11473)
11472	BC				 Shale Partings	Peloidal	MS	.004 - .031	LG	D	
		No Recovery									
11482		No Recovery									

Depth (ft.)	Pore Type	Mineral Composition (Incl. Porosity)			Structures	Texture	Fabric	Grain Size (mm)	Color	Cement	Comments
		0%	50%	100%							
11492	BC	No Recovery			Shale Partings	Peloidal	WS	.004 - .062	DG	C	Very Shaley Increasing Organics
	BC, F										
11502	BP					Ooid Peloidal Pelletal	WS	.004 - .062	DG	C	Crumbly till top of cored segment (11495)
	BC				Shale Partings	Pelletal	WS	.004 - .062	LB	D	
11512	BC				Shale Partings Vague Laminations	Pelletal	WS	.004 - .125	DB	D	Significant Oil Stain
	BC										
11522	BC				Vague Laminations	Pelletal	WS	.004 - .125	DB	D	Interbedded brown/gray laminations
	BC					Peloidal	MS	.004 - .031	LG	D	
11532	BC				Shale Partings Vague Laminations	Peloidal	WS	.004 - .125	LB	D	Shaley, vague laminations
	BC					Peloidal Pelletal	WS	.004 - .062	DG	D	Shaley, vague laminations
11542	BC				Shale Partings Vague Laminations	Peloidal Pelletal	WS	.004 - .125	G	D	Shaley, vague laminations
								.004 - .062	G		
11552					Vague Laminations						
11555											

Depth (ft.)	Pore Type	Mineral Composition (Incl. Porosity)			Structures	Texture	Fabric	Grain Size (mm)	Color	Cement	Comments			
		0%	50%	100%										
11421					Shale Partings 	Chickenwire Anhydrite	--	--	W	A	Buckner Anhydrite Sabkha			
11431						Sucrosic	MS	.004 - .125	G	D	Pyrite Common			
11441	M BC				Shale Partings 									
	M BC													
	M BC							Shale Partings 	Peloidal Oolitic	WS	.004 - .5	B	D	Oomoldic Porosity
	M BC								Micrite	MS	.004 - .031	DG	D	Silty
	WP M								Oolitic Peloidal	PS	.004 - .5	G	C	
	WP M					Algal Oolitic	BS/GS	.004 - .5	G	C	Top Patch Reef?			
11451														

Stratigraphic Interval: Smackover Formation 11318 - 11500

Depth (ft.)	Pore Type	Mineral Composition (Incl. Porosity)			Structures	Texture	Fabric	Grain Size (mm)	Color	Cement	Comments
		0%	50%	100%							
11318		No Recovery									
11328	V				Shale Partings	Oolitic Oncoidal	GS	.004 - .5	G	C	Red Shale Exposure Near Top
	WP										
11338	V	No Core				Algal Peloidal	BS	.004 - 4.0	B	C	Coarsening Upwards Gastropod & Pelecypod Frags Till Top Algal Boundstone Patch Reef?
	WP										
11388		No Core									
11398	F				Shale Partings	Oolitic Peloidal	PS	.004 - .25	LG		
	BP										
11408	F				Shale Partings	Peloidal	WS	.004 - .25		C	Rare Oncoids Anhydrite Filled Vugs Coarsening Upwards
	V										
	BP										
	BP										
11418	M				Vague Bedding	Oncolitic Peloidal	PS	.004 - 4.0			
	BP										
11428	M	No Recovery						.004 - 4.0			
	BP										
11448	M					Oncoidal		.004 - .5		C	Small molds of encrusting algae
	BP										
	BP										
	BP										
	M										

Depth (ft.)	Pore Type	Mineral Composition (Incl. Porosity)			Structures	Texture	Fabric	Grain Size (mm)	Color	Cement	Comments
		0%	50%	100%							
11458	M M WP M WP					Peloidal	WS	.004 - .25	LG	C	Many small molds of round colonial algae
11468		No Recovery									
11478	M					Oncolitic Peloidal	WS	.004 - 4.0	G	C	Abundant large oncoids and rounded colonial algae
	M M					Peloidal	MS	.004 - .062	DG	C	
	M					Anhydritic Peloidal	WS	.004 - .5	DG	C	Abundant Anhydrite Vugs
11488						Peloidal	MS	.004 - .062	DG	C	Anhydrite laths along laminations
11498											Vague laminations
11508											

Depth (ft.)	Pore Type	Mineral Composition (Incl. Porosity)			Structures	Texture	Fabric	Grain Size (mm)	Color	Cement	Comments
		0%	50%	100%							
11400	V					Oolitic	GS	.031 - 1.0	G	C	cross-bedded
	WP					Oolitic Peloidal	PS	.031 - .25	LB	C	
	V					Peloidal	WS	.004 - .062	LB	C	
	WP					Oolitic Peloidal	PS	.031 - .5	LB	C	
11410	M					Oolitic Peloidal	WS	.031 - .25	LB	C	
	V					Oolitic Peloidal	GS	.031 - .5	LB	C	
	WP										
	M										
11420	V					Oolitic Peloidal	PS	.004 - .25	LB	C	Some ooids dolomitized
	WP										
	BP	No Recovery									
11430	V				Shale Parting 	Oolitic Peloidal	PS	.004 - .25	LB	C	Some ooids dolomitized
	WP					Oolitic Peloidal	WS	.004 - .25	LG	C	
	BP										
	BP										
11440	BP					Oolitic Peloidal	WS	.004 - .25	LG	C	Some ooids dolomitized
		No Recovery									
11450	M					Oolitic Peloidal Skeletal	WS	.004 - .5	G	C	Pelecypod shell fragments common
	WP										
	V										
	M										
	WP										
	V										
11460	M					Oolitic Peloidal	WS	.004 - .5	MG	C	Oncoids and pelecypods Bioturbated
	WP					Oolitic Peloidal	PS	.004 - .5	LB	C	
	M										
	WP										
11470	BP					Peloidal	WS	.004 - .5	LB	C	Oncoids
	WP					Peloidal	GS	.004 - .5	LB	C	
	FR										
	WP										
	WP										
11480	WP					Oolitic Peloidal	WS	.004 - .25	LG	C	Oncoids and pelecypods
	WP										
		No Recovery									

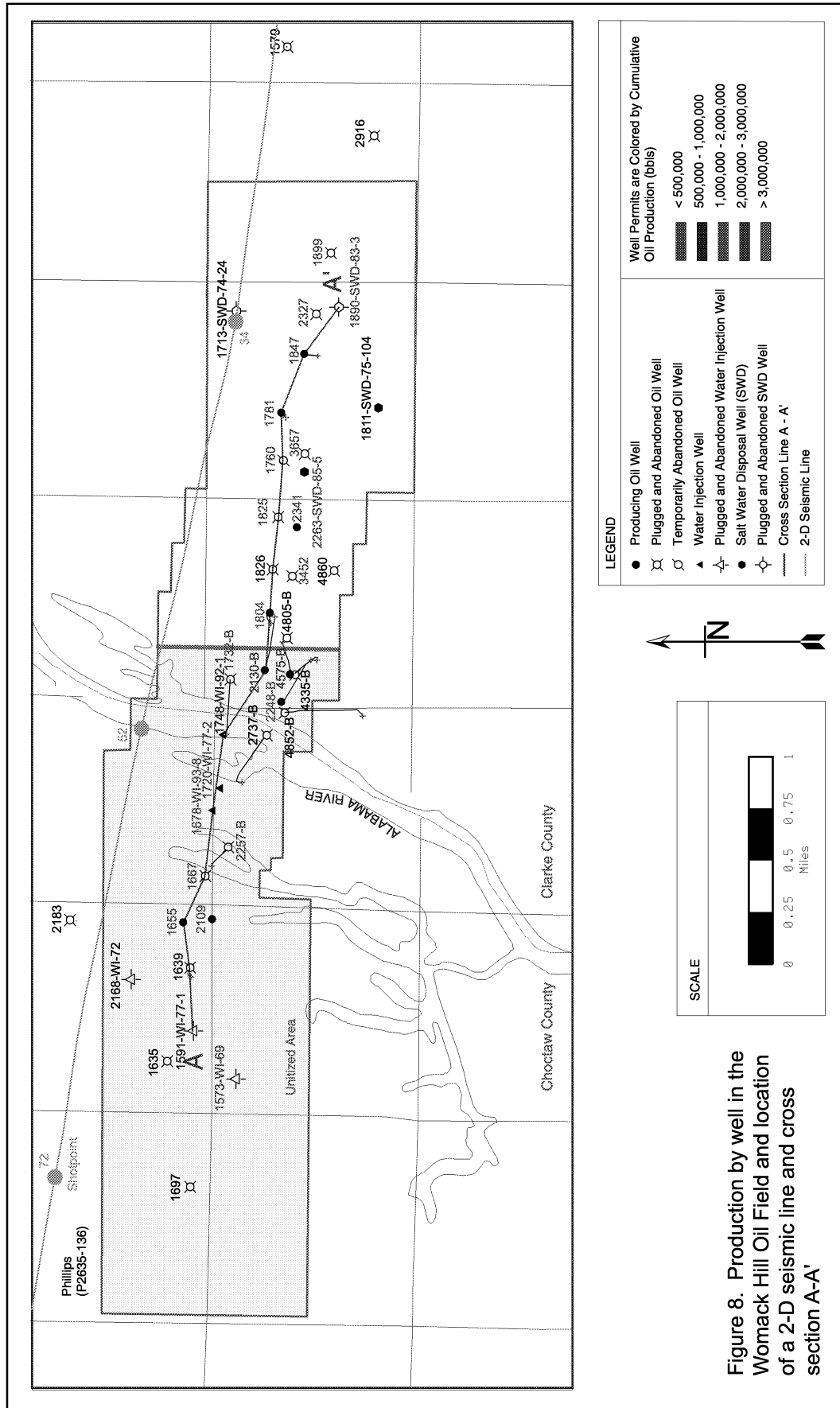
Depth (ft.)	Pore Type	Mineral Composition (Incl. Porosity)			Structures	Texture	Fabric	Grain Size (mm)	Color	Cement	Comments
		0%	50%	100%							
11490		No Recovery									
	WP					Peloidal	WS	.004 - .25	LB	C	
11500	WP				Shale Partings	Peloidal	PS	.031 - .5	G	C	Healed fractures off of stylolite Pelecypods and oncoids
	WP										
	WP										
	WP BP										
11510	WP BP					Peloidal	WS	.004 - .125	LG	C	
		No Recovery									
	WP BP V							.004 - .25			
11520	WP BP V				Shale Partings	Oolitic Peloidal	WS	.004 - .125	LG	C	Oncoids
11530											

Depth (ft.)	Pore Type	Mineral Composition (Incl. Porosity)			Structures	Texture	Fabric	Grain Size (mm)	Color	Cement	Comments		
		0%	50%	100%									
11115	M WP V				Shale Partings	Oolitic Intraclasts	WS	.004 - 4.0	LG	C	Red Shale - Exposure Surface		
								Oolitic Peloidal Oncoidal	PS	.062 - .5	LB	D	Dense Limestone Anhydrite Laths Pelecypods, Gastropods, Oncoids, and Forams Finger Stromatolite
11125	M WP V  M WP V				Cloudy	Oolitic	GS	.031 - .5	MGB	C	Dissolution Surface? Large Anhydrite Nodules		
													Bitumen healed fracture
11135	WP M  WP M  WP M				Shale Partings	Oolitic Peloidal	WS	.004 - .5	LB	D	Shaley		
					Cloudy						Resembles Lagoonal Depositional Environment		
											Shaley		
11145	WP M  WP M							.004 - 1.0 .004 - .5	LB	D	Vague cross-laminations		
						Oolitic Peloidal	PS	.031 - .25			G	C	pelecypods
11155	WP M  M Wp V								G	C	Numerous Pelecypods		
11165	WP M  WP M  WP M					Oolitic Peloidal	PS	.004 - 1.0	LB	D	Small Nautiloid Fossil		
						Peloidal	WS	.004 - 1.0			LB	D	
11175	M WP V  WP BC V								DB	D	Pelecypods and Gastropods		
						Peloidal	MS	.004 - .25					Pelecypods, Gastropods, Oncoids
11185	BC  BC  BC				Faint Laminations				DB	D	Chert Nodules		
						Peloidal	WS	.004 - .5					
													Bioturbation, Oncoids Fabric probably destroyed
11195	BC  BC V BP V				Faint Laminations			.004 - .25	LB	D			
					Shale Partings	Peloidal	MS	.004 - .5					Oncoids
11206											Finely Laminated		

Gas Board. Thin section petrography was conducted using standard-sized, polished thin sections, with one half of each section stained with Alizarin Red-S and Potassium ferricyanide. Thin sections were described using a Nikon microscope and Swift Model F point counter. Stable carbon and oxygen isotopic analysis were conducted at the Stable Isotope Laboratory of the University of Miami Rosenstiel School of Marine and Atmospheric Science following standard procedures and are reported relative to the Peedee Belemnite standard (PDB). Reproducibility for isotope data is better than 0.05 ‰ for oxygen and better than 0.1 ‰ for carbon. Cathodoluminescence petrography was conducted on polished thin sections using a Technosyn Cold Cathode Luminescence Model 8200 MK II with a 450 – 550 nA current, 15-20 kV, and a 0.05 torr vacuum. Detailed component microsampling was done using a JEOL 733 Superprobe. Probing was completed with an accelerator voltage of 15 kV, 12 nA sample current and a 10 μ spot.

**Well Log Study.**--Electrical and geophysical well logs were obtained and analyzed for 42 wells within and immediately adjacent to Womack Hill Field (Fig. 8) and core analysis for 24 cores in the field area were studied. Log types studied include resistivity, compensated neutron, bulk density, gamma ray, SP, and acoustic. Compensated neutron, bulk density and resistivity logs were used to pick and distinguish the Smackover, Buckner, and Norphlet units. Three upward-shoaling cycles in the upper Smackover Formation (labeled A, B, and C) were also determined and picked on all logs (Fig. 9). These picks were correlated across the field and used to create cross-sections (Fig. 10). Core descriptions were also added to the logs, allowing correlation of rock types, facies, and reservoir units across the field. The core data were calibrated to the well log patterns to establish electrofacies for correlation, mapping and modeling.

The three shallowing-upward cycles (A, B, and C) (Fig. 11) are generally composed of a basal peloidal carbonate mudstone, overlain by peloidal wackestone. The tops of each cycle are comprised of peloidal to ooid packstone and are capped by ooid and oncoidal grainstone. The cycles suggest a gradual regression of sea level. There are general increases in porosity, permeability, and dolomite toward the tops of each cycle suggesting some stratigraphic control on reservoir development at Womack Hill Field.



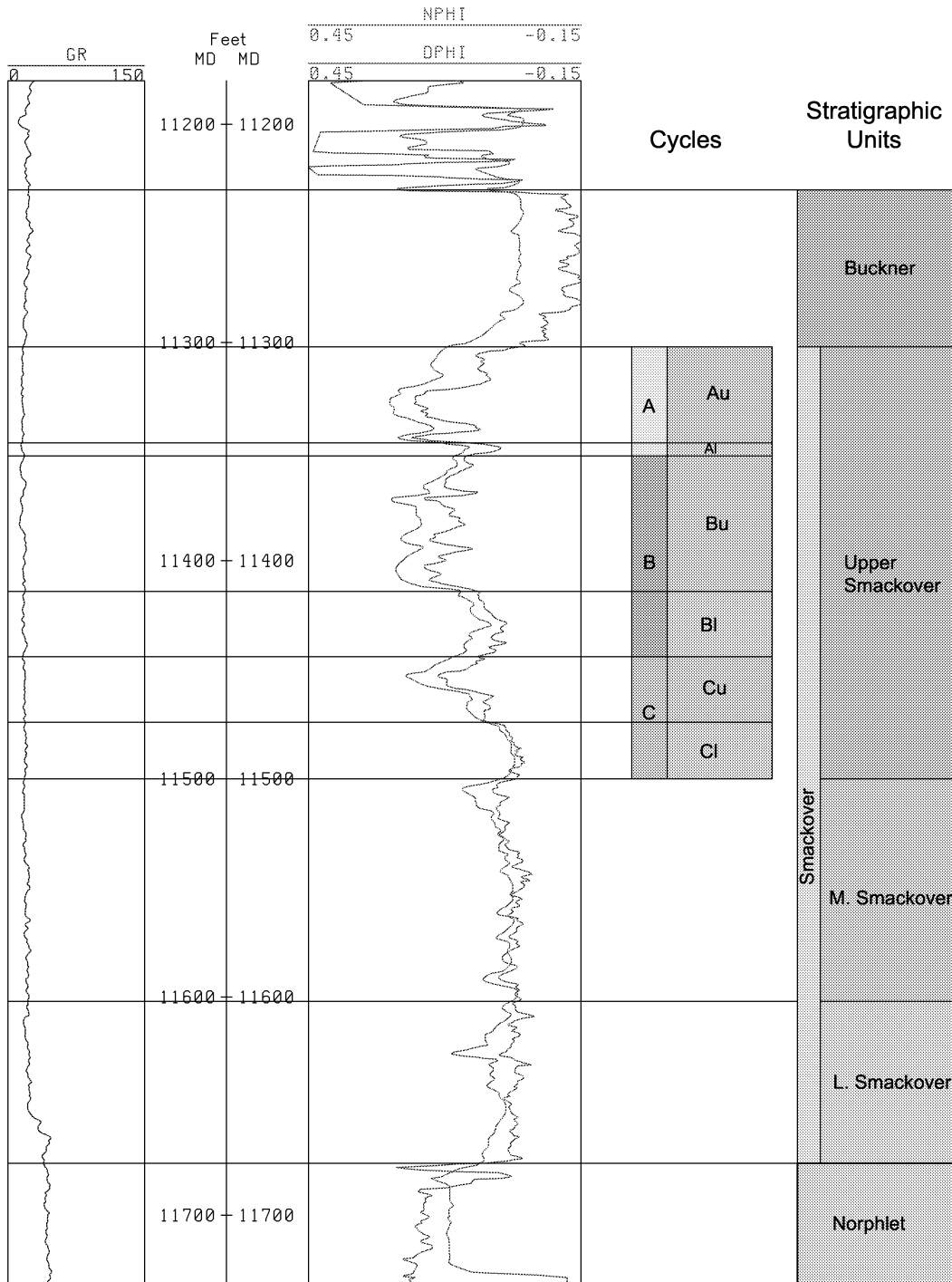


Figure 9. Well log patterns of the Louise Locke 10-14 well (Permit #1667) illustrating Smackover stratigraphic units and upper Smackover cycles at Womack Hill Oil Field. GR=gamma ray log, NPHI=neutron porosity log, DPHI=density porosity log; Au=upper Cycle A, Al=lower Cycle A, Bu=upper Cycle B, Bl=lower Cycle B, Cu=upper Cycle C, Cl=lower Cycle C. See Figure 8 for location of well.

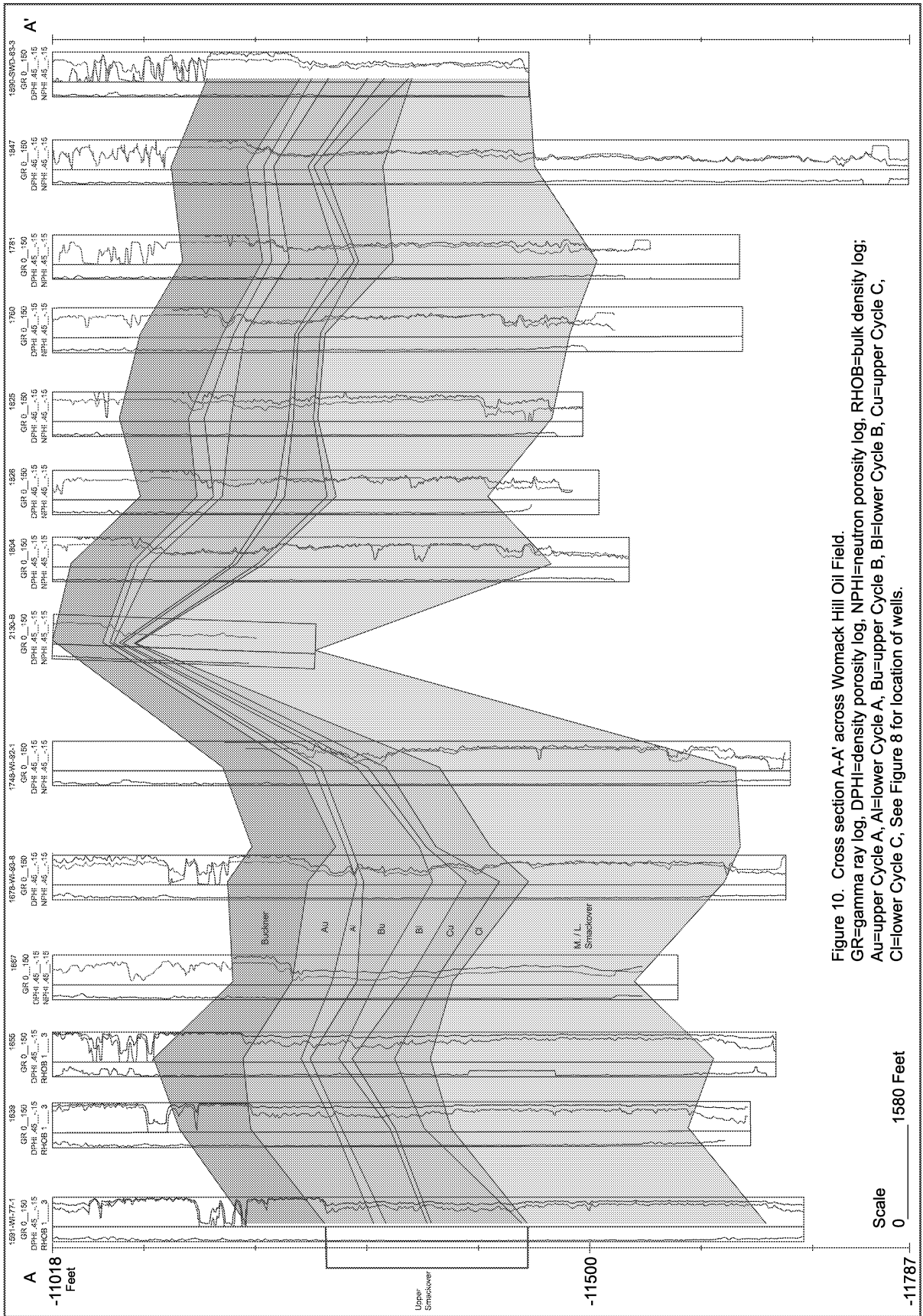


Figure 10. Cross section A-A' across Wormack Hill Oil Field.  
 GR=gamma ray log, DPHI=density porosity log, NPHI=neutron porosity log, RHOB=bulk density log;  
 Au=upper Cycle A, Al=lower Cycle A, Bu=upper Cycle B, Bl=lower Cycle B, Cu=upper Cycle C,  
 Cl=lower Cycle C. See Figure 8 for location of wells.

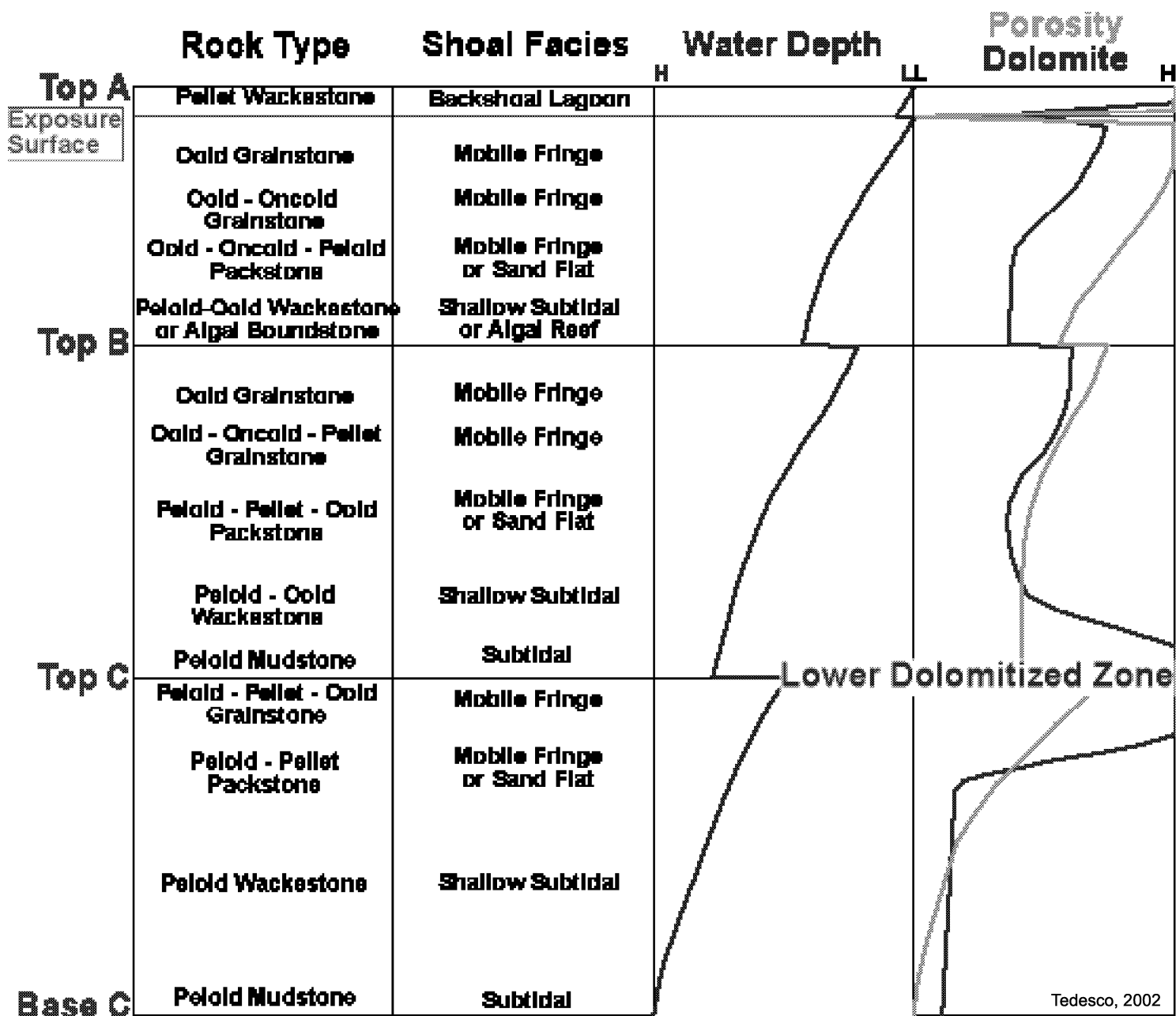


Figure 11. Idealized cycle facies in Upper Smackover at Womack Hill Field. Each cycle comprised of an upward-shallowing sequence of facies on an ooid shoal. Porosity, permeability and dolomite percents generally increase towards the top of each cycle. Location of lower dolomitized zone idealized for a well near the crest of the field structure. Upper dolomitized zone at top of Cycle A.

Two completely dolomitized zones (Fig. 12) were identified and named the upper and lower dolomitized zones. These zones consist of completely dolomitized carbonate rock and are the best reservoir zones at Womack Hill Field. The upper dolomitized zone is found in the upper 10-15 feet of the Smackover Formation, just beneath the Buckner Anhydrite Member. The lower dolomitized zone cuts across depositional lithofacies in the field. This zone is commonly 40 to 50 feet thick and is stratigraphically higher in the structurally lower parts of the field.

**Subsurface Mapping.**--Several different subsurface maps of the Womack Hill Field have been constructed to assist with analysis of production controls in the field. Structure maps of the top of the Smackover Formation (Fig. 13) and Buckner Anhydrite Member of the Haynesville Formation (Fig. 14) have been made using depths determined from the geophysical logs. Isopach maps of the Smackover (Fig. 15), upper Smackover (Fig. 16), Cycle A (Fig. 17), Cycle B (Fig. 18), and Cycle C (Fig. 19) have been made using log derived thicknesses.

**Seismic Interpretation.**--Seismic reflection data (2-D) have been acquired from Seismic Exchange, Inc. These data (Fig. 20) were reprocessed by Geo-Seis Processing and interpreted. Figure 8 shows the location of the seismic data acquired.

**Petrographic Analysis.**--Thin section petrographic analysis is completed. All 184 thin sections available at Womack Hill field have been described. A clasticity index was determined for all thin sections and then compared to porosity and permeability data. Clasticity index is a measure of the largest coated grain present in each sample (Carozzi, 1958; Erwin *et al.*, 1979; Humphrey *et al.*, 1986). In general, a direct relationship with permeability and porosity was found with the clasticity index. With increasing clasticity there is a corresponding increase in porosity and permeability. The only zones not following this trend are zones with complete or near complete fabric-destructive dolomitization. In these zones, clasticity index drops to zero, whereas porosity and permeability increase. At the top of Cycle A, a low clasticity index also correlates well with an exposure surface identified and mapped across the field.

One hundred twenty-two powders for isotope analysis were prepared from thin section butts and core pieces for stable carbon and oxygen isotopic analysis. Sampling ensured that all rock

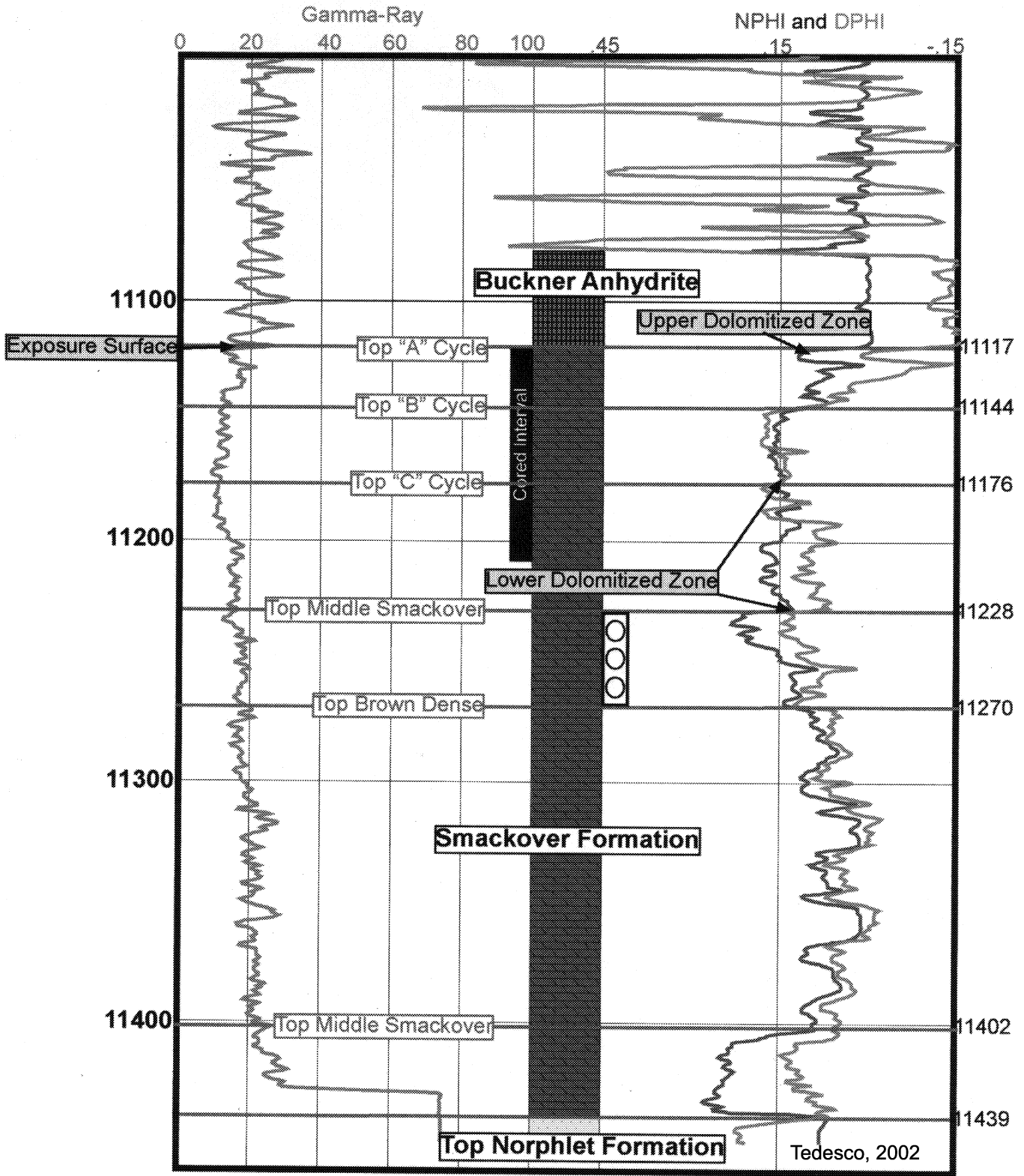


Figure 12. Porosity and gamma-ray logs for Womack Hill Field Unit 14-5 No. 2 well. Formation boundaries and cycles denoted by brown lines. Exposure surface identified at top of Smackover Formation from core data correlates with gamma-ray spike near Buckner-Smackover contact. "Type 1" dolomitized zone just below exposure. Lower dolomitized zone comprised of "Types 2 & 3" dolomite.

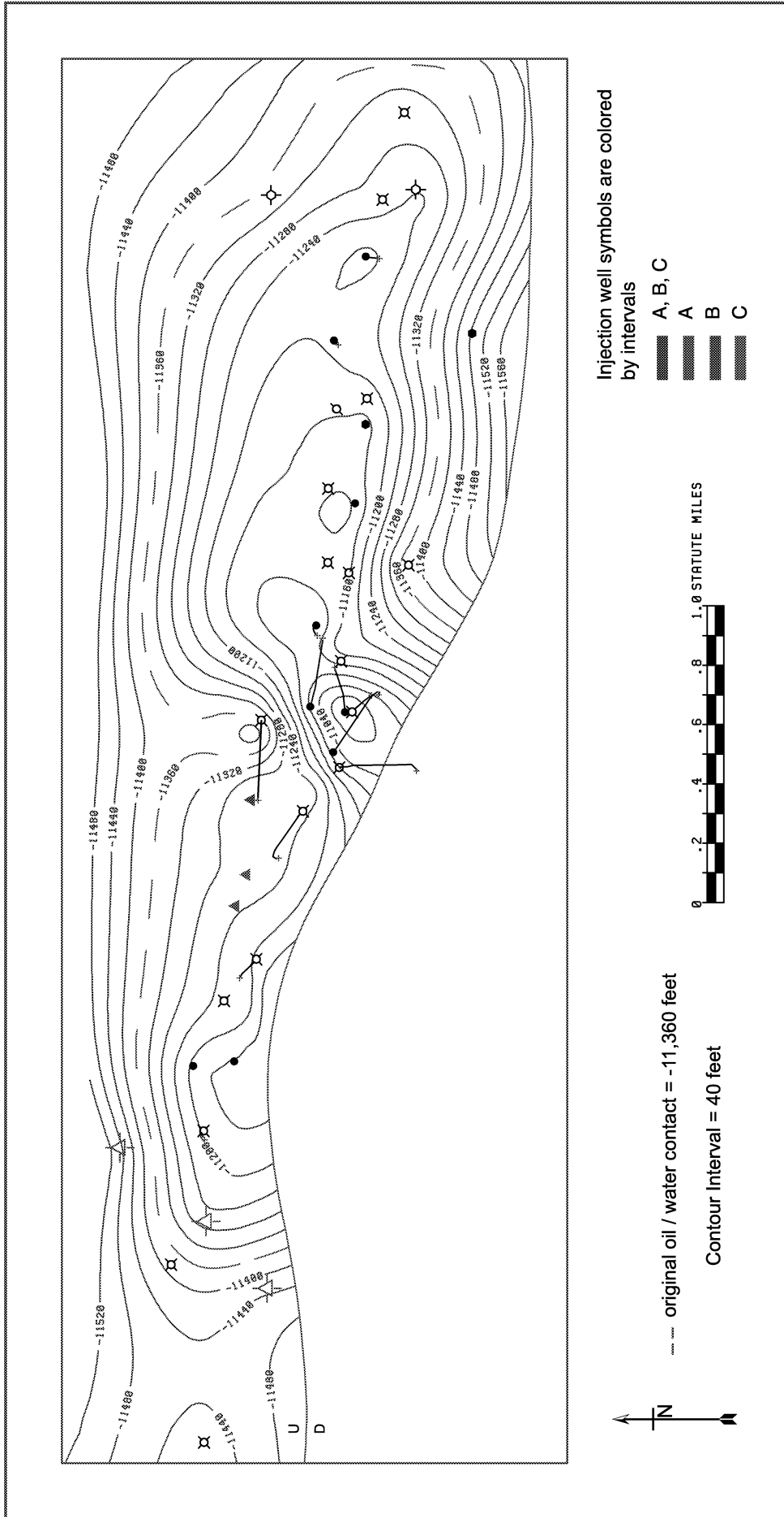


Figure 13. Structure map on top of the Smackover Formation at Womack Hill Oil Field. See Figure 8 for well symbols.



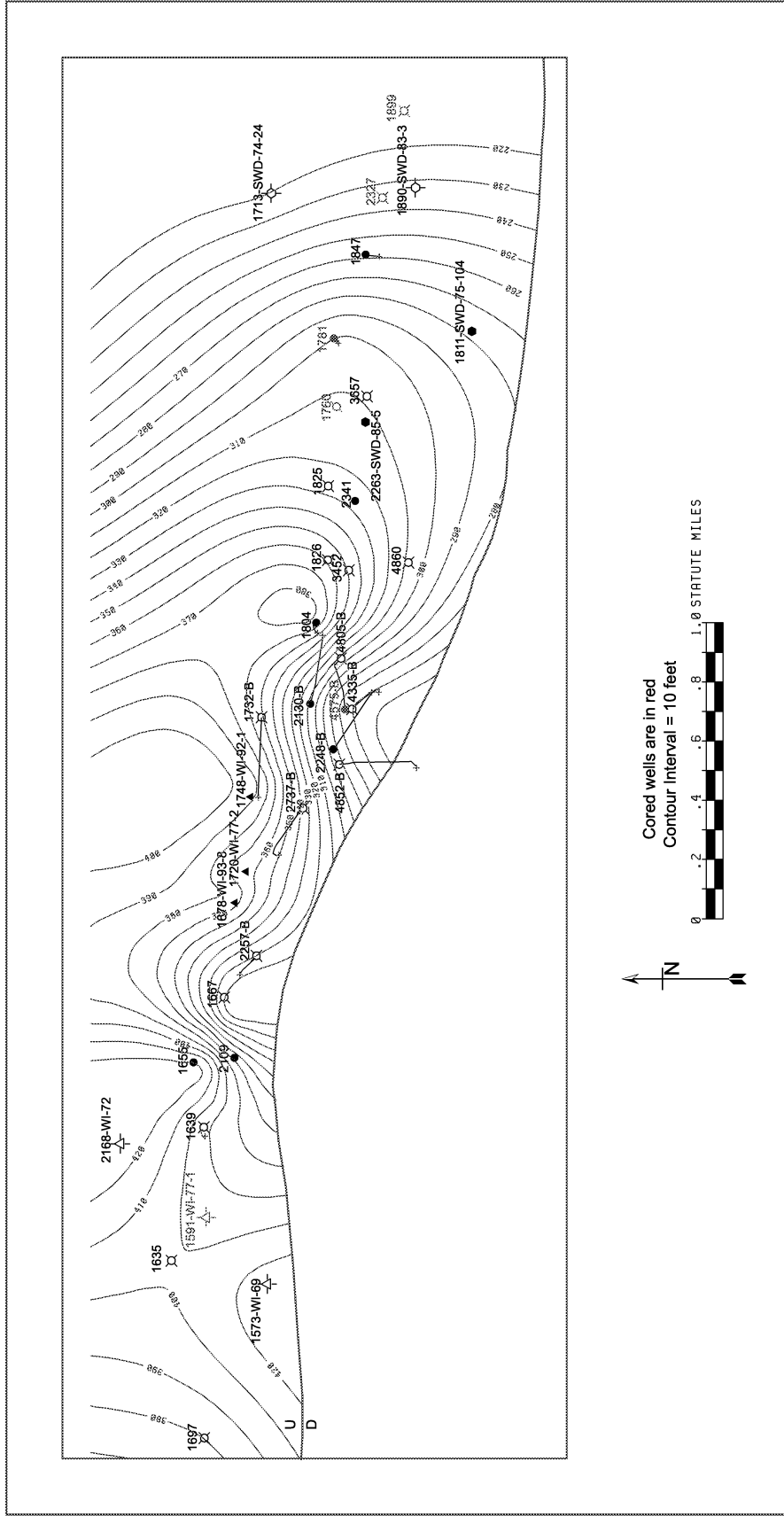


Figure 15. Isopach map of the Smackover Formation at Womack Hill Oil Field. See Figure 8 for well symbols.

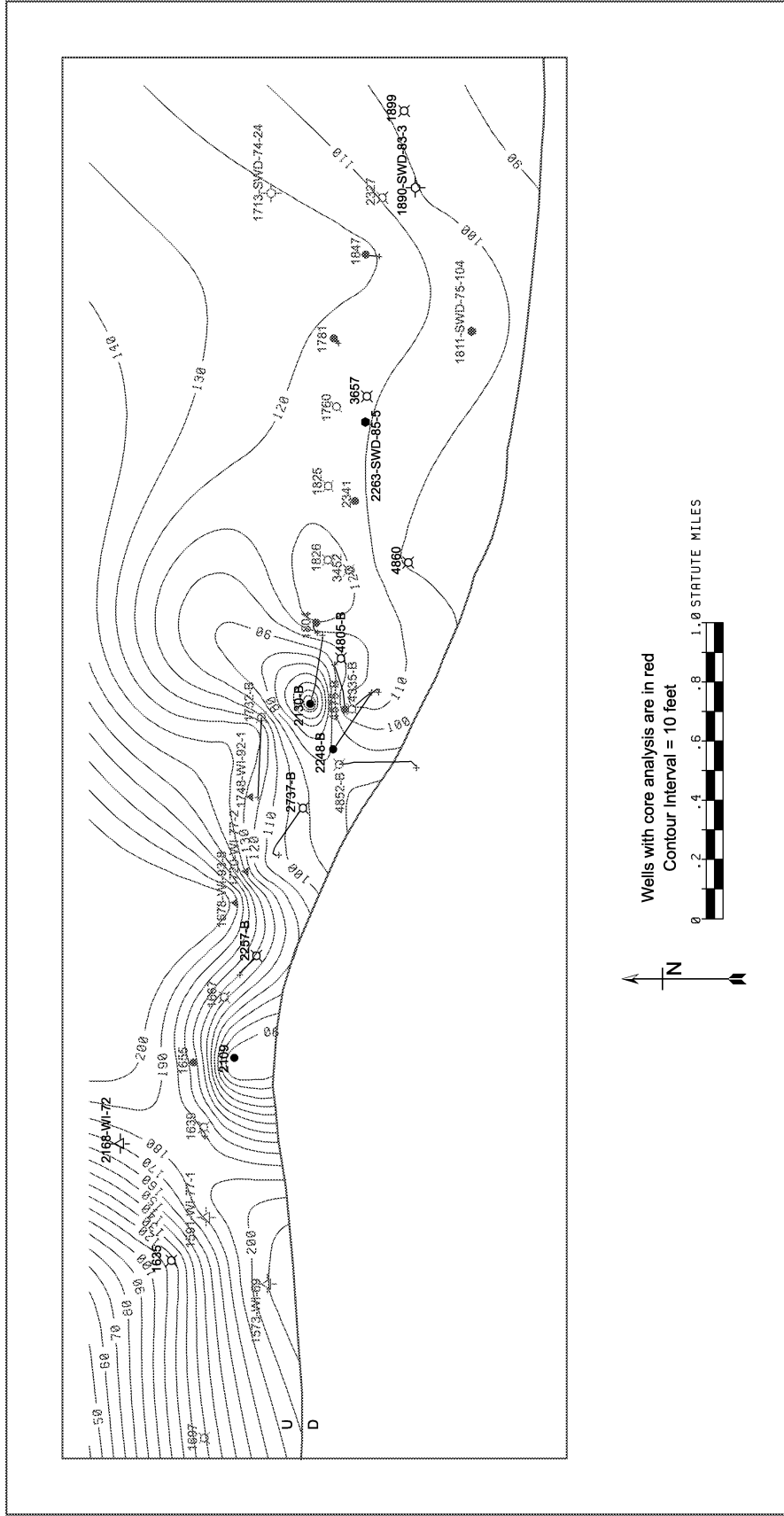


Figure 16. Isopach map of the upper part of the Smackover Formation at Womack Hill Oil Field and location of wells with core analysis data. See Figure 8 for well symbols.



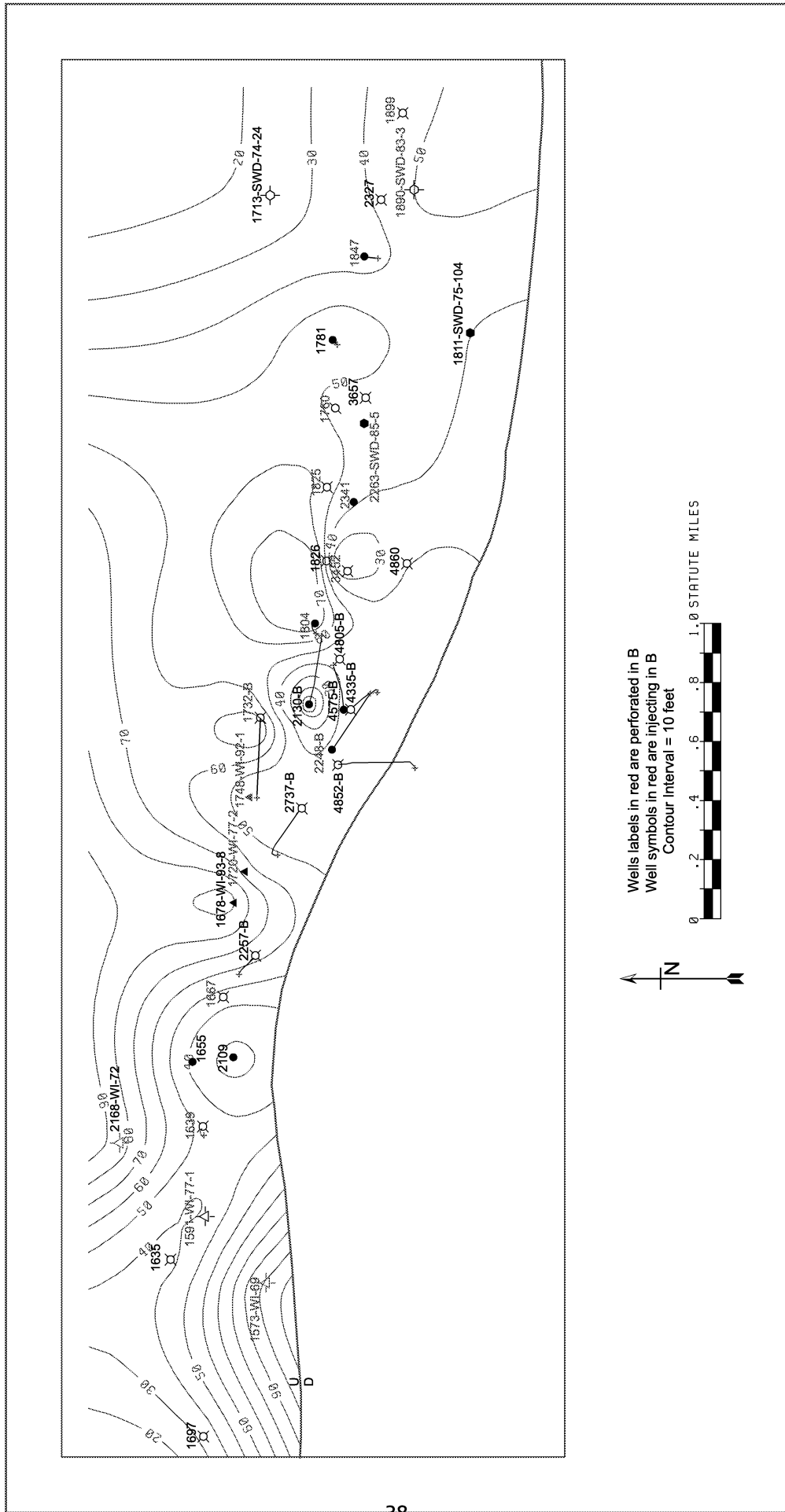


Figure 18. Isopach map of Cycle B and locations of wells perforated in Cycle B and wells injecting water into Cycle B. See Figure 8 for well symbols.

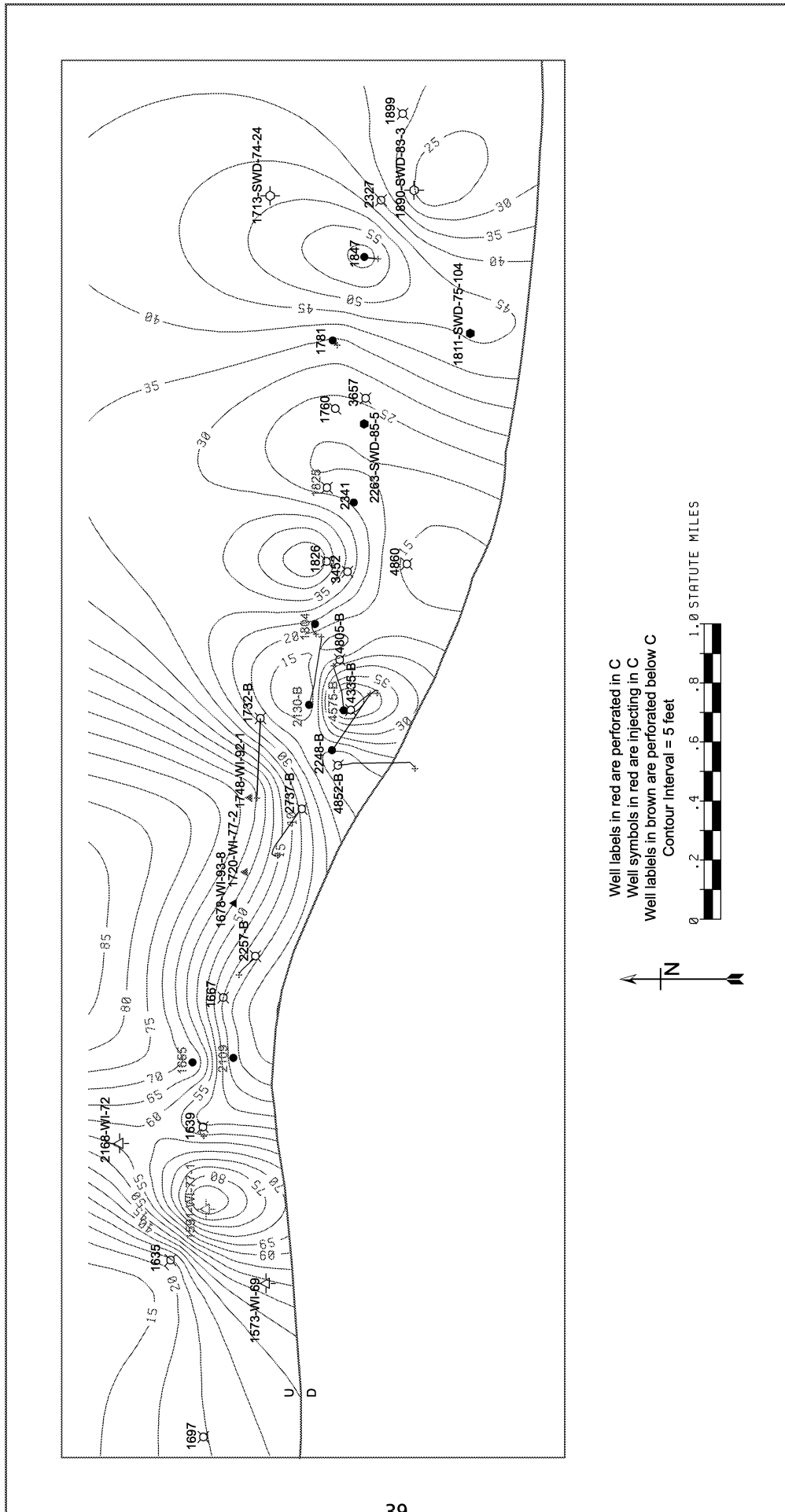


Figure 19. Isopach map of Cycle C and locations of wells performed in Cycle C, wells perforated immediately below Cycle C, and wells injecting water into Cycle C. See Figure 8 for well symbols.

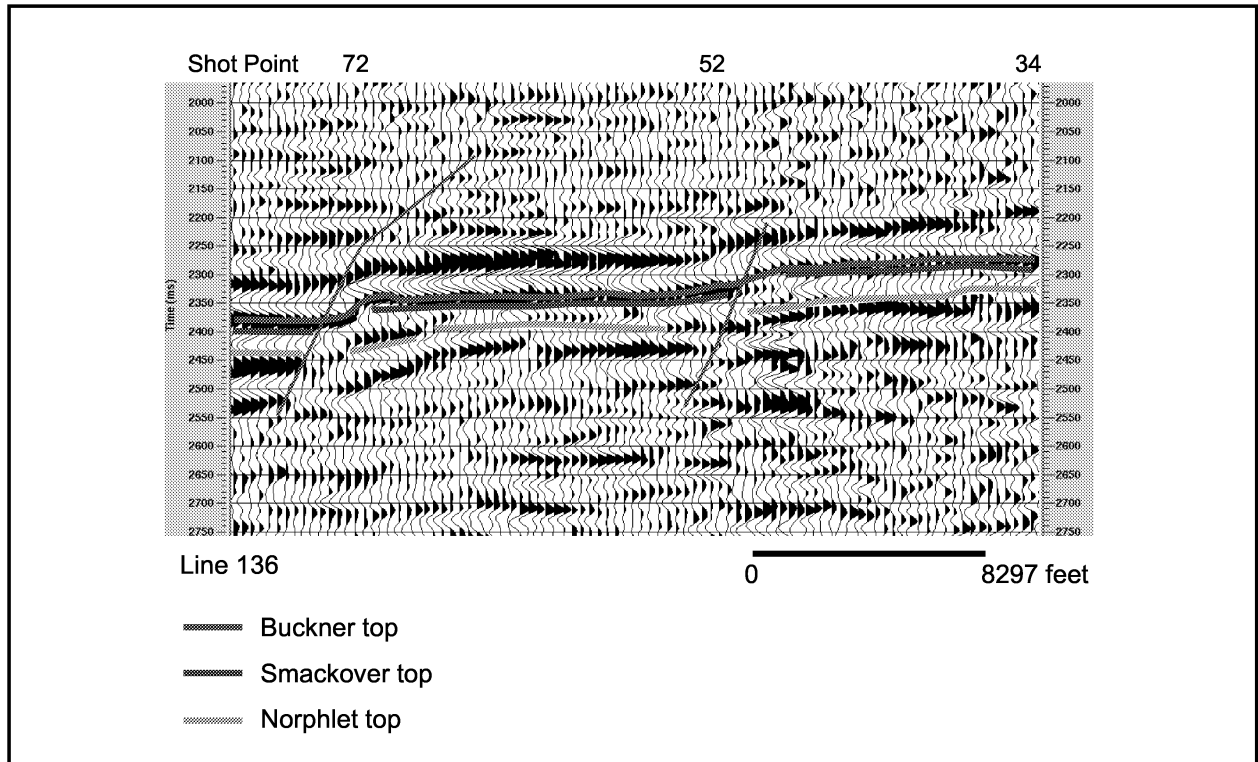


Figure 20. 2-D reflection profile, west-east line, Phillips P2635-136. See Figure 8 for location of seismic line.

types present in each of the cores were analyzed. Data from isotopic analysis (Fig. 21) show clear separation of the upper and lower dolomitized zones. Dolomite in the upper dolomitized zone has isotopically enriched  $\delta O^{18}$  values compared to the lower dolomitized zone. This suggests that the dolomitizing fluid for the upper zone was supersaturated brine at relatively low temperature. Analysis of the lower dolomitized zone isotopic data is ongoing. Calcite cements form a linear trend probably reflecting a transition from earlier precipitated cement at cooler temperature through later burial calcite cements.

Cathodoluminescence (CL) petrography was conducted on all petrographically identified dolomite and calcite cements and grains. Zoned cements and bimineralic ooid grains were recognized during petrography. In addition, changing CL intensities in some dolomite crystals suggests changing fluid chemistry during precipitation. Detailed CL mapping was used to determine traverse and sampling locations for microprobe study. Results of CL study will be discussed in the diagenesis section below.

Strontium, calcium, magnesium, iron, and manganese concentrations have been determined through detailed component microsampling using a JEOL 733 Superprobe. We collected 98 data points, which include data from each dolomite type identified during transmitted light and cathodoluminescence petrography. Analysis of probe data is currently be conducted at The University of Mississippi.

**Diagenetic Study.**--Core descriptions, openhole well log analysis, thin section petrography, and stable isotope geochemistry have been used to create a model of Smackover diagenesis at Womack Hill Field. Smackover diagenesis began with early marine cementation of grains by fibrous aragonite and development of micrite envelopes through algal borings. Partially preserved fabrics in ooids suggest these grains had three different original compositions: aragonite, Mg-calcite, and bimineralic. These unstable sediments were highly altered in the meteoric diagenetic realm, creating large amounts of moldic porosity. Isopachous rim and equigranular drusy spar cements precipitated in intergranular and moldic pores. Both cements precipitated

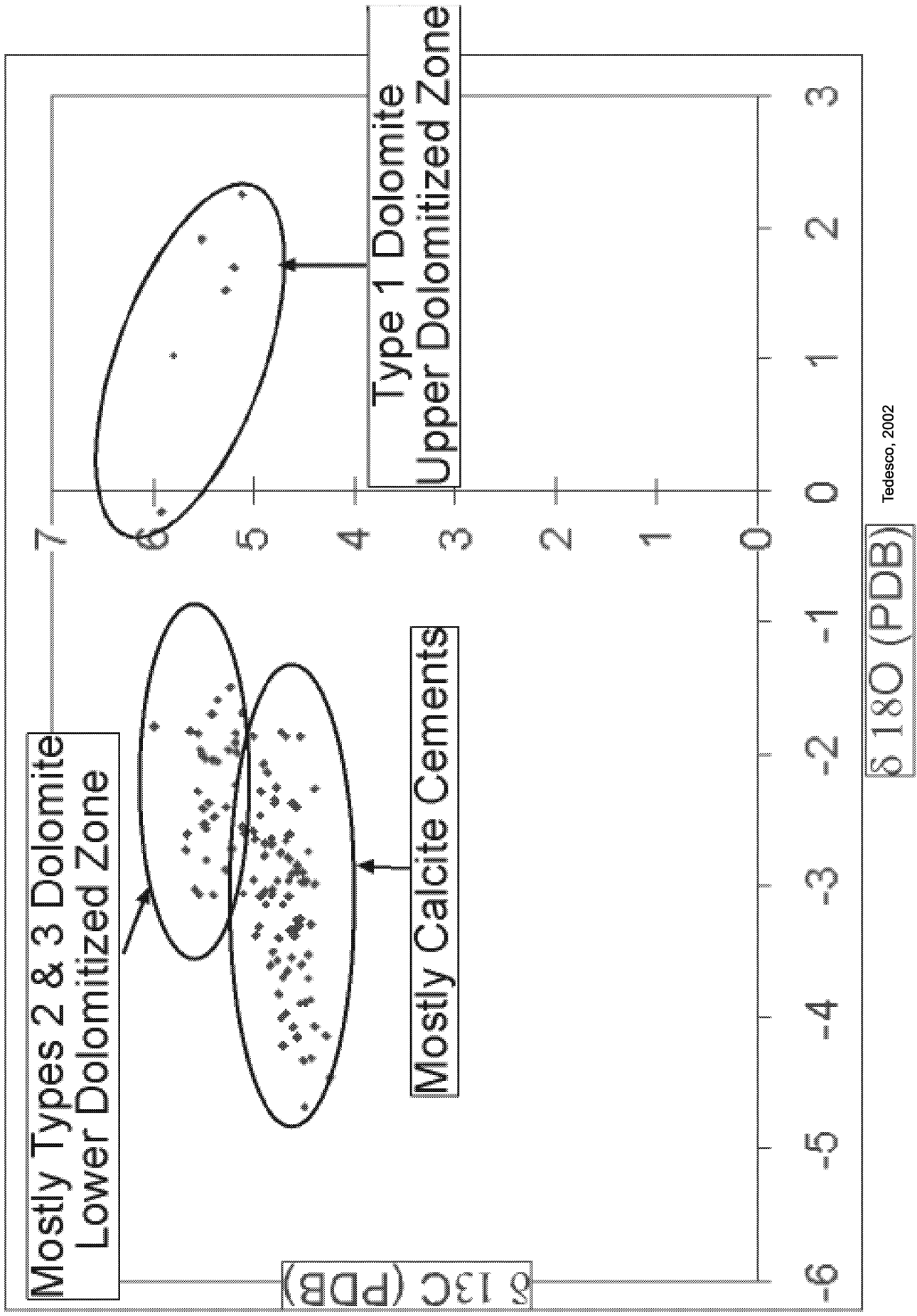


Figure 21. Stable isotope geochemistry. Upper dolomitized zone enriched relative to lower dolomitized zone suggesting two separate dolomitizing fluids. Upper dolomitized zone isotopic signature suggests dolomitization by hypersaline brine at near-surface temperatures.

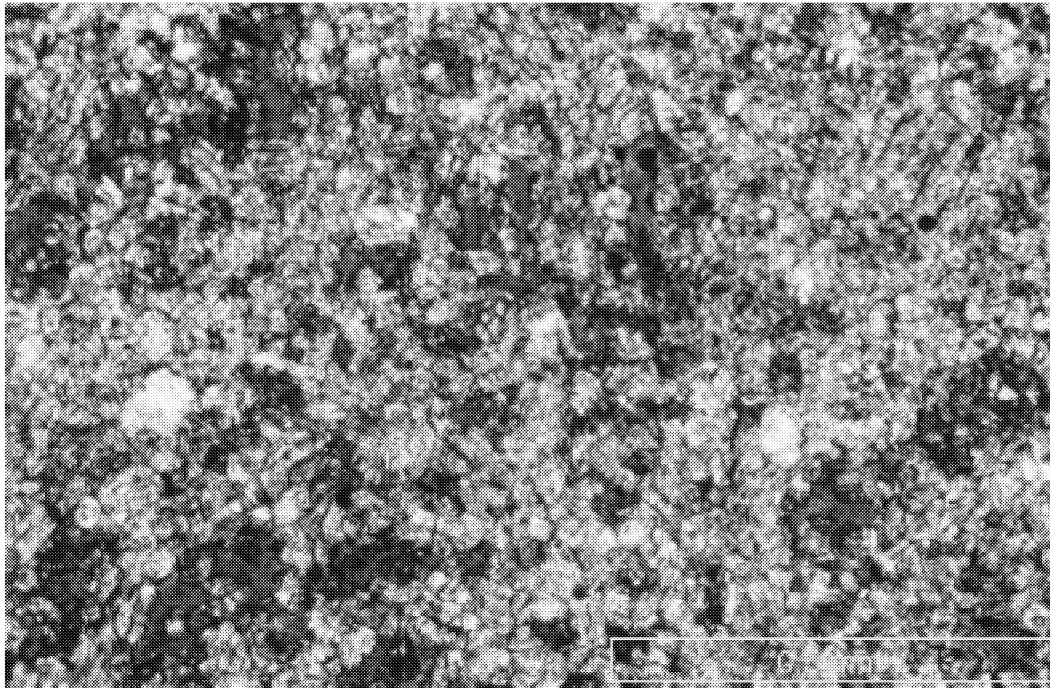
contemporaneously with dissolution and can be found in intergranular and moldic pores. Meteoric cementation was followed by at least four major phases of dolomitization.

The first event was a fabric-destructive dolomitization in the uppermost Smackover (Cycle A; upper dolomitized zone) (Fig. 22). This event likely occurred soon after deposition by penecontemporaneous, downward-moving, evaporitically-concentrated brine. The dolomite phase is associated with an exposure event identified from core and petrographic analysis (Fig. 23). At wells located on the structural high area of the field, the exposure is located above the phase 1 dolomitized zone near the Buckner-Smackover contact. In wells off the structural high, the exposure is located at or near the base of the dolomitized zone. A gamma-ray spike commonly occurs at the exposure surface, allowing for recognition and correlation of this surface. The dolomite is composed of inclusion-rich, euhedral to subhedral dolomite crystals, is completely fabric destructive, and exhibits a dull red luminescence (Fig. 22). The dolomitized zone is commonly 4 to 15 feet thick, has high porosity (15-30%) and high permeability (5-45 md). This first dolomitization event can be recognized on logs across the entire field.

The second phase of dolomitization likely occurred during or immediately following meteoric leaching of unstable aragonite grains, occluding much of the moldic porosity. The dolomite is characterized by inclusion-rich, xenotopic, fine-crystalline to microcrystalline (commonly less than 50 microns), anhedral crystals selectively replacing ooids and peloids (Fig. 24). The dolomite has a slightly brighter red luminescence than other dolomite phases. This event occluded moldic porosity and is a porosity destructive event.

The third dolomitizing event was fabric-destructive, creating large amounts of intercrystalline porosity and increasing permeability. This dolomite event is the most common throughout the wells, except where dolomite type 1 is present. Reservoir zones in the lower part of Cycle A, Cycle B, and Cycle C are commonly associated with dolomite phase 3. The lower dolomitized reservoir zone, which is primarily composed of type 3 dolomite, climbs stratigraphically higher in north to south transects. Two distinct dolomite crystal morphologies are recognized in this phase. The two morphologies may represent two separate phases of dolomitization from different brines or may

A.



B.

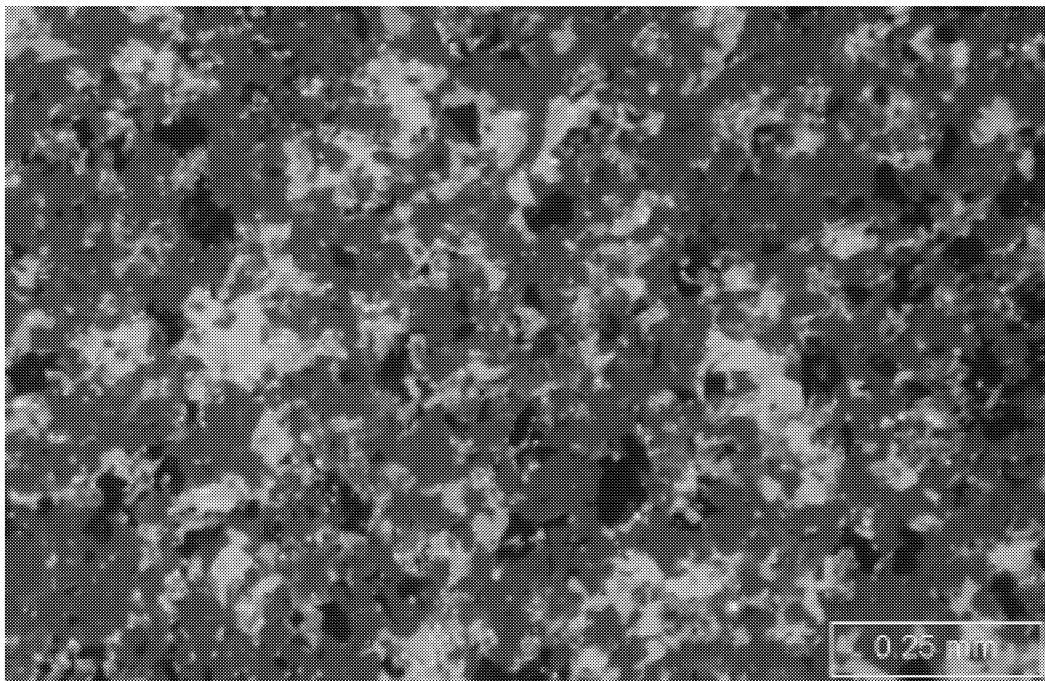


Figure 22. "Type 1" dolomite from near the top of the Smackover Formation.

A. Note inclusion-rich sucrosic dolomite crystals and large amount of intercrystalline porosity, Turner 13-25 well (11,434.4 ft).

B. Cathodoluminescence in Type 1 dolomite. Dolomite has red luminescence, burial calcite cement exhibits yellow luminescence, and bitumen exhibits green luminescence, Counselman 18-12 well (11,462 ft.).

(photographs by Tedesco).

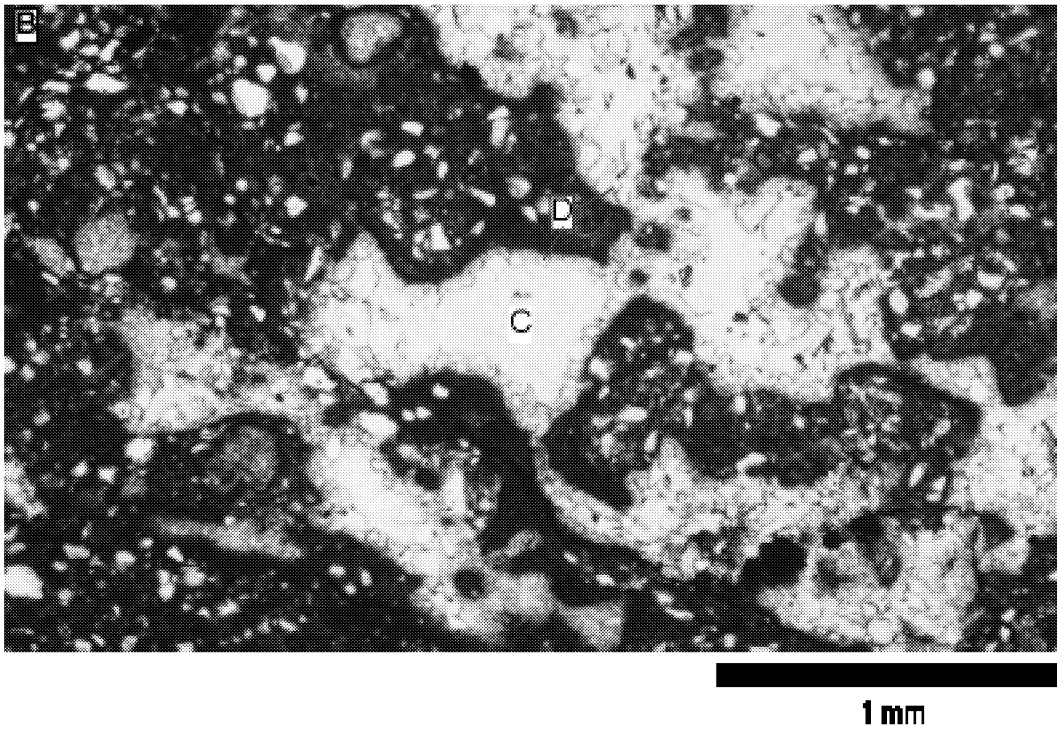
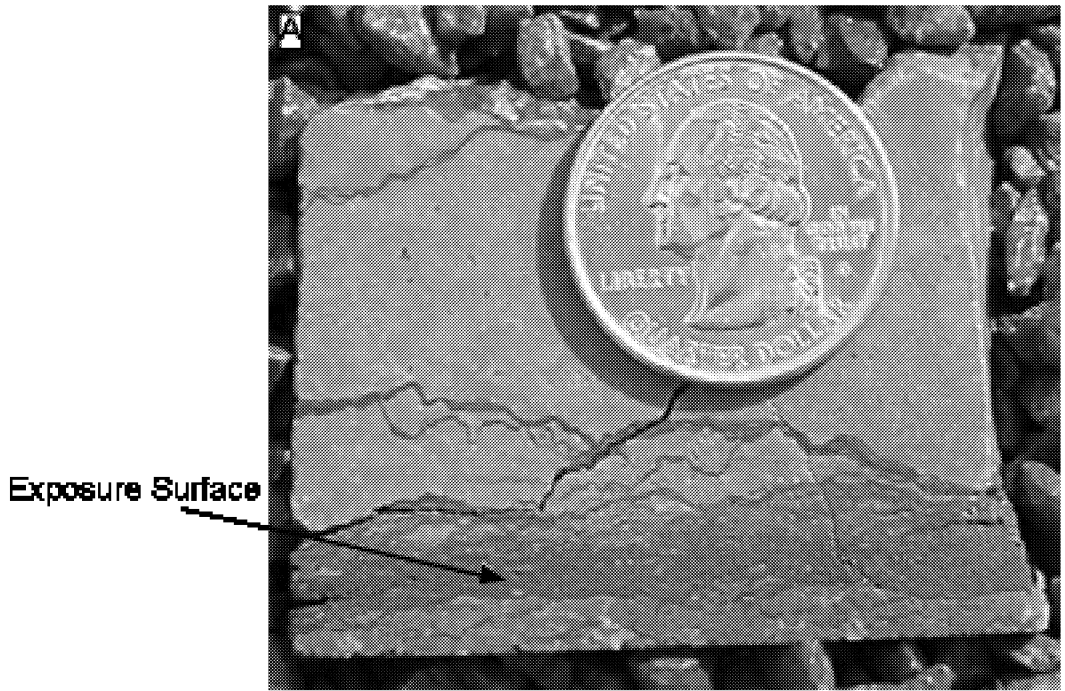
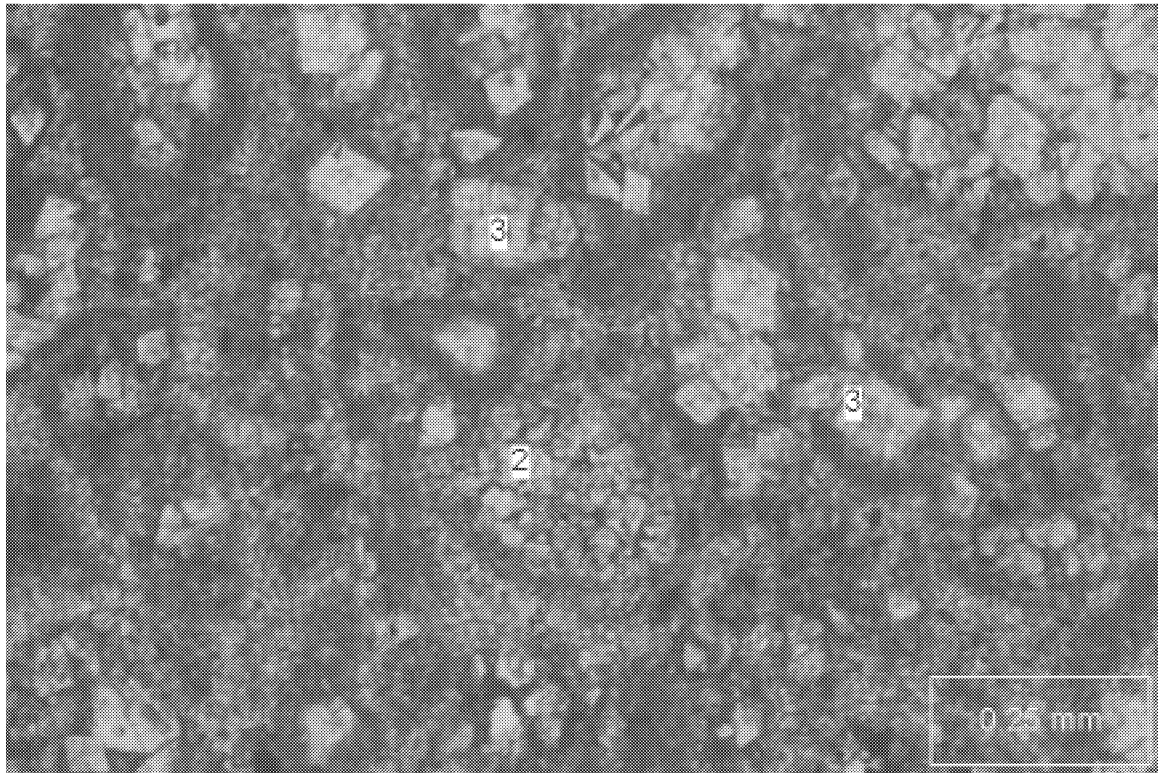


Figure 23. Upper "A" cycle exposure surface. Turner 13-5 well (11,326 ft.).  
 A. Red shale lamina at exposure surface.  
 B. Photomicrograph at exposure surface. Dark brown groundmass composed of microcrystalline dolomite. Note alveolar texture. Pore lined idiopathic-C dolomite cement (D) followed by blocky calcite (C) cements that completely occlude porosity. Note high clastic content which is responsible for gamma ray spike characteristic of exposure surface. (photographs by Tedesco).

A.



B.

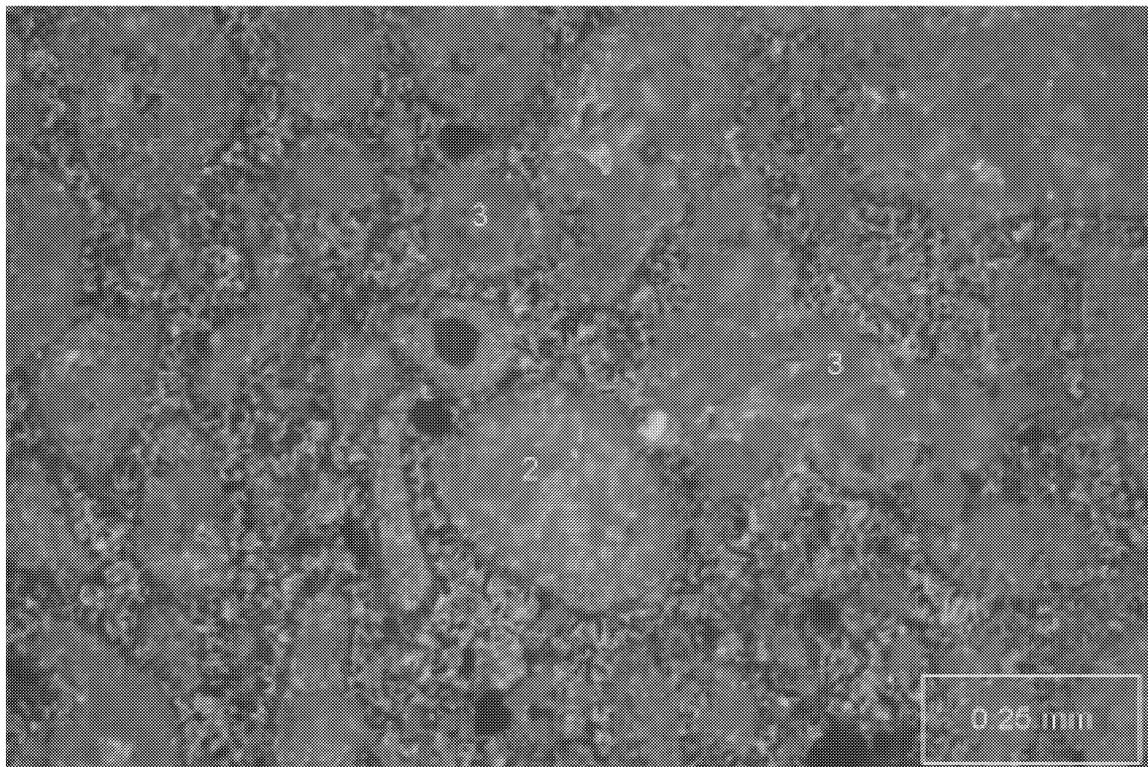


Figure 24. "Types 2 and 3" dolomite. Womack Hill Field Unit 14-5 well (11,116.5 ft.).  
A. Note Type 2 (2) fabric selective replacement of grains by anhedral fine-crystalline dolomite and Type 3 (3) fabric destructive dolomitization by euhedral rhombs.  
B. Cathodoluminescence view of A. Note brighter luminescence by Type 2 (2) dolomite. (photographs by Tedesco).

represent a continuum of dolomitization with changing water chemistry. The first dolomite morphology is characterized by subhedral hypidiotopic to idiotopic, relatively inclusion-free crystals 50 to 100 microns in diameter (Figs. 24 and 25). The second morphology is comprised of euhedral, ideotopic, inclusion-free crystals 50 to 150 microns in diameter. Larger crystals commonly have an inclusion-rich core and more inclusion-free outer zone (Fig. 25). Both morphologies are commonly associated with stylolites and fractures throughout the cores, suggesting stylolites may have been fluid migration pathways.

The fourth dolomitization phase is comprised of idiotopic-c (Gregg and Sibley, 1984) dolomite cement lining vuggy pores in the Cycle A (Fig. 26). The cement commonly follows an early phreatic isopachous calcite cement and is followed by syntaxial blocky calcite spar cement. This cement is found in Cycle A near the identified exposure surface. The dolomite commonly has a bright red luminescence with quenched crystal terminations, suggesting changing fluid chemistry during precipitation. Microprobe data indicate a decrease in Mn concentration across the crystals, explaining the change in luminescence.

A minor dolomitization phase occurred in the deep burial environment and is characterized by precipitation of large saddle dolomite rhombs in fractures and vuggy pores. Other late burial cements include syntaxial and poikilotopic calcite spar cements, potassium feldspar overgrowths, blocky and poikilotopic anhydrite and celestite cement, and rare gypsum and sulfur cements.

Burial effects include both physical and chemical compaction (Fig. 27). These have led to significant reductions of porosity and permeability in sediments not already dolomitized or altered to stable calcite. Burial features include crushed and deformed or broken grains, spalled oolites, stylolites and microstylolites, stylolitic grain contacts, interpenetrating grains, and fractures.

**Pore System and Petrophysical Study.**--The pore systems in the Smackover reservoir at Womack Hill Field have been studied and classified using the classification of Choquette and Pray (1970). Pore types include interparticle, intraparticle, vuggy, intercrystalline and moldic (Table 3). The probe permeameter (mini-permeameter) was used to determine horizontal and vertical permeabilities from the 118 billets cut from the cores for thin sections. Average log vertical

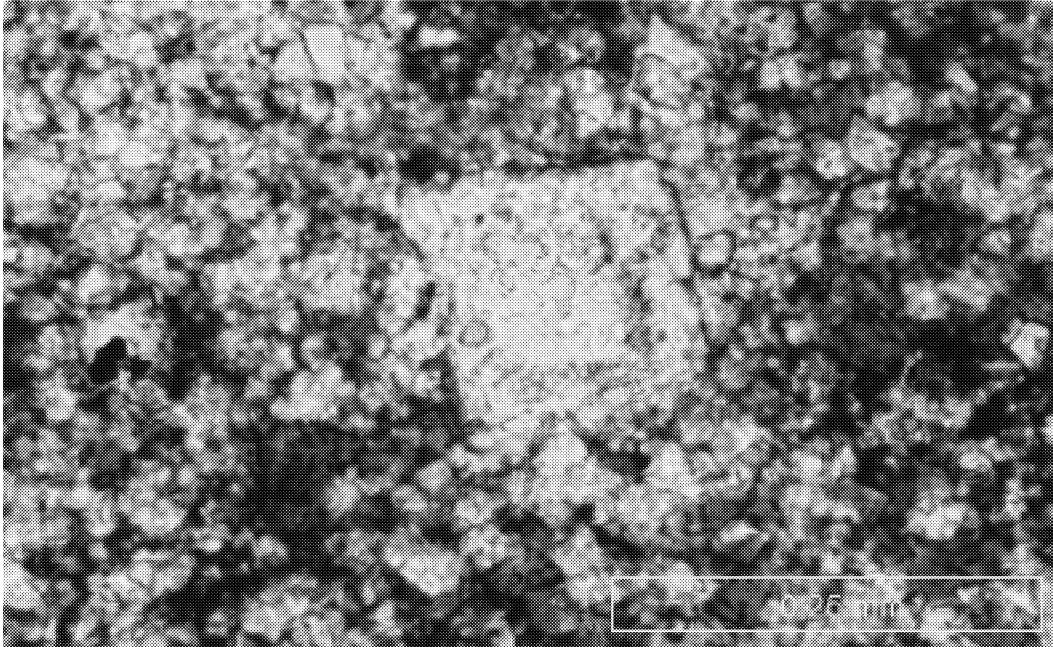
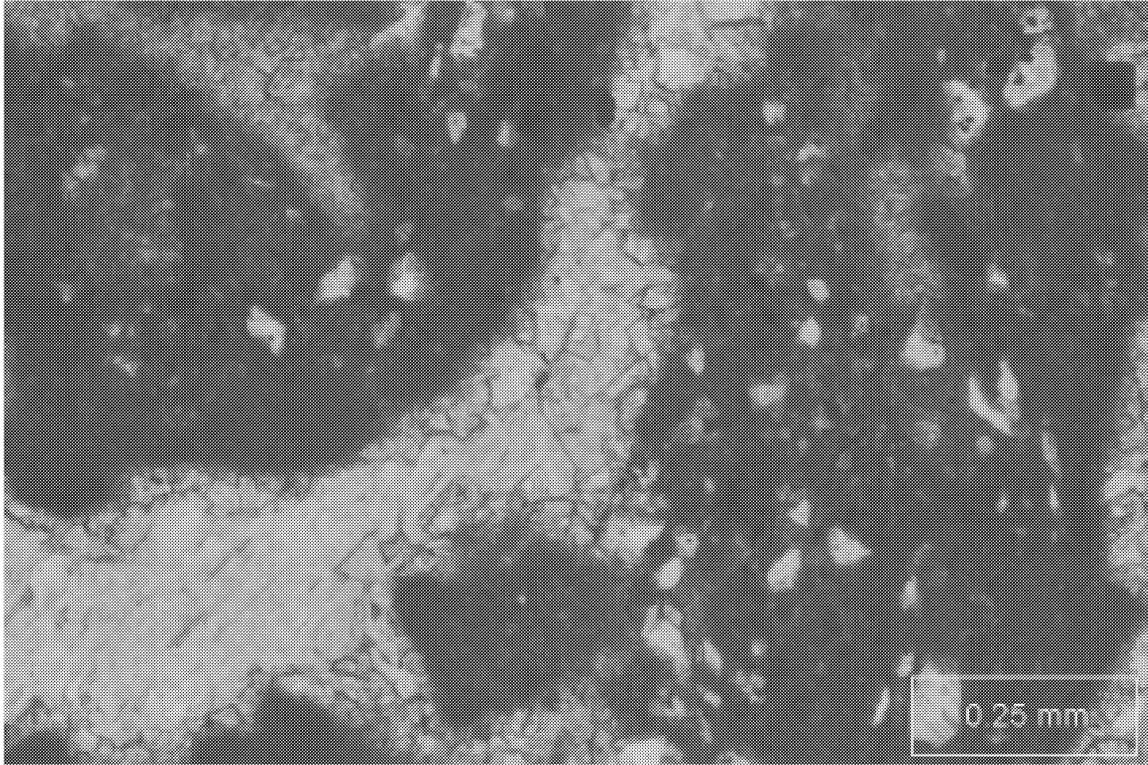


Figure 25. Close-up of "Type 3" dolomite crystal. Zones of inclusions toward center of crystal is a common observation across the field. Scruggs, Parker, Norton 9-14 well (11,413 ft.). (photograph by Tedesco).

A.



B.

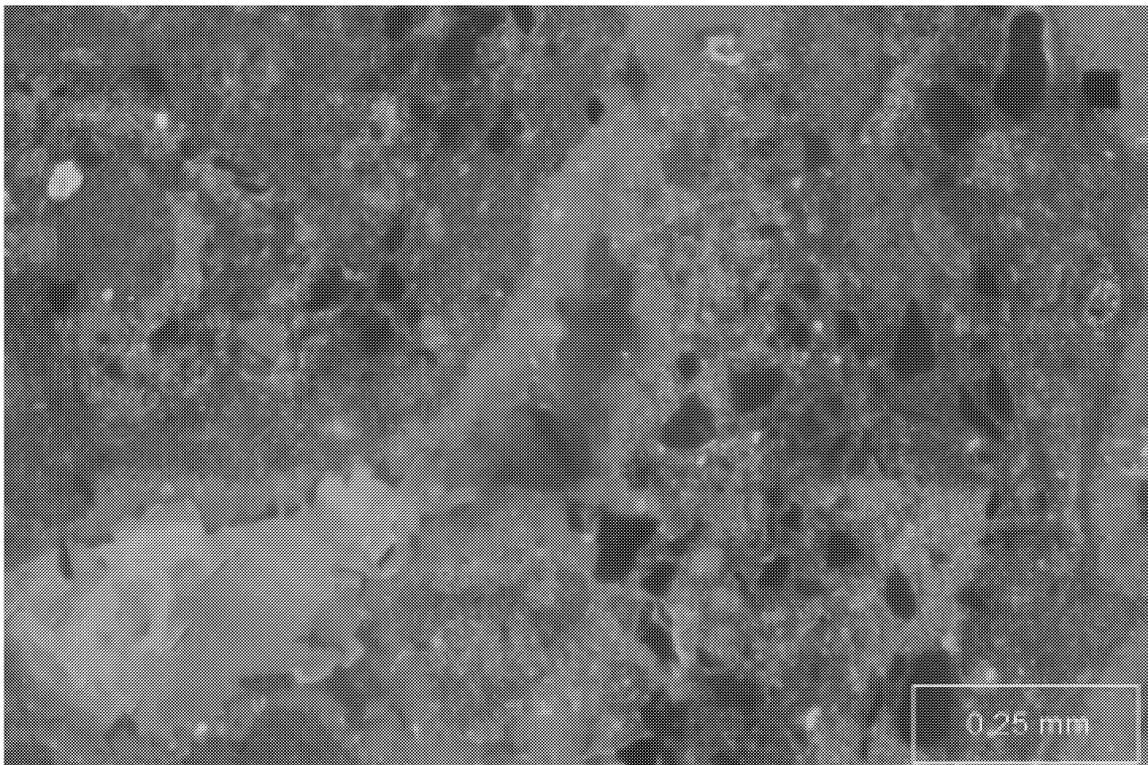


Figure 26. Idiopathic-C dolomite cement. Turner 13-5 well (11,327 ft.).

- A. Note dolomite cement lining pore walls and following isopachous calcite cement. Dolomite followed by coarse syntaxial calcite cement which completely occludes porosity.
- B. Cathodoluminescence of same view as in A. Note red luminescence and quenched crystal edges in dolomite cement.  
(photographs by Tedesco).

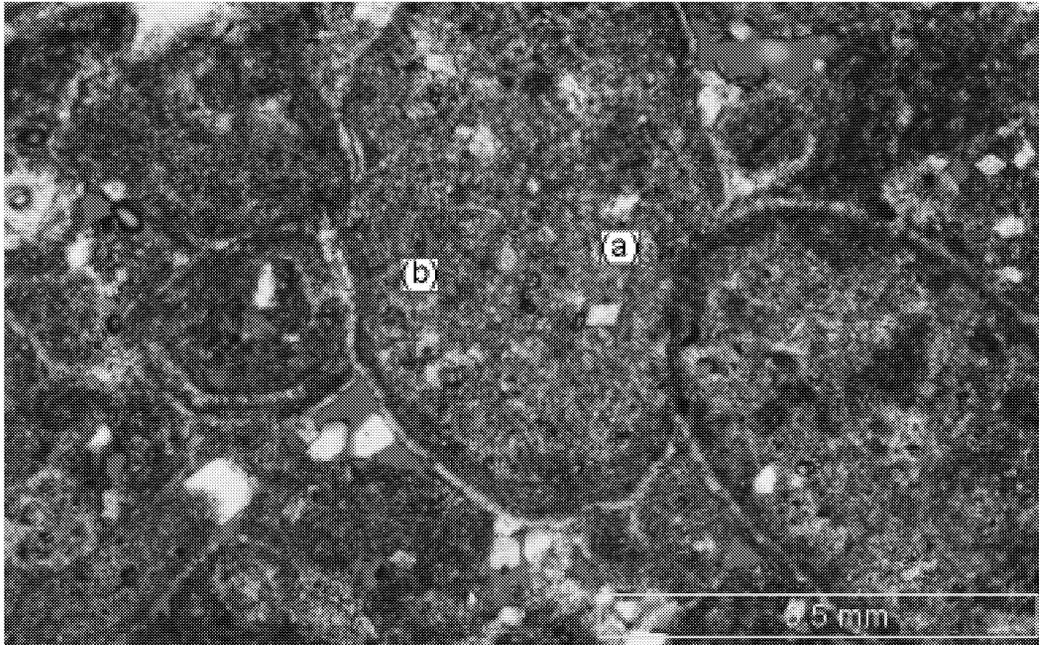


Figure 27. Deformation features in calcite-dominated zones. Note interpenetration and deformation of grains. These features can significantly reduce porosity. Deformation occurred both before (a) and following (b) early marine cementation. Rare "Type 3" dolomite rhombs scattered in interparticle pores. Turner 13-6 well (11,412 ft.). (photograph by Tedesco).

**Table 3. Data on plugs chosen for capillary pressure testing (from Hopkins, 2002).**

<b>Well Permit #</b>	<b>Cycle</b>	<b>Core Depth</b>	<b>Lithology</b>	<b>Est % Dolomite</b>	<b>Pore Types</b>	<b>(Cleaned) He % Porosity</b>	<b>Cleaned Pr Permeability (md)</b>
1591	A	11,405.0	pel, oo ws	90	ic 21.	52	35.07
1591	A	11,411.0	ms	80	ip, vg	12.10	5.60
1591	A	11,413.0	oo, pel ws	80	ic 17.	15	8.19
1591	C	11,515.0	pel ws	88	ic 18.	33	41.83
1591	C	11,528.0	pel ms	90	ic 16.	39	9.04
4575b	A	11,120.0	oo, pel ps	20	vg 8.	56	19.90
4575b	A	11,129.0	oo, pel ps	10	ip, ap, vg	20.73	22.40
4575b	B	11,146.0	onc, pel, oo gs	15	ip, ap	17.68	6.87
4575b	B	11,156.0	onc, oo gs	15	ip, ap, vg	18.22	7.46
4575b	B	11,174.0	onc, pel, oo gs	20	ip, ap, vg	15.25	2.27
4575b	C	11,192.0	pel ws	87	ic 17.	27	42.67

ms=mudstone  
ws=wackestone  
ps=packstone  
gs=grainstone

ip=interparticle  
ap=intraparticle  
vg=vuggy  
ic=intercrystalline  
mo=moldic

*Est - Visually Estimated*  
He - Helium Porosimeter  
Pr - Probe Permeameter

permeabilities were plotted with average log horizontal permeabilities, and no significant difference was observed between vertical and horizontal permeabilities (Figs. 28 and 29). High pressure mercury injection capillary pressure (MICP) analysis was performed on 11 core plugs representative of the pore systems (Table 4). See Figures 30 through 42 for results of the MICP testing.

Porosity and permeability data representative of the pore systems and acquired from the plugs were combined with mercury derived data to compare porosities and permeabilities (Table 5). Helium derived porosity values were found to average 2% higher than the mercury derived values (Figs. 43 and 44). Probe permeability values closely approximate the mercury derived permeabilities, except where the permeability value is below 1 md (Figs. 45 and 46). Capillary pressure permeability correlates with measured probe permeabilities (Fig. 47). Capillary pressure porosity has a high correlation with helium derived porosity values (Fig. 48); however, porosity from core analysis correlates poorly with the mercury and helium derived porosities (Figs. 48 and 49). There is a general relation between porosity and permeability (Fig. 50). See cross plots of porosity and permeability for the range of correlation values between these two parameters (Figs. 51 through 53).

Pore types exhibit general trends to their relation to porosity and median pore throat aperture (Table 6). See Figures 54 through 64 for median pore aperture size distribution for certain depths in well Permits #1591 and 4575B. Median pore throat aperture (MPA) increases with increasing porosity (Fig. 65), and probe permeability and mercury derived permeability strongly correlate with MPA (Fig. 66). The intercrystalline pore system is characterized by the highest porosities.

Capillary pressure data were available for wetting phase (air) saturations. Wetting phase saturation at 77 psia was approximated from its relation with MPA through the equation graphed on Figure 67. No clear relation was observed for entry pressures (displacement pressures) and any parameters. Utilizing a series of equations where porosity, permeability, and capillary radius (=MPA) can be determined, the equation:  $y = \tau = (\phi r^2) / 8k$  was graphed to solve for  $\pi$  or tortuosity

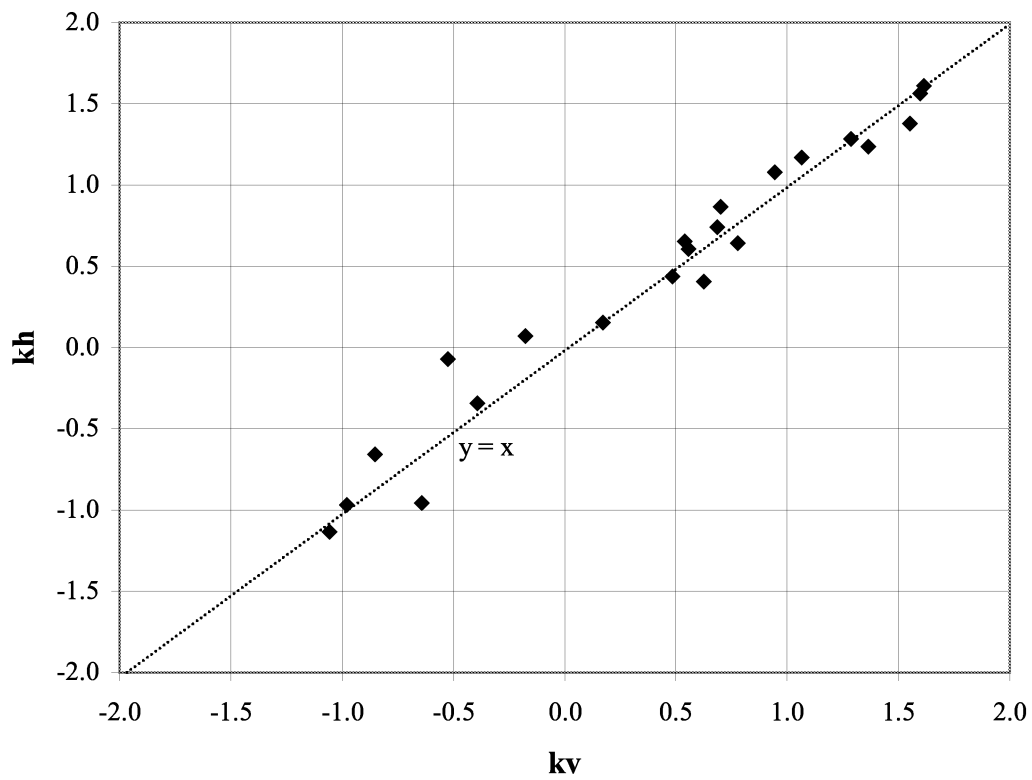


Figure 28. Average log vertical permeability (kv) vs. average log horizontal permeability (kh) measured from the probe permeameter for Well Permit 1591 (from Hopkins, 2002).

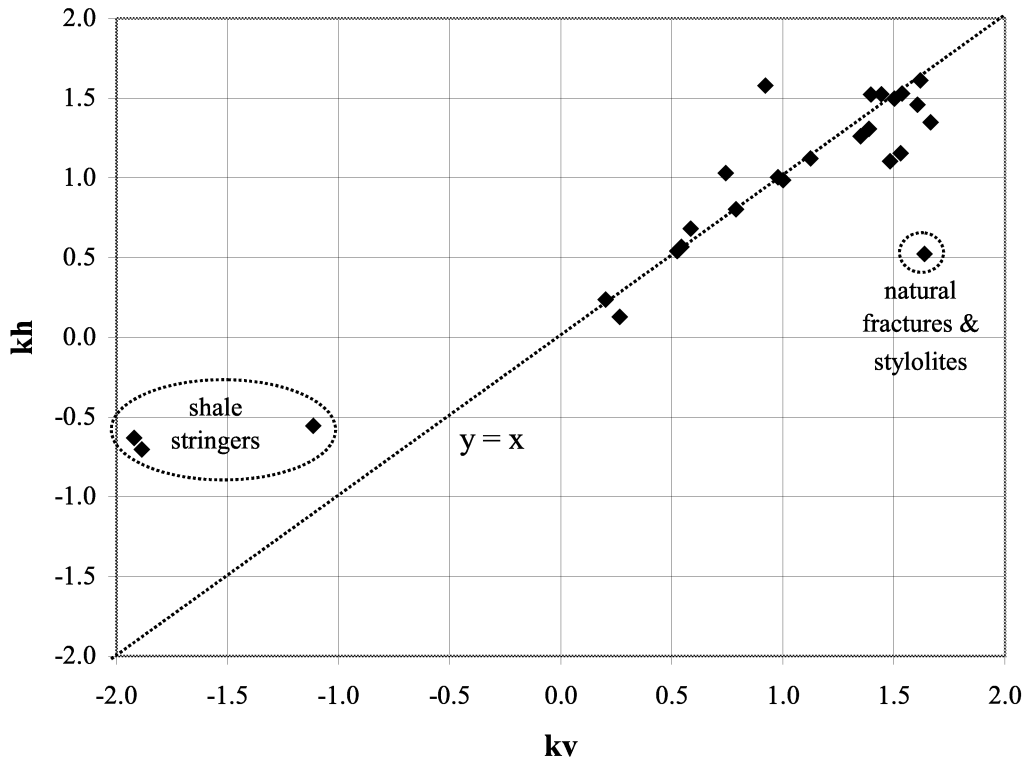


Figure 29. Average log vertical permeability (kv) vs. average log horizontal permeability (kh) measured from the probe permeameter for Well Permit 4575-B (from Hopkins, 2002).

**Table 4. List of mercury injection capillary pressure plugs and associated data (from Hopkins, 2002).**

Permit #	Sample Depth (ft)	Plug #	Core Analysis		Mercury Derived		Median Pore Aperture (μm)	Saturation At End of Initial		Pore Structure
			phi (%)	k (md)	phi (%)	k (md)		Drainage Cycle	Imbibition Cycle	
1591	11,405.0	1	21.52	35.1	19.6	35.3	4.62	3	34	unimodal sharp
	11,411.0	2	12.10	5.6	9.02	0.982	1.07	12	25	unimodal broad
	11,413.0	3	17.15	8.19	15.3	8.83	2.59	7	29	unimodal sharp
	11,515.0	4	18.33	41.8	16.4	34.7	5.20	4	24	unimodal sharp
	11,528.0	5	16.39	9.04	15.0	8.95	2.33	2	52	unimodal sharp
4575b	11,120.0	11	8.56	19.9	2.27	0.021	0.262	44	46	poorly defined
	11,129.0	12	20.73	22.4	18.7	17.8	3.33	3	44	unimodal broad
	11,146.0	14	17.68	6.87	16.6	8.67	2.36	2	37	unimodal sharp
	11,156.0	15	18.22	7.46	15.9	7.19	2.22	4	44	unimodal broad
	11,174.0	16	15.25	2.27	12.9	2.07	1.28	8	40	unimodal broad
	11,192.0	18	17.27	42.3	16.0	49.5	6.75	3	23	unimodal sharp

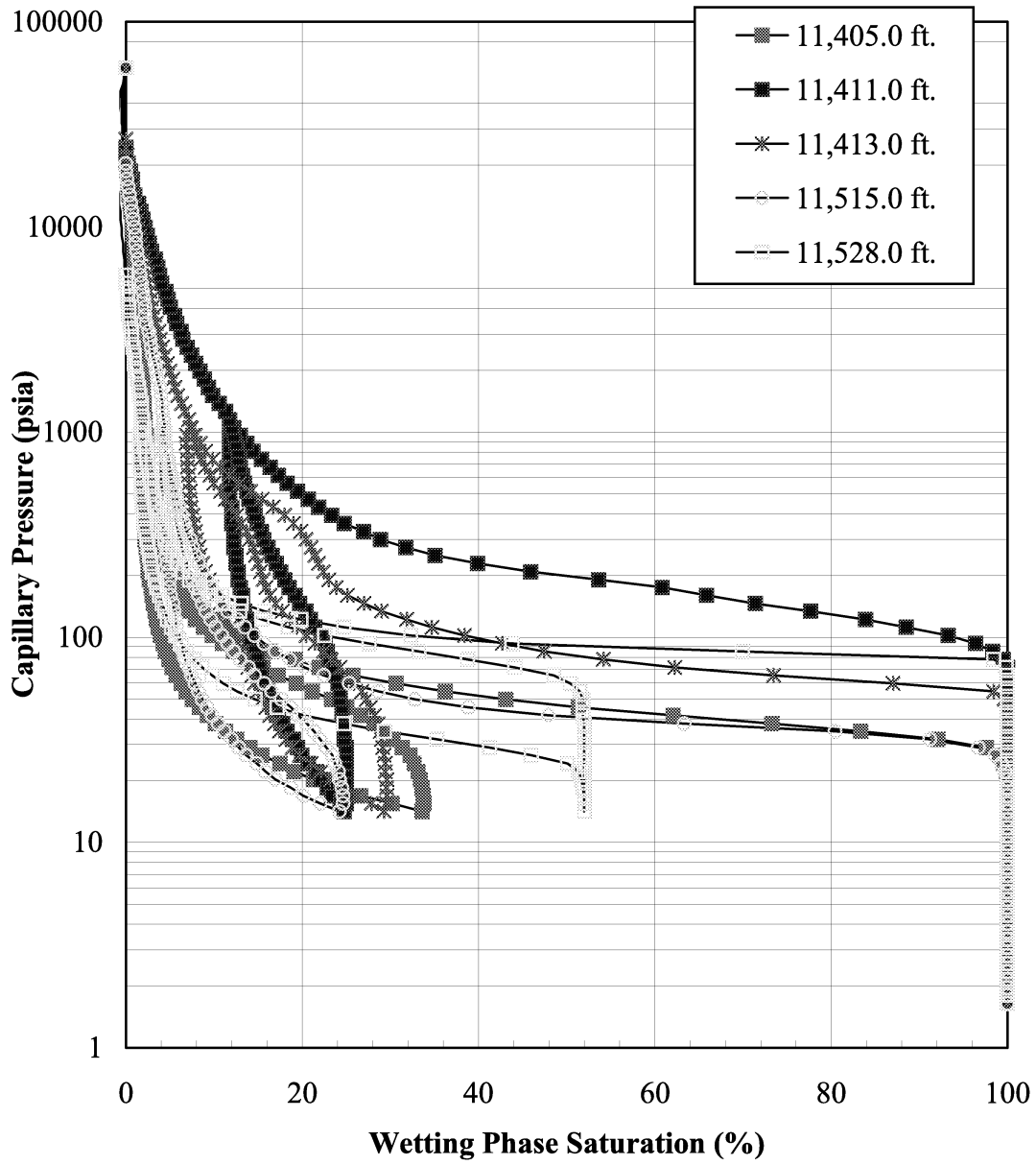


Figure 30. Mercury injection capillary pressure (pore volume) for Well Permit 1591  
(from Hopkins, 2002).

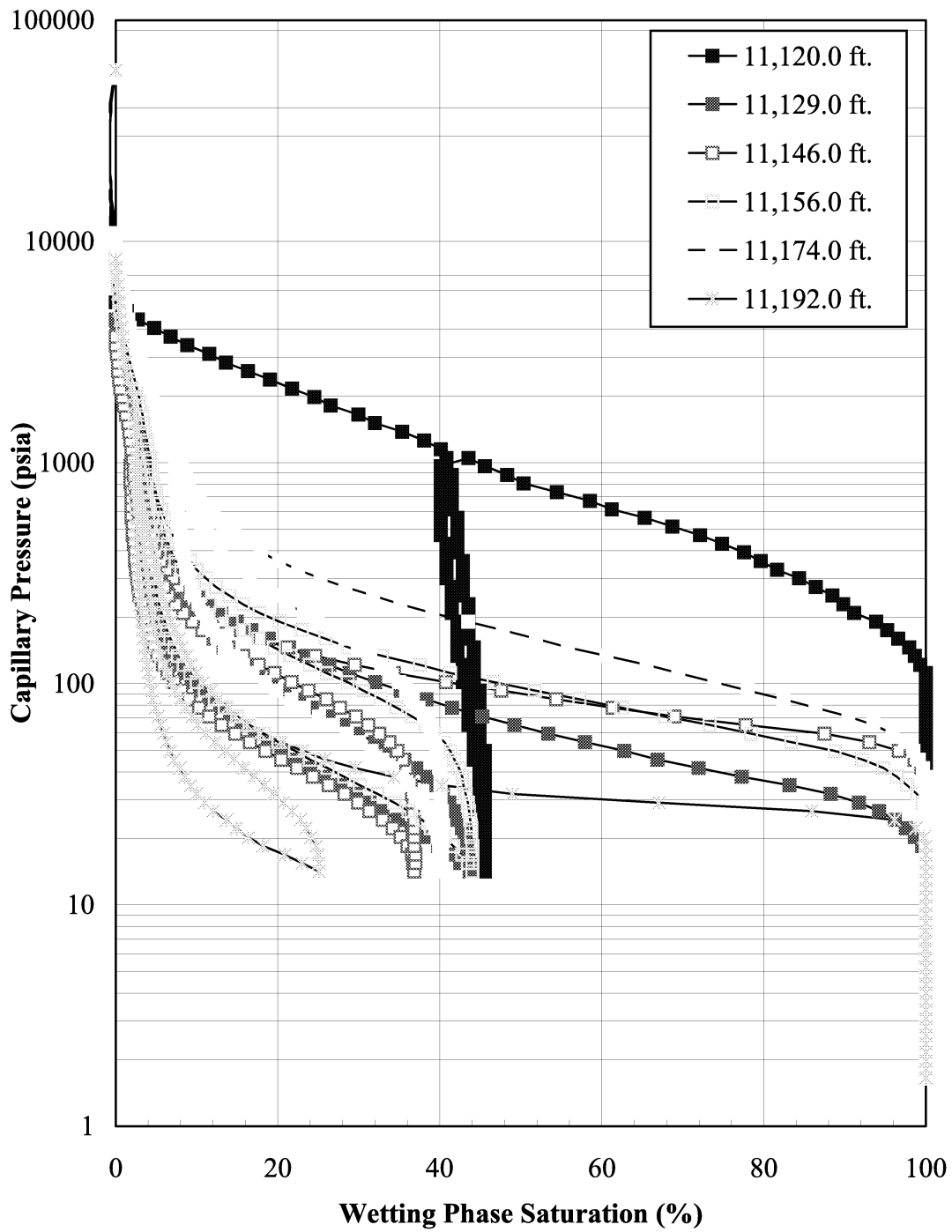


Figure 31. Mercury injection capillary pressure (pore volume) for Well Permit 4575-B  
(from Hopkins, 2002).

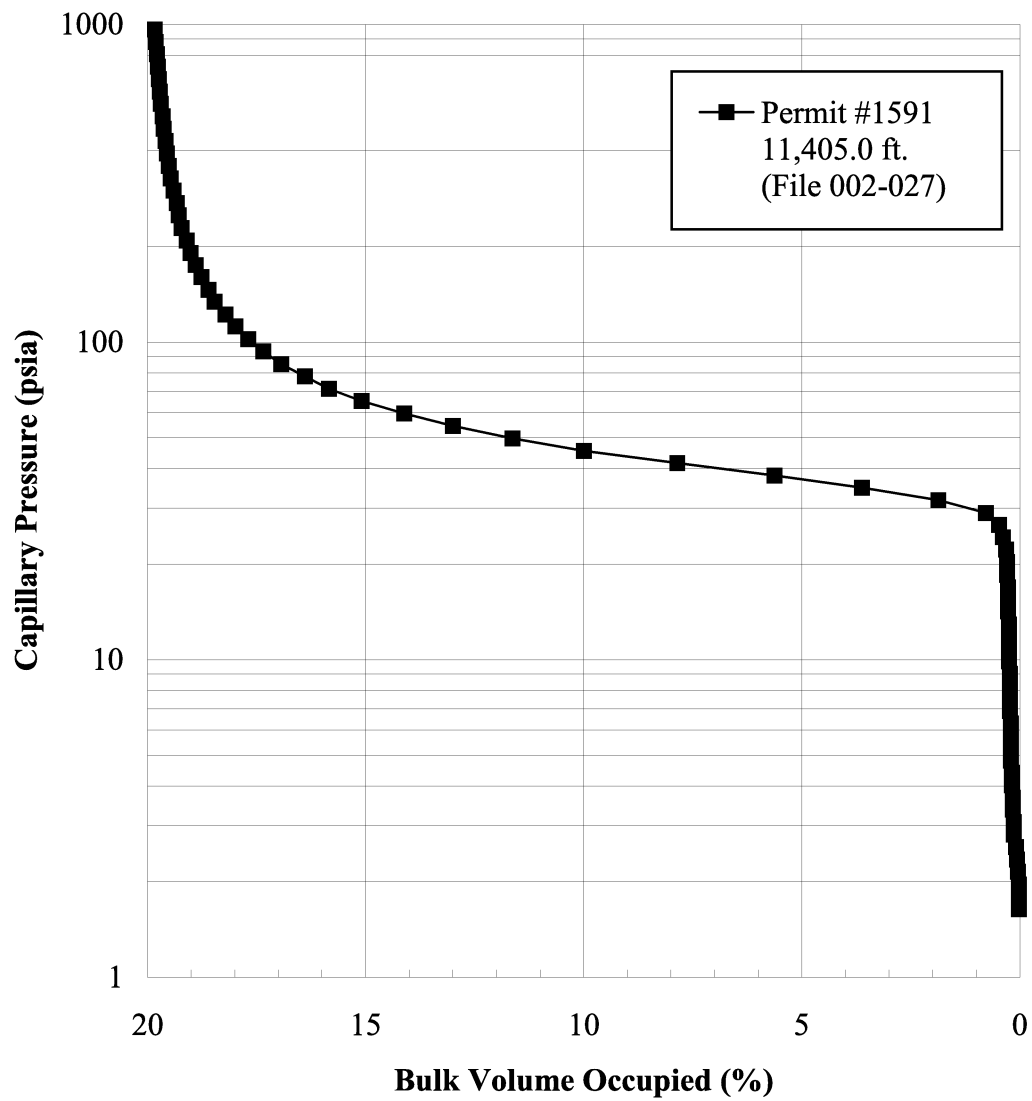


Figure 32. Mercury injection capillary pressure (pore volume) for Well Permit 1591 at 11,405 ft (from Hopkins, 2002).

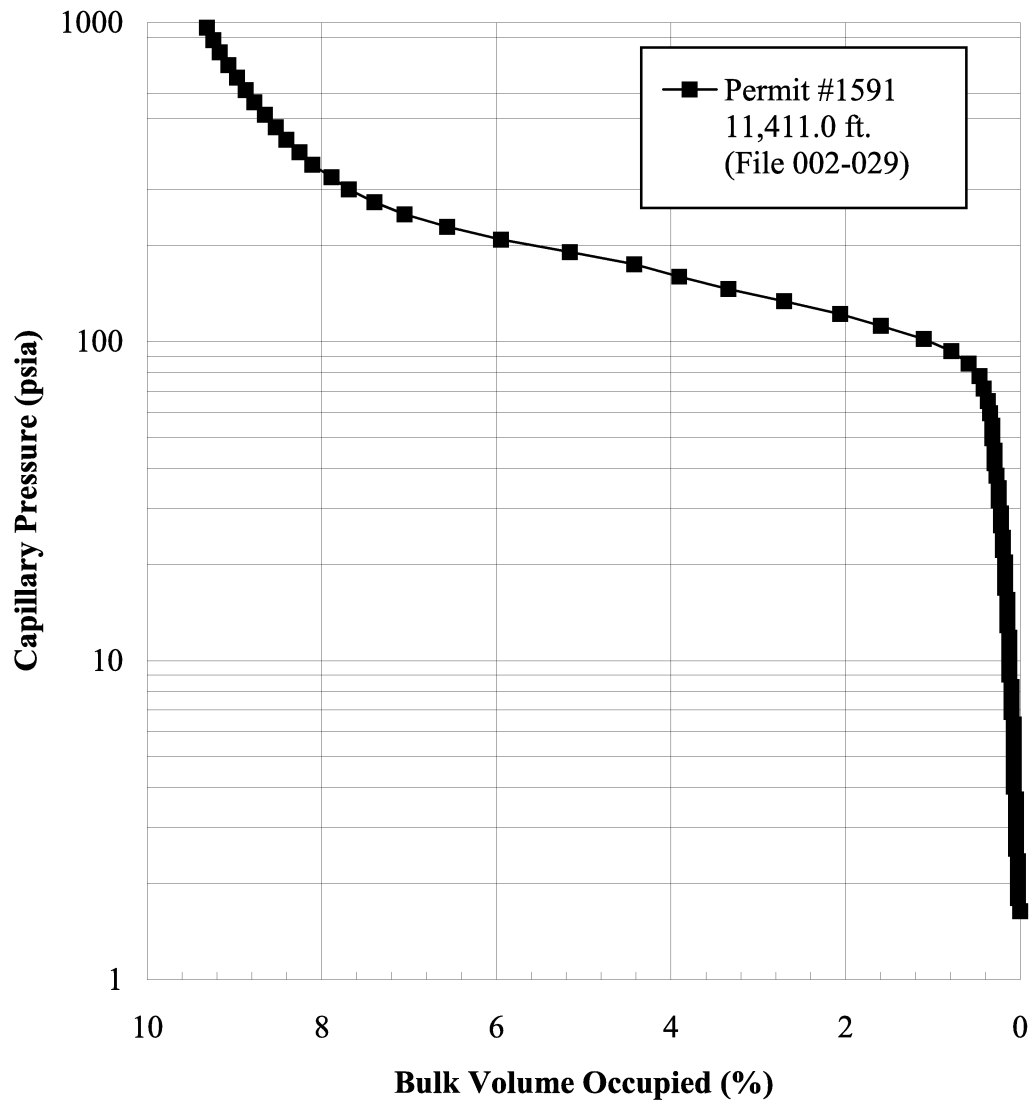


Figure 33. Mercury injection capillary pressure (pore volume) for Well Permit 1591 at 11,411 ft (from Hopkins, 2002).

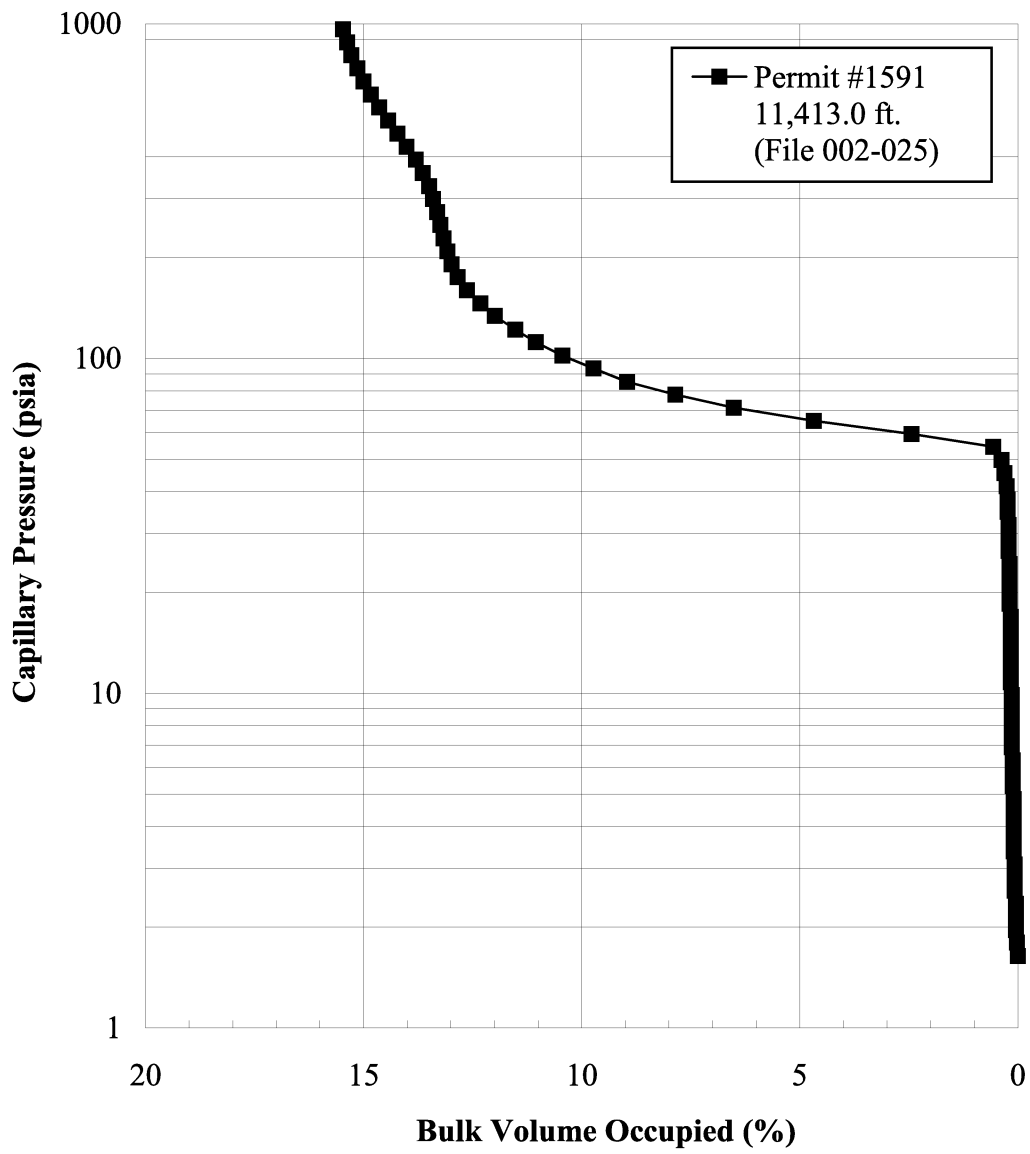


Figure 34. Mercury injection capillary pressure (pore volume) for Well Permit 1591 at 11,413 ft (from Hopkins, 2002).

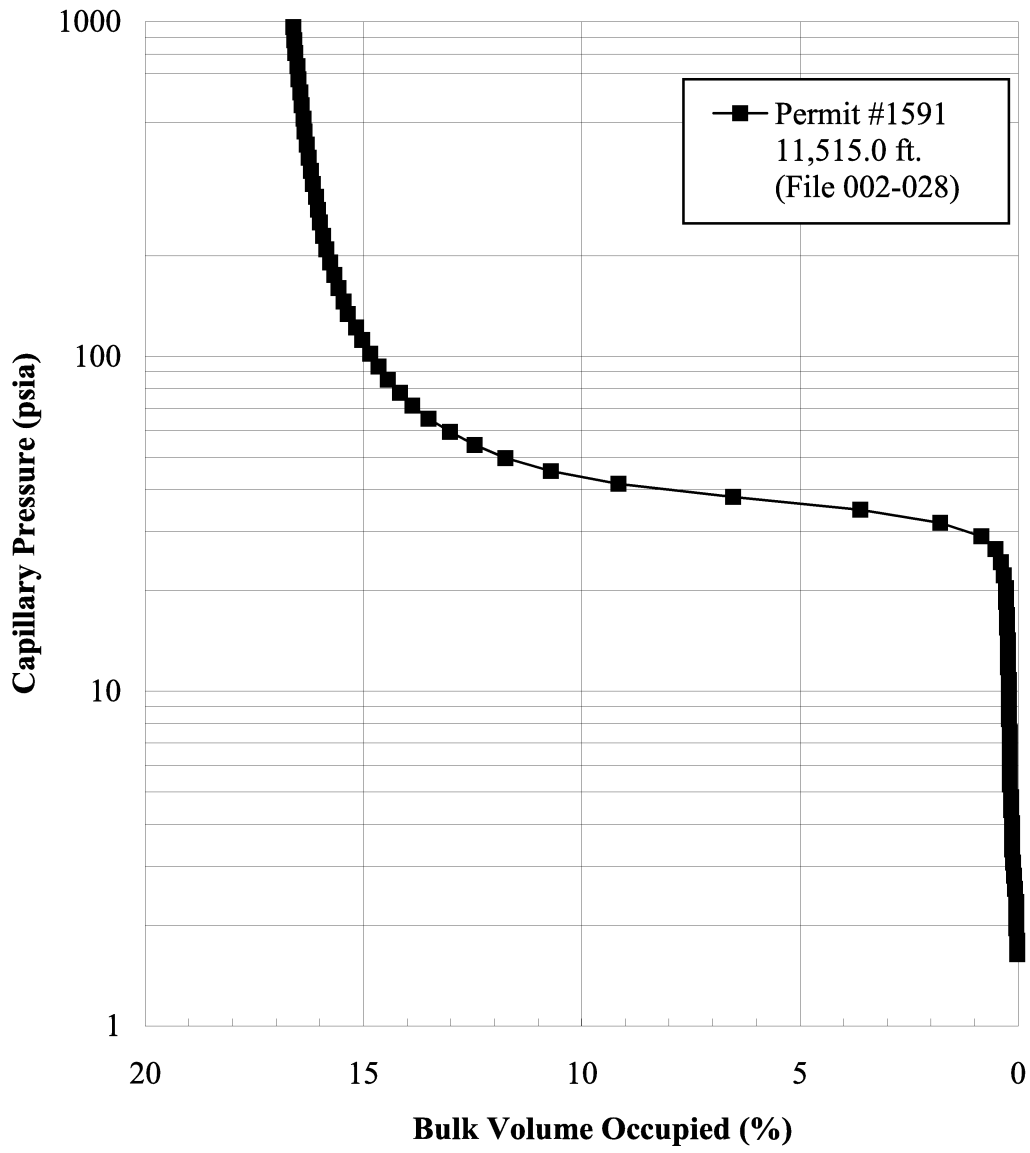


Figure 35. Mercury injection capillary pressure (pore volume) for Well Permit 1591 at 11,515 ft (from Hopkins, 2002).

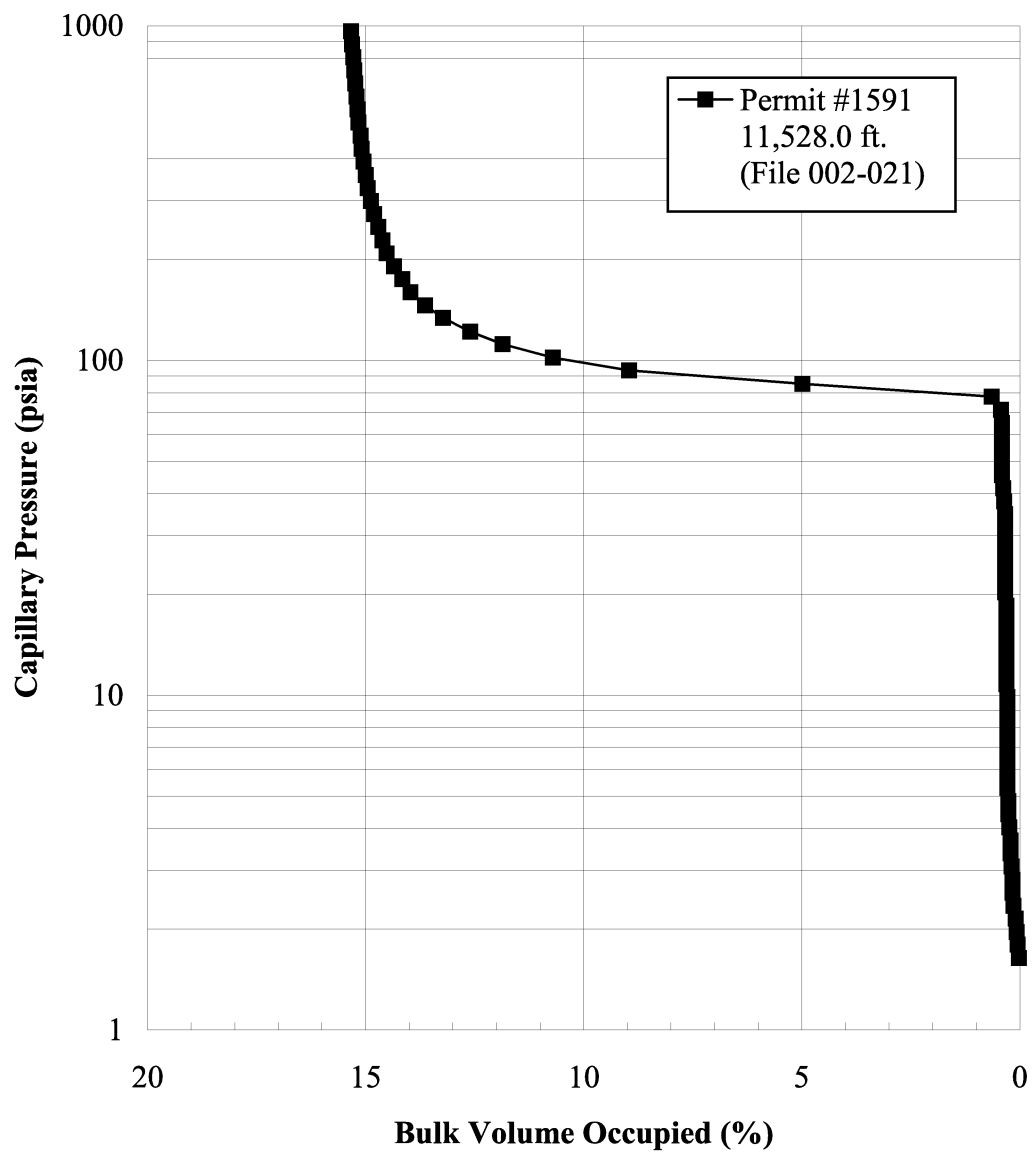


Figure 36. Mercury injection capillary pressure (pore volume) for Well Permit 1591 at 11,528 ft (from Hopkins, 2002).

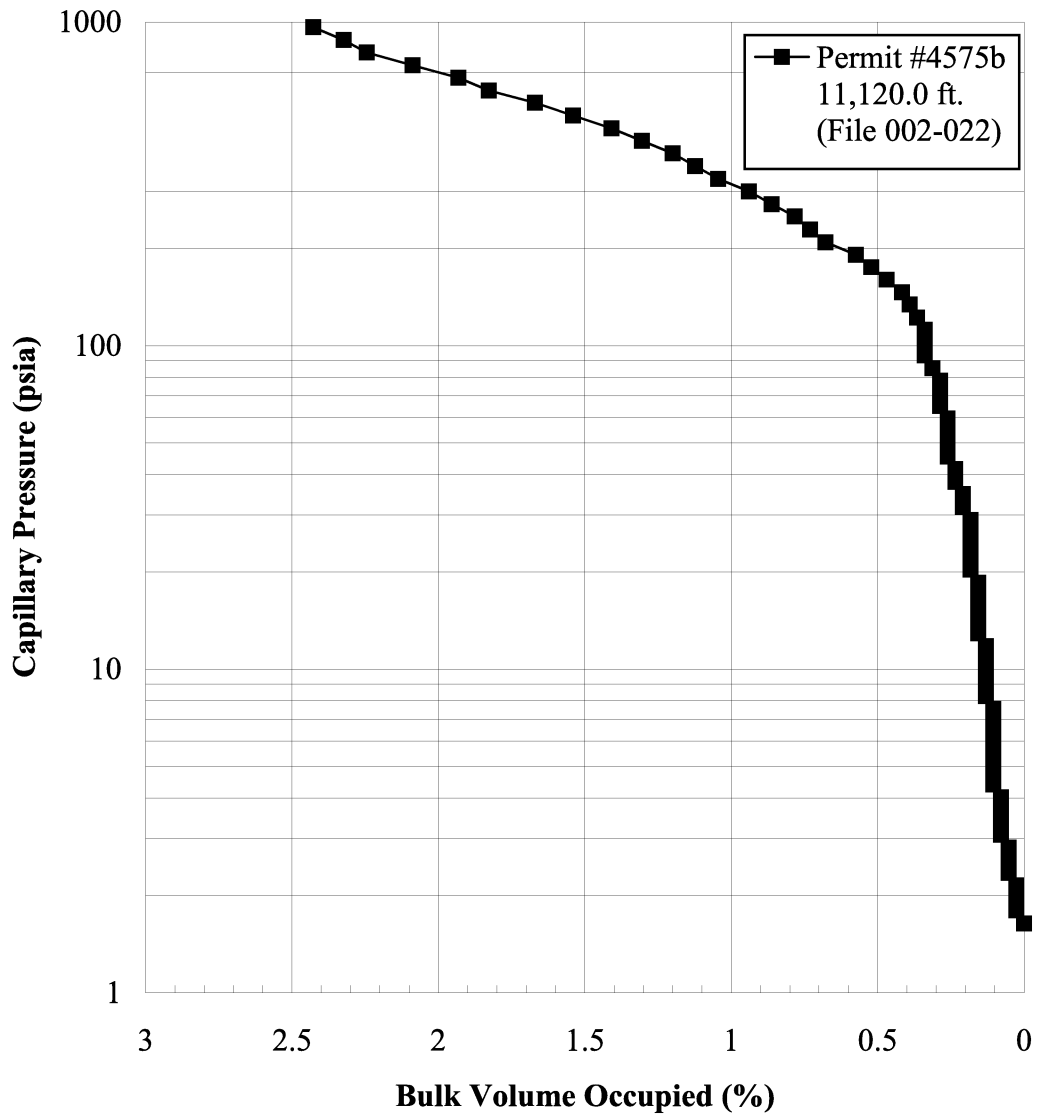


Figure 37. Mercury injection capillary pressure (pore volume) for Well Permit 4575B at 11,120 ft (from Hopkins, 2002).

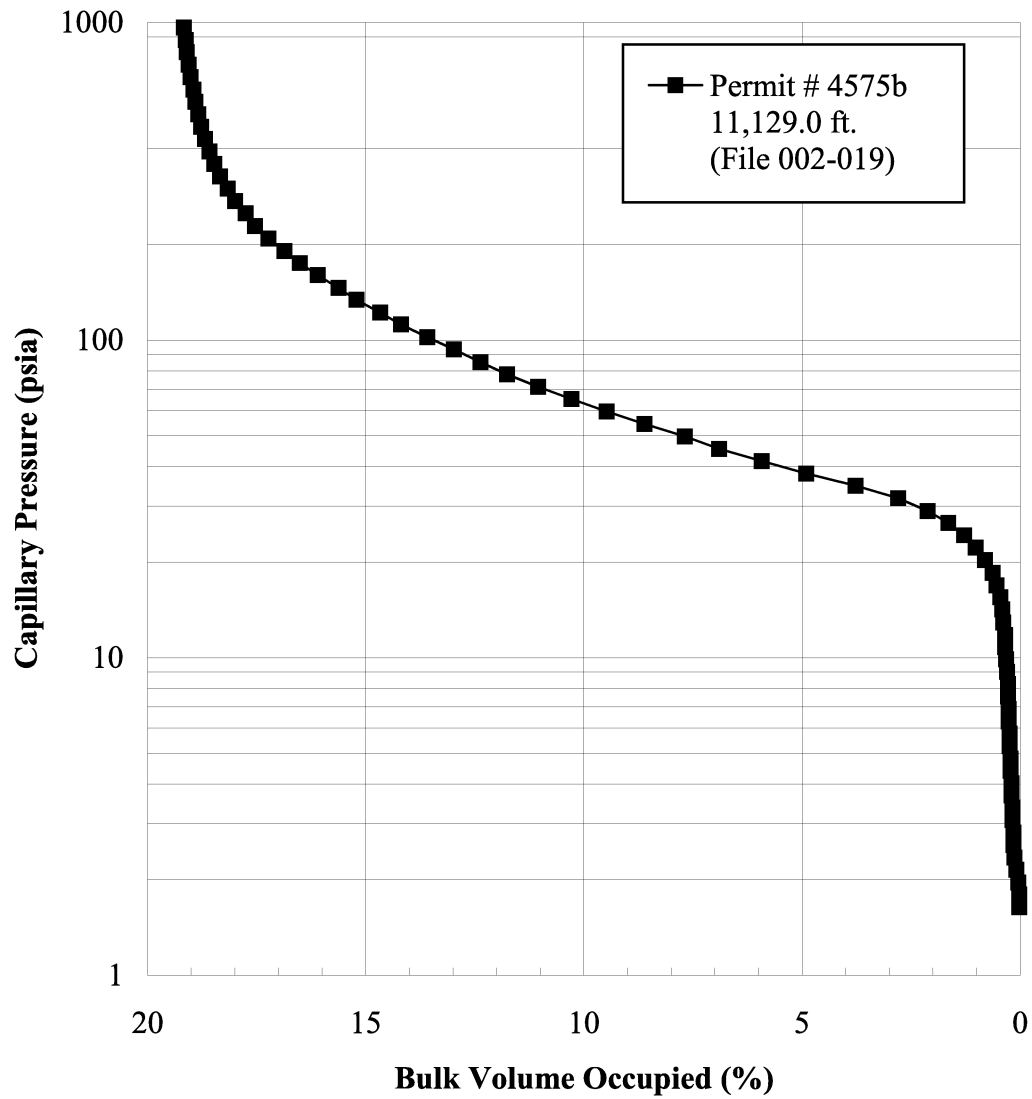


Figure 38. Mercury injection capillary pressure (pore volume) for Well Permit 4575B at 11,129 ft (from Hopkins, 2002).

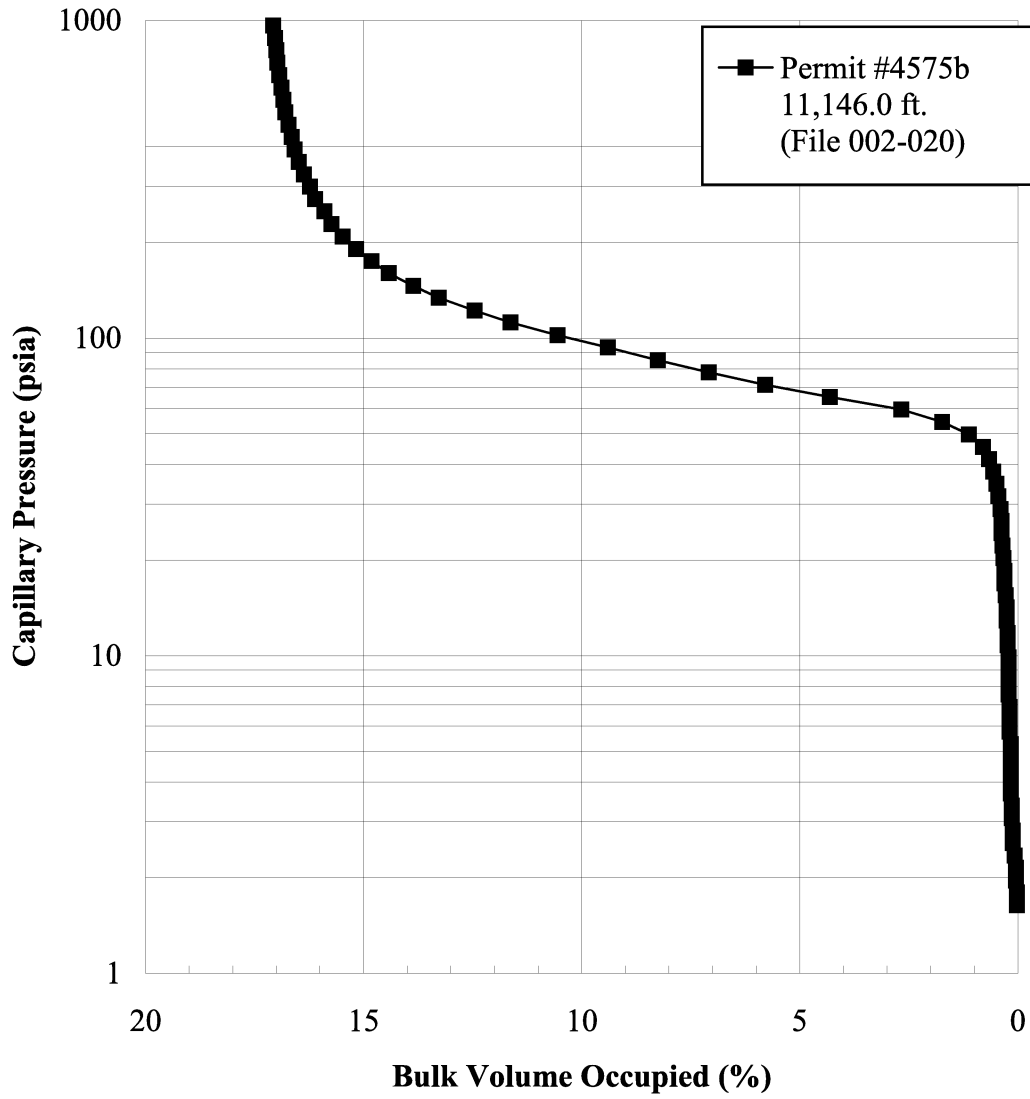


Figure 39. Mercury injection capillary pressure (pore volume) for Well Permit 4575B at 11,146 ft (from Hopkins, 2002).

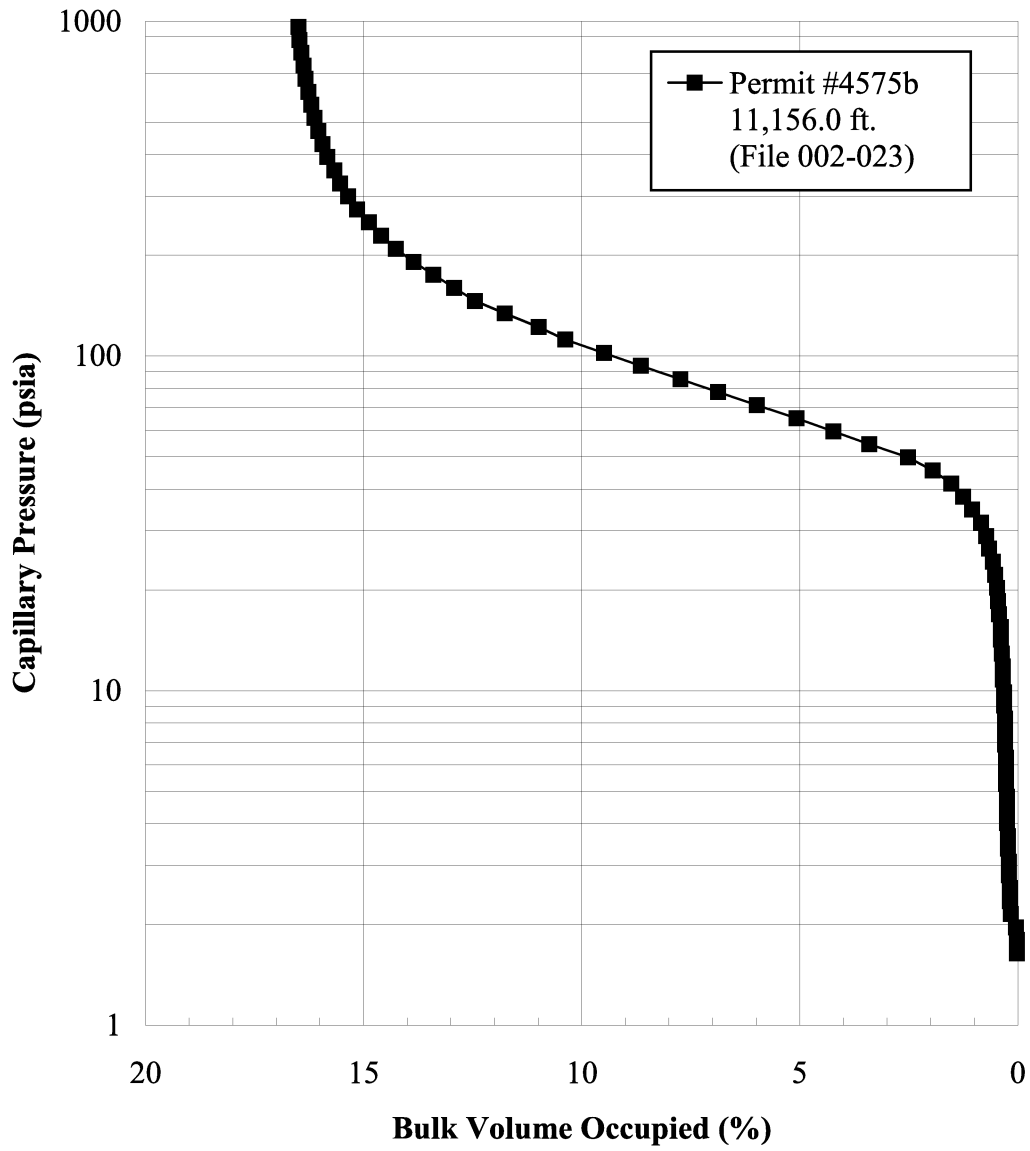


Figure 40. Mercury injection capillary pressure (pore volume) for Well Permit 4575B at 11,156 ft (from Hopkins, 2002).

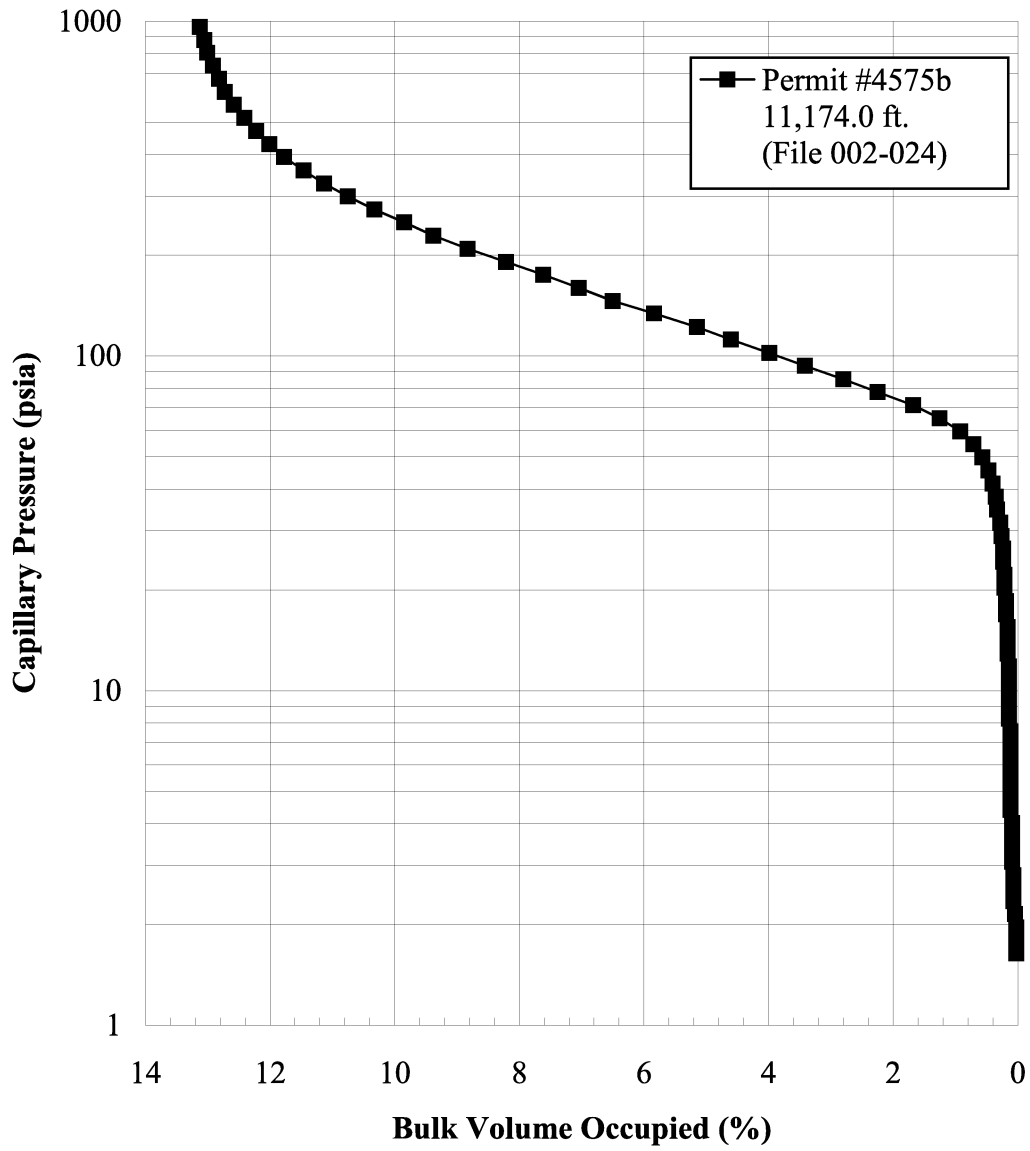


Figure 41. Mercury injection capillary pressure (pore volume) for Well Permit 4575B at 11,174 ft (from Hopkins, 2002).

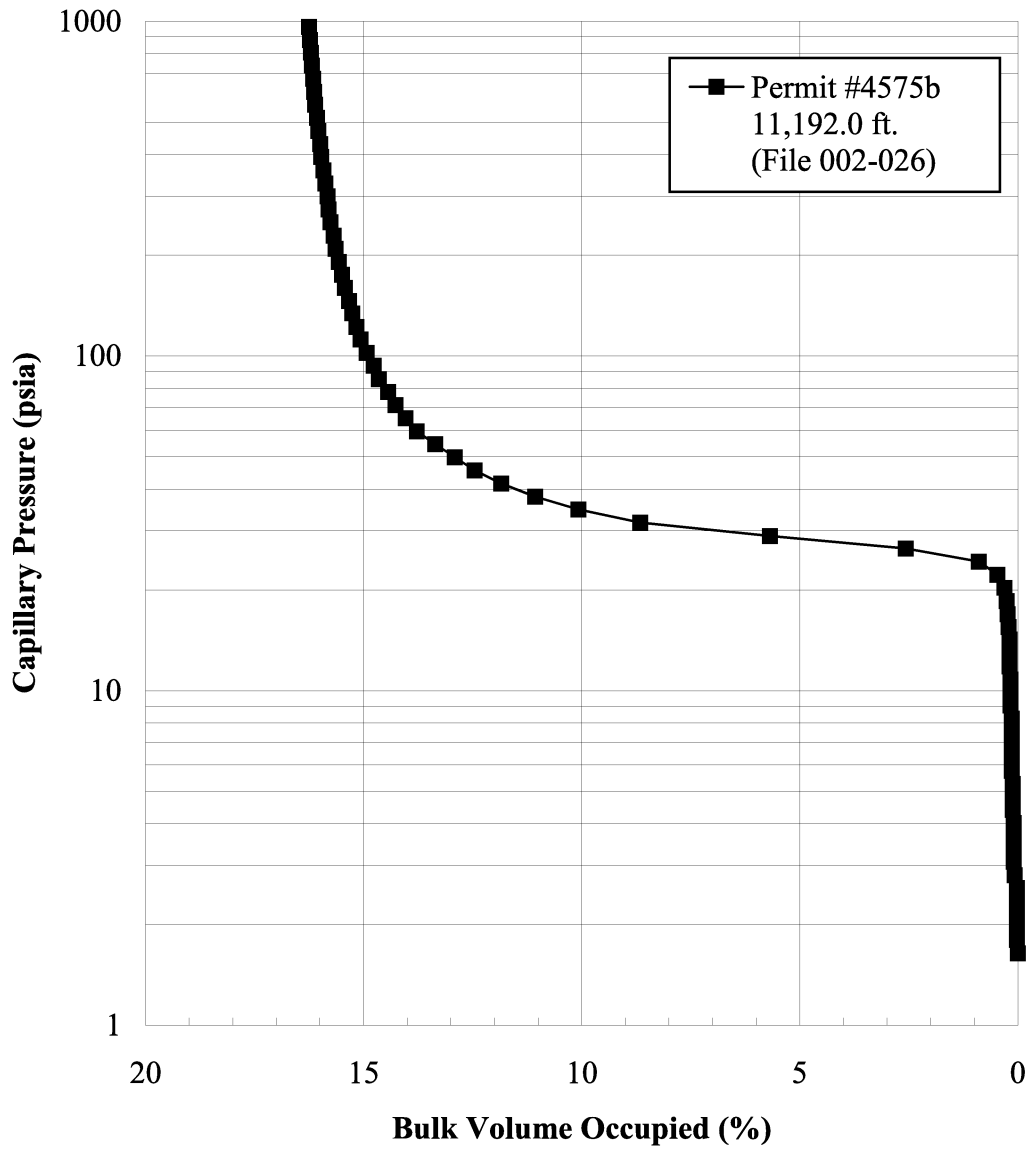


Figure 42. Mercury injection capillary pressure (pore volume) for Well Permit 4575B at 11,192 ft (from Hopkins, 2002).

**Table 5. Plug data: measured values versus mercury (Hg) derived values (from Hopkins, 2002).**

<b>Plug Number</b>	<b>Well Permit #</b>	<b>Core Depth</b>	<b>Pore Types</b>	<b>Hg Median Pore Aperture (μm)</b>	<b>He % Porosity</b>	<b>Hg % Porosity</b>	<b>Pr Permeability (md)</b>	<b>Hg Permeability (md)</b>
1	1591	11,405.0	ic	4.62	21.52	19.6	35.07	35.3
2	1591	11,411.0	ip, vg	1.07	12.10	9.02	5.60	0.98
3	1591	11,413.0	ic	2.59	17.15	15.3	8.19	8.83
4	1591	11,515.0	ic	5.20	18.33	16.4	41.83	34.7
5	1591	11,528.0	ic	2.33	16.39	15.0	9.04	8.95
11	4575b	11,120.0	vg	0.26	8.56	2.27	19.90	0.02
12	4575b	11,129.0	ip, ap, vg	3.33	20.73	18.7	22.40	17.8
14	4575b	11,146.0	ip, ap	2.36	17.68	16.6	6.87	8.67
15	4575b	11,156.0	ip, ap, vg	2.22	18.22	15.9	7.46	7.19
16	4575b	11,174.0	ip, ap, vg	1.28	15.25	12.9	2.27	2.07
18	4575b	11,192.0	ic	6.75	17.27	16.0	42.67	49.5

ic=intercrystalline    Hg - Mercury Derived  
ip=interparticle        He - Helium Porosimeter  
vg=vuggy                Pr - Probe Permeameter  
ap=intraparticle

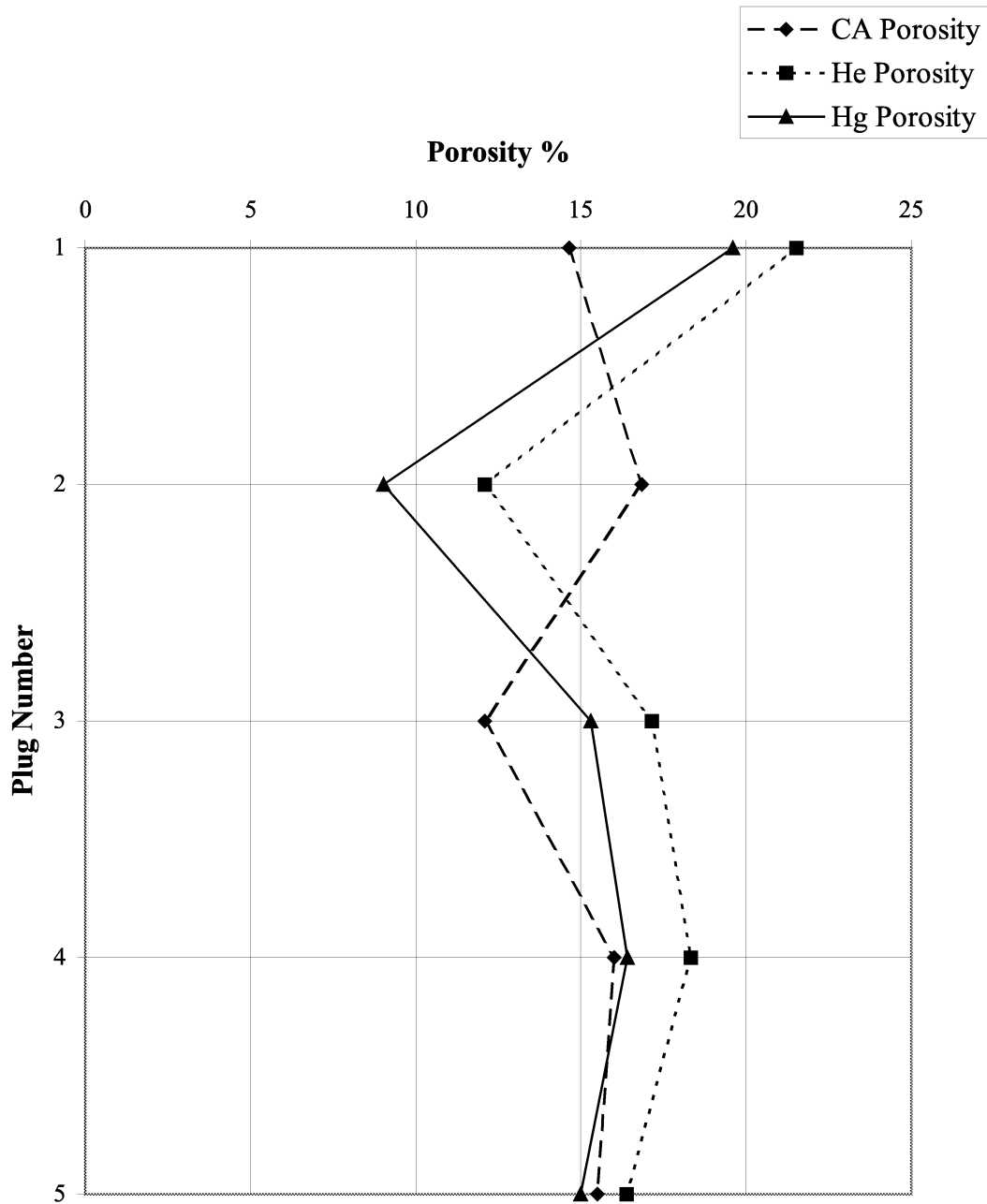


Figure 43. Comparison of porosities derived from various tests for Well Permit 1591. CA=core analysis, He=helium derived, Hg=mercury derived (from Hopkins, 2002).

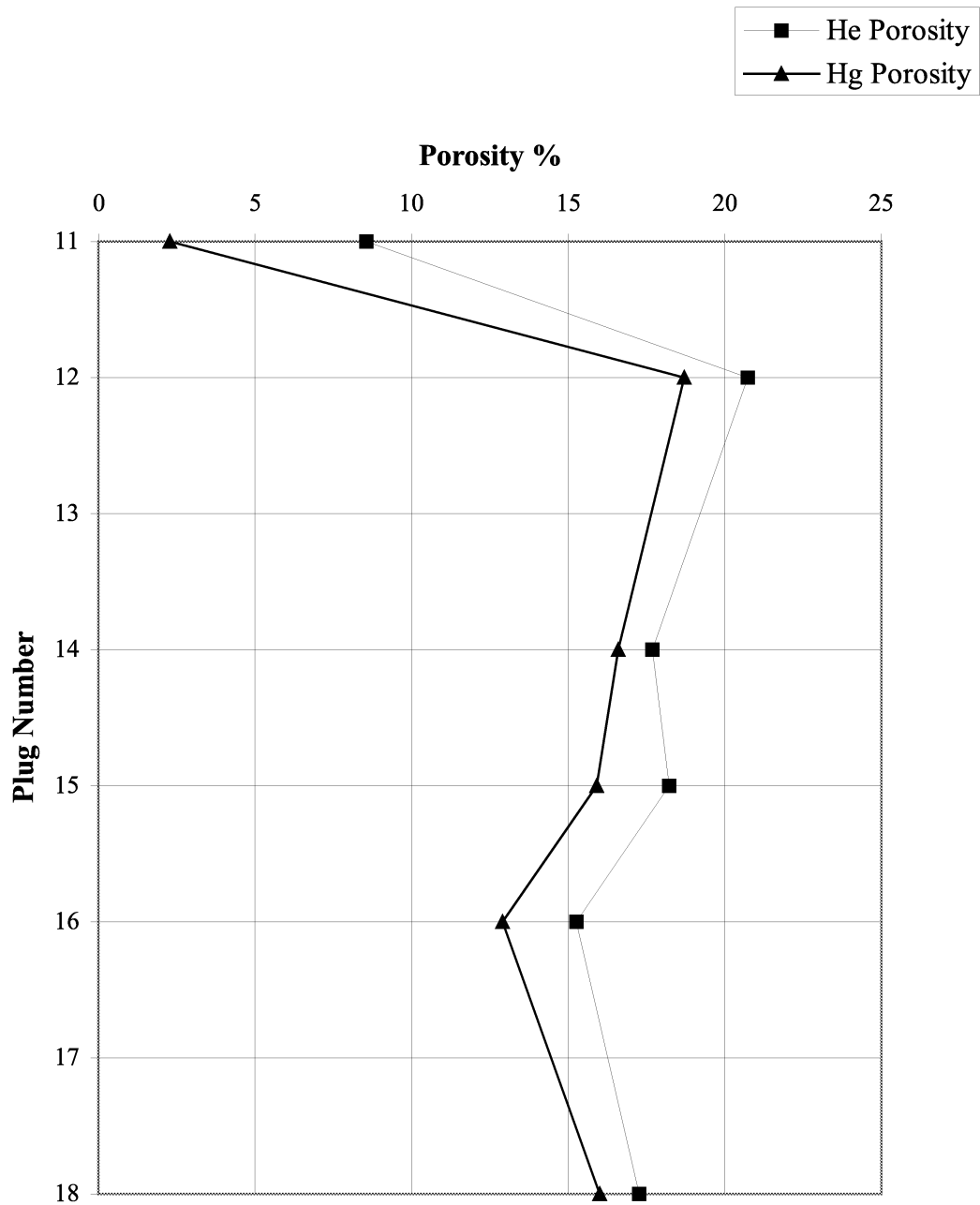


Figure 44. Comparison of porosities derived from various tests for Well Permit 4547B. CA=core analysis, He=helium derived, Hg=mercury derived (from Hopkins, 2002).

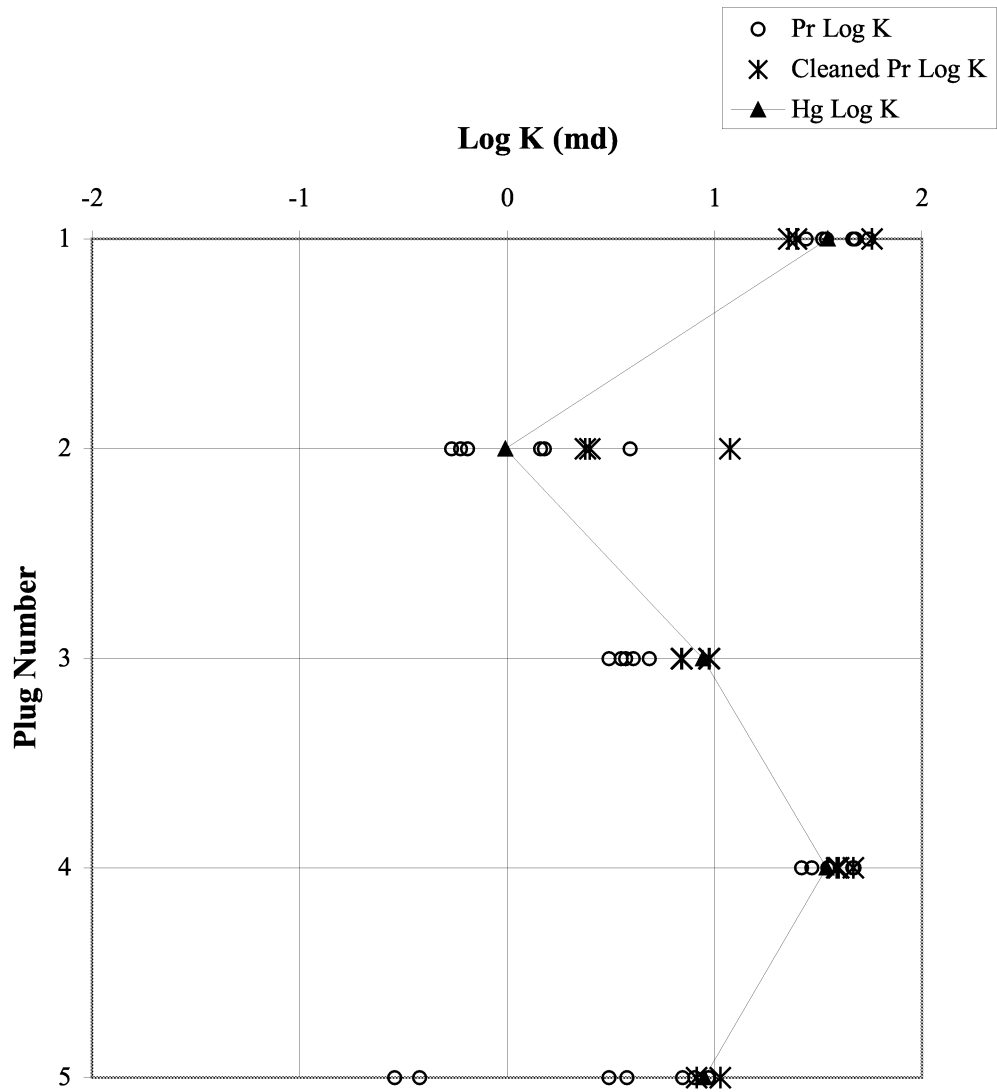


Figure 45. Comparison of log permeabilities derived from various tests for Well Permit 1591 (from Hopkins, 2002).

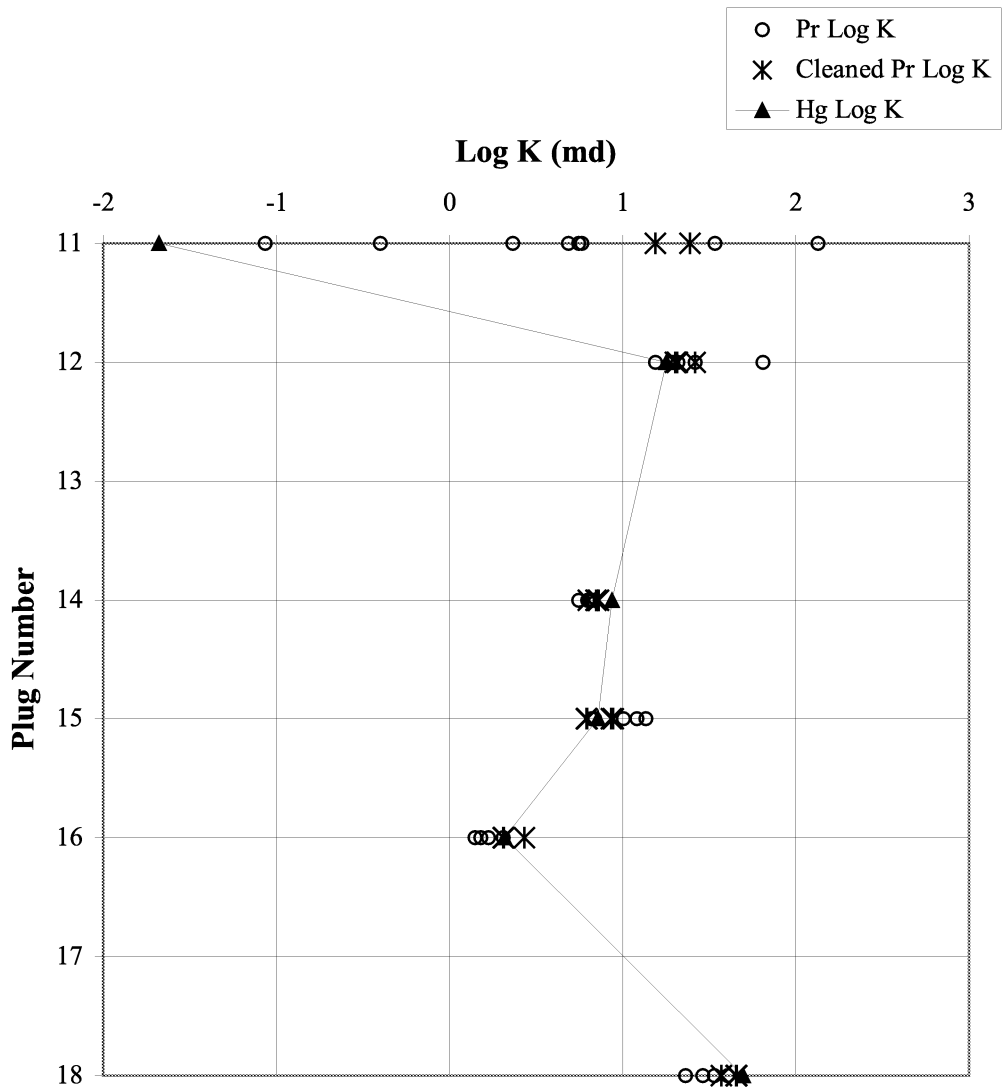


Figure 46. Comparison of log permeabilities derived from various tests for Well Permit 4575B (from Hopkins, 2002).

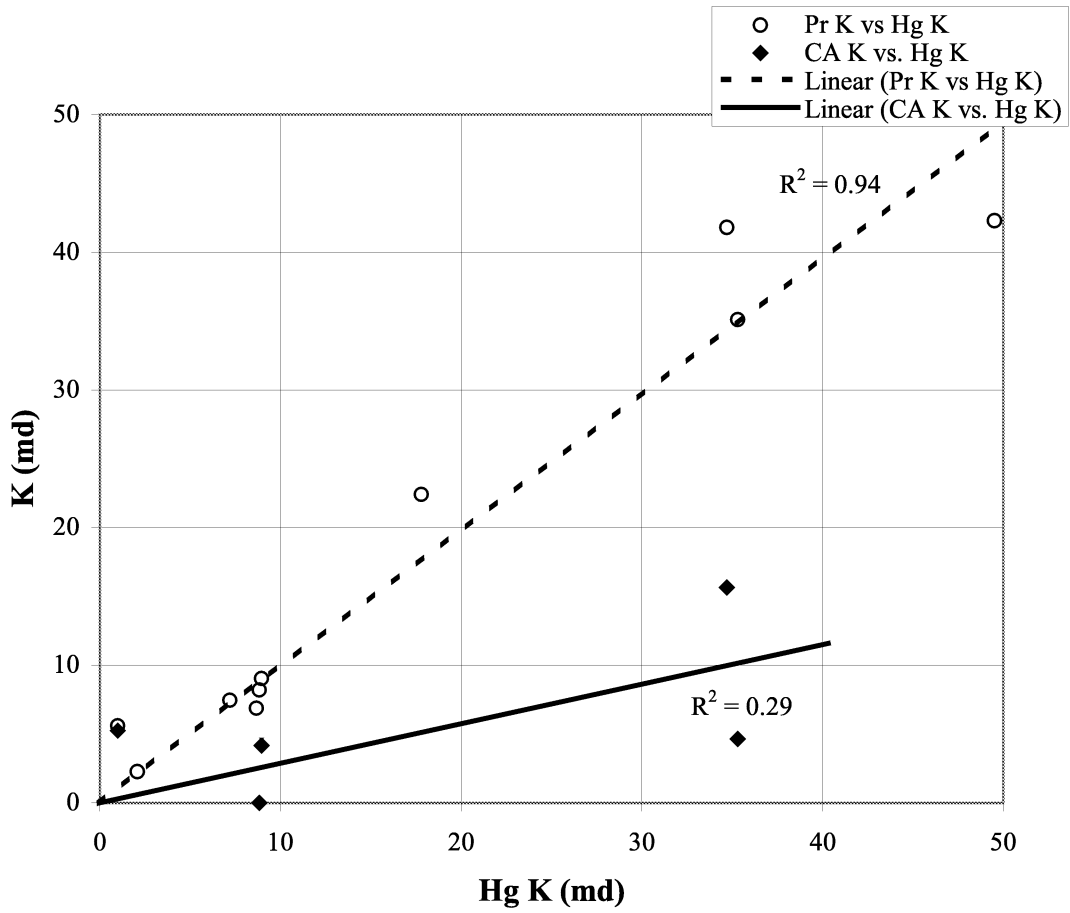


Figure 47. Comparison of mercury derived (Hg), core analysis (CA), and probe permeability (Pr) data (from Hopkins, 2002).

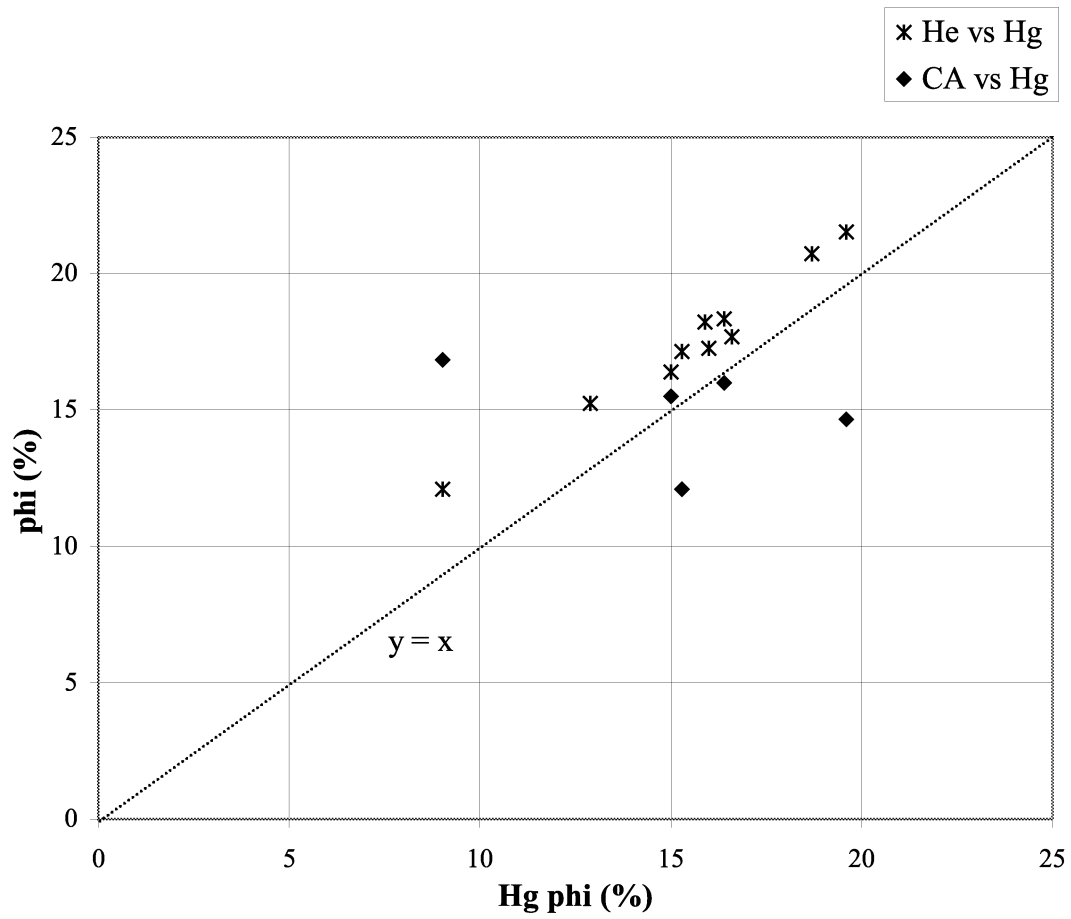


Figure 48. Comparison of helium and core analysis porosities with mercury (capillary pressure) porosity (from Hopkins, 2002).

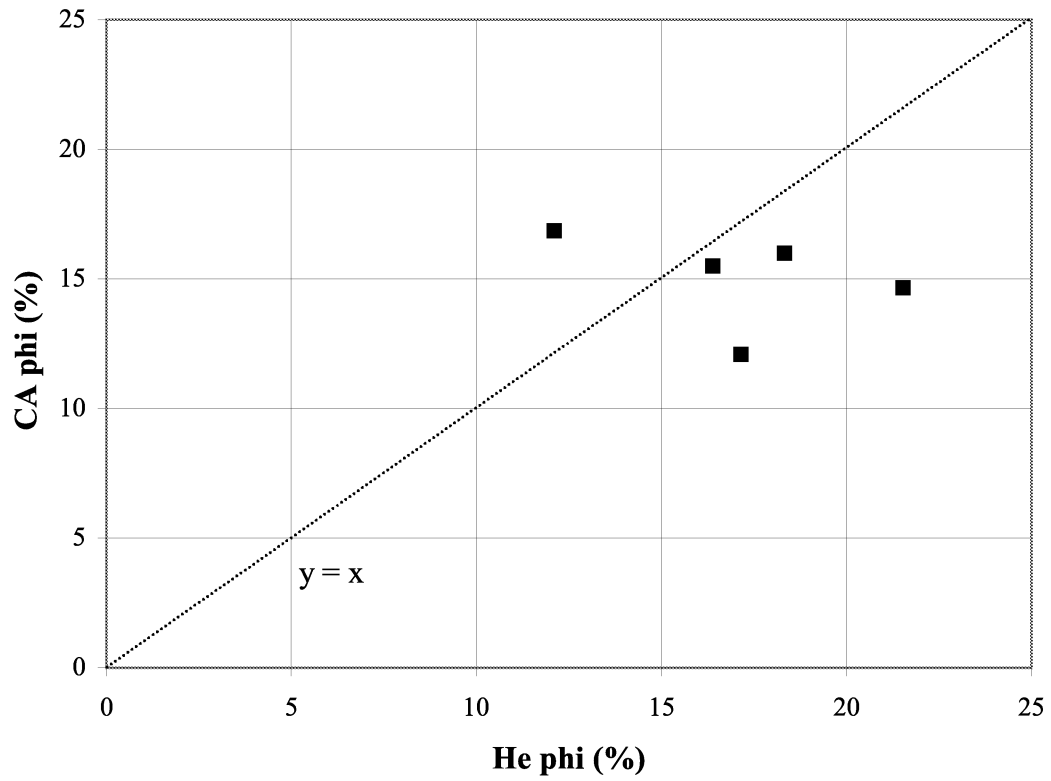


Figure 49. Comparison of core analysis porosity and helium porosity (from Hopkins, 2002).



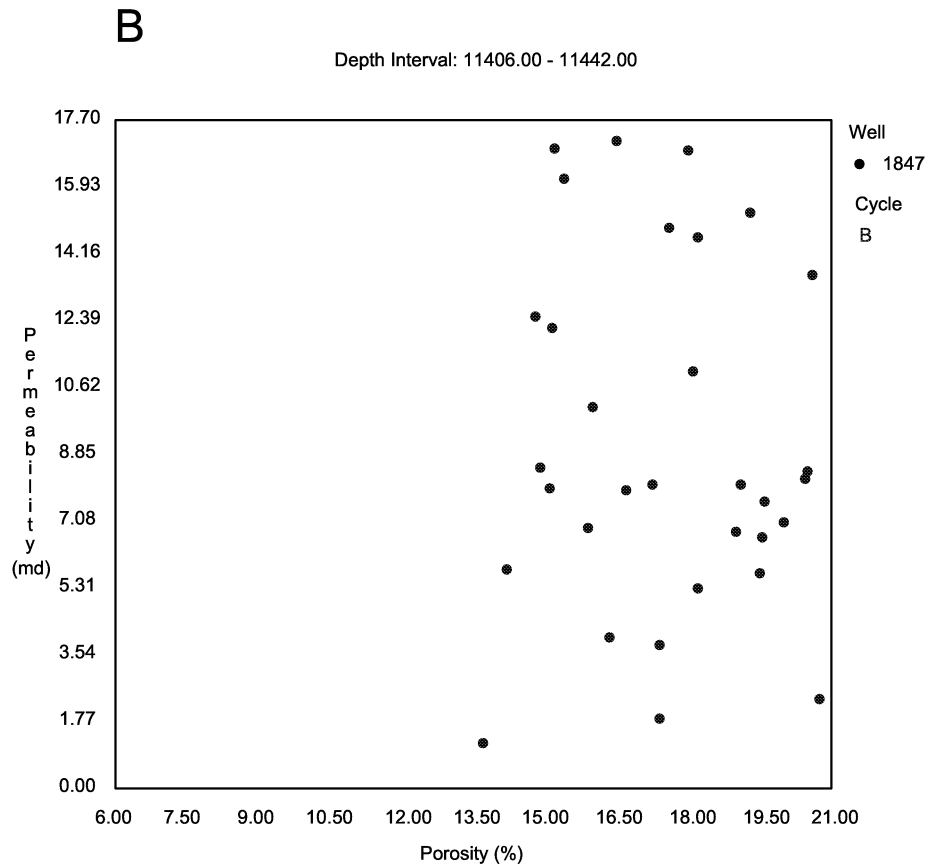
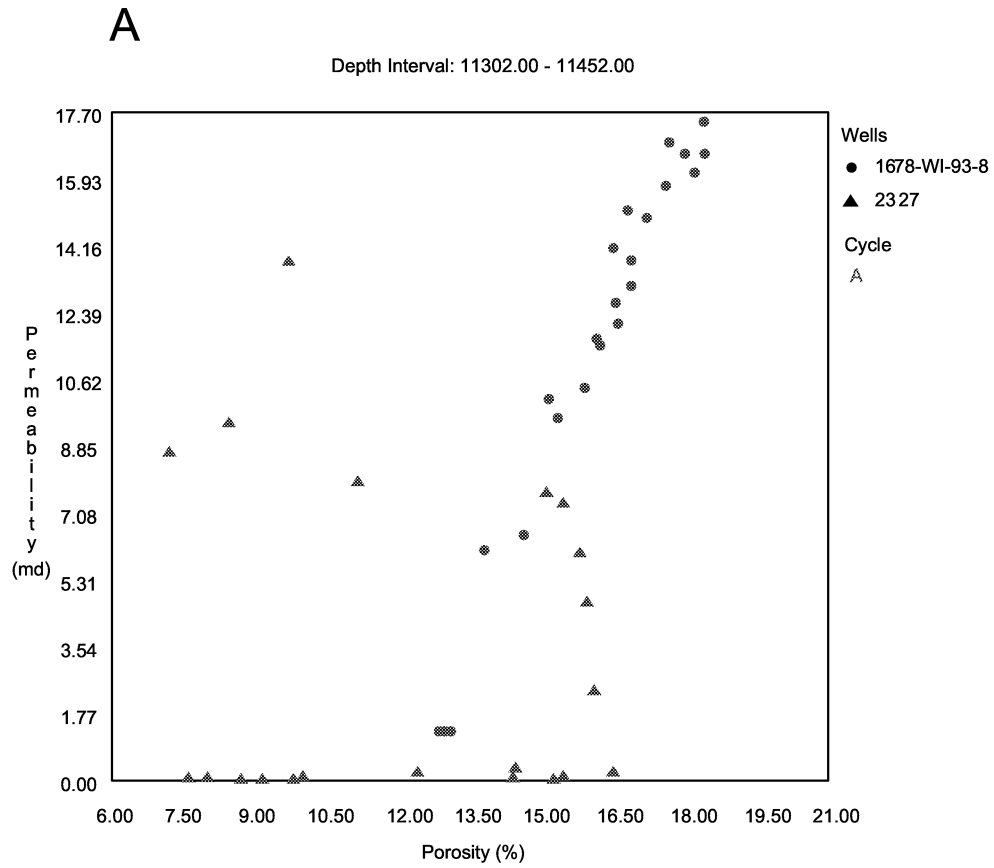


Figure 51. Porosity vs. permeability plots for: (A) Cycle A for wells, Permit # 1678, high production well and Permit #2327, low production well, (B) Cycle B for well, Permit #1847.

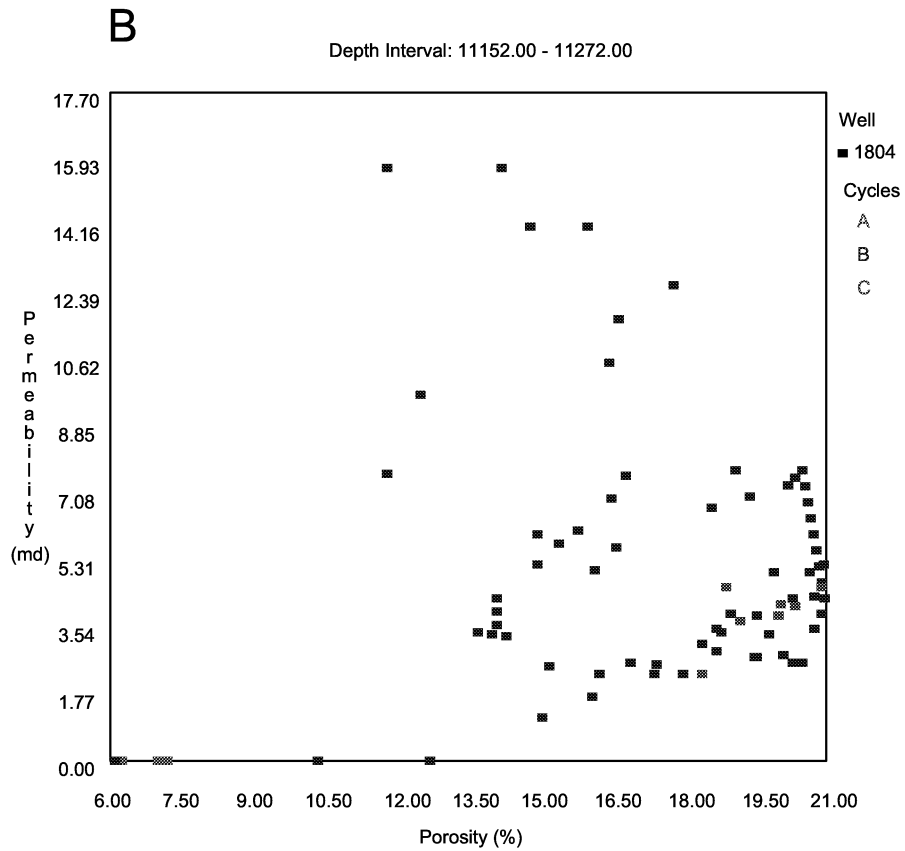
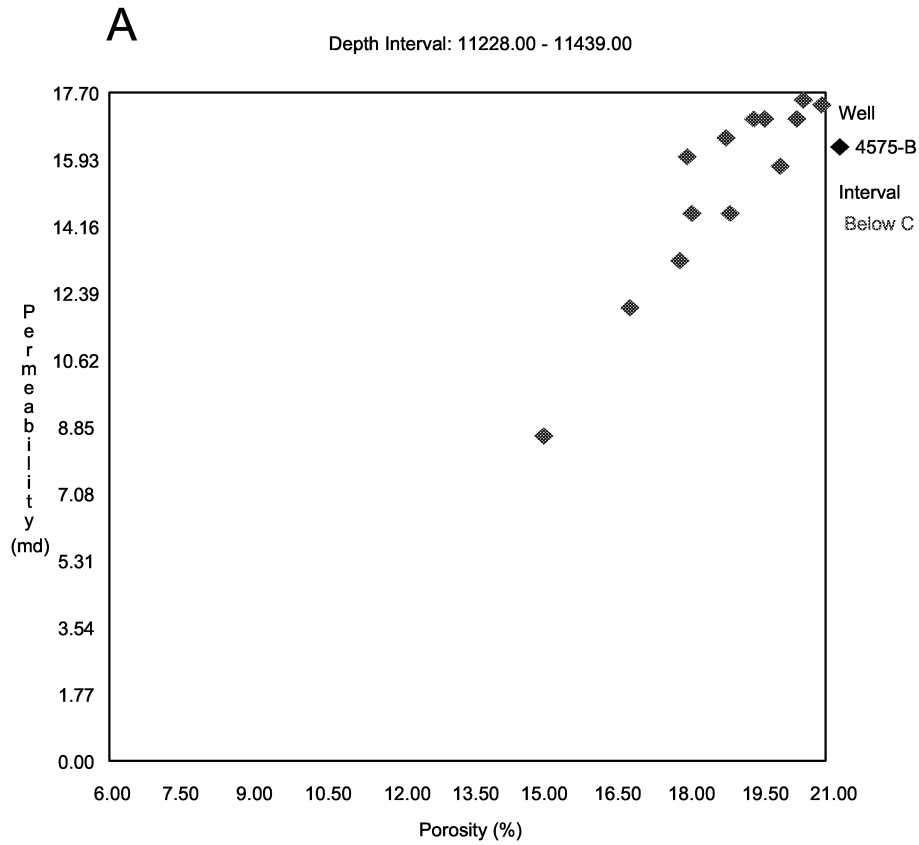


Figure 52. Porosity vs. permeability plots for: (A) Interval immediately below Cycle C for well Permit #4575B, (B) Cycles A, B, and C for well, Permit #1804.

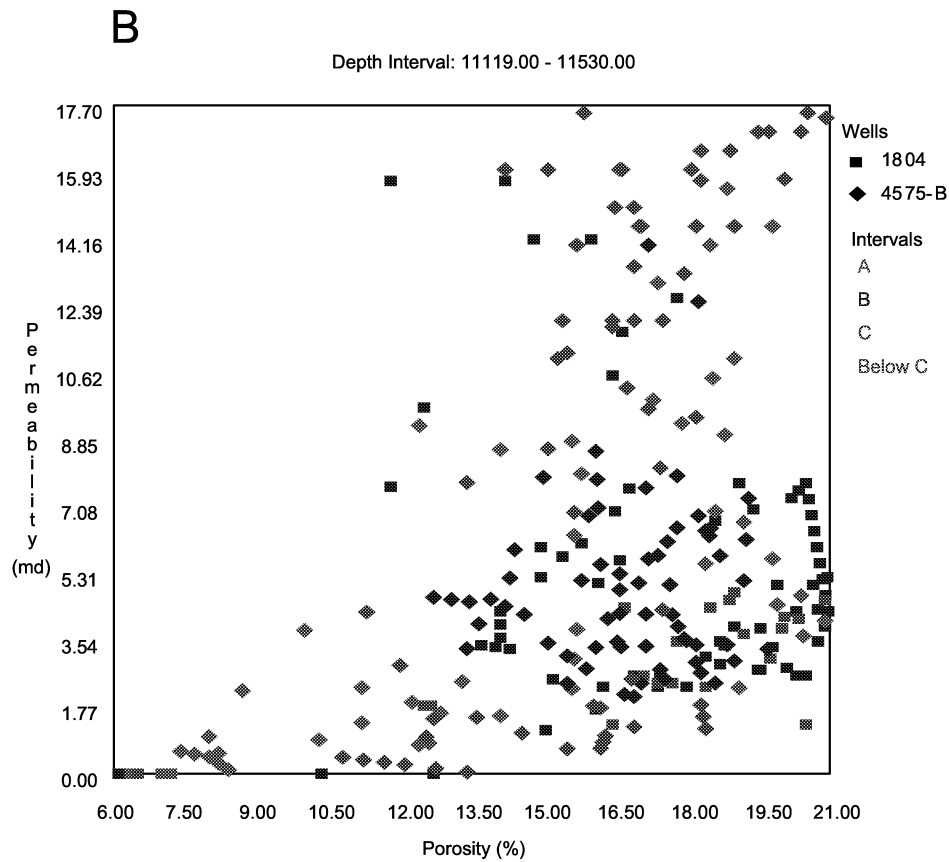
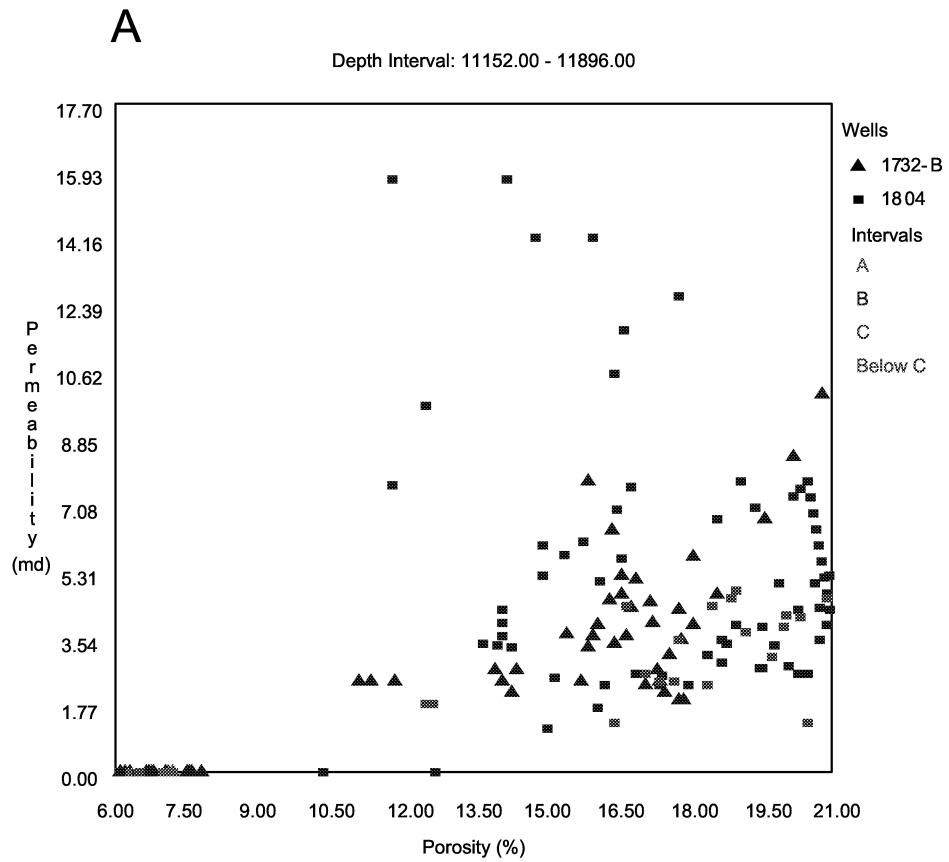


Figure 53. Porosity vs. permeability plots for: (A) Cycles A, B, C and interval immediately below Cycle C for wells, Permit #1732B and Permit #1804, and (B) Cycles A, B, C and interval immediately below Cycle C for wells, Permit #1804 and Permit #4575B. See Figure 8 for location of wells.

**Table 6. Common pore type associations in the mercury injection capillary pressure sample set, with the average porosity and median pore throat aperture (from Hopkins, 2002).**

<b>Common Pore Type Associations</b>	<b>Average Sample Porosities (%)</b>	<b>Average MPA (<math>\mu\text{m}</math>)</b>
intercrystalline 1	6.5	4.3
interparticle, intraparticle, moldic	16.3	2.3
interparticle, intraparticle	15.8	2.3
interparticle, vuggy	9.0	1.1
channel, vuggy	2.3	0.3

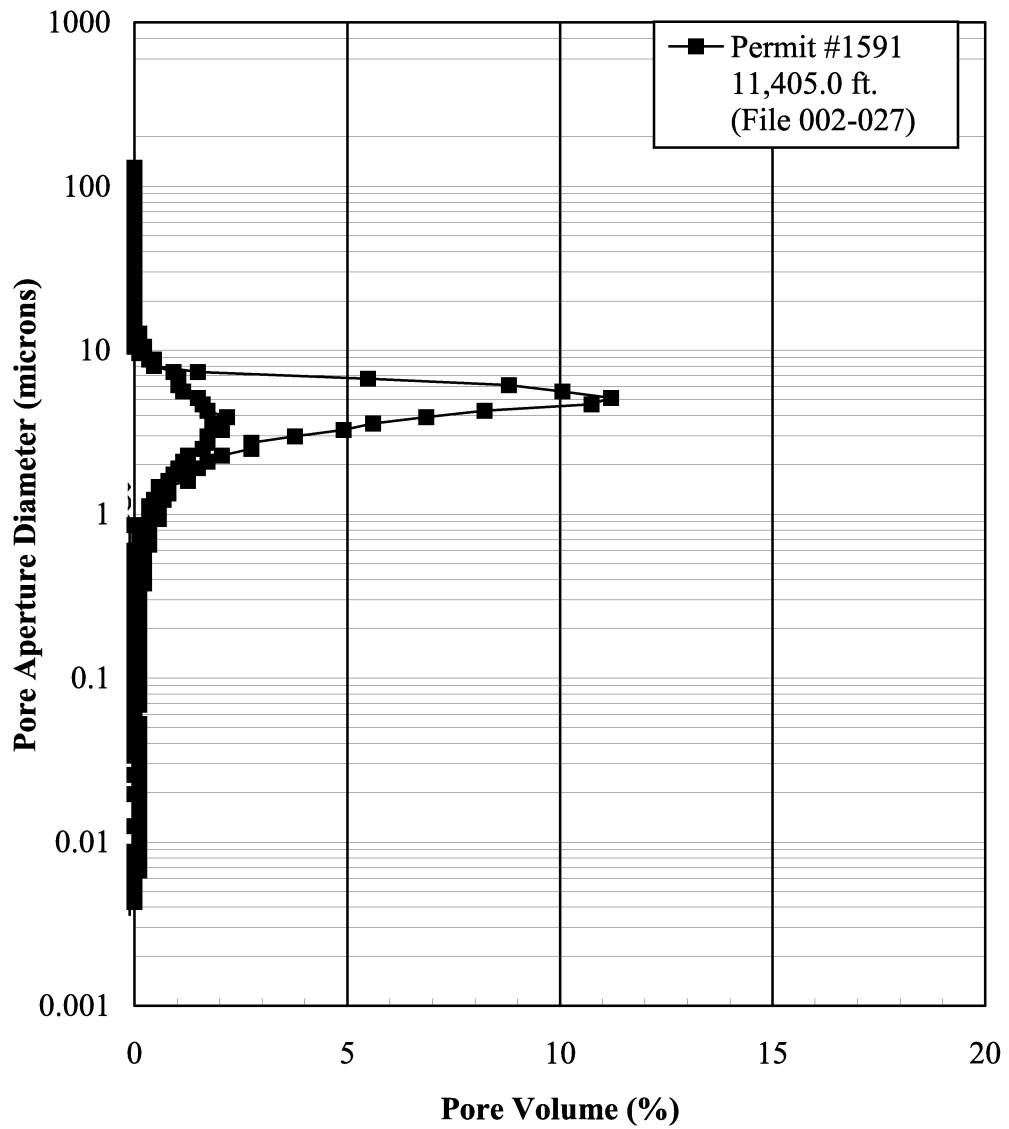


Figure 54. Pore aperture size distribution for Well Permit 1591 at 11,405 ft.

(from Hopkins, 2002).

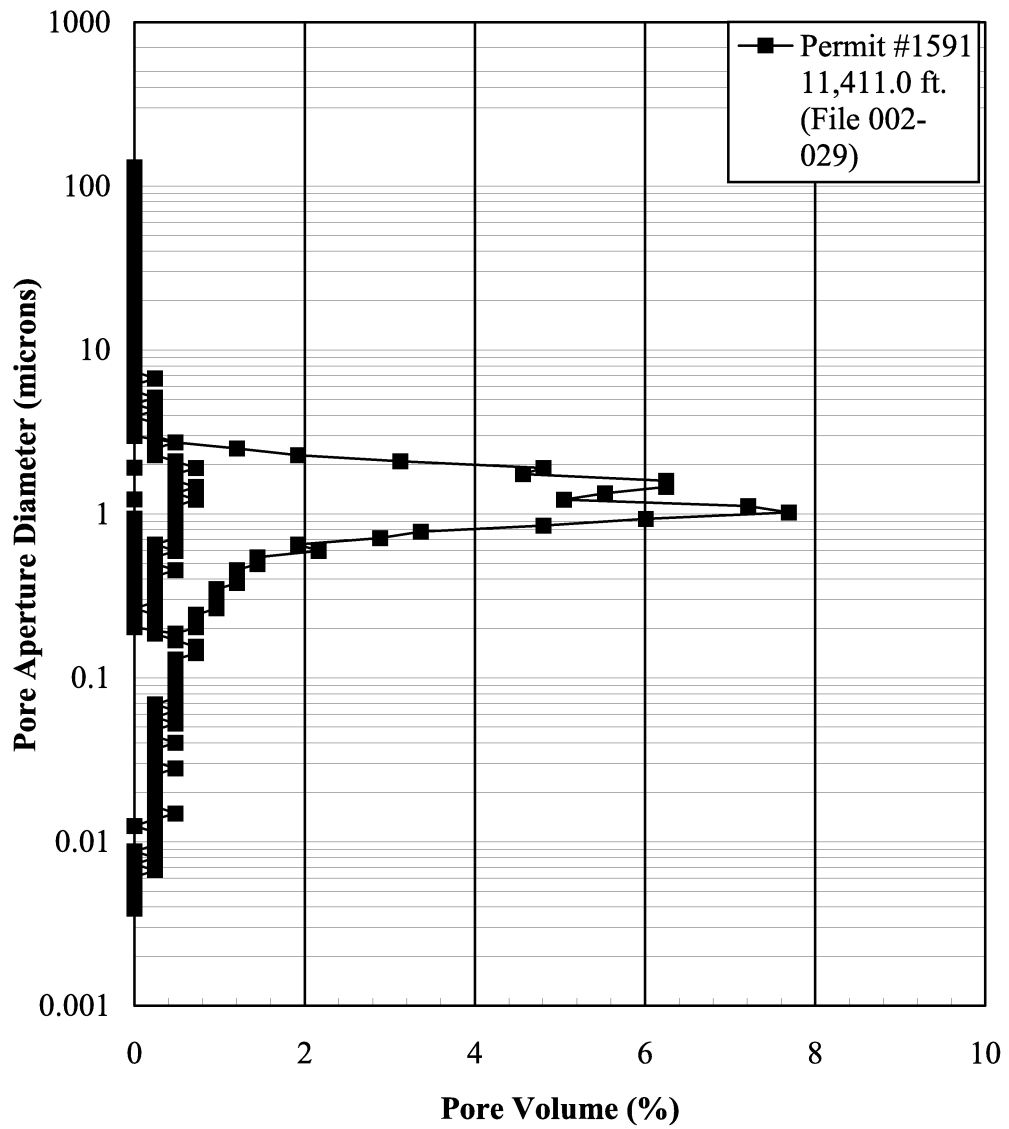


Figure 55. Pore aperture size distribution for Well Permit 1591 at 11,411 ft.

(from Hopkins, 2002).

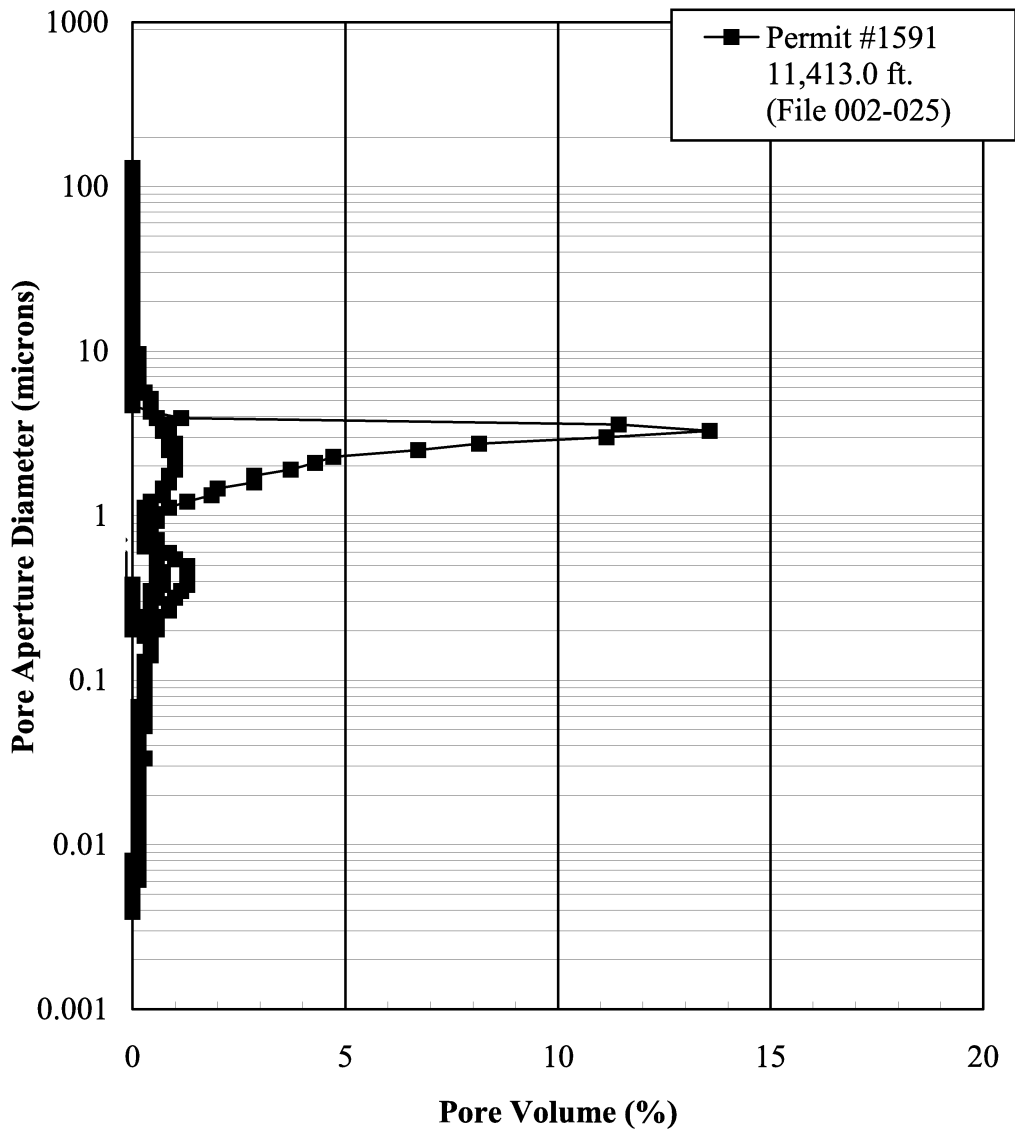


Figure 56. Pore aperture size distribution for Well Permit 1591 at 11,413 ft.

(from Hopkins, 2002).

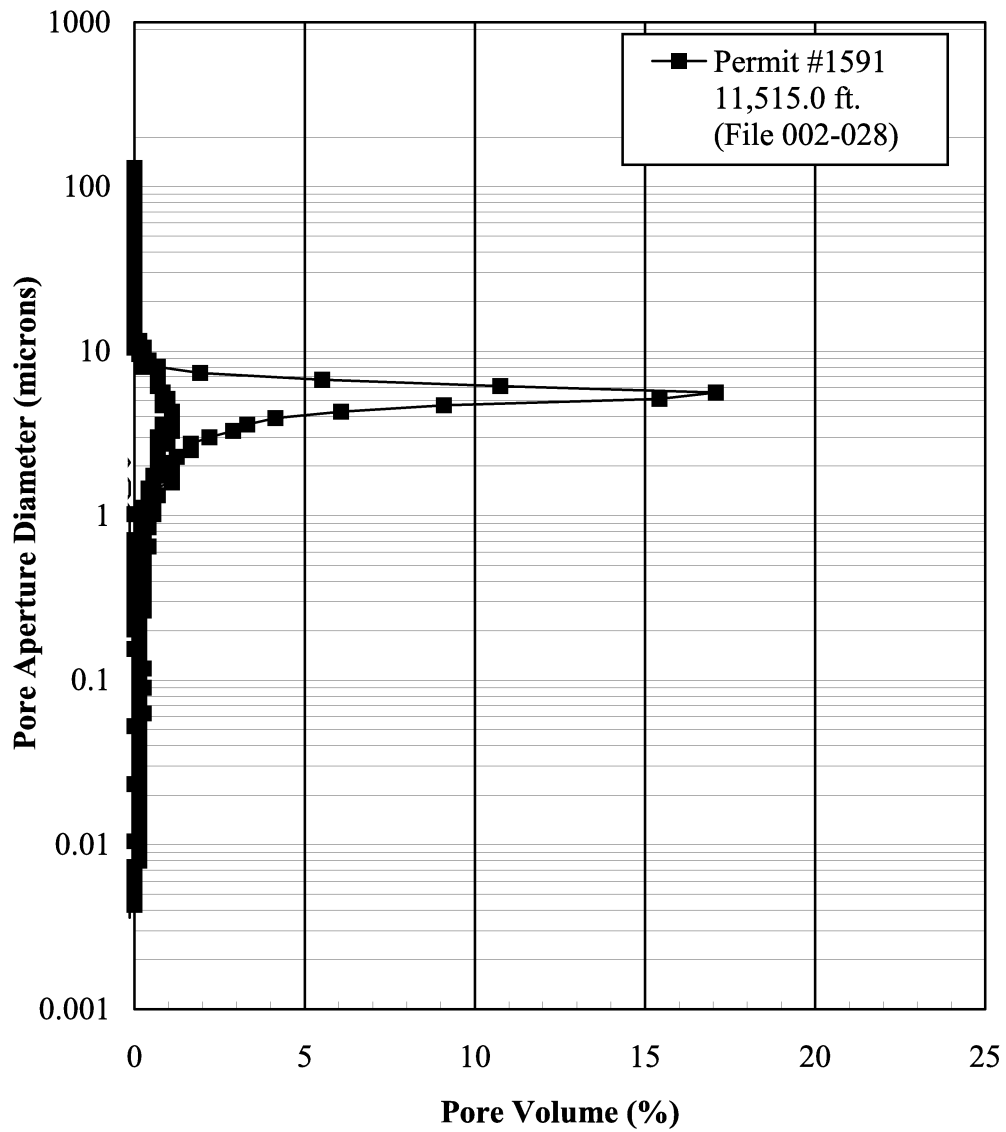


Figure 57. Pore aperture size distribution for Well Permit 1591 at 11,515 ft.

(from Hopkins, 2002).

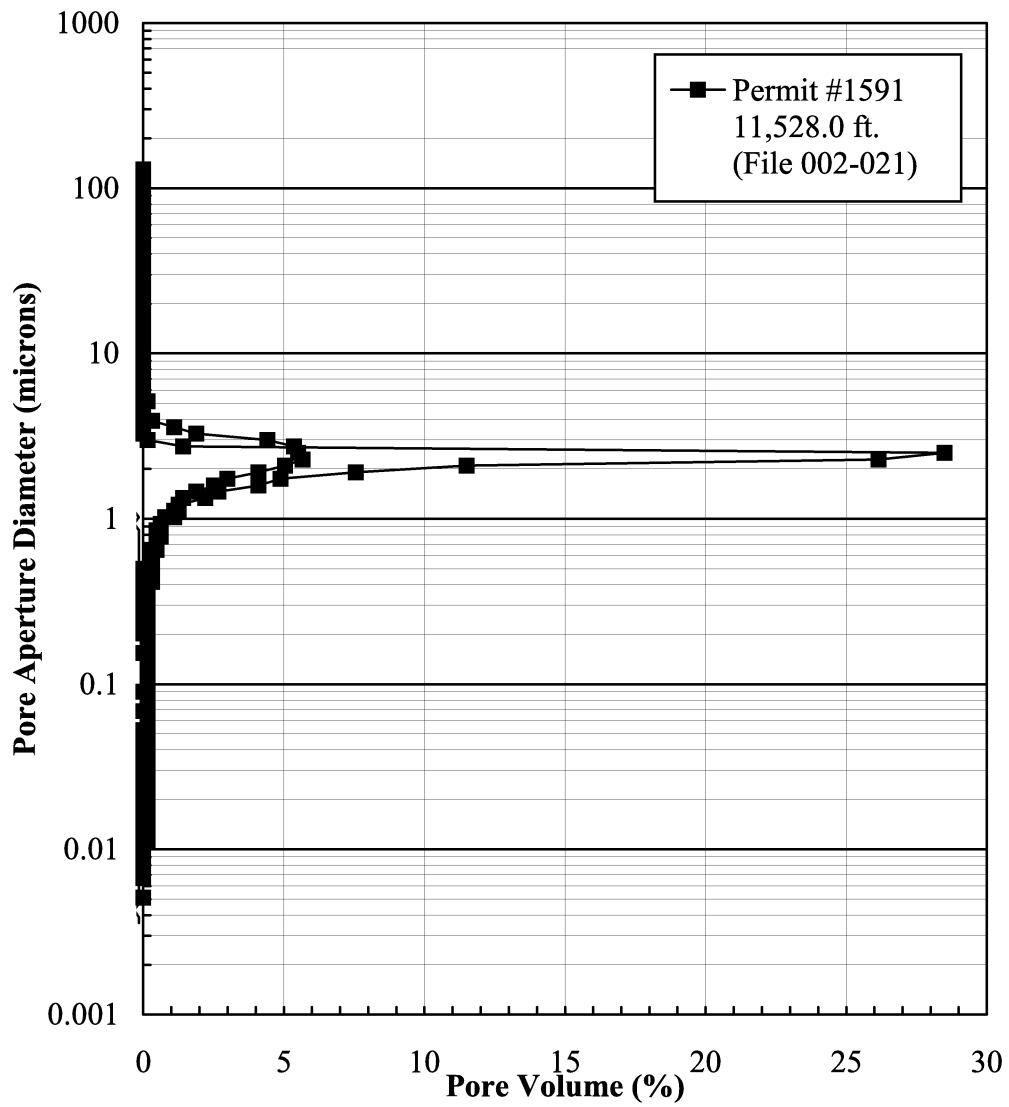


Figure 58. Pore aperture size distribution for Well Permit 1591 at 11,528 ft.

(from Hopkins, 2002).

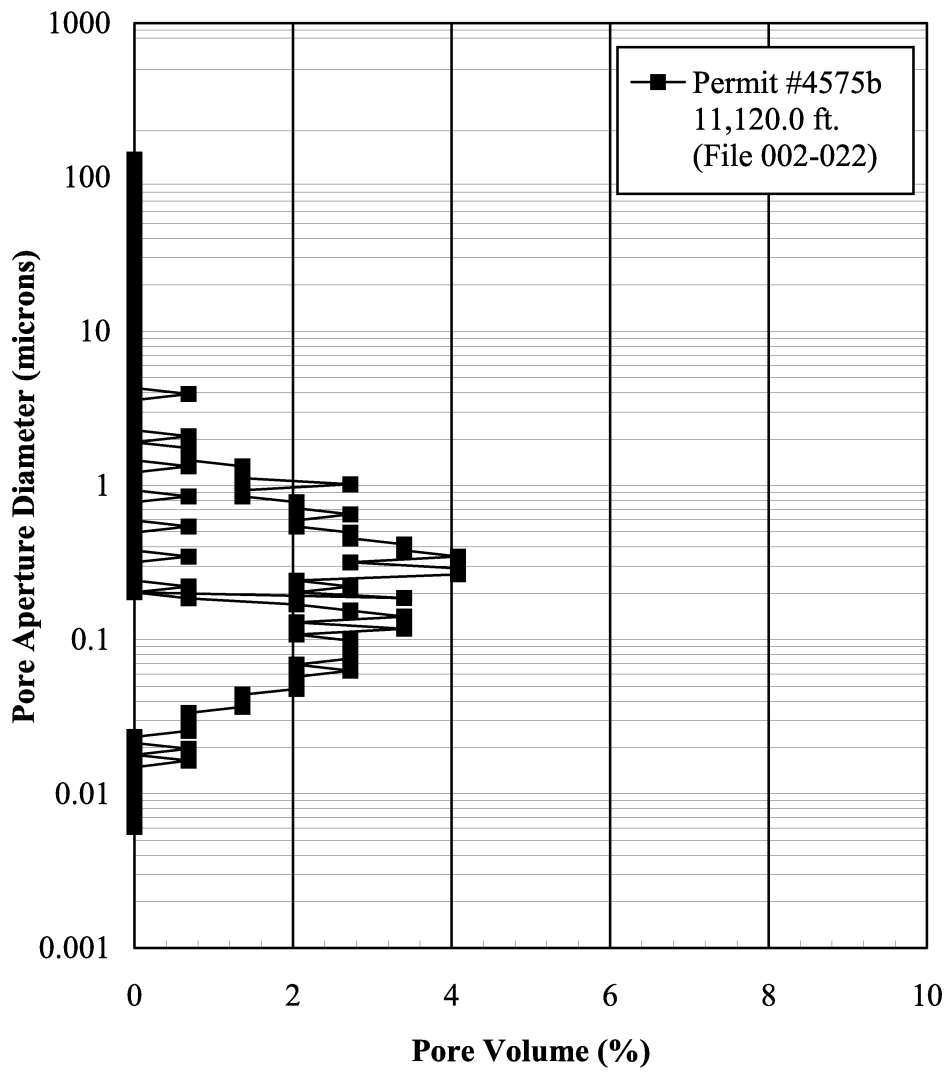


Figure 59. Pore aperture size distribution for Well Permit 4575B at 11,120 ft.  
(from Hopkins, 2002).

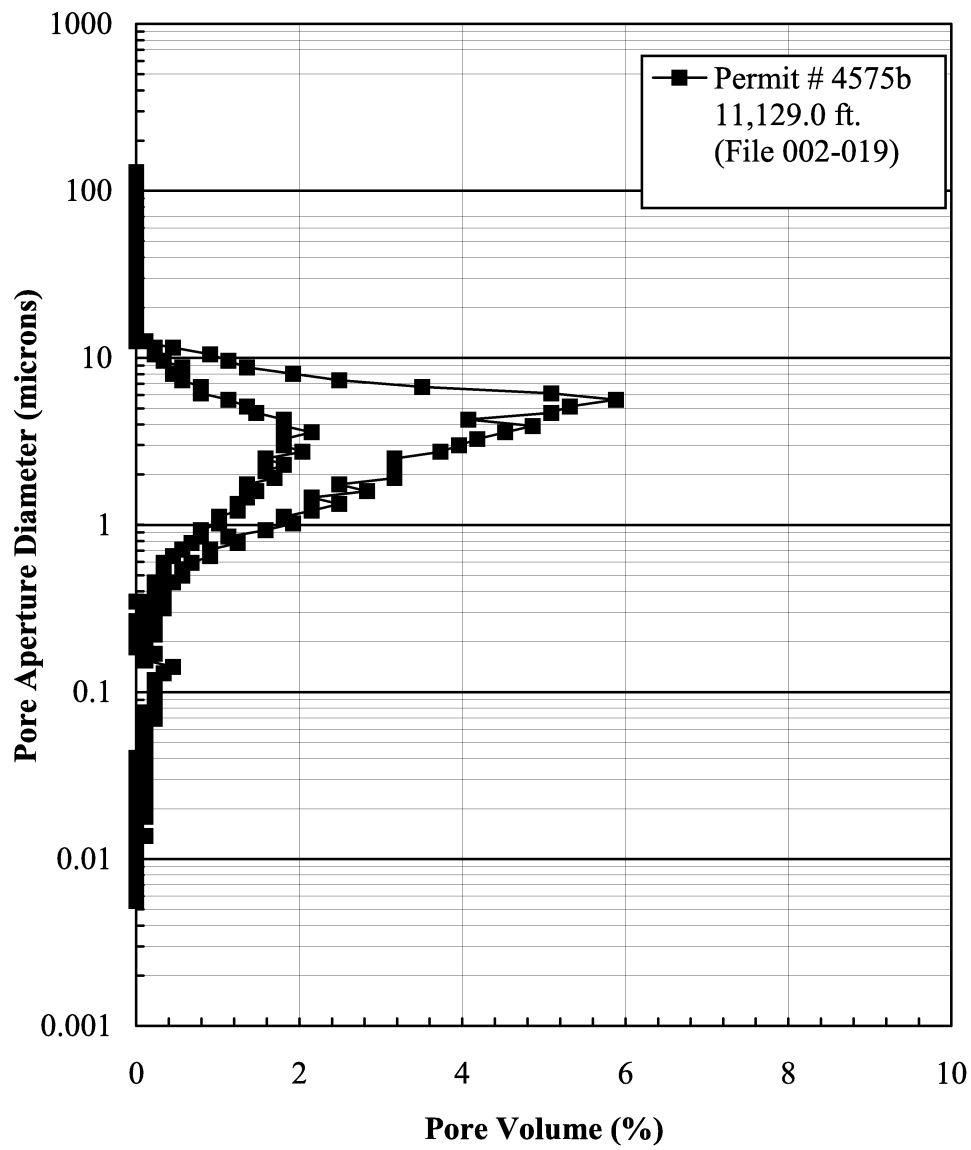


Figure 60. Pore aperture size distribution for Well Permit 4575B at 11,129 ft.

(from Hopkins, 2002).

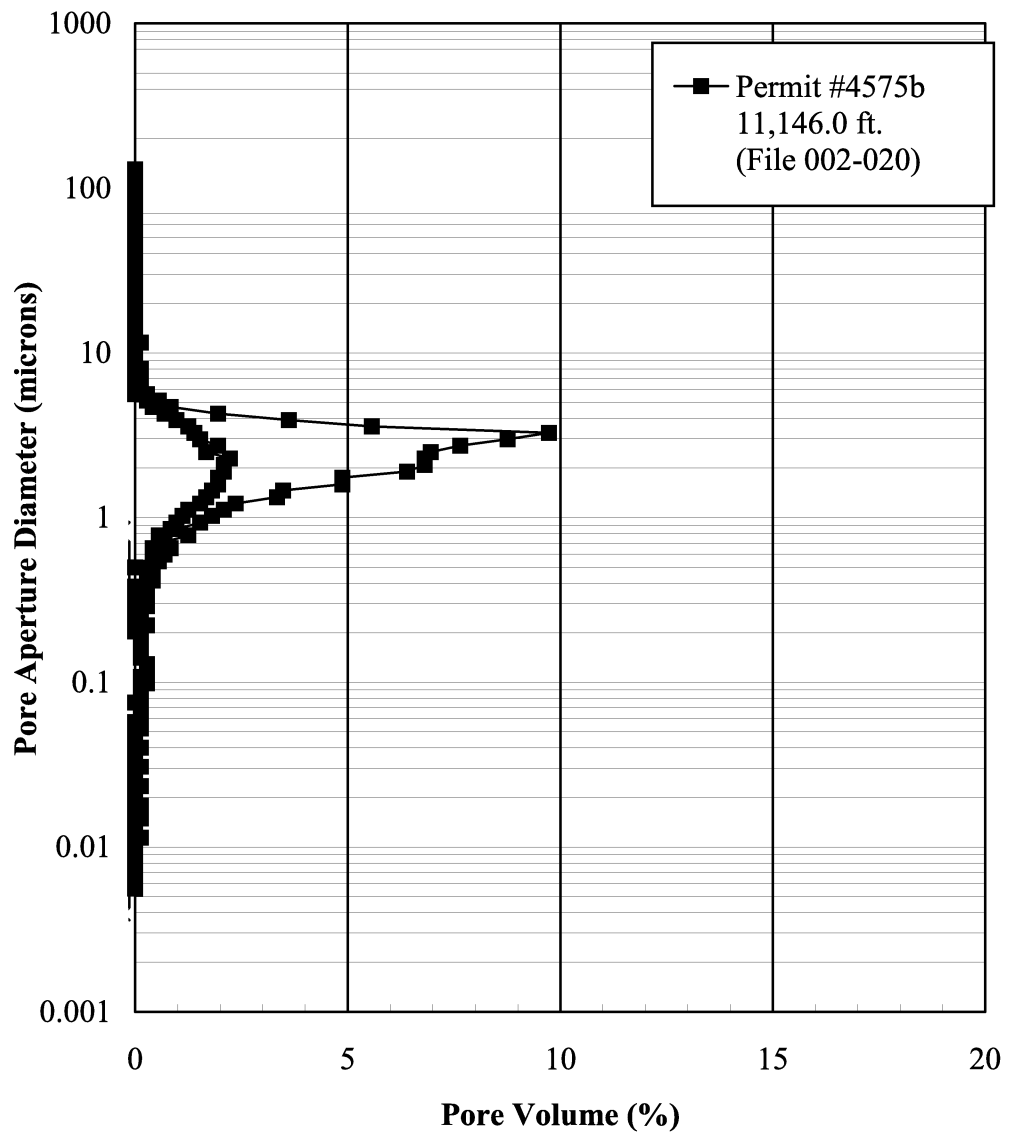


Figure 61. Pore aperture size distribution for Well Permit 4575B at 11,146 ft.

(from Hopkins, 2002).

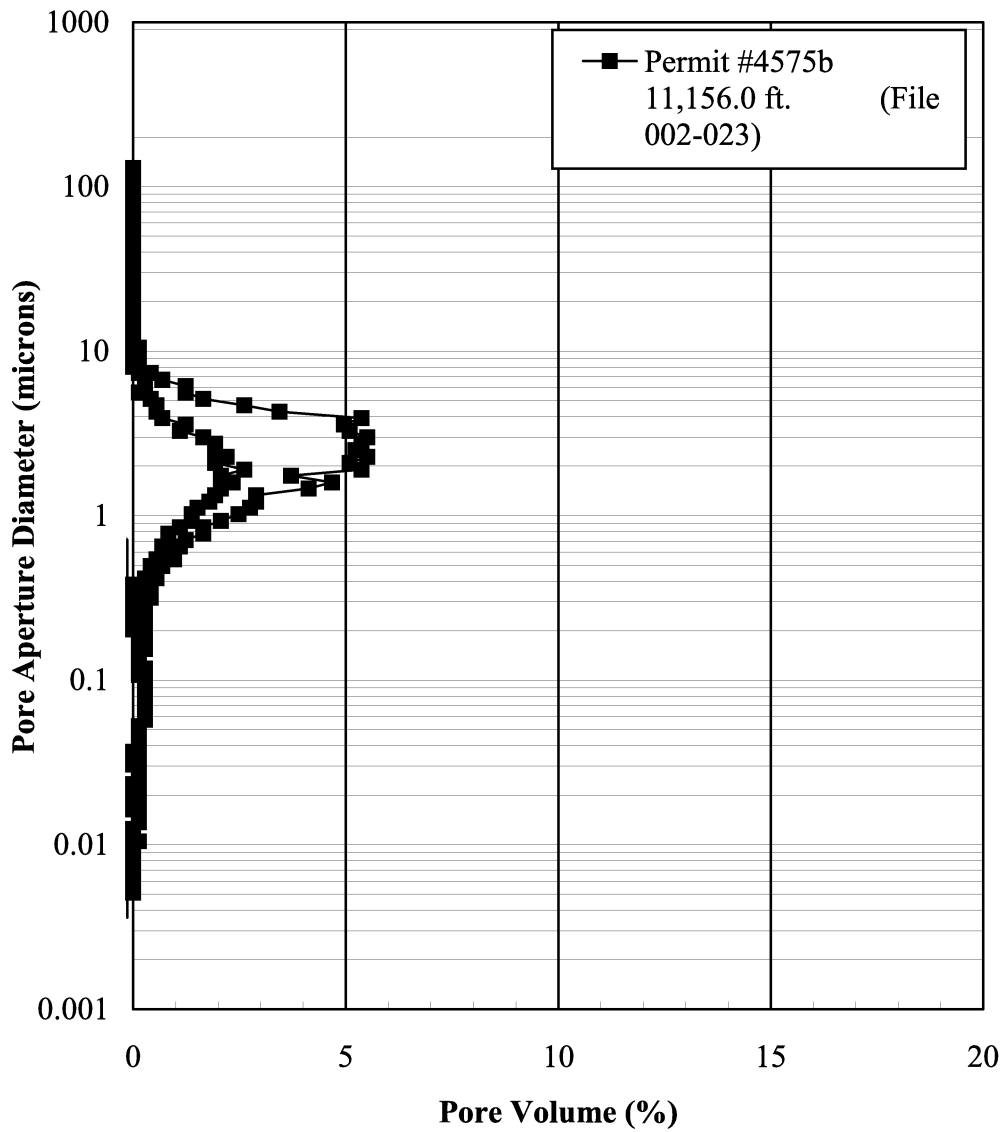


Figure 62. Pore aperture size distribution for Well Permit 4575B at 11,156 ft.

(from Hopkins, 2002).

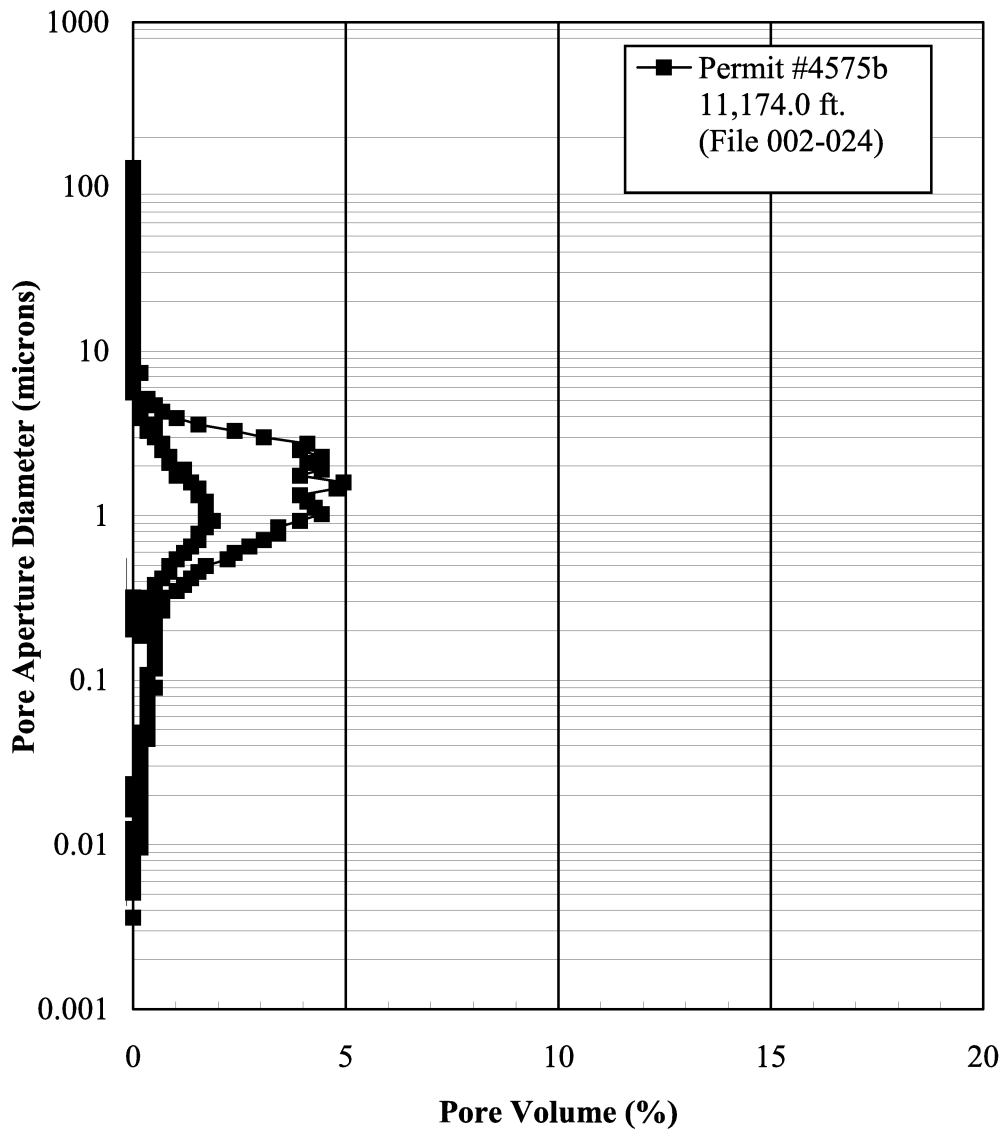


Figure 63. Pore aperture size distribution for Well Permit 4575B at 11,174 ft.

(from Hopkins, 2002).

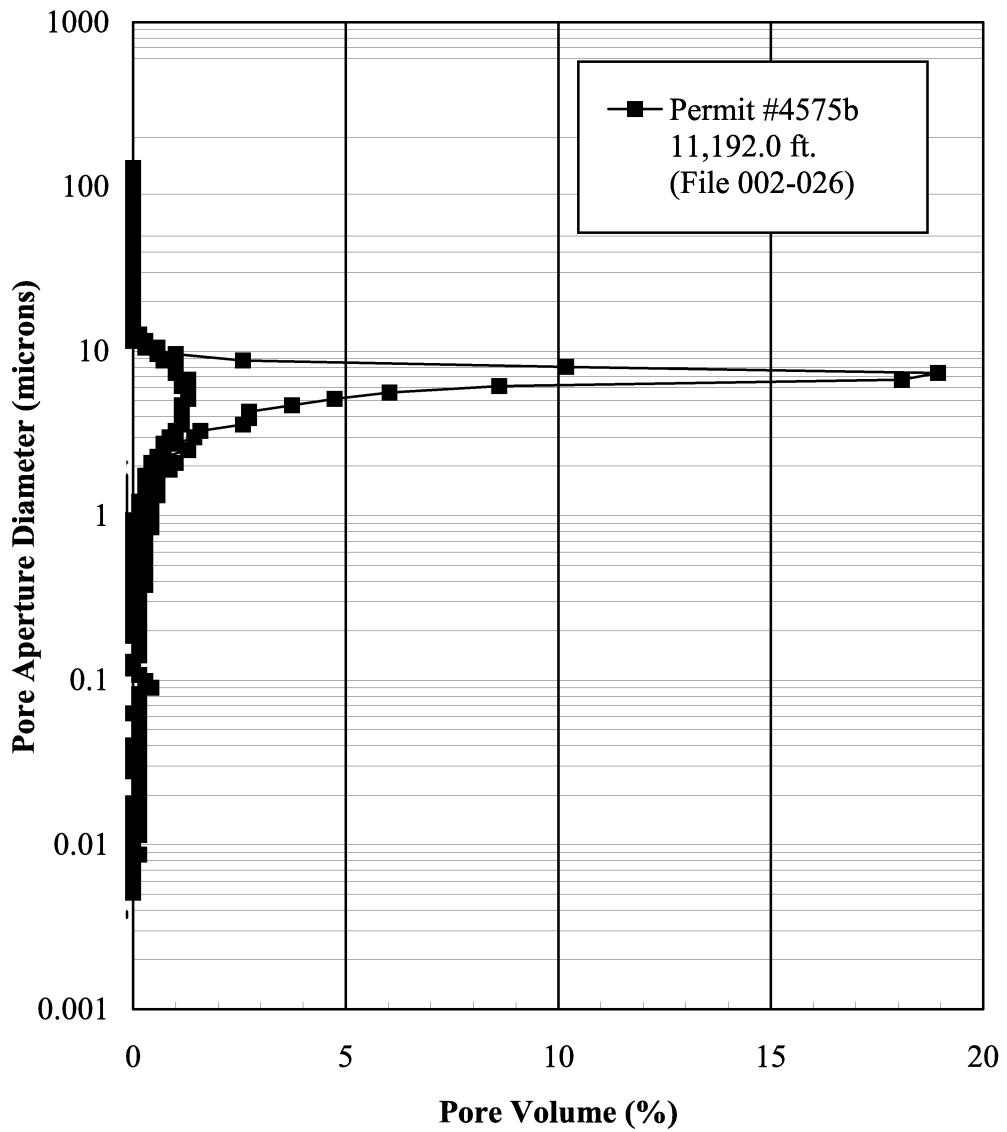


Figure 64. Pore aperture size distribution for Well Permit 4575B at 11,192 ft.

(from Hopkins, 2002).

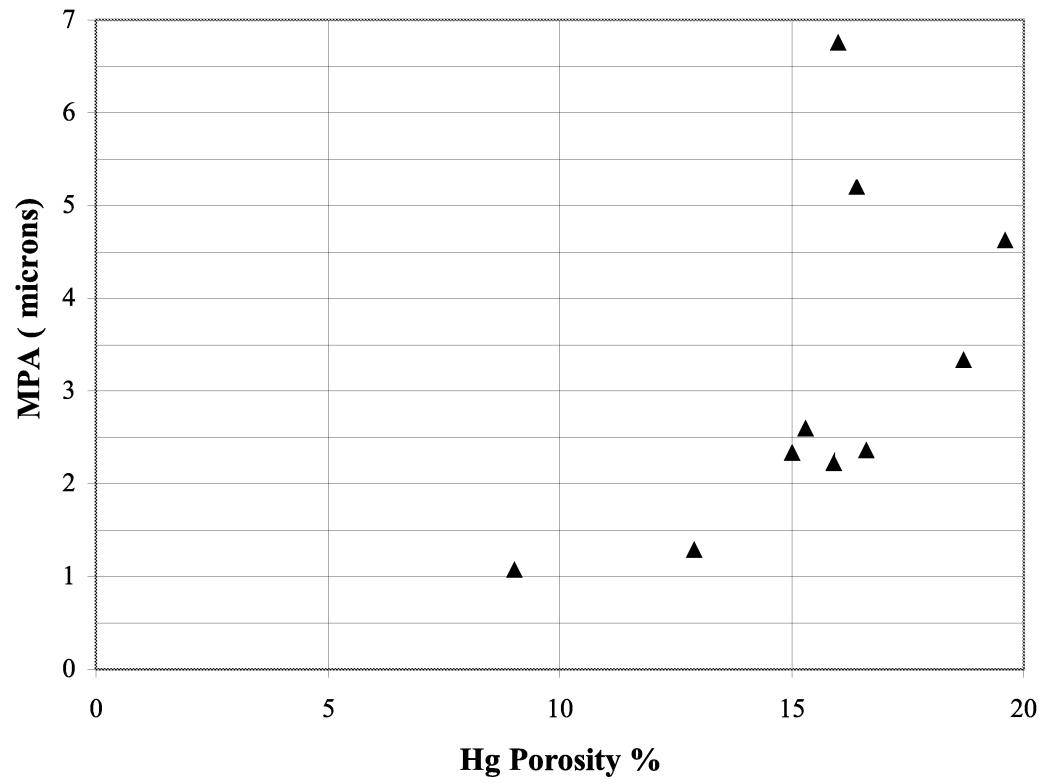


Figure 65. Graph of median pore throat aperture versus mercury derived porosity (from Hopkins, 2002).

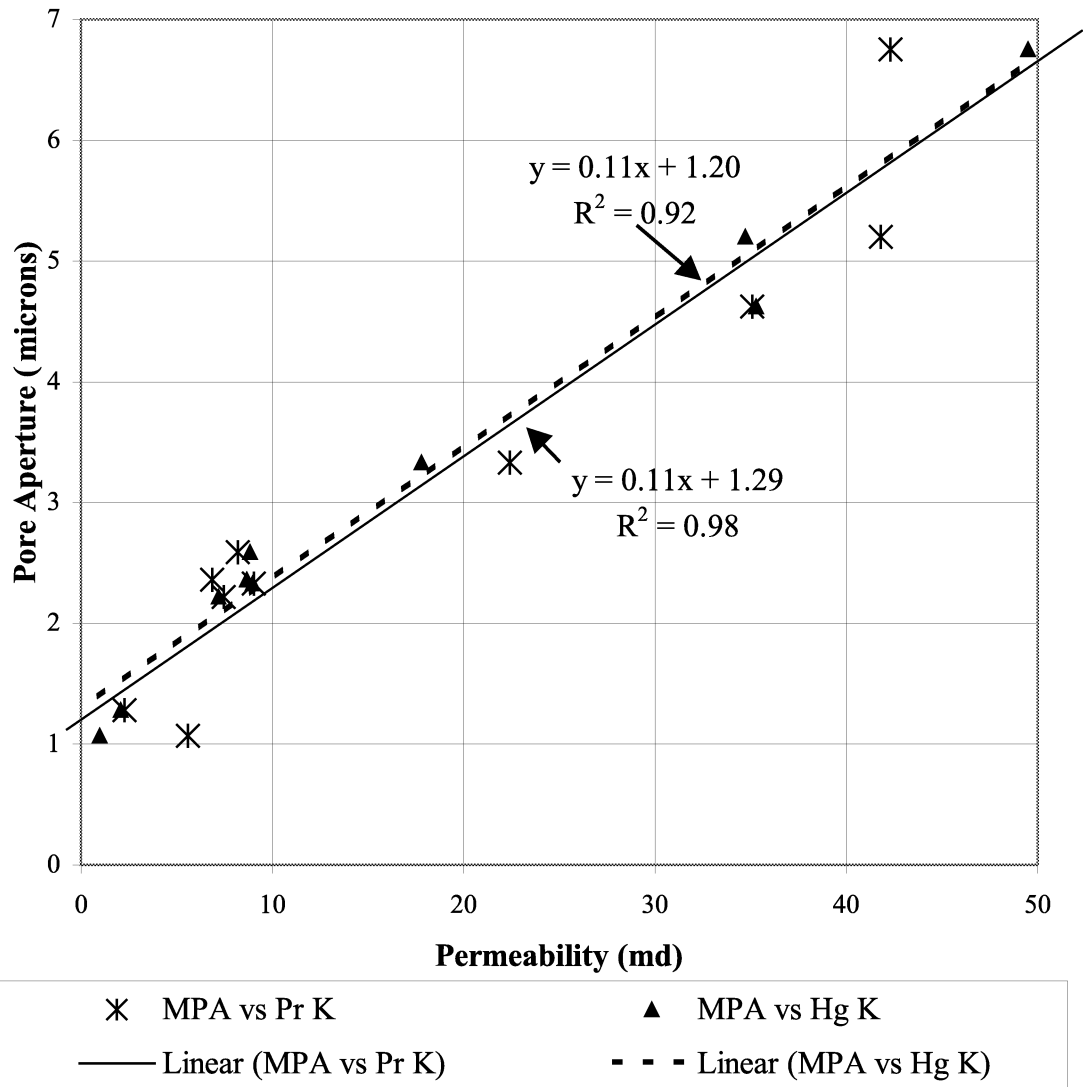


Figure 66. Graph showing the relationship between median pore throat aperture and probe permeability (from Hopkins, 2002).

**Sw @ Pc=1050 vs MPA**

$$y = 9.43x^{-0.90}$$
$$R^2 = 0.70$$

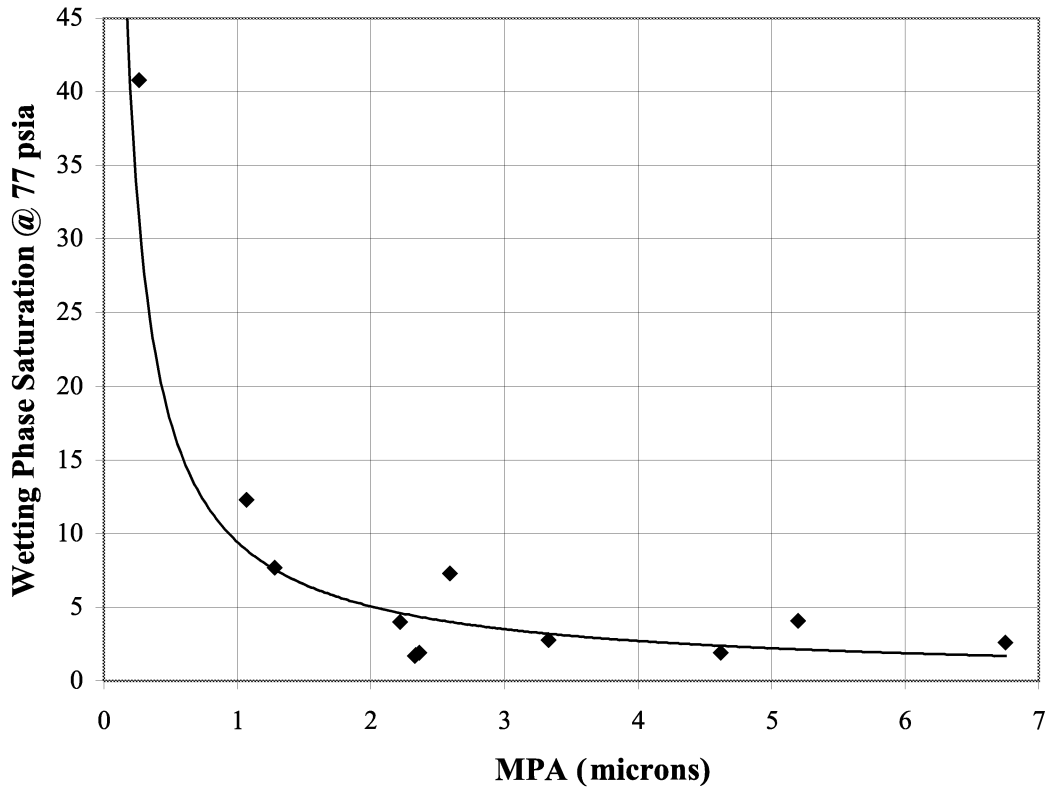


Figure 67. Wetting phase saturation at 77 psia versus median pore throat aperture (from Hopkins, 2002).

(Fig. 68). Figure 68 shows that tortuosity increases with increasing MPA. This relation is related to pore type: the larger MPA and tortuosity values are observed to be associated with intercrystalline pores. Figure 69 shows that entry pressure conditions can be predicted using the inverse of the pore throat radius.

### ***Task RC-2. Petrophysical and Engineering Property Characterization***

**Description of Work.**--This task is designed to focus on the characterization of the reservoir rock, fluid, and volumetric properties. These properties can be obtained from petrophysical and engineering data. This task will assess the character of the reservoir fluids (oil, water, and gas), as well as quantify the petrophysical properties (rock type, grain density, porosity, permeability, electrical properties, etc.) of the reservoir rock. In addition, considerable effort is devoted to the fluid-rock behavior (i.e., capillary pressure and relative permeability). The production rate and pressure histories are cataloged and analyzed for the purpose of estimating reservoir properties such as permeability, well completion efficiency (skin factor), average reservoir pressure, as well as in-place and movable fluid volumes. A major goal is to assess current reservoir pressure conditions and develop a simplified reservoir model (i.e., drive mechanism). New pressure and tracer survey data are scheduled to be obtained in Year 2 to assess communication within the reservoir fieldwide, including among and within the various pay zones in the Smackover. This work will both serve as a guide and provide bounds for the reservoir simulation modeling.

**Rationale.** Petrophysical (core, well logs, etc.) and engineering data (production rate and pressure histories, pressure tests, well completion data) are fundamental to the reservoir characterization process. Petrophysical data are often considered static (non-time dependent) measurements, while the engineering data are considered dynamic. The reservoir characterization concept is (almost by definition) the coupling or integration of these two classes of data. The data are analyzed to identify fluid flow units (reservoir-scale flow sequences), barriers to flow, as well as reservoir compartments. The petrophysical data are essential for defining the quality of the reservoir rock, and engineering data (performance data) are crucial for assessing the producibility of the

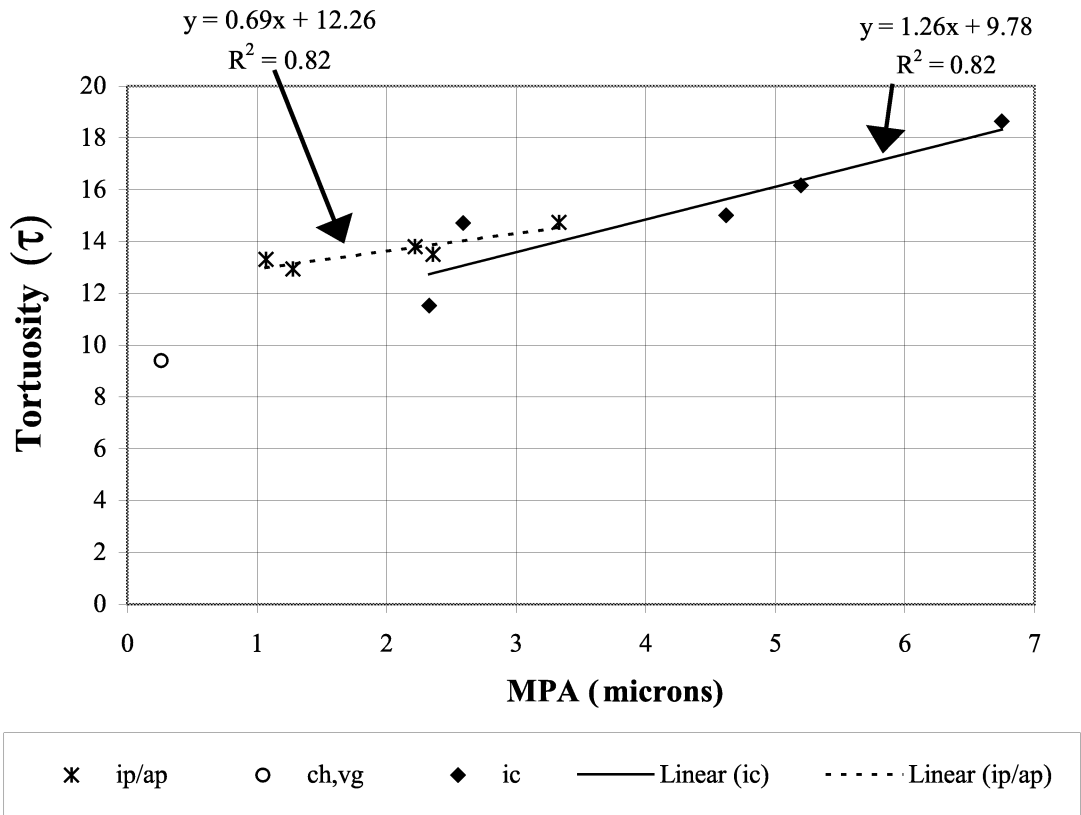


Figure 68. Graph of equation to determine tortuosity ( $\tau$ ) (from Hopkins, 2002).

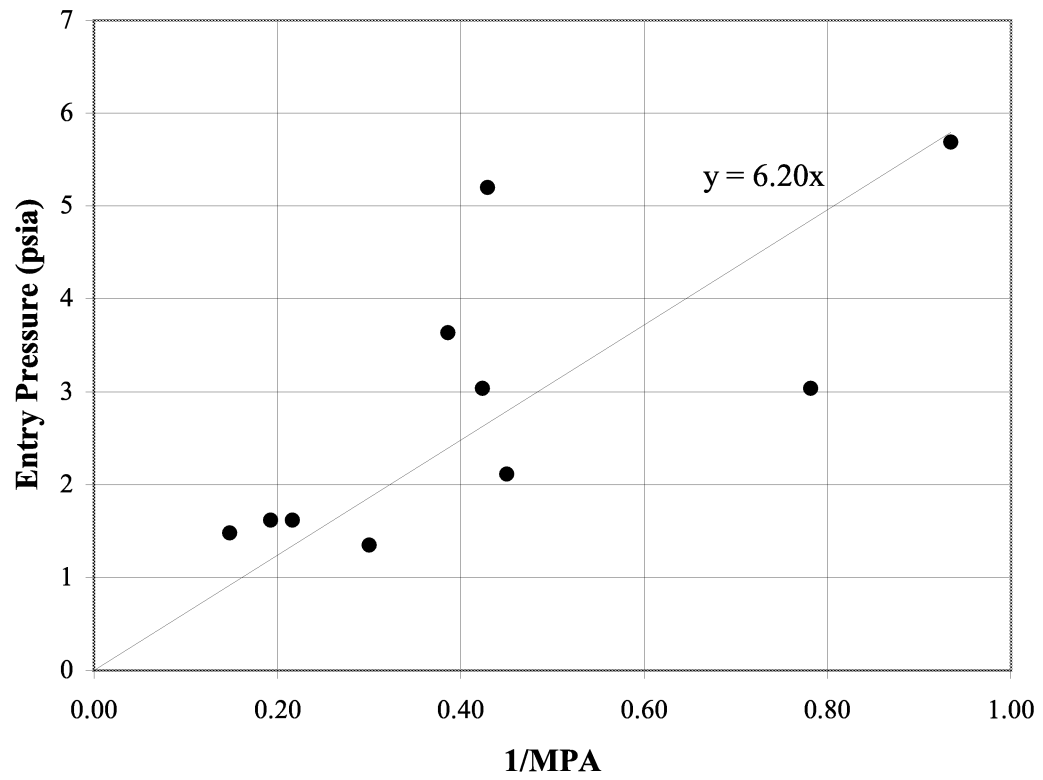


Figure 69. Predicting entry pressure from the inverse of pore throat radius (from Hopkins, 2002).

reservoir. Coupling these concepts, via reservoir simulation or via simplified analytical models, allows for the interpretation and prediction of reservoir performance under a variety of conditions.

**Analysis/Interpretation/Integration Procedure.--**Womack Hill Field is a mature oil field (Figs. 70 and 71). Since the discovery of the field production rates have steadily declined. The following tasks are employed as the mechanisms to analyze, interpret, and integrate the petrophysical and engineering data from Womack Hill Field.

1. Collect and catalog the well log, core, and production data.
2. Convert these data into an appropriate electronic format.
3. Develop correlations between core and well log data to predict reservoir permeability using well log responses.
4. Analyze and interpret the reservoir performance data using decline type curve analysis and estimated ultimate recovery analysis.
5. Integrate the geological data and the results of reservoir performance analysis by generating maps of distributions of reservoir properties throughout the field.
6. Establish recommendations to optimize the reservoir management strategies, such as: infill drilling, producer/injector conversions, special testing procedures to obtain more information regarding reservoir behavior, etc.

Our work to date has essentially focused on points 1-5.

**Correlation of Petrophysical Data—Core-Well Log Data Correlation.--**At Womack Hill Field the following well log responses are typically available:

- (SP) Spontaneous potential
- (ILM) Shallow resistivity
- (LLS) Deep resistivity
- (GR) Gamma ray
- (ROHB) Bulk density
- (DPHI) Density derived porosity
- (NPHI) Neutron derived porosity

In addition, substantial volumes of whole and sidewall core data are available. Admittedly, all of these data are 1970's vintage, and we have encountered significant difficulty in trying to correlate the core and well log data.

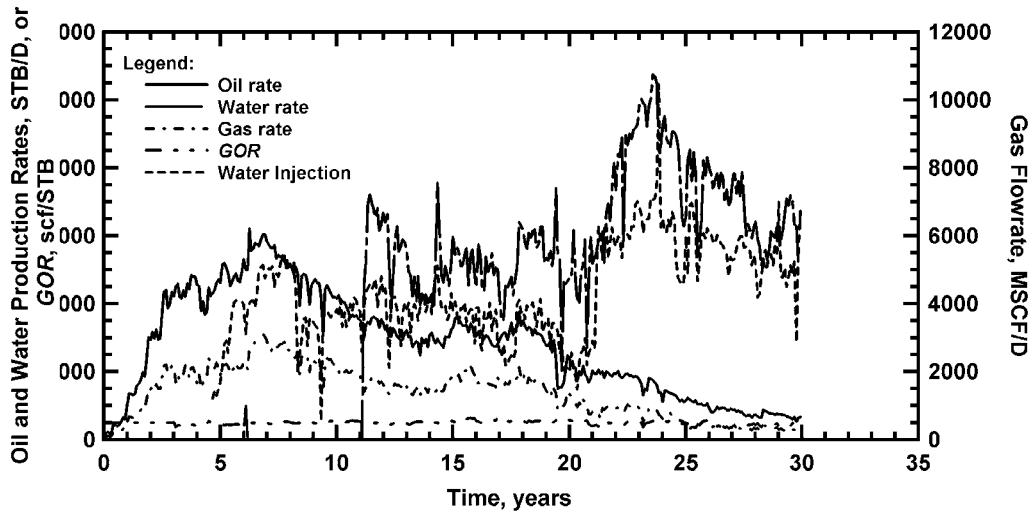


Figure 70. Production history of Womack Hill Field. Since 1997, oil and gas rates have steadily declined, while the water production rate has increased. GOR has remained essentially constant.

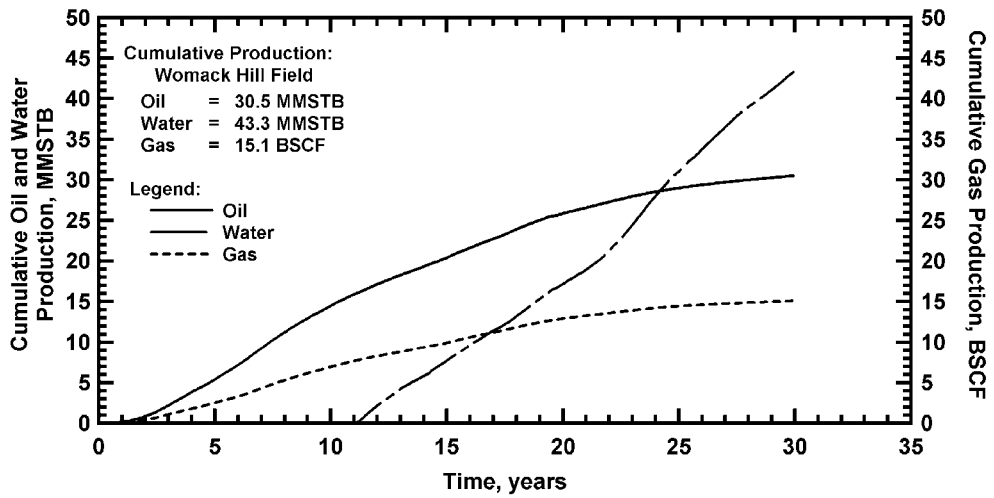


Figure 71. Cumulative production of Womack Hill Field. Oil and gas curves are on the plateau and the water continues rising.

As an example, in Figure 72 we provide a presentation of the core and well log data—showing the well log data and core permeability profiles for well Permit #1639. The reservoir has been divided into three flow units, based originally on geological data, and we note that our work with the core and well log data also confirmed these assignments. As shown, the core permeability data are quite scattered, giving us an indication of the level of heterogeneity in the reservoir. The wells at Womack Hill Field produce from the upper Smackover carbonate reservoir, which is typically characterized by a high level of heterogeneity. This makes it difficult to find correlations between the petrophysical variables on a regional scale. Therefore, our approach is to establish correlations for each of the three flow units at a local scale (i.e., for individual wells).

As part of our characterization of the petrophysical data, we distributed the core data (porosity and permeability) into the appropriate flow units and aligned the corresponding well log measurements to construct the data tables for correlation purposes. We selected the core and well log data for 9 wells. We find that there is no consistent suite of well logs for all wells; however, we do note that the GR, LLS and some sort of porosity log are generally available. As such, we selected GR, LLS, and (core) porosity as independent variables to keep the same set of input data for all correlations.

To develop our correlations of the petrophysical data we selected a nonparametric technique that is based on estimating the optimal transformation of each variable (the dependent as well as the independent variables). This method has an advantage over conventional multiple regression algorithms in that it does not require an assumed correlating function (i.e., model) between the variables—where a pre-established model could yield an inaccurate representation. The nonparametric method uses an iterative process involving a set of "alternating conditional expectations" (ACE) to generate a transform value for each data point of the dependent and independent variables. Once the transform for each of the variables has been established, a nonparametric correlation is generated between the dependent variable and the sum of the transform values, this is called the optimal transformation. Parametric correlations can be generated by fitting these curves using the appropriate functions, generally polynomial functions (GRACE (1996)) The



dependent variable is estimated by determining the inverse of the optimal transform. The details for this process are given by Breiman and Friedman (1985).

Our first approach in developing the core-log correlations was to analyze simple relationships between the variables, which could allow us to obtain less complex correlations if a strong relationship is found between these variables. We then studied the relationship between core permeability and each well log signal. Figure 73 presents crossplots of core permeability against GR, RHOB, LLS, and ILM for flow unit in well Permit #1639. No single plot indicates a clear tendency between the core permeability and any of the well log variables. GR and RHOB do not provide significant character to the correlation since the behavior of these variables is essentially constant through the section. Although the resistivity data do exhibit some variation, the overall relationship of resistivity with the core permeability is quite random (no clear pattern is evident).

This behavior (i.e., the lack of a univariate relationship) was found in each of the three flow units for each well. This observation leads us to pursue the application of regression on several well log variables simultaneously as a mechanism to generate correlations between the core permeability and the well log data. We believe that the use of several well log variables in these correlations will improve the overall behavior of a correlation and establish a more consistent statistical model (when we move to convert the non-parametric relation into a parametric relation).

During the depth shifting effort we observed that a significant variation exists between the core and well log-derived porosity, over the entire scale of porosity values. As an effort to try to resolve these differences, we considered the relationship between these two variables (core and well log porosity) on the flow unit scale. Figure 74 shows the relation between the porosity derived from the bulk density log and the core porosity for well Permit #1639 (Flow unit A). We note that the relationship is extremely poor, and that the only positive comment is that the data appear evenly distributed (although randomly) about the 45° line (i.e., the perfect correlation line).

Generally speaking, well log derived porosity values are among the most consistent variables that can be estimated—unfortunately, this is not the case in Womack Hill Field. To use the well log

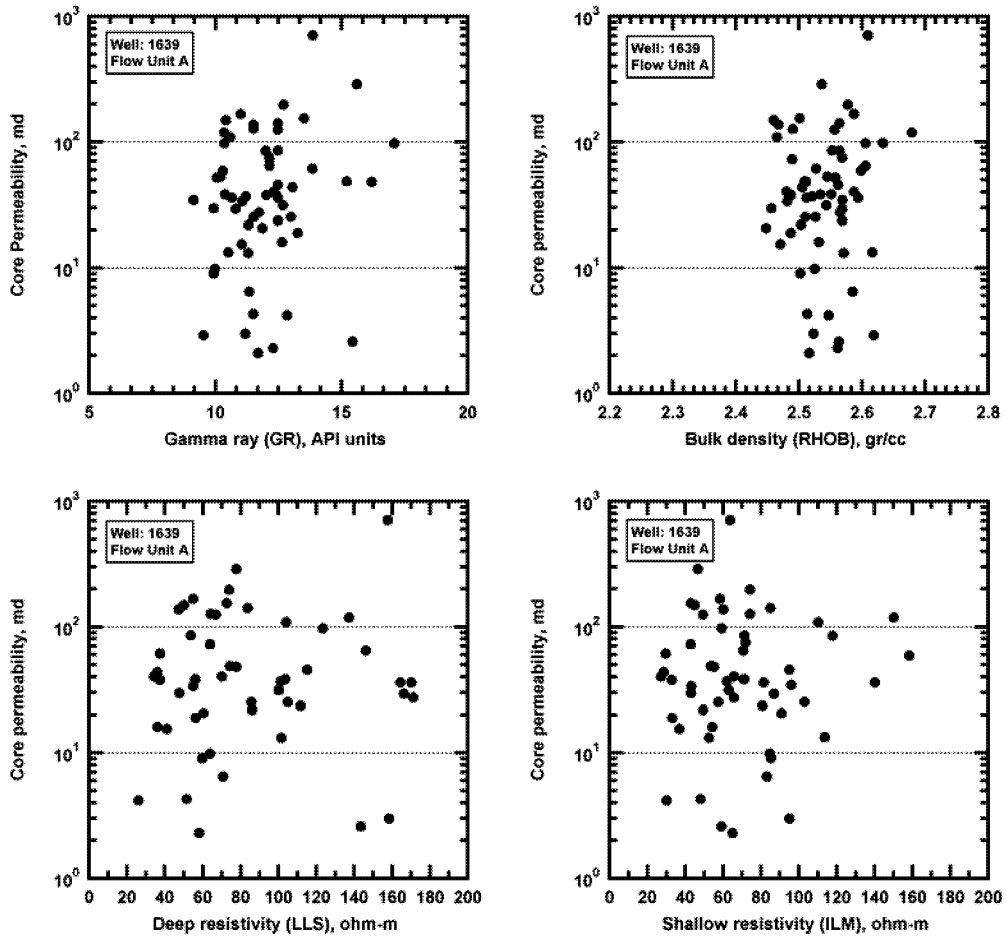


Figure 73. Core permeability univariate correlations — Womack Hill Field, Well 1639 (Flow unit A). No clear trend is present.

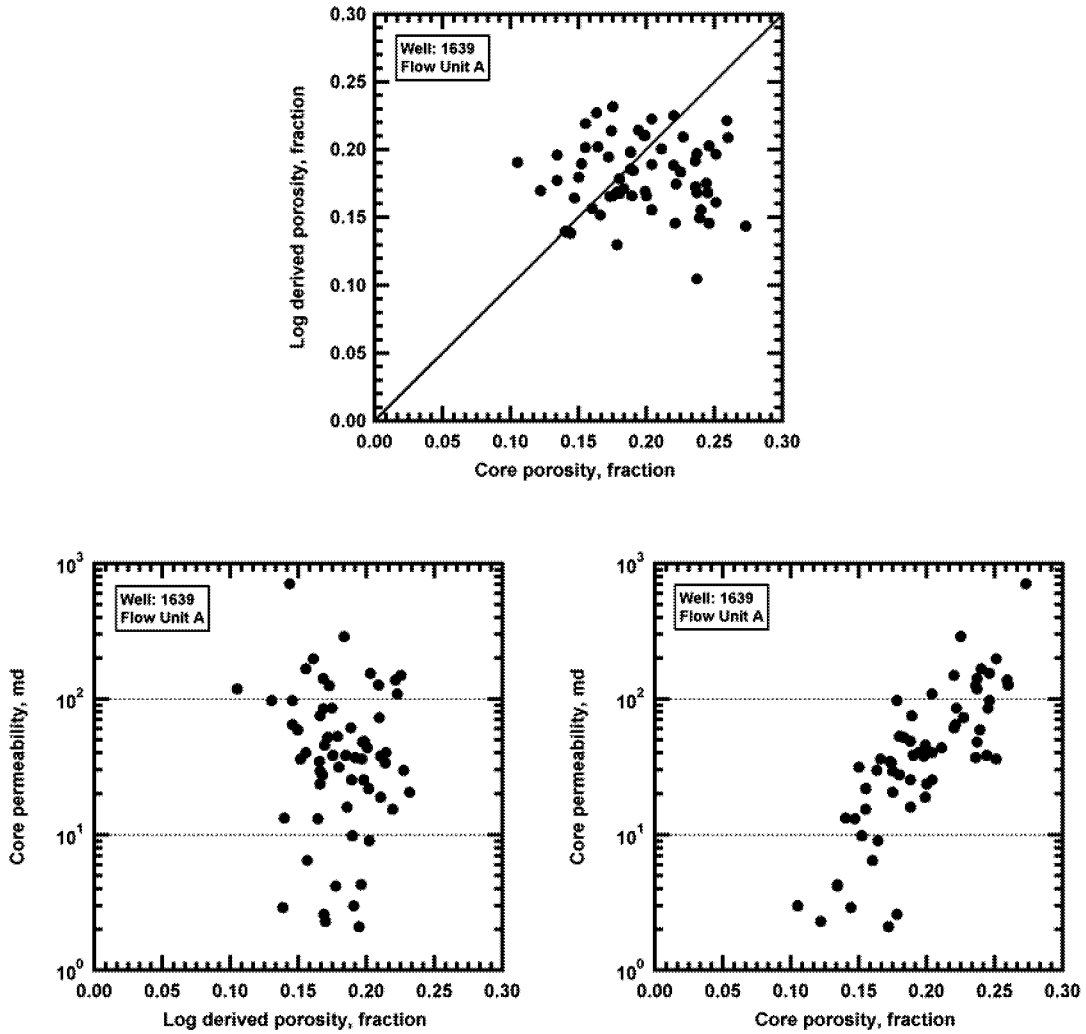


Figure 74. Core permeability and porosity plots — Womack Hill Field, Well 1639 (Flow unit A). Log derived porosity does not match either core porosity or have a clear trend with core permeability — core porosity and permeability show a clear relationship.

derived porosity as input data for the correlation would produce significant errors, as it has little or no relation to the formation permeability. However, a comparison of the logarithm of the core permeability with core porosity yields a reasonably linear trend (Fig. 74). As such, we elected to use the core porosity in lieu of the well log-derived porosity to obtain more consistent results. To generate correlations that can be used for most of the wells, we selected the GR, LLS, and core porosity as input data for the correlations. Although the GR log is thought to have relatively little character, it does provide certain petrophysical characteristics, as the accuracy of the correlation tends to improve when the GR data are included. Typically, the ILM and LLS responses follow essentially the same tracks; however, we prefer the deep resistivity (LLS) over the shallow resistivity (ILM) because the LLS resistivity utilizes information at distances further into the reservoir, and because the LLS is the more common well log acquired in Womack Hill Field.

Having prepared the data sets for correlation, we use the GRACE program (1996) to establish the nonparametric correlations for each variable—generating the corresponding optimal transformations. As we require some functional form, in order to apply the correlation, we utilize parametric correlations that are generated by fitting the data using quadratic polynomials (a feature of the GRACE program). As an example, in Figure 75 we present the transformations for each variable (well Permit #1639—Flow unit A). Finally, the correlation that is used to predict the dependent variable is obtained by calculating the inverse of the optimal transformation. We noted that the correlating function matches the tendency exhibited by the measured data, which confirms the robustness of the non-parametric method.

**Correlation of Petrophysical Data—Statistical Analysis of Core-Data.**--In order to generate a petrophysical model of the reservoir we need to establish a distribution of the formation properties throughout the reservoir drainage area. Our ultimate goal in this effort is to provide a reservoir description that can be used for numerical simulation. To accomplish this goal we segregate the data according to flow units and develop histograms of porosity and the logarithm of permeability. These histograms confirm that porosity and the logarithm of permeability both follow a normal distribution.

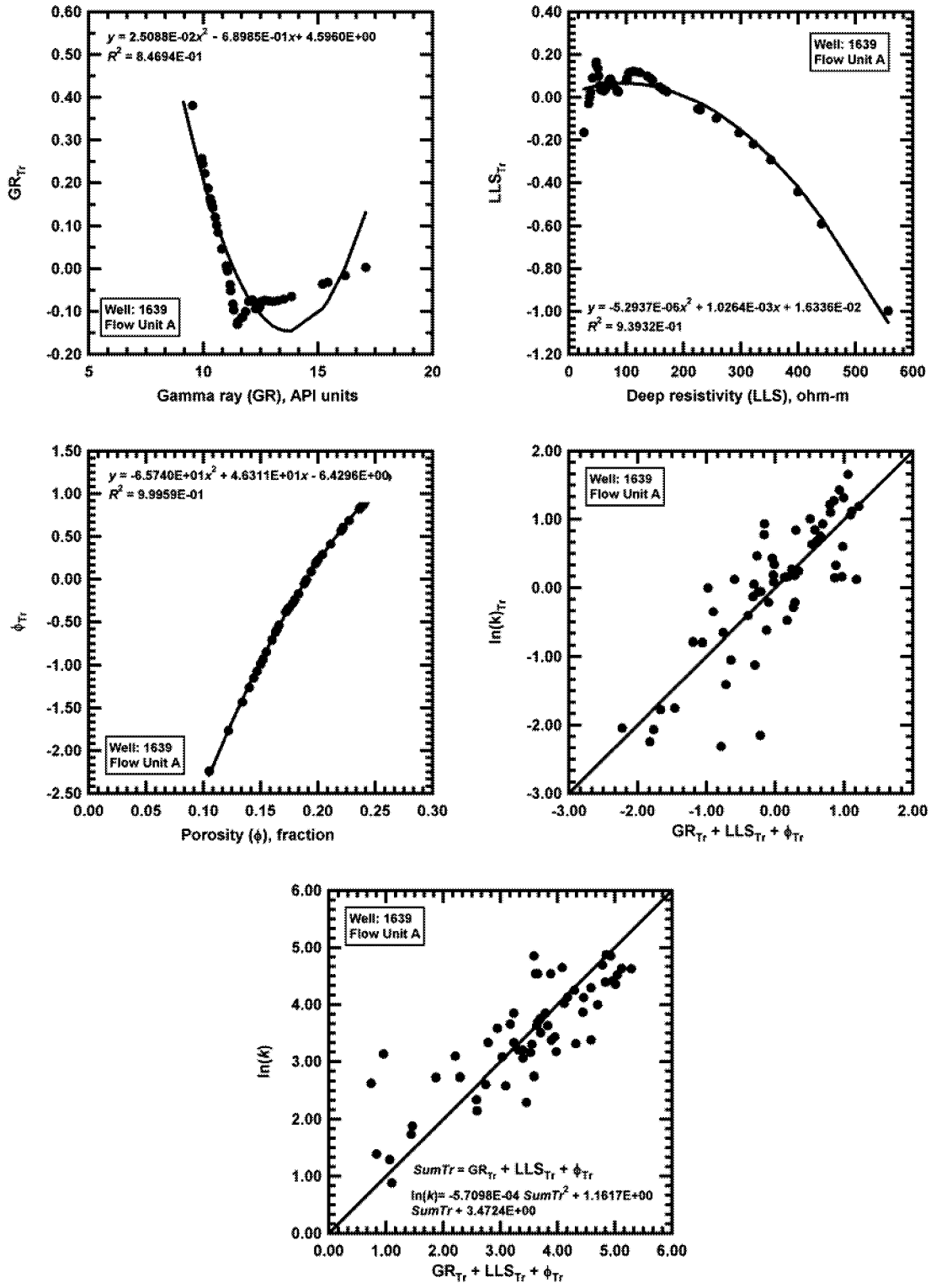


Figure 75. Optimal transformations for independent and dependent variables and core permeability correlation — Womack Hill Field, Well 1639 (Flow unit A).

Figure 76 provides an example of this behavior for well Permit #1639—Flow unit A. We note that most of the wells in Womack Hill Field yield similar histogram trends. It is our intention to use the mean value of porosity and the logarithm of permeability established from a particular histogram to represent the average for a particular flow unit. Using these results we developed maps of porosity and permeability based on the average values for each flow unit—which will be part of our proposed geological model for numerical simulation.

**Analysis of Reservoir Performance—General.**--Figure 70 presents the historical behavior of the oil, gas, and water production rates at Womack Hill Field since production began in December 1970. Oil and gas production peaked in 1977 at 6,200 STB/D and 3,200 MSCF/D of oil and gas, respectively. Since then, oil and gas flow rates have steadily declined, while the water rate has consistently increased. This production decline has reduced the profitability of the field—which leads to the current program of production optimization and field management strategies to improve the performance and overall recovery. Currently there are 3 injection wells (in the Smackover) which are active, although there are also some injection wells which are also used periodically. The producing gas-to-oil ratio (GOR) has remained relatively constant (approximately 500 scf/STB) indicating that the reservoir pressure remains above the bubblepoint pressure (approximately 1925 psia).

Figure 71 presents the fieldwide cumulative production for oil, gas, and water. The oil and gas curves are nearing their respective "plateaus" and should not be expected to change their behavior without substantial intervention (i.e., infill drilling, well stimulation, improved artificial lift, etc.). We also note from Figure 71 that the cumulative water production curve is still increasing at a substantial rate although it does appear to be trending towards a plateau (probably in the range of 55-60 MMSTB of water). To date, the total oil production is 30.5 MMSTB, along with 43.3 MMSTB of water and 15.1 BSCF of gas. The field is divided the field into two areas—the Eastern and Western Unit areas, based presumably on geological information. In Figure 77 we present the production profiles for the Eastern area, and in Figure 78 the hydrocarbon production for the Western Unit area is presented.

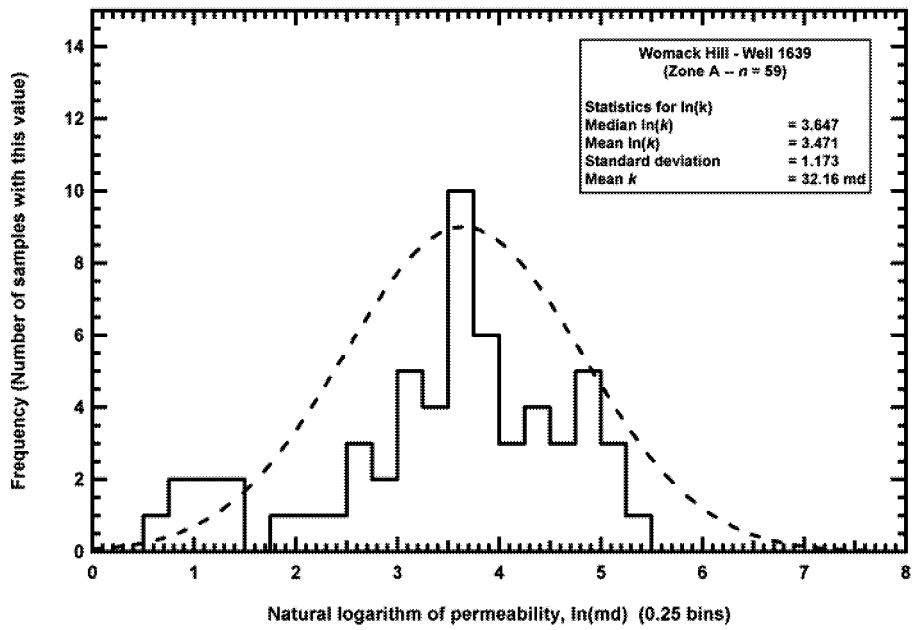
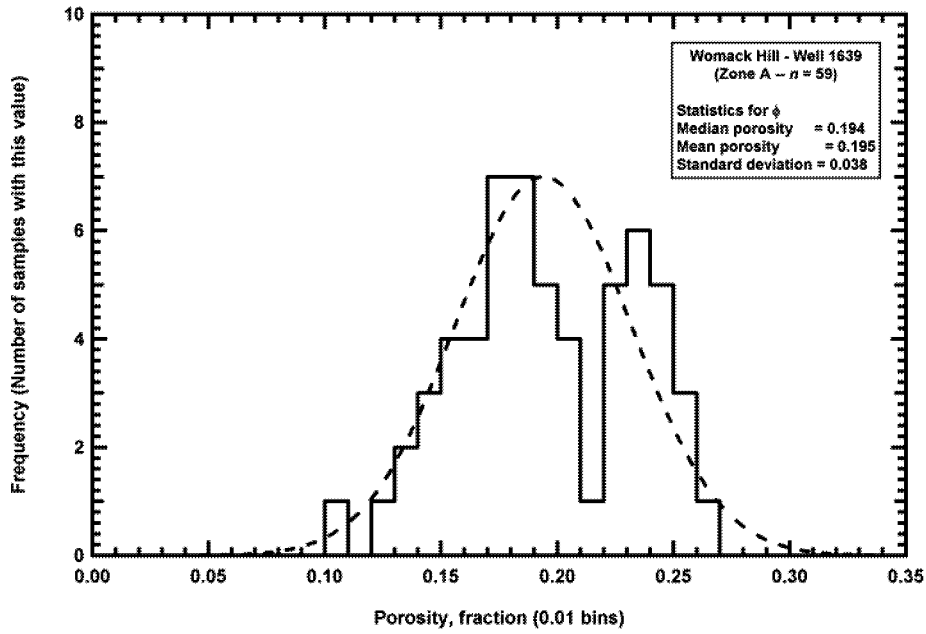


Figure 76. Core porosity and logarithm of core permeability histograms — Womack Hill Field, Well 1639 (Flow unit A). Both porosity and the logarithm of permeability have a normal distribution.

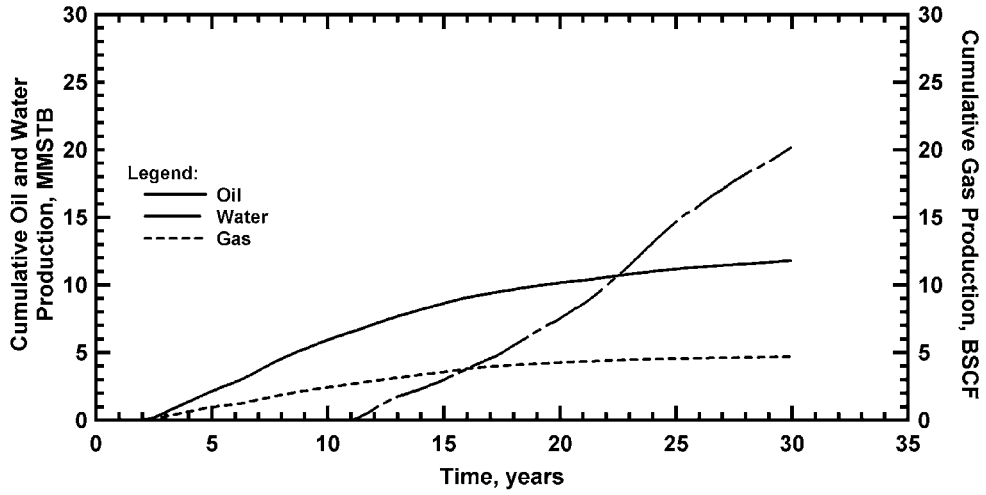


Figure 77. Cumulative Production in Eastern Area — Womack Hill. This area produces 38.7 percent of total oil production.

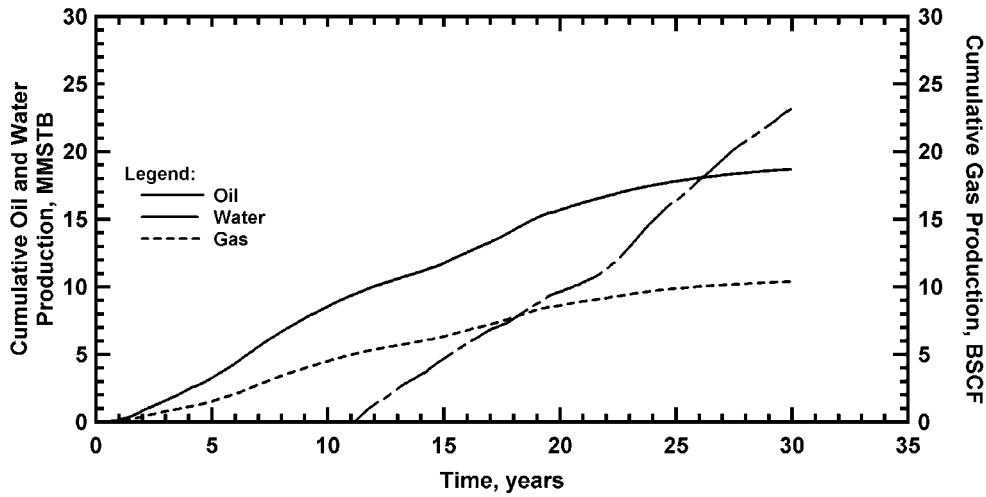


Figure 78. Cumulative Production in Western Area — Womack Hill. This area produces 61.3 percent of total oil production.

In Figure 79 we present a curve of the logarithm of the fractional flow of water ( $f_w$ ) versus cumulative oil production ( $N_p$ )—these plots are widely used for evaluation and prediction of reservoir performance—in particular, to estimate total recovery at 100 percent water production. The technique only applies at later times and presumes a log-linear relationship of WOR (or  $f_w$ ) and oil recovery, which allows us to extrapolate the presumed straight-line trend to any desired water cut in order to determine the corresponding oil recovery. In our case, this extrapolation yields an oil recovery of approximately 34.5 MMSTB, which is consistent with the result obtained by the hyperbolic extrapolation of the cumulative oil curve (34.6 MMSTB).

Another way to estimate remaining reserves is using "estimated ultimate recovery" (or *EUR*) analysis on the production performance for each well. *EUR* analysis is a semi-empirical technique that consists of extrapolating the production rate ( $q_o$ ) versus cumulative production ( $N_p$ ) curve to  $q_o=0$ . The corresponding value of  $N_p$  at  $q_o=0$  represents the "recoverable" oil ( $N_{p,max}$ ). In Figure 80 we illustrate this process for well Permit #1591. For the wells at Womack Hill Field the recoverable oil estimate is often close to current cumulative production because of the lateness in the productive life of an individual well (as well as the field). We performed this analysis on all of the producing wells in the field as a mechanism to estimate the remaining field-wide recoverable oil at current conditions.

In Figure 81 we summarize the *EUR* analysis results by plotting the cumulative oil production ( $N_p$ ) for each well against its corresponding *EUR*. As expected, a strong correlation of  $N_p$  with *EUR* emerges because of the mature status of the field. The slope of this curve represents the percentage of oil produced with respect to the total recoverable oil. As a fieldwide average, we estimate that 94 percent of the total oil at current conditions has been recovered—which means that 6 percent of recoverable oil remains to be produced.

**Analysis of Reservoir Performance—Field-Scale Flow Behavior.**—Early in the productive life of Womack Hill Field a concept emerged that the field had two compartments (or areas)—one in the west and one in the east. For field management purposes, and based on the belief that a geological division exists in the field, Womack Hill Field has been developed and managed in two

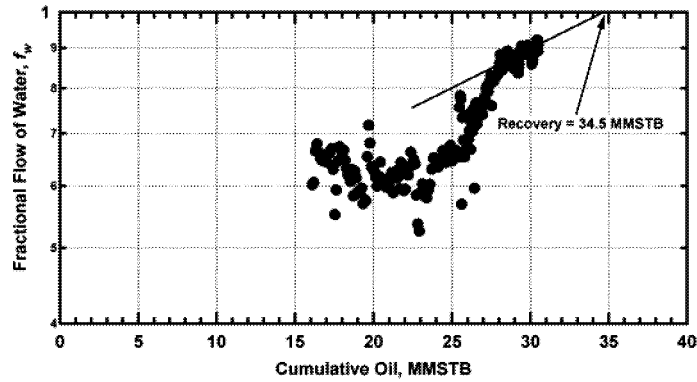


Figure 79. Logarithm of the fractional flow of water versus cumulative oil production. The straight-line extrapolation at  $f_w=1$  yields an oil recovery of 34.5 MMSTB.

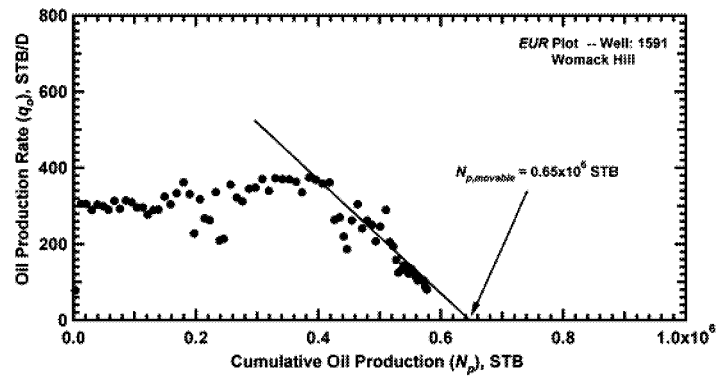


Figure 80. EUR plot for Well 1591 — Womack Hill Field. Cumulative production is approaching total recoverable oil.

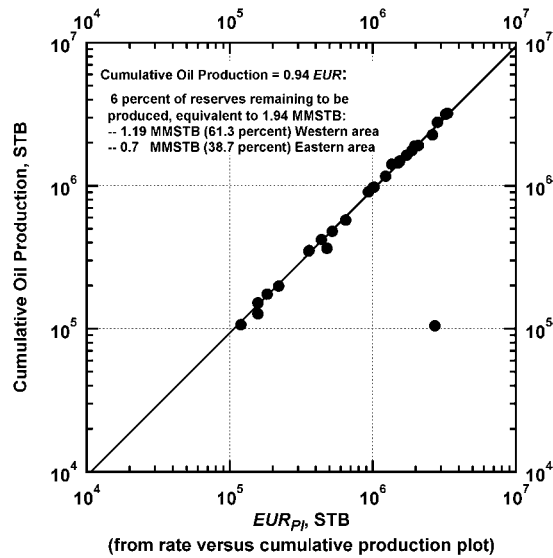


Figure 81. Summary of EUR Analysis — Womack Hill Field. Strong correlation — likely a consequence maturity of production.

independent areas. It appears, however, that some pressure support is benefiting wells in the Eastern area, while all of the injection wells are in the Western Unit area.

A "flow barrier" in the Womack Hill Field area was identified early in the development of the field and was used as demarcation to separate the Western Unit area from the Eastern area. It is important to note that all of the water injection wells are located in the Western Unit area, so the water injection influence should not affect the Eastern area if a "barrier" exists. Figure 71 shows that the water injection rate has always exceeded the oil production rate—the cumulative water injected has reached 42 MMSTB, which is 11.5 MMSTB higher than the oil withdrawal. So the amount of injected water appears to be more than sufficient to maintain the reservoir pressure. Figures 82 and 83 present the limited pressure data available for the Western Unit and Eastern areas, respectively. Figure 82 illustrates clearly the pressure increase (or maintenance) in the Western Unit wells due to the water injection. However, the pressure maintenance has not been as effective in the Eastern area (Fig. 83), where the pressure in most of the wells has declined (although there are exceptions). This pressure data suggests that a geological separation could exist between the two areas—but it does not serve to confirm this concept. As noted, some of the wells in the Eastern area have experienced pressure maintenance—which suggests that the "barrier" is not completely sealing and that some flow paths may communicate to both areas.

Figure 84 presents the historical field-wide oil production and water injection rates. We first note that from the beginning of the water injection program up to about year 20 (1990), the reservoir performance was approximately a 1:1 ratio (the volume of injected water per volume produced oil). Since then the injected water has increased steadily and the oil production has declined. This sharp change almost certainly cannot be attributed to a reservoir mechanism—it is far more likely to be a consequence of operational practices. In fact, in 1990 the operator first installed hydraulic "jet pumps" in the production wells in order to improve the productivity—but as revealed in Figure 84, this installation has not been as effective as desired.

We also consider the phenomenon of "overproduction" of water where the ratio of water production rate to water injection rate ratio versus time is presented in Figure 85. This profile shows

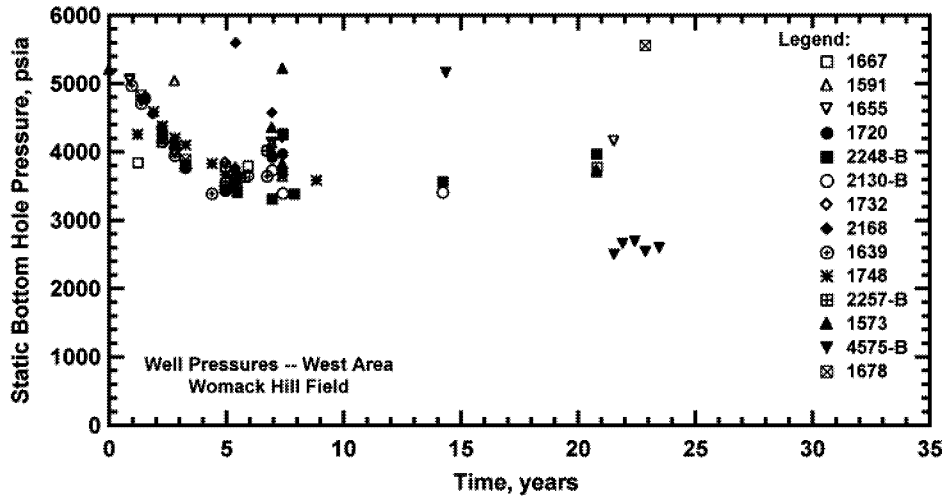


Figure 82. Well pressures in Western Area — Womack Hill Field. The effect of water injection is clearly shown from year 5.

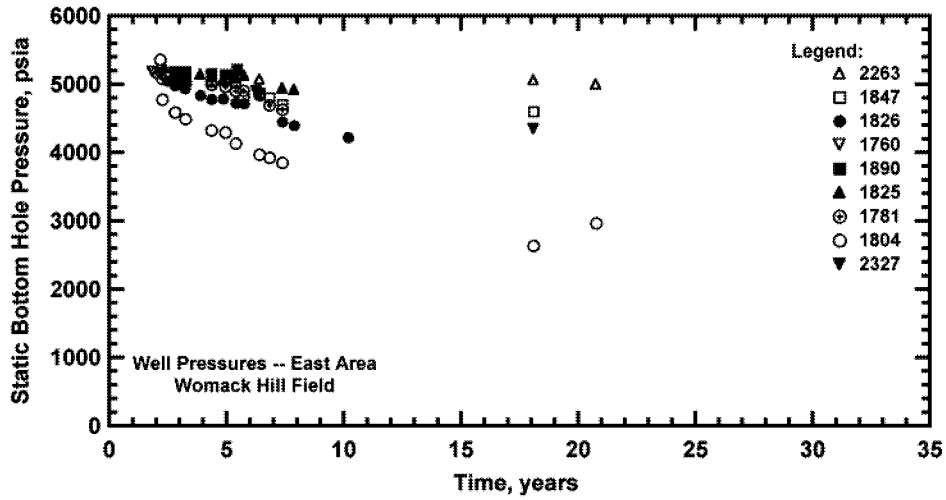


Figure 83. Well pressures in Eastern Area — Womack Hill Field. Despite water injection, well pressures for some wells are declining "normally," while other wells appear to be receiving pressure support.

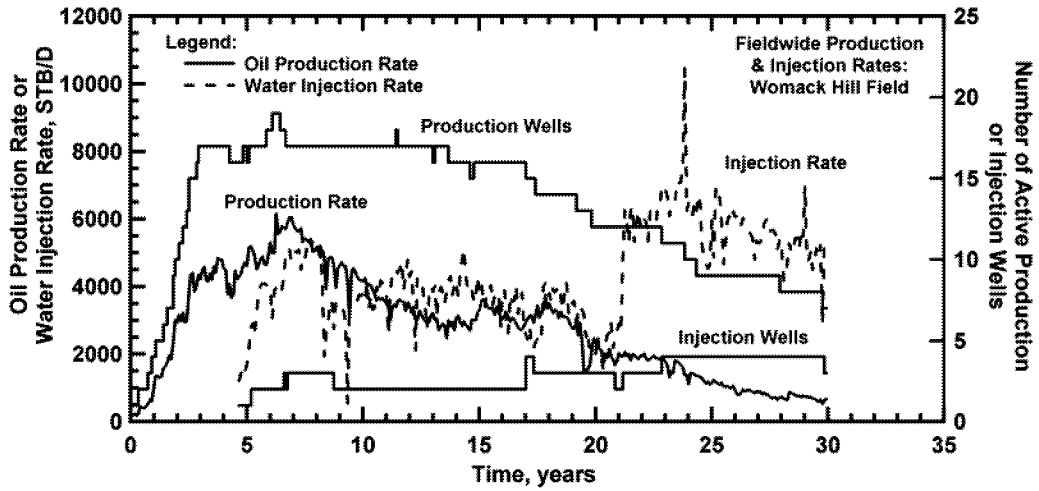


Figure 84. Water injection and oil production rate profiles — Womack Hill Field. Water injection appears to be less efficient over the last 10 years.

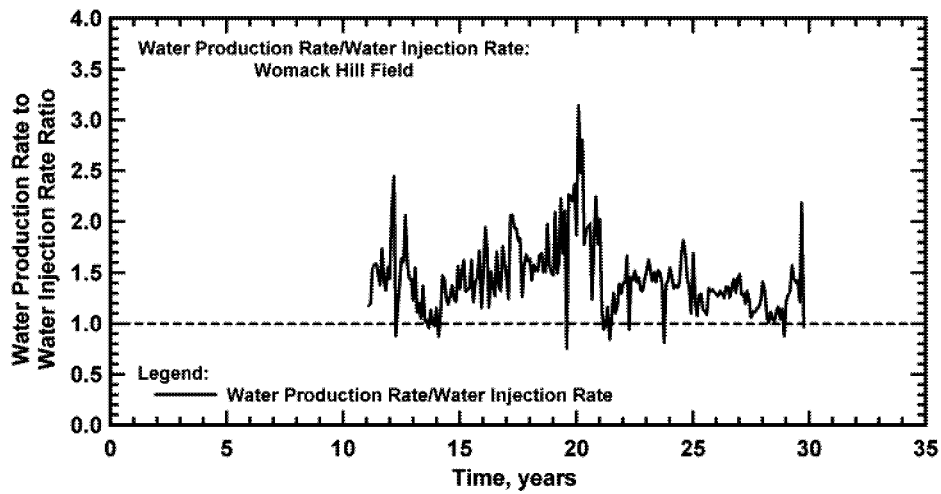


Figure 85. Water production rate to water injection rate ratio — Womack Hill Field. The higher volume of produced water is likely due to water coning or a strong water influx.

a ratio over unity—so the volume of produced water is higher than the volume of injected water. Water coning, water channeling, and/or strong water influx can cause this phenomenon. Empirical evidence from a site visit to Womack Hill Field suggests the possibility of water channeling and water influx. A numerical simulation model should consider the causes and effects of this "overproduction" of water phenomenon.

**Analysis of Reservoir Performance—Decline Type Curve Analysis.**--To analyze and interpret the well production profiles for each well we used the decline type curve technique (Fetkovich, 1980; Doublet *et al.*, 1994; Doublet and Blasingame, 1996). The application of this methodology is based in theory, but in practice we must often apply the technique without certain data — typically wellbore pressure data are not available. This is a limitation, and it is the case for our analysis of the production performance at Womack Hill Field.

For this work we have specifically used the Fetkovich-McCray family of decline type curves (Doublet, *et al.* (1994)) where these type curves are formulated based on pseudosteady-state (or boundary-dominated) flow behavior. We use pressure-drop normalized rate functions as well as a "material balance time" formulation to eliminate the constant  $p_{wf}$  constraint associated with the original Fetkovich method. In addition, by adding the rate integral and the rate integral-derivative functions to this analysis technique, we are able to achieve much more consistent (*i.e.*, unique) type curve matches and we generally obtain better matches of transient data for the estimation of formation flow properties.

The software *WPA* (Blasingame, *et al.*, 1998) provides us a mechanism to apply this technique. The input data required for the *WPA* program consists of a table containing the following production data functions:

Time, $t$ (days)	Flowing bottomhole pressure, $p_{wf}$ (psia)	Flow rate, $q$ (STB/D)
xxx	xxx	xxx

In addition to production data, we also require reservoir and fluid properties, as well as an estimate of the initial reservoir pressure. Once the analysis process is completed in the *WPA* software, we should obtain estimates of the following parameters:

Flow terms:	Volumetric results:
<ul style="list-style-type: none"> <li>•Effective permeability, <math>k_p</math>, md</li> <li>•Skin factor for near-well damage/stimulation, <math>s</math></li> <li>•Fracture-half length, <math>x_f</math></li> </ul>	<ul style="list-style-type: none"> <li>•Reservoir radius, <math>r_e</math>, ft</li> <li>•Drainage area, <math>A</math>, acres</li> <li>•<math>Nc_t</math> product, STB/psi</li> </ul>

Figure 86 illustrates the type curve match we obtained for Well 1847. As shown, the  $q/\Delta p$ , the "integral" of  $q/\Delta p$ , and the "integral-derivative" of  $q/\Delta p$  are matched against the corresponding type curves. We note that most of the data lie in the "boundary-dominated flow region"—which is logical since the "transient flow region" contains few (if any) representative data (due to the proration of the field). Further, a lack of wellbore pressure data amplifies the problems encountered with the transient flow region—we simply have to provide a "best guess" analysis in this region, which really implies that the "flow property" results are qualitative at best.

As noted, we can only use the transient "flow property" results qualitatively, but we can utilize the "volumetric" results in a somewhat more quantitative fashion because for each well analyzed we clearly observe the late-time "harmonic" trend—which confirms the material balance correctness of this technique. Unfortunately, the parameters estimated using the "late time" data are tied to the value of total compressibility ( $c_t$ ) specified for the analysis—this is not a value for which we have substantial confidence. Having prescribed a value for  $c_t$  we can calculate the oil-in-place ( $N$ ) and the reservoir drainage area ( $A$ ). In this particular case we believe that it may be more valuable to report the  $Nc_t$ -product because our estimate of  $c_t$  yields estimates of  $N$  and  $A$  which are clearly unrealistic. Our intention is to obtain a "tuned" value of  $c_t$  and calibrate our analysis.

Therefore, for this case, we will use the  $Nc_t$  product as a surrogate variable to represent the distribution of oil in the reservoir. Figure 87 presents a crossplot  $EUR_{PI}$  versus  $Nc_t$  for all of wells that were analyzed. As shown, this plot shows a very strong correlation between  $EUR_{PI}$  and  $Nc_t$ , even though these results are estimated independently.  $EUR_{PI}$  is estimated from the rate versus

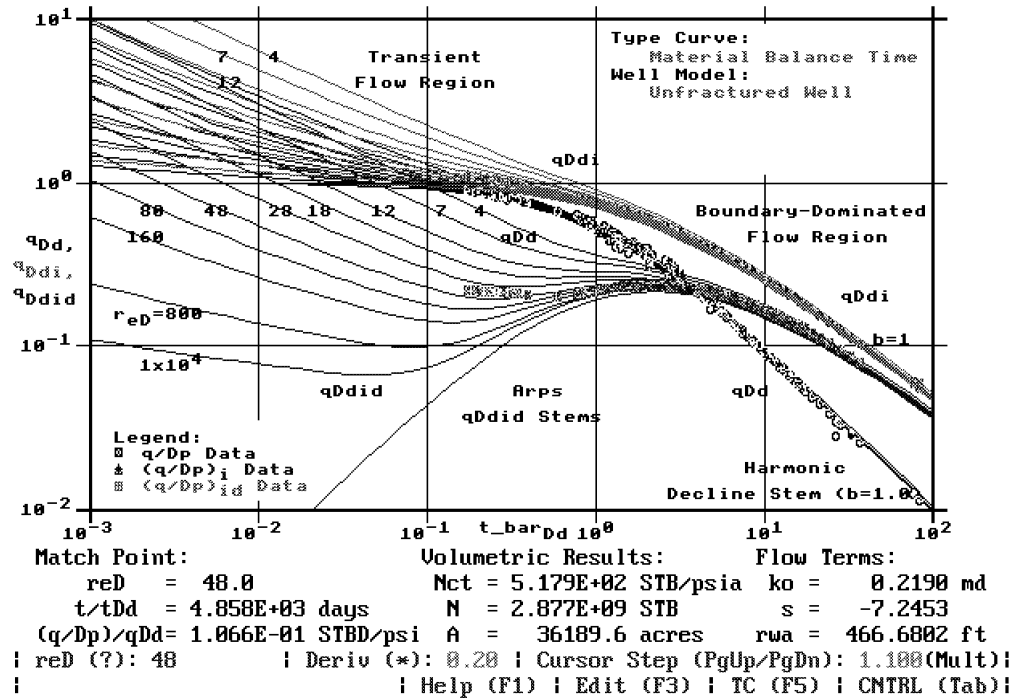


Figure 86. Decline type curve analysis — match plot, Womack Hill Field Well 1847. Most of the data lie in the boundary-dominated flow region 1848. The transient flow regime is less well-defined.

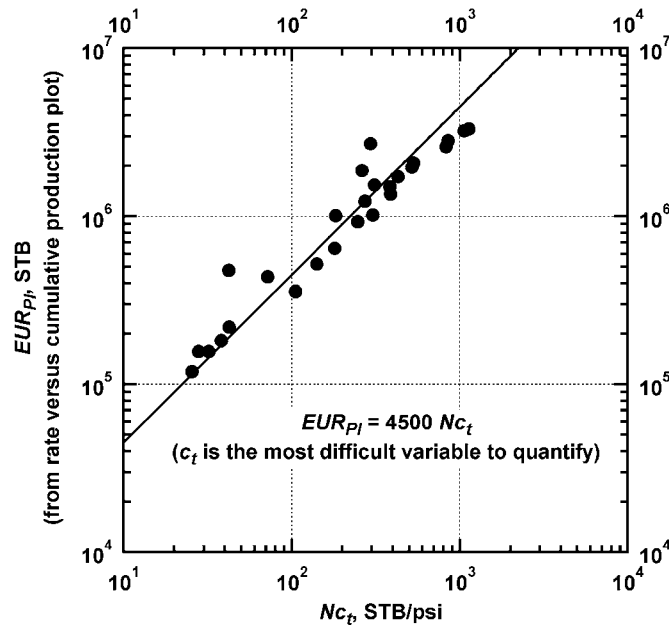


Figure 87. EUR<sub>Pi</sub> versus N<sub>ct</sub> — Womack Hill Field. EUR<sub>Pi</sub> and N<sub>ct</sub> are estimated using independent mechanisms — however, these variables are clearly correlated.

cumulative production plot and  $Nc_t$  from using decline type curve analysis. The observation of this strong relationship is logical, and it suggests that the recovery is proportional to the fluid-in-place (which is logical — but this evidence does confirm this behavior).

In Table 7, we present a summary of the results we obtained using decline type curve analysis for each well. The "flow properties," effective permeability ( $k_o$ ) and skin factor ( $s$ ) are only qualitative estimates at best due to the lack of competent data in the transient flow region. The  $N$  and  $A$  estimated depend on an accurate estimate of  $c_t$ , and these values are also suspect since a "tuned" estimate of  $c_t$  has not been defined. At this point in our work, the  $Nc_t$ -product is our most reliable variable for representing oil-in-place.

**Analysis of Reservoir Performance—Material Balance.**--As Womack Hill Field is presumed to still be producing at pressures above the bubblepoint, we elected to attempt a material balance calculation using the production and pressure data. Our goal was simply to attempt an "initial analysis," if material balance appears viable, we will refine these analyses later to include other potential drive mechanisms. The material balance equation for a slightly compressible liquid in a volumetric reservoir is given by: (Dake, 1977).

$$p_i - \bar{P} = \frac{1}{Nc_t} \frac{B_o}{B_{oi}} N_p \dots\dots\dots(1)$$

On a plot of  $\bar{P}$  versus  $N_p$  the extrapolation of the straight-line trend to  $\bar{P} = 0$  yields the "recoverable" oil,  $N_{p,max}$ . Figure 88 presents a material balance plot constructed for Womack Hill Field. This plot yields an estimate of  $N_{p,max}$  of 76 MMSTB—which appears to be quite high. The slope of the straight-line trend can be used to estimate the original oil-in-place ( $N$ ), but once again an accurate estimate of  $c_t$  is required. This high estimate of recoverable oil suggests that the reservoir pressure is too high for a volumetric model, and may be receiving external energy support. The most logical source of this "external" energy would be an aquifer—whose characteristics should be considered during the construction of the reservoir simulation model. Again, this exercise

Table 7. Summary results for decline type curve analysis — Womack Hill Field.

Well permit	Region	$N_p$ (STB)	$Nc_t$ (STB/psi)	$N$ (STB)	$A$ (acres)	$k_o$ (md)	$s$
1639	West	977305	183.30	1.02E+07	6688.80	0.1833	-6.401
1655	West	1772155	261.80	1.46E+07	11135.80	0.1235	-7.195
1667	West	1168145	272.80	1.52E+07	12443.70	0.3950	-1.372
1760	East	349215	104.60	5.81E+06	10697.30	0.2792	-6.125
1781	East	1923054	529.90	2.94E+07	48353.80	0.3605	-4.577
1804	East	3217813	1083.00	6.01E+07	80988.80	0.7045	-2.309
1825	East	364831	42.10	2.34E+06	3184.90	0.1854	-5.519
1826	East	981820	304.00	1.69E+07	65494.40	0.2521	-7.542
1847	East	1901848	517.90	2.88E+07	36189.60	0.2190	-7.245
1899	East	152230	32.10	1.78E+06	4096.80	0.0821	-6.695
2109	West	1637015	420.10	2.33E+07	27513.00	0.7026	-5.904
2327	East	421841	71.80	3.99E+06	30376.40	0.6467	-5.954
2341	East	1417137	387.30	2.15E+07	41360.70	0.4650	-7.312
3452	East	481699	141.30	7.85E+06	16665.20	1.2105	-1.518
3657	East	127460	29.10	1.62E+06	8168.80	0.3776	-6.501
1732-B	West	198755	42.40	2.36E+06	2675.70	0.2383	-4.739
2130-B	West	2793767	800.00	4.45E+07	194229.70	0.7249	-10.011
2248-B	West	3177666	1057.00	5.87E+07	41355.40	0.2514	-7.851
2257-B	West	1443996	382.30	2.12E+07	34397.20	0.6226	-7.220
4575-B	West	2280222	829.00	4.61E+07	66367.20	0.5044	-7.549
SWD-1890-83-3	East	106874	26.60	1.48E+06	2221.00	0.0689	-7.775
SWD-2263-85-5	East	352008	104.30	5.79E+06	44128.90	1.2025	-6.834
WI-1573-69	West	105302	294.30	1.64E+07	11621.30	0.1041	-6.677
WI-1591-77-1	West	576835	180.10	1.00E+07	6043.80	0.1648	-3.537
WI-1678-93-8	West	1489082	309.90	1.72E+07	20128.80	0.4208	-4.139
WI-1720-77-2	West	174337	38.10	2.12E+06	1699.30	0.1139	-6.255
WI-1748-92-1	West	909261	247.10	1.37E+07	16818.90	0.3155	-5.658

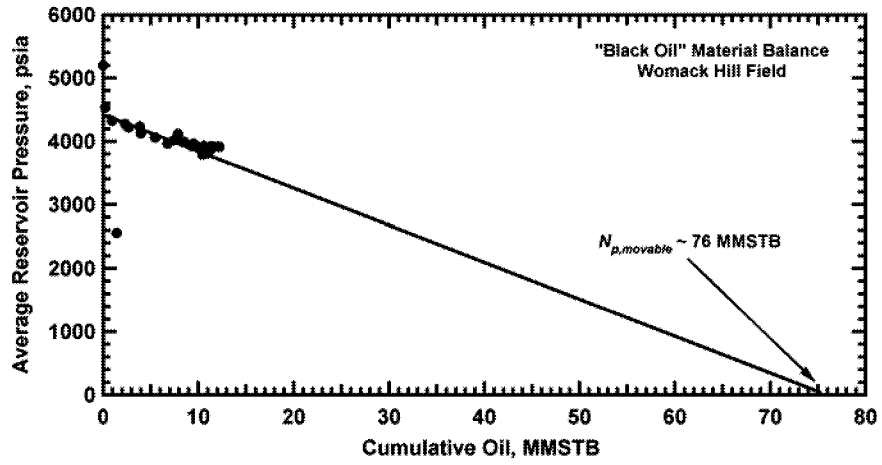


Figure 88. Material balance plot — Womack Hill Field. The straight-line trend produces an estimate of oil-in-place that is presumed to be high due to injection support and possible water influx.

was more for the benefit of confirming the external energy than for estimating the oil-in-place—this work will continue.

**Integration of Results.**--In this section, we present the integration of the results we obtained from the petrophysical and production data analyses. We utilized contour maps in order to establish spatial relationships of reservoir properties and to compare performance-derived parameters with other data such as geological and petrophysical descriptions. Reservoir structure based on the "top of structure" for the Upper Smackover sequence shows two ridges, one in the Eastern area and another toward the central-Western Unit area. Most of the wells are located on these ridges, the water injection wells are located on the periphery in the Western Unit area of the reservoir. The anhydrite of the Buckner Member is presumed to provide the reservoir seal, and laterally, the reservoir is bounded on the south by a fault and controlled on the west, east, and north by the water-oil contact.

In Figures 89 through 91, we present the porosity distributions generated using the statistical analysis of data for Flow units A, B, and C, respectively. The contours show a homogeneous trend in Flow unit A; however, in Flow unit C there is insufficient data to produce a meaningful map. From Figures 89 to 91, we can conclude that a porosity estimate of 18 percent would serve as a reasonable average value for the entire Smackover sequence (Flow units A, B, and C). Likewise, Figures 92 to 94 present the permeability distributions generated using the statistical analysis on the core data given for Flow units A, B, and C. Again, the shortage of data in Flow unit C prohibits us from making any conclusions. However, in Flow units A and B the contours show a apparent permeability contrast between the Eastern and Western Unit areas.

Permeability reaches a maximum for the field just on the Western Unit ridge area and its minimum on the south of the Eastern ridge area. The pressure data suggest that a flow barrier may exist between both areas, and the permeability distributions (Figs. 92 to 94) tend to confirm this hypothesis. This permeability contrast has to be considered as the "barrier" between the two areas. Using pressure transient tests (production or injection wells), we can attempt to quantify the

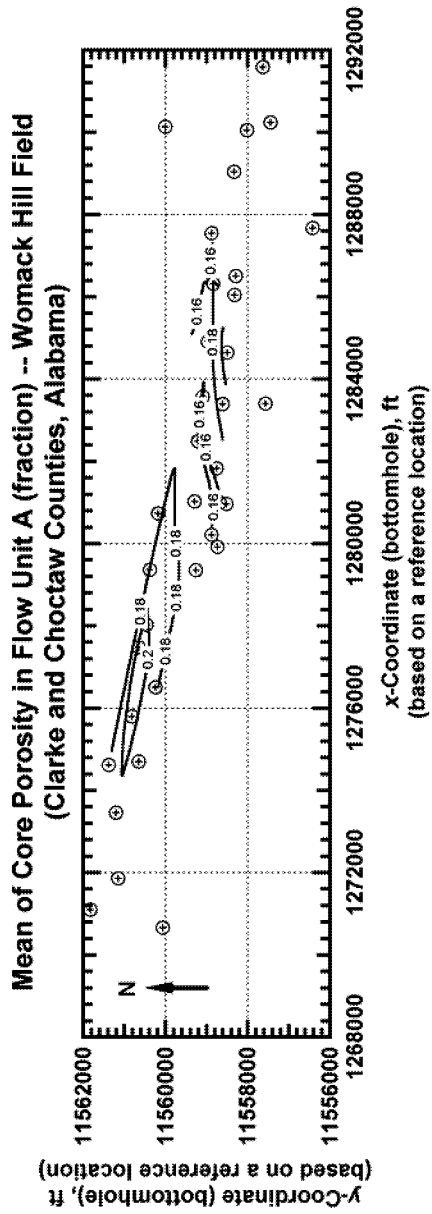


Figure 89. Flow Unit A — Core porosity distribution obtained from statistical analysis (histogram for each well) —the contours tend to indicate a homogeneous reservoir model.

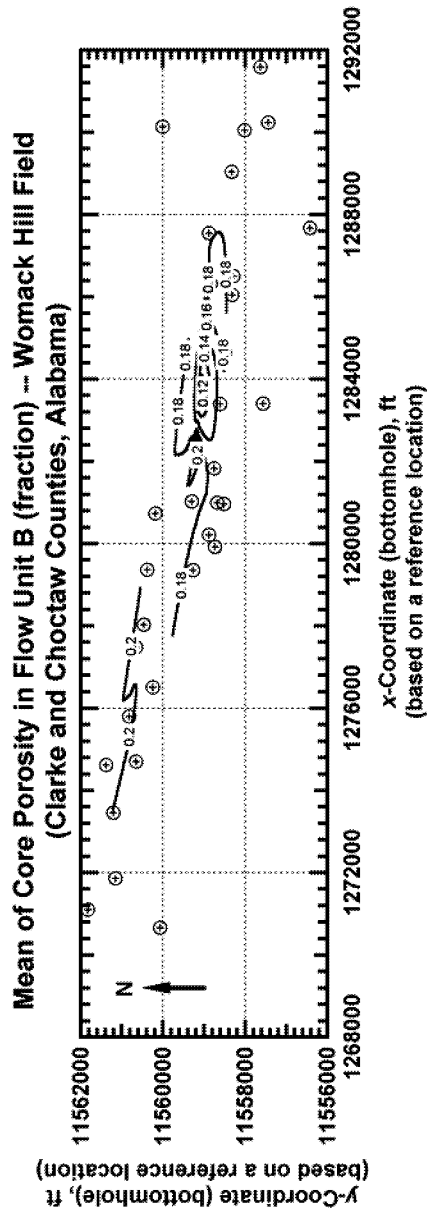


Figure 90. Flow Unit B — Core porosity distribution obtained from statistical analysis (histogram for each well) —the contours tend to indicate a homogeneous reservoir model.



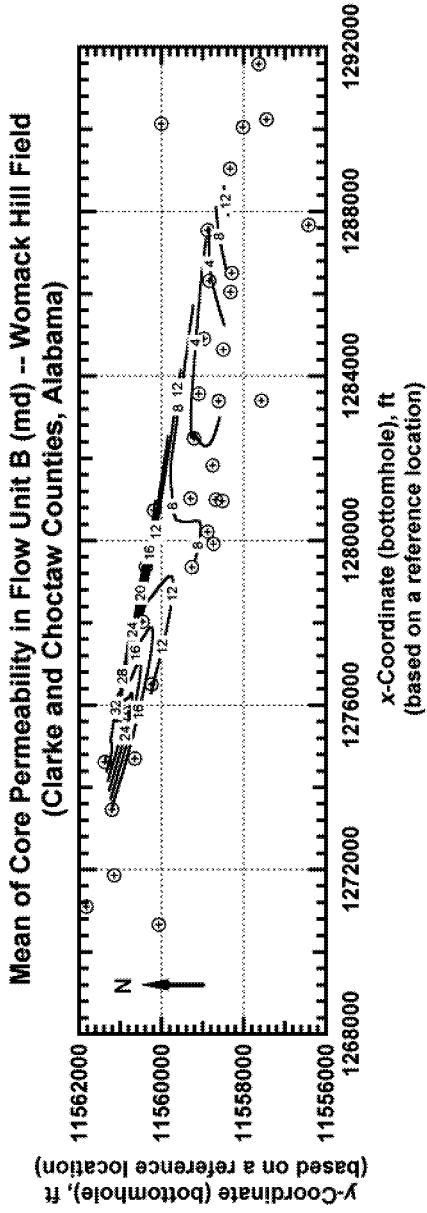


Figure 93. Flow Unit B — Core permeability distribution obtained from statistical analysis (histogram for each well) — a permeability contrast is evident between the Eastern and Western areas.

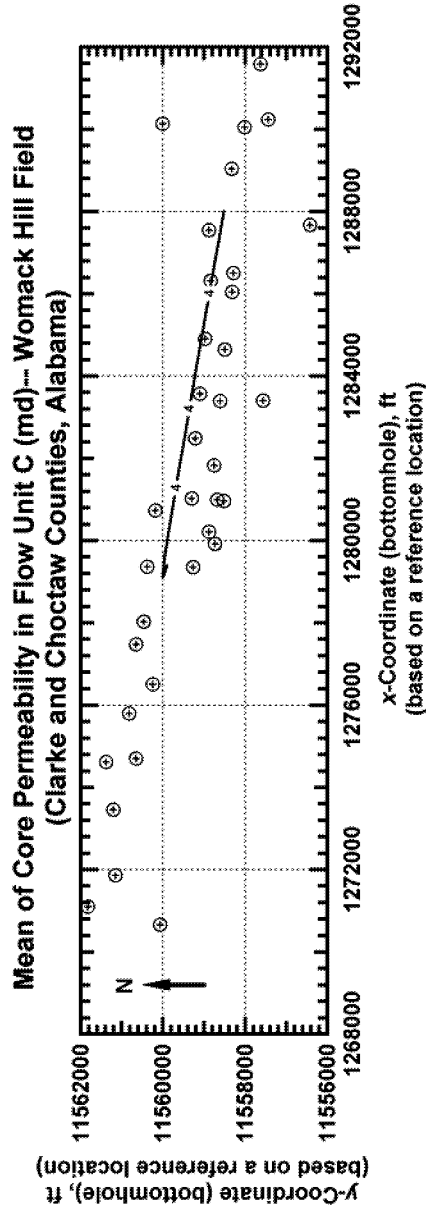


Figure 94. Flow Unit C — Core permeability distribution obtained from statistical analysis (histogram for each well) — insufficient data.

existence/influence of this of this barrier. In summary, the "barrier" could simply be a reduction of permeability that was caused by a change in mesoscopic heterogeneity (depositional facies), a change in microscopic heterogeneity (diagenetic changes), or a combination of the two processes—at this point in time we simply confirm the apparent existence of this flow "contrast."

Figure 95 shows the distribution of the cumulative oil production throughout the field area—this plot shows that the best production is in the Western Unit area (where the formation is thicker and permeabilities are higher). In the Eastern area the oil production is less, presumably as consequence of the lower reservoir quality. Figure 96 shows the 3-month initial oil rate distribution, this variable behaves consistently throughout most of the reservoir area (probably because of regulatory constraints), and only a few values lie out of the average range (350-450 STB/D)—these values are in the margin of the Eastern area, where the gross pay thickness is relatively small.

A map of the *EUR* estimated from the rate versus cumulative production plots is presented on Figure 97; this map reveals that the highest recovery is in the vicinity of the Eastern ridge area, reaching a maximum value of 3 MMSTB per well. However, this higher recovery is very localized, and is surrounded by contours of much lower magnitudes. Towards the west, the distribution is more consistent and averages 1.5 MMSTB per well. As we saw earlier, *EUR* and the  $N_{C_f}$ -product correlate quite well—on Figure 98 we can see that the area with higher  $N_{C_f}$ -products generally coincides with the area of higher *EUR*. The distribution reflects the fact that most of the oil-in-place lies in the area associated with the two ridges in the field. Outside of this area, the  $N_{C_f}$ -product is significantly lower. Finally, we note in Figures 98 and 99 evidence of irregular performance behavior at Womack Hill Field as the zone with higher *EUR* and  $N_{C_f}$ -products is in the area of lower permeability and variable reservoir thickness.

**Reservoir Modeling (Simulation).**--Reservoir simulation efforts have been initiated and have focused on quantifying the sources of reservoir energy. Qualitatively we believe that fluid compressibility, water injection, and aquifer influx provide various components of reservoir energy.

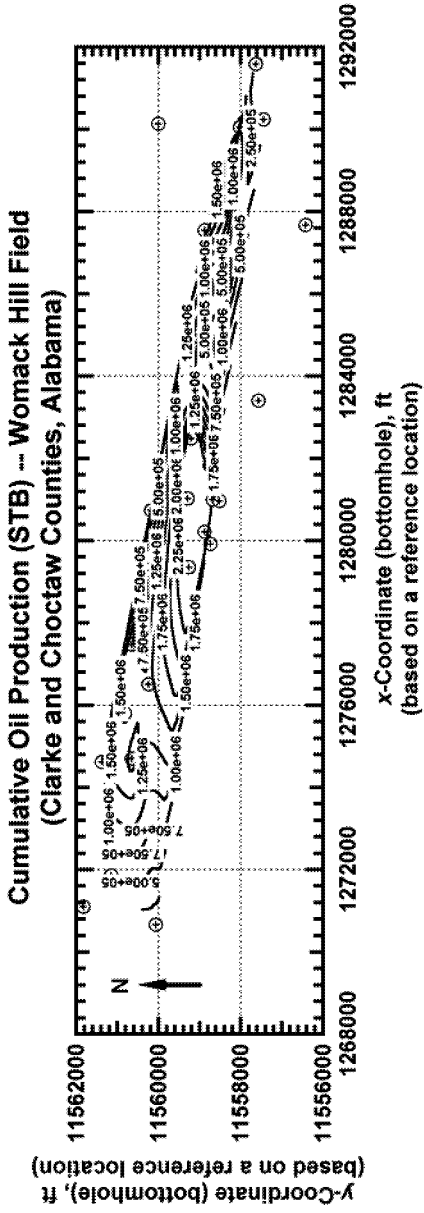


Figure 95. Distribution of cumulative oil production — the best productive area is the Western part of the structure, this area is presumed to have the highest reservoir quality.

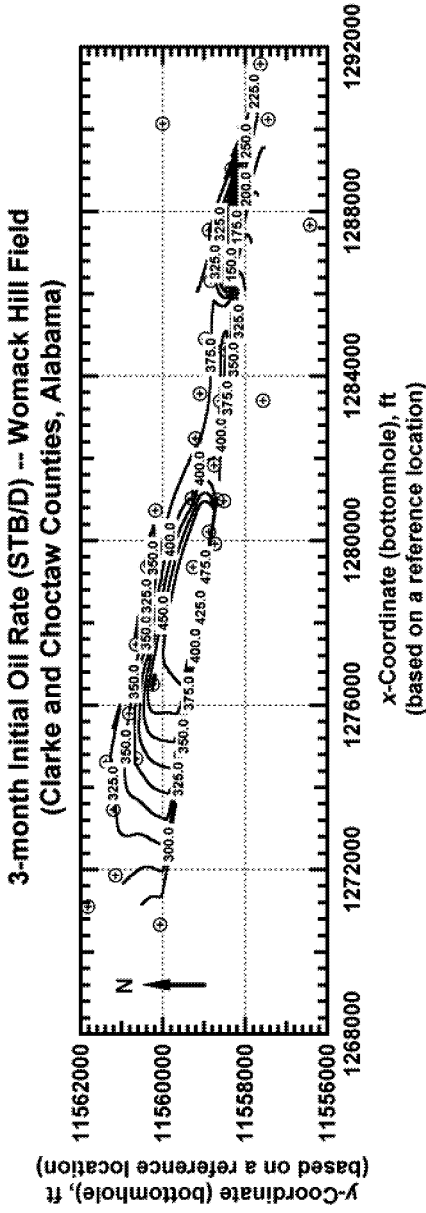


Figure 96. Distribution of the 3-month initial (oil) production (IP) — the trend is consistent throughout most of the field, with the exception of the Eastern edge of the structure.



We are therefore trying to establish the strength and orientation of the aquifer. In simulations made without an aquifer, the average reservoir pressure declines to very low levels (under 1000 psi) which would not have yielded the flow rates we observed in the production wells

The available static bottomhole pressure data suggests that the average reservoir pressure in the model should not drop below about 3000 psia. This is also consistent with the fieldwide gas-oil ratio, which has remained approximately constant over the life of the field. If the average reservoir pressure dropped below the bubblepoint (1938 psi) we would expect an increase in the field gas-oil ratio with time. In the current model, using a strong aquifer causes the model to suffer convergence failures (*i.e.*, the computational scheme is unable to solve the equations modeling fluid flow with sufficient accuracy and a reasonable timestep length).

Based on production data, the distribution of water influx across the reservoir is not believed to be uniform. Water production is highest in a group of wells (Permits #1639, #1655, #1667, #1678 and #2109) in the western portion of the field. This non-uniformity in the distribution of water influx may be due to discontinuities in the nonporous layers between the productive zones. There is insufficient well control to fully characterize the continuity of these reservoir layers, so additional simulations are being performed to assess the effect of the continuity of the nonporous layers on the production history. This continuity issue is also likely to contribute to the convergence failures mentioned above.

We are also trying to ascertain the initial location of the water-oil contact. The performance of the field in terms of water production is very sensitive to this estimate. However, the estimates of the water-oil contact significantly under-predict water production for the field.

Water-oil contact depth, ft	Cumulative water production, MSTB
11340	2603
11360	1210
11380	672

Another problem we face in matching the volumes of produced water is that apparently no water production data are available until after 1982. We know that substantial volumes of water were produced prior to January 1982 as some wells had very high water rates (*e.g.*, Well 1639,  $q_w = 13,300$  STB/D). This means that we can not necessarily "fine-tune" the relative permeability profiles by matching water breakthrough times.

The history matching process in the simulation process has been initiated. Our first target is to match field-wide performance (*i.e.*, cumulative produced oil, water and gas). Once we are satisfied with this match we will then pursue matches of individual well performance.

### ***Task RC-3.--Microbial Characterization***

**Description of Work.--**This task will determine whether *in-situ* micro-organisms are present in the Smackover carbonate reservoir at Womack Hill Field and will determine through laboratory experiments the ability of these microbes to produce a single by-product (acid) by supplying them with only enough nutrients to sustain the cells but not enough to support cell proliferation.

**Rationale.** Researchers at Mississippi State University have demonstrated the cost-effectiveness of utilizing the growth of indigenous microbes in enhancing the efficiency of an active waterflood for the recovery of incremental oil. The technology involves injecting a regulated stream of nutrients into a sandstone reservoir at a subsea depth of -2,300 ft to stimulate indigenous microbe growth. Cell proliferation by these micro-organisms acts to reduce the flow of injected water in more permeable zones of the reservoir by selective plugging, thereby diverting the water to other areas of the reservoir. This diversion and altering of flow patterns in the reservoir serve to enhance the sweep efficiency of the waterflood. This technology will be expanded upon in this study by using the ability of these microbes to produce a single by-product (acetic acid).

This immobilized enzyme technology will be applied to the carbonates at a depth of 11,300 ft in Womack Hill Field. It is anticipated that the acetic acid will act to break down the Smackover reservoir through dissolution thereby creating enhanced reservoir connectivity.

**Microbial Identification and Characterization.--**The objectives of this subtask are to characterize the microflora present in the Womack Hill Oil Field in terms of their ability to convert

alcohols to acids and to determine the nutritional requirements to maintain cells in a metabolically active state with minimal replication.

Four water samples from Womack Hill Field Well Turner 13-6 and two cores taken from the Womack Hill Field a number of years ago were analyzed for micro-organisms capable of growing at 90°C, but none were found in any of the samples. This was not unexpected since the cores had been exposed to the air for years. Likewise, it was not surprising that no micro-organisms capable of growth at 90°C were found in the water samples since micro-organisms prefer to grow attached to a substrate and consequently may be absent in the water. At the time that these samples were tested, the equipment necessary to maintain an anaerobic environment was inadequate and may have prevented the growth of strict anaerobes. A Coy® Anaerobic Flexible Vinyl Chamber, which efficiently maintains an anaerobic atmosphere, was purchased and resolved the problem.

In order to design the amounts and schedule for the introduction of nutrients into the injection wells for the field demonstration of the immobilized enzyme technology, cultures from the Smackover Formation were required. Attempts to obtain a core from a well being drilled near the Womack Hill Field were unsuccessful for several reasons. As an alternative, cuttings and drilling mud were obtained from Crosby's Creek Oil Field located in Washington County, AL, that is situated near Womack Hill Oil Field.

When attempting to isolate micro-organisms from petroleum reservoirs it is expected that most, if not all, will be in the form of ultramicrobacteria (UMB). They are extremely small in size due to lack of essential nutrients and are metabolically dormant. Specifically, the oil reservoir is deficient in nitrogen- and phosphorus-containing nutrients. Furthermore, UMB's normally cannot be reactivated using conventional strength media and more dilute media must be employed in isolation procedures. Therefore, approximately two g of the cuttings were placed into nine 60 ml volatile organic analysis (VOA) vials containing 20 ml of either  $1/2$ ,  $1/10^{\text{th}}$ , or  $1/20^{\text{th}}$  strength mineral salts broth (MSB). MSB consisted of 1 g  $\text{KNO}_3$ , 0.38 g  $\text{K}_2\text{HPO}_4$ , 0.20 g  $\text{MgSO}_4 \cdot 7\text{H}_2\text{O}$ , and 0.05 g  $\text{FeCl}_3 \cdot 6\text{H}_2\text{O}$  per liter of distilled water. The pH was adjusted to 7.0 with 10% HCl (vol/vol). Of the nine VOA vials prepared, three contained 20 ml of  $1/2$ -strength mineral salts broth (MSB), three

contained 20 ml of  $1/_{10}$ -strength MSB, and three contained 20 ml of  $1/_{20}$ -strength MSB. To each of the VOA vials, ~100  $\mu$ l of Womack Hill Oil Field crude oil was added. All 9 vials were incubated under stationary conditions at 90°C.

After 21 days of incubation, growth of micro-organisms was evident in all of the vials. It was next decided to determine if the micro-organisms in these enrichments had the ability to convert the ethanol into acetic acid. Five  $\mu$ l of 95% ethanol was added to each of the nine vials and the vials placed in the 90°C incubator to allow the ethanol to reach equilibrium between the gas and aqueous phases. The concentration of ethanol in the headspace of the vials was determined using a Varian® Model 3800 Gas Chromatograph equipped with a flame ionization detector. Additionally, carbon dioxide was determined using a Fisher dual column, dual detector, gas partitioner fitted with thermal conductivity detectors.

As shown in Figure 99, the enrichments from all three dilutions of media consumed ethanol. The difference in the amounts of ethanol consumed is probably a reflection of a difference in cell concentration rather than a difference in species of micro-organism. It should be pointed out that after four days of incubation, 6.9 mg of bicarbonate was added to each vial to react with the acids to form carbon dioxide.

Figure 100 shows the amount of carbon dioxide produced by the enrichments cited above. As may be seen, a large quantity of carbon dioxide was produced by the enrichments and was considerably more than could be accounted for by the reaction of acetic acid with the carbonate. This additional carbon dioxide could be derived from utilization of the ethanol or oil. Also, carbon dioxide may have been derived from organic acids produced from the oil directly reacting with the carbonate.

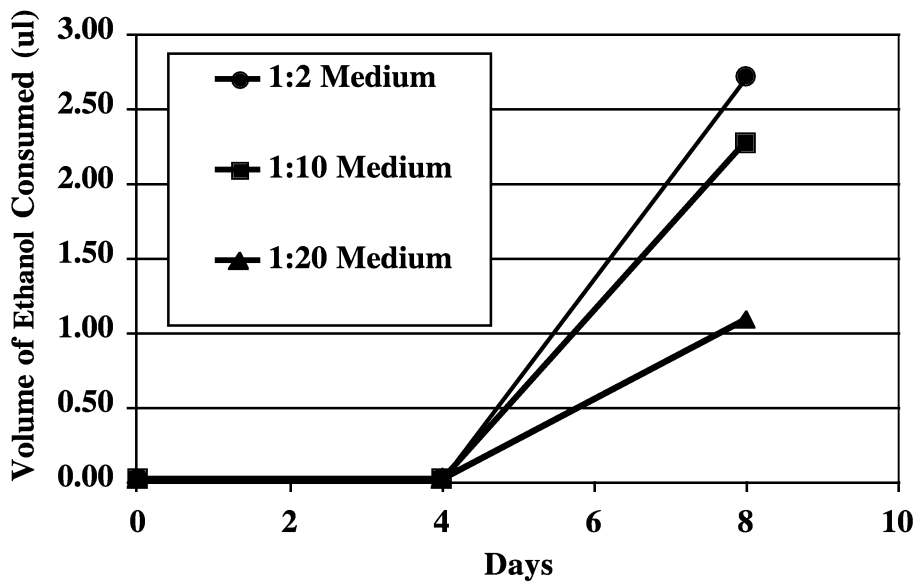


Figure 99. The utilization of ethanol by enrichment cultures.

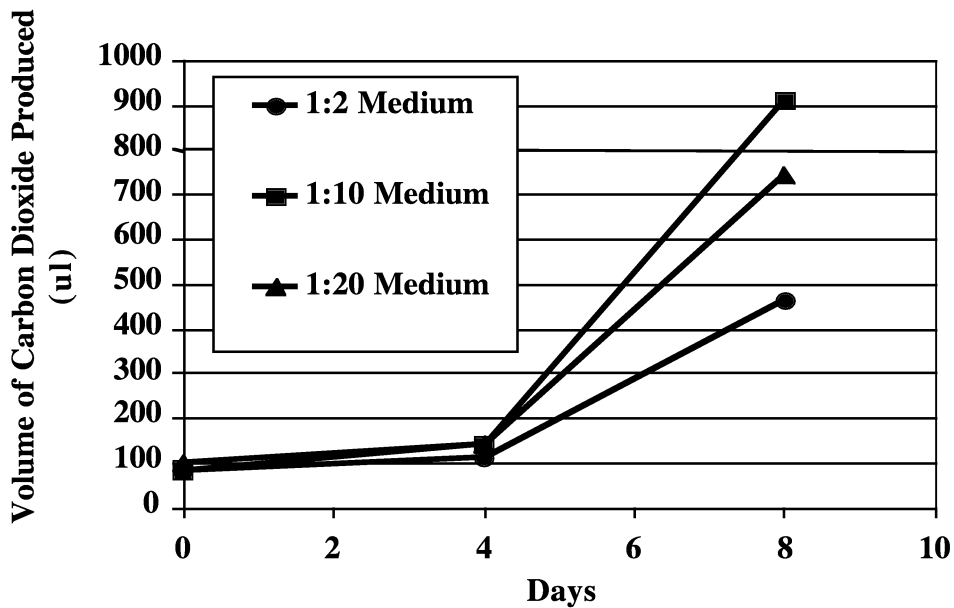


Figure 100. The production of carbon dioxide by enrichment cultures.

These enrichment cultures were subcultured into new medium with oil. Also, the original cultures were again tested for their ability to utilize ethanol and the results are given in Table 8. As may be observed, all of the cultures consumed ethanol.

Table 8. Utilization of Ethanol by Enrichment Cultures Growing at 90°C Under Anaerobic Conditions

MSM/H <sub>2</sub> O (Dilution)	Ethanol Utilization in 5 Days (%)	Ethanol Utilization in 9 Days (%)
1:2	75	88
1:10	74	85
1:20	60	82

Samples of these enrichments were examined using a confocal laser-scanning microscope. In transmitted light, the bacteria are visible within menisci of oil as shown in Figure 101. These bacteria auto fluoresce (fluoresce without staining) when stimulated with the laser (see Figure 102). A reverse negative picture of the cells is given in Figure 103.

These findings are highly encouraging and suggest that micro-organisms capable of producing acetic acid from ethanol will be present in the Womack Hill Oil Field reservoir and that they can be induced to grow and be metabolically active at the temperature in the reservoir. Nevertheless, cores from near the Womack Hill Oil Field and/or from the same producing formation are still being sought.

Ultimately, the ability of the microflora to grow and produce acetic acid from ethanol in live cores needs to be determined. Toward this end, a core plug testing system designed to operate at 90°C has been fabricated and is depicted in Figure 104.

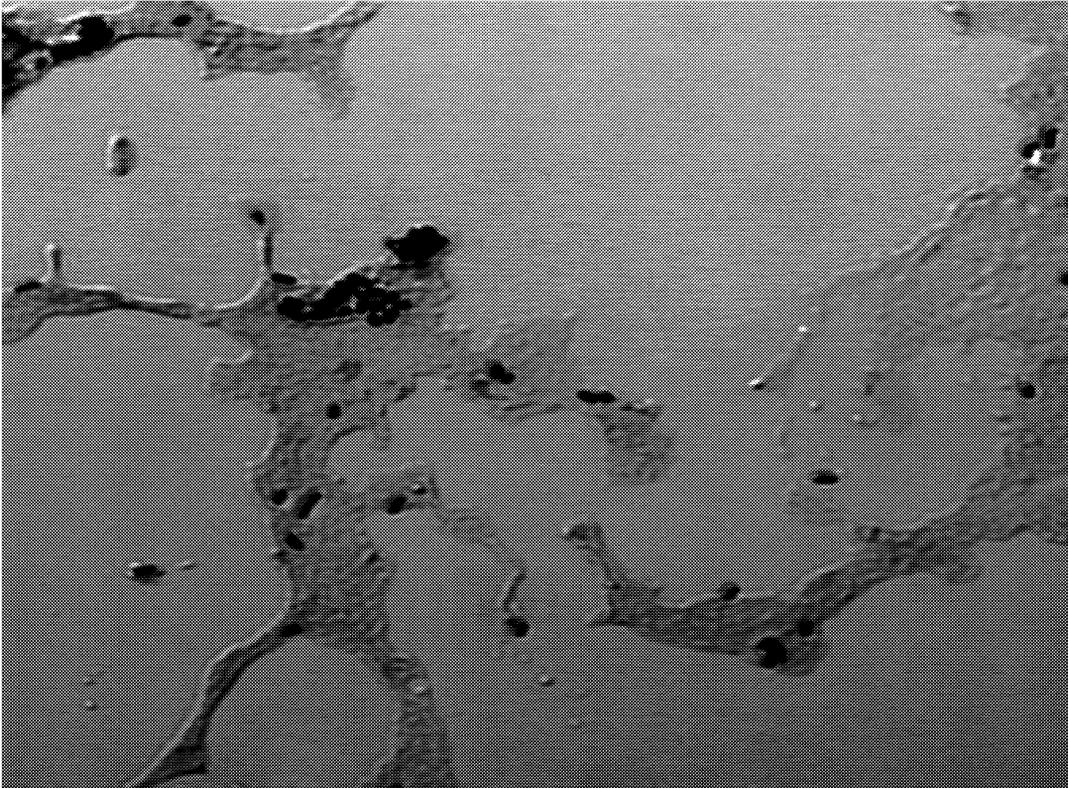


Figure 101. Laser confocal microscope image of oil-degrading grown anaerobically at 90°C.

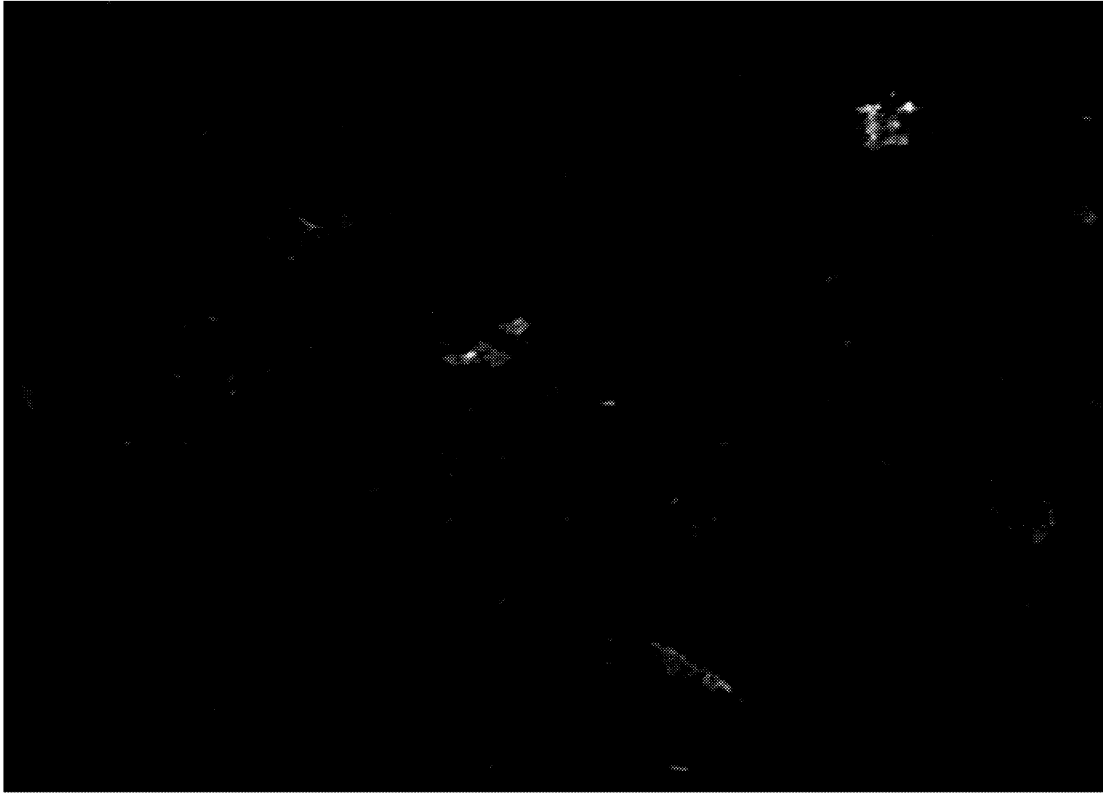


Figure 102. Auto fluorescence of bacteria grown anaerobically at 90°C when stimulated by laser using a confocal laser-scanning microscope.

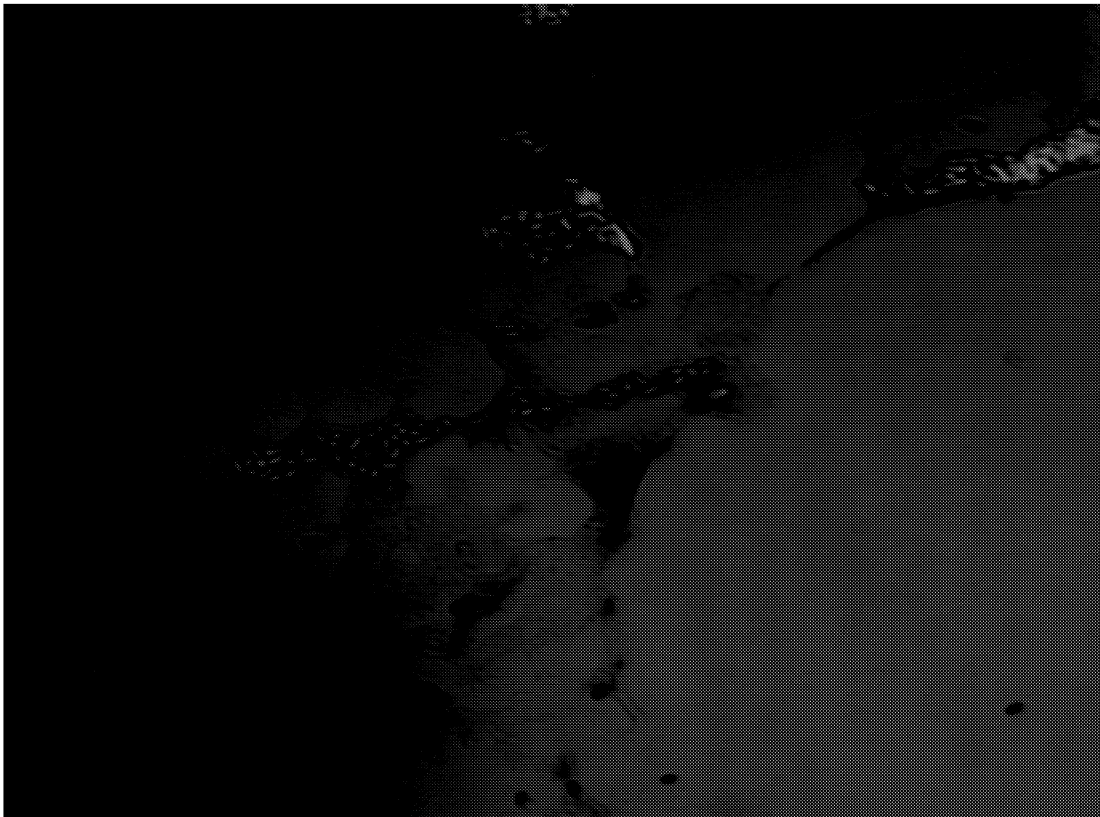
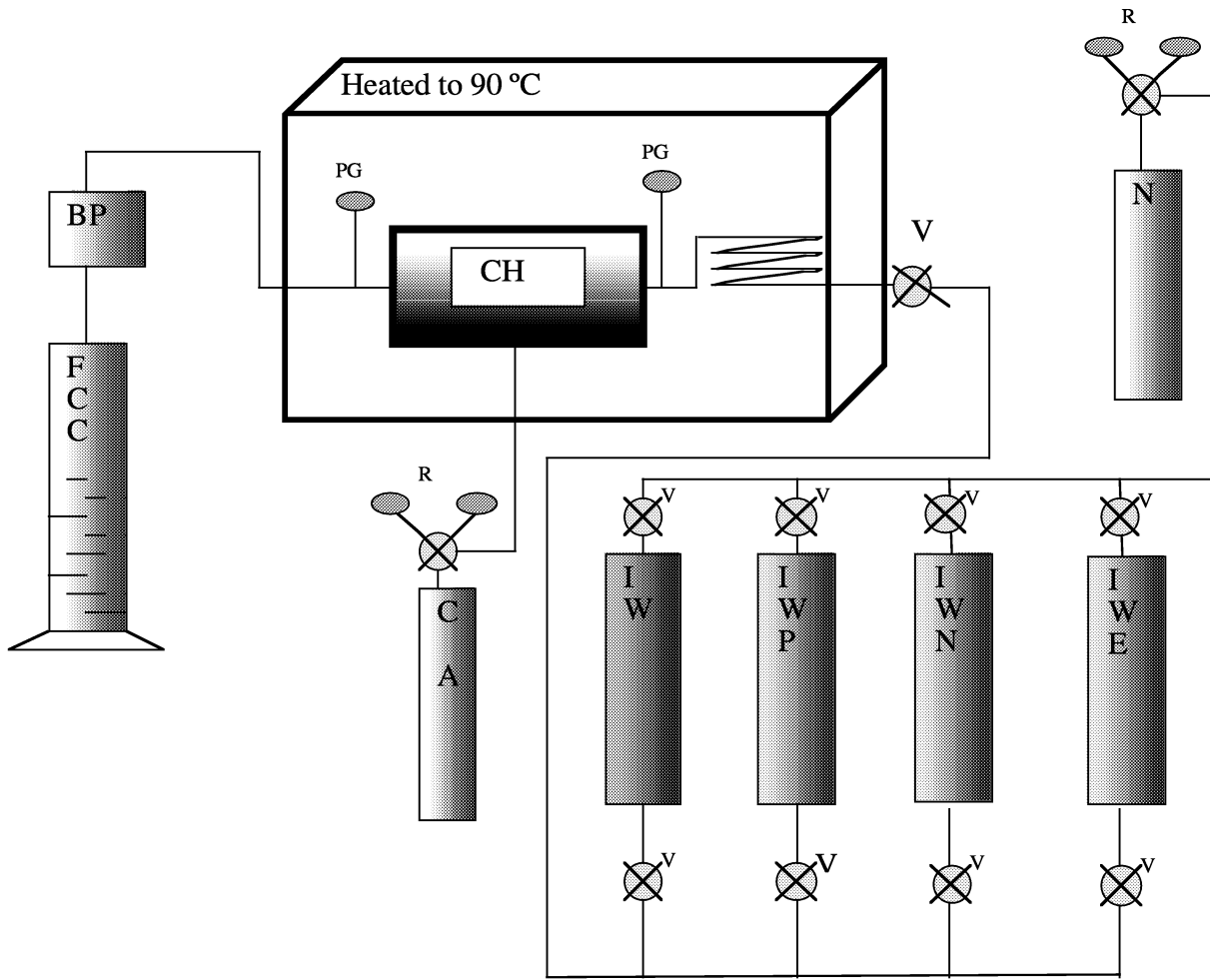


Figure 103. A reverse negative confocal laser-scanning microscope image oil-degrading bacteria grown at 90°C.



- BP:** Back Pressure regulator  
**CA:** Compressed Air  
**CH:** Core Holder  
**FCC:** Fluid Collection Container  
**IW:** Injection Water  
**IWE:** Injection Water with Ethanol  
**IWN:** Injection Water with  $\text{NO}_3$   
**IWP:** Injection Water with  $\text{PO}_4$   
**N:** Nitrogen gas  
**PG:** Pressure Guage  
**R:** Regulator

Figure 104. Diagram of the core plug testing system.

As shown, the core holder is enclosed in a 90°C incubator. All fluids entering the core will be preheated to 90°C and the effluent from the core will be collected in the Fluid Collection Container where the quantities of oil and water can be measured.

Once cores become available, experiments will be conducted in the core plug testing system shown above at 90°C to determine the effects of nutrient concentrations on the indigenous micro-organisms and evaluate the ability of these micro-organisms to convert ethanol to acetic acid. Scanning electron microscopy (SEM) will be used to gain some insight into the manner of attachment of cells in the cores and follow their reproduction. This is especially important in the immobilized enzyme technology since the goal is to maximize metabolic activity (conversion of ethanol to acetic acid) rather than cell proliferation. One of the problems in scanning electron microscopic studies of bacteria has been the preservation techniques being employed. Five techniques have been tested thus far, including air-drying, 10% glutaraldehyde fixation, standard ethanol dehydration with hexamethyldisilazane, ethanol dehydration with critical point drying, and ethanol/acetone dehydration with critical point drying.

Ethanol dehydration and critical point drying are the standard preservation procedures used for microbiological studies, and our investigation shows that bacterial cells preserved according to these techniques maintain their vital shape. However, our investigation also has shown that these techniques greatly change the morphology of the polysaccharide capsule. Simple air-drying and glutaraldehyde fixation best preserved the shape of polysaccharide biofilm. It was concluded that an accurate investigation requires two samples, one preserved by glutaraldehyde fixation for characterization of the biofilm, and one by ethanol dehydration for examination of the bacterial cells themselves.

It has been proposed that a third major species of organic material, along with bacteria and humus (or kerogen), is present in soils and rocks. Nannobacteria are 25-300 nm ovoid shapes that are observed during high-magnification SEM research. Because of their general resemblance to eubacterial cocci or bacilli, and because of their tendency to occur in chains or clusters, they have been characterized as nannobacteria. They have been implicated in the formation of mineral deposits

in terrestrial and extraterrestrial samples, and in the development of arterial plaque in the human body (Folk, 1993; McKay *et al.*, 1996; Folk and Lynch, 1997, 1998, 2001; Kirkland *et al.*, 1999; Folk *et al.*, 2001).

It would be difficult to find a more contentious geologic or biologic topic than the existence or non-existence of these nanobacteria. Critical attention from the microbiology community has been focused on the small size of the nanobacteria, which are often 1/1000<sup>th</sup> the volume of typical bacteria. Nonetheless, confirmation of the biological affinity of some of these features, especially the larger ones, has been made using molecular biology techniques (Spark *et al.*, 2000). However, laboratory experiments have shown that the suspect textures also can be formed by mineral precipitation in an organic-rich, though abiotic, environment (Kirkland *et al.*, 1999). Our current research also shows that textures very similar to the purported nanobacteria can be produced by dehydration of polysaccharide capsule or biofilm (Fratesi and Lynch, 2001). The relationship between the textures, different minerals, and different organic compounds requires further research.

#### ***Task RC-4. Integration of Data***

**Description of Work.**--This task will integrate the geological, geophysical, petrophysical and engineering data for the Womack Hill Field into a single comprehensive digital database for reservoir characterization, 3-D geologic and seismic modeling, 3-D reservoir simulation, cost-effective field management, and for making operational decisions in the field.

**Rationale.** This task serves as a critical effort to the project because the construction of a digital database is an essential tool for the integration of large volumes of data. This task also serves as a means to begin the process of synthesizing concepts. The database also provides a mechanism for quality control in that core and log data can be compared to geophysical, petrophysical and engineering data. These measured and calculated data are utilized in developing predictive algorithms for calculating variable values for interwell areas. The database serves as an archival record that can be updated in the future. The database is built using a spreadsheet approach. The data are accessed, managed, and analyzed by using standard industry software. The goal is to develop a relevant and transportable database.

**Data Integration.**--All geological, geophysical, petrophysical and engineering data for the Womack Hill Field acquired to date have been integrated into a comprehensive digital database.

***Task RTA-1. 3-D Geologic Model***

**Description of Work.**--This task involves using the integrated database which includes the information from the reservoir characterization tasks to build a 3-D stratigraphic and structural model of the Womack Hill reservoir. Previous reservoir models constructed for the Smackover and for the Permian carbonate shoal reservoirs in West Texas and the depositional modeling of modern ooid sand shoals of the Great Bahama Bank are used as analogs in building the 3-D stratigraphic and structural model for the Smackover shoal reservoir at Womack Hill Field.

**Rationale.** This task provides the framework for the reservoir simulation model. Sequence stratigraphy in association with structural interpretation will form the framework for the model for Womack Hill Field. The model will incorporate data and interpretations from the core and well log analysis, sequence stratigraphic, depositional history and structural studies, petrographic analysis, and diagenetic, pore system, and petrophysical and engineering studies. The purpose of the 3-D stratigraphic and structural model is to provide an interpretation for the interwell distribution of systems tracts, lithofacies, and reservoir-grade rock. This work is designed to improve well-to-well predictability with regard to reservoir parameters, such as primary depositional lithologies, diagenetic features, pore types and systems, porosity and permeability values, and heterogeneity. This layer-based model will be built utilizing data mining and associated neural networks to populate and distribute property and attribute data. Key data include structural features, physical surfaces, depositional sequences, stratigraphic event beds, sedimentary structures, carbonate textures and mineralogy, diagenetic features, pore types and throats, and porosity and permeability. Geologic modeling sets the stage for reservoir simulation and for the recognition of flow units, barriers to flow and flow patterns in the respective fields. The reservoir model and integrated database become effective tools for cost-effective reservoir management for making decisions regarding operations in the field. Accepted industry software, such as Stratamodel, will be used to build the 3-D geologic model.

**3-D Geologic Model.**--Building a 3-D geologic (stratigraphic and structural) model (Figs. 105 and 106) to illustrate the geometry of the reservoir(s) at Womack Hill Field requires understanding of the stratigraphic framework of the reservoir and the structural framework in the field area (Kerans and Tinker, 1997). The Smackover stratigraphic, sedimentologic and petrophysical information (stratigraphic units, carbonate lithologies, lithofacies, cycles, porosities, and permeabilities) obtained from core, well log and thin section studies and from core analysis are fundamental to the construction of the model for this field. These data and information from the subsurface structure and isopach maps and cross sections are integrated into the model to illustrate Smackover cycle distribution, thickness, and reservoir quality and structural configuration. The 2-D seismic data (Fig. 20) for the field provide an independent confirmation of the location of faults in the Womack Hill Field.

### **Work Planned in Year 3**

The work planned for Year 3 includes the following (Table 9):

#### ***Task RTA-2. 3-D Reservoir Simulation***

**Description of Work.**--This task builds a numerical simulation model for the Womack Hill Field that is based on the 3-D geologic model (stratigraphic and structural framework), petrophysical properties, fluid (PVT) properties, fluid-rock properties, and the results of the well performance analysis. The geological/geophysical model will be coupled with the results of the well performance analysis to determine flow units, as well as reservoir-scale barriers to flow. The purpose of this work is to build forecasts for the Womack Hill Field that consider the following scenarios: base case (continue field management as is); optimization of production practices (optimal well completions, including stimulation, injection/production balancing, etc.); active reservoir management (includes replacement and development wells); targeted infill drilling program; and enhanced oil recovery scenarios of gas injection, water/chemical injection, and immobilized enzyme technology.

**Rationale.** This task is the critical step for any enhanced oil recovery technology. Reservoir simulation is used to forecast expected reservoir performance, to forecast ultimate recovery, and

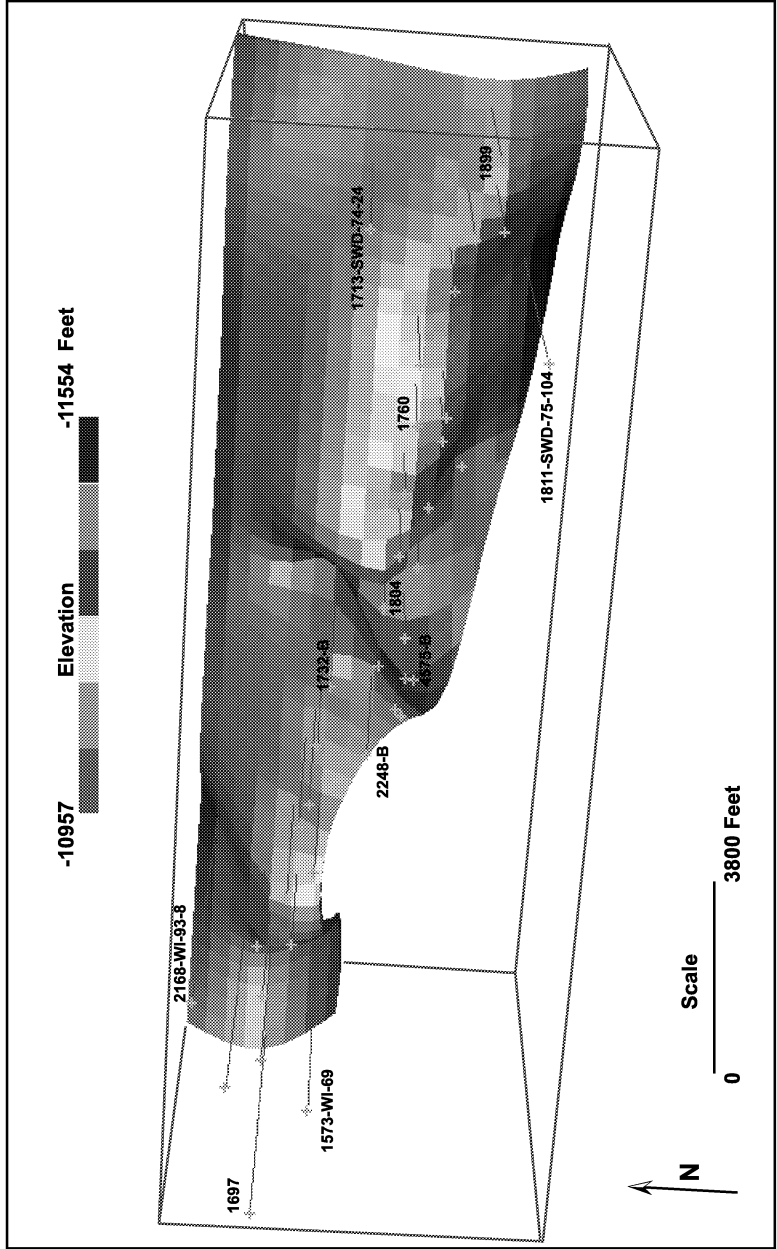


Figure 105. 3-D geologic model of Womack Hill Oil Field. Model depicting elevation of top of Smackover Formation. Model constructed using Stratamodel software. See Figure 8 for location of wells.

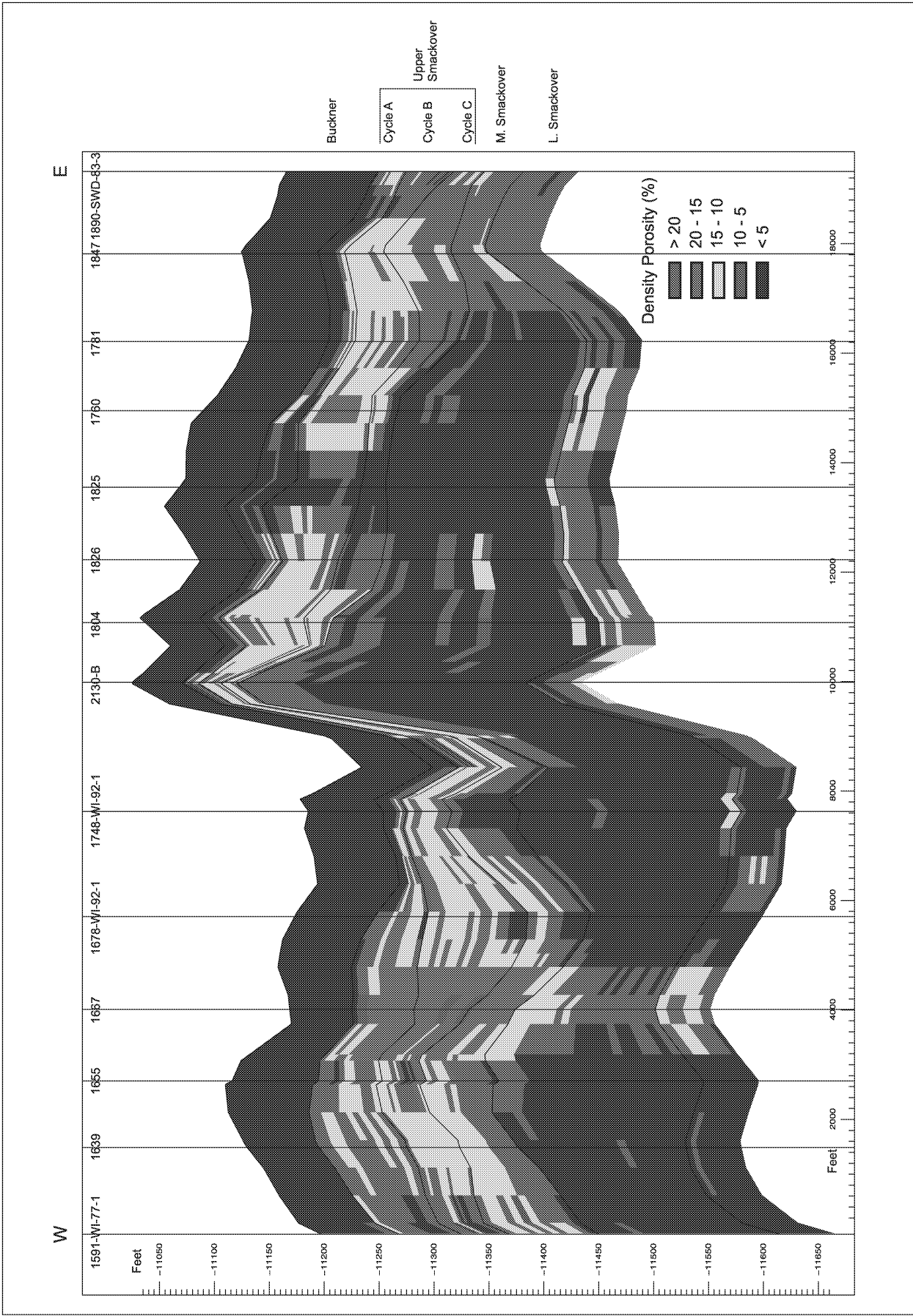


Figure 106. Cross section across Wornack Hill Oil Field showing changes in porosity, as determined from density log analysis, in the Smackover Formation, including Cycles A, B, and C. Cross section constructed using Stratamodel software. This cross section corresponds to line of cross section A-A' in Figure 8.

**Table 9  
Milestone Chart—Year 3**

<b>Reservoir Characterization Tasks (Phase I)</b>	<b>M</b>	<b>J</b>	<b>J</b>	<b>A</b>	<b>S</b>	<b>O</b>	<b>N</b>	<b>D</b>	<b>J</b>	<b>F</b>	<b>M</b>	<b>A</b>	
Recovery Technology Analysis													
3-D Simulation	■												
Core Experiments	■												
Recovery Technology Evaluation													
3-D Seismic							■						
Pressure Maintenance												■	
IET Concept												■	
Decision for Implementation												■	

Work Planned

evaluate different production development scenarios. In itself, modeling of the current scenario at Womack Hill Field is necessary to establish whether or not the existing efforts in reservoir management (i.e., evaluation of the existing pressure maintenance program) are sufficient, and if not, how could these activities provide optimal performance. Conceptually, it is important to understand (i.e., be able to model) the current behavior at Womack Hill Field prior to initiating any new activities. Probably the most important aspect of the simulation work will be the setup phase. Developing a detailed reservoir model for the Womack Hill Field is essential because this is a geologically complex system, and the long production/injection history has not been evaluated relative to a detailed reservoir description. Much should be learned about the reservoir, including in particular, insight regarding the carbonate reservoir architecture and regarding the inherent heterogeneities in such a complex reservoir system.

**Subtask 1** is the setup phase and will be conducted in conjunction with the creation and validation of the integrated reservoir description. However, this work has more specific goals than simply building the simulation data file. Considerable effort will go into the validation of the petrophysical, fluid (PVT), and fluid-rock properties to establish a benchmark case, as well as bounds (uncertainty ranges) on these data. In addition, well performance data will be thoroughly reviewed for accuracy and appropriateness.

**Subtask 2** is the history matching phase. In this phase we will continue to refine and adjust data similar to the previous subtask, but in this work the focus will be to establish the most representative numerical model for the Womack Hill Field. Adjustments will undoubtedly be made to all data types, but as a means to ensure appropriateness, these adjustments will be made in consultation and collaboration with the geoscientists on the research team. In this phase, the goal is not to obtain a perfect match of the model and the field data, but rather to scale-up the small-scale information (core, logs, etc.) in order to yield a representative reservoir model. We envision the use of a black oil formulation, but it is conceivable that a compositional model may be incorporated if the black oil formulation is deemed insufficient.

**Subtask 3** is the forecasting phase. In this phase, the goals for forecasting are to establish the viability of individual scenarios, where these cases include: a base case (no changes), optimal well practices, continued field development, and enhanced recovery activities (water, gas, or chemical injection). As the project progresses to Phase II, this work will be refined and the focus will be to establish the most viable improved recovery strategy.

***Task RTA-3. Core Flood Experiments***

**Description of Work.**--This task involves the maximization of the chemical addition program using core flood experiments. Live cores are anticipated for use in this work. If live cores are not available, artificial cores will be prepared from stratal material from archived cores. The cores will be incorporated into the core flood apparatus. The chemical addition program from Task RC-3 will be employed initially and changes made to maximize acid production while minimizing cell proliferation. All experiments will be conducted under anaerobic conditions at reservoir temperature. In addition to the parameters monitored in Task RC-3, a variety of other parameters will be monitored including oil recovery and petrophysical characteristics. These studies will finalize the chemical addition program to be implemented in the field demonstration project.

**Rationale.** As stated in Task RC-3, researchers at Mississippi State University have demonstrated the cost-effectiveness of utilizing the growth of indigenous microbes in enhancing the efficiency of an active waterflood for the recovery of incremental oil. This technology expands on the previous study by using the ability of *in-situ* microbes to generate acetic acid as a growth by-product. This IET is applied to a carbonate reservoir at a depth of 11,300 ft. It is anticipated that the acetic acid will act to break down the reservoir through dissolution, thereby increasing porosity and permeability in less permeable zones of the reservoir. This should result in reduced reservoir compartmentalization and more contacted oil, thereby increasing producibility of the reservoir.

***Task RTE-1. Evaluation and Acquisition of 3-D Seismic Data***

**Description of Work.**--This task involves the use of the 3-D geologic model to determine whether there are zones in the Womack Hill reservoir where uncontacted oil remains and whether there is attic oil remaining in the field. The task also includes evaluating whether the acquisition of

3-D seismic data is required to confirm the presence of uncontacted oil, including attic oil in the Womack Hill Field Unit. If so, 3-D seismic data will be acquired, processed and interpreted as part of this task to facilitate the implementation of the integrated demonstration project of the Womack Hill Field Unit.

**Rationale.** Petroleum companies have been extremely successful in the Eastern Gulf Region in exploring for and developing Upper Jurassic Norphlet, Smackover and Haynesville Fields using 3-D seismic data. Utilizing 3-D seismic data, in combination with well logs, has proven to be a powerful tool in imaging Smackover structures and reservoirs in the Eastern Gulf Region. It is anticipated that 3-D seismic imaging of the reservoir structure, in combination with the 3-D geologic model, which incorporates the 3-D structural interpretation of the Womack Hill petroleum trap, generated by using GeoSec software and a series of balanced cross sections for the field, will provide the information required to determine whether uncontacted oil and attic oil remain in the Womack Hill Field Unit. The importance of using petrophysics data and balanced cross sections in combination with 3-D seismic data for reservoir and structure modeling has been shown by a study of the Ellenberger in West Texas. Standard industry software, such as 2d/3d Pak and SeisWorks, will be used to perform this task.

***Task RTE-2. Evaluation of the Pressure Maintenance Project***

**Description of Work.**--This task is designed to verify/dispute the effectiveness of the existing pressure maintenance activities being conducted at Womack Hill Field Unit. The reservoir simulation history matches will be used as a mechanism to establish water loss and to provide insight as to large-scale water movement within the unit. The well performance activities will be designed to determine if the water injection program is being effective. Efforts will be made to: evaluate pressure and fluid communication in the field (data analysis, data correlation), review injection/ production behavior on a pattern basis to verify pressure support in a particular area, and review completion and production practices. The short-term goal of this work is to determine if modifications are required for the injection strategy, as well as to determine whether or not an advanced oil recovery technology (such as the introduction of chemicals) should be considered or

discarded. The long-term goal is to establish the practices and procedures for implementing optimal pressure maintenance, regardless of the mechanism (waterflood, chemical injection, etc.).

**Rationale.** Profitability is currently down at Womack Hill Field Unit because production is declining and the cost of operations is escalating. The operator has cited water loss due to the heterogeneous nature of the Smackover reservoir as a major source of the production decline (i.e., pressure support is insufficient to provide good pressure/fluid communication). It is clear that modification of the existing pressure maintenance project and/or the addition of an advanced oil recovery technology has the potential to extend the life of this reservoir by increasing profitability.

**Subtask 1** consists of additional analyses of the production/injection data to establish the state of pressure/fluid communication at Womack Hill Field. In particular, a separate evaluation of the production and injection data on a per-well basis using a multiwell reservoir model will be considered. In theory, it is possible to analyze per-well performance using an analytical solution for a closed multiwell reservoir; but, because of reservoir heterogeneities, it may not be feasible to implement a multiwell solution. Interference and/or injector/producer communication, as well as utilizing the conventional (albeit simplified) analysis of injection well rates and pressure (the Hall and Hearn plots), will be studied.

**Subtask 2** will focus on the use of the results from the history-matches obtained in the reservoir simulation tasks. The focus will be to correlate simulated performance with other analysis results to verify pressure/fluid movement in different areas of the field. The work in this subtask will guide the efforts to optimize injection/production behavior, as well as to identify possible target areas for infill drilling and/or enhanced recovery activities (cyclic injection, IET, etc.)

### ***Task RTE-3. Evaluation of the Immobilized Enzyme Technology Project Concept***

**Description of Work.**--This task involves the evaluation of the laboratory results of the proposed IET project at Womack Hill Field Unit to determine whether it is feasible to implement an IET field-scale demonstration project at Womack Hill Field Unit.

**Rationale.** MEOR technology has been demonstrated to be profitable at North Blowhorn Creek Field Unit, Alabama. The reservoir at this field is a sandstone at a depth of -2,300 ft. The

application of this biological technology to Smackover carbonates at a depth of 11,300 ft has the potential to increase oil production at Womack Hill Field Unit, thereby increasing profitability and saving this endangered mature field from premature abandonment.

***Task. Decision to Integrate Demonstration Project***

**Description of Work.**--The project results, to date, will be evaluated by Pruet Production Co. and DOE to determine whether project continuation is justified.

**Rationale.** This activity represents the decision process on whether it is feasible for Pruet Production Co. to implement the technologies addressed and evaluated in Phase I of this study. The decision may be to implement an enhanced pressure maintenance project, initiate an advanced oil technology application, implement a strategic infill drilling program, and/or initiate an immobilized enzyme technology project at Womack Hill Field Unit. This activity also presents DOE with the opportunity to decide whether DOE will continue to support the project.

## **RESULTS AND DISCUSSION**

The Project Management Team and Project Technical Team are working closely together on this project.

### **Geoscientific Reservoir Characterization**

In the Womack Hill Field, the Smackover Formation ranges in thickness from 220 to 422 feet with an average thickness of 340 feet (Fig. 15) and overlies sandstone beds of the Norphlet Formation. The Norphlet Formation overlies the Jurassic Louann Salt, which in combination with faulting, is responsible for the petroleum trap at the field. The Smackover Formation is overlain by the Buckner Anhydrite Member of the Haynesville Formation. These anhydrite beds form the seal in the field. The Smackover Formation includes lower, middle and upper units in the Womack Hill Field (Fig. 9). The Smackover lower member or unit typically is composed of peloidal packstone and wackestone (Benson, 1988), which has reservoir potential in the field area but generally is not the reservoir in the Womack Hill Field. The middle member or unit includes laminated carbonate mudstone and fossiliferous wackestone and mudstone. The upper member or unit ranges in thickness from 30 to 209 feet with an average thickness of 120 feet (Fig. 16), and consists of a

series of three cycles, Cycle A, Cycle B, and Cycle C (Fig. 9). Porosity is developed in the upper part of the middle Smackover in the central part of the field along the Tombigbee River on the Clarke County side of the river. Cycle A (carbonate shoal) is an upward shoaling cycle composed of lower energy, carbonate mudstone and peloidal wackestone at the base and is capped by higher energy, ooid grainstone. The carbonate mudstone and wackestone have been interpreted as restricted bay and lagoon sediments, and the grainstone has been described as beach shoreface and shoal deposits (McKee, 1990). Although Cycle A is present across the field (Fig. 10), the reservoir quality in this cycle varies. The thickness of Cycle A ranges from 9 to 82 feet with an average thickness of 30 feet (Fig. 17). The grainstone associated with Cycle A is dolomitized (upper dolomitized zone) in much of the field area (Fig. 12), and is the main reservoir perforated in the field. Hydrocarbons have been produced from Cycle A in 21 of the 27 productive wells in the field. Six wells (Permit #1678, #1781, #1826, #2257B, #2327 and #3657) only have been perforated in Cycle A, and the cumulative oil production ranges from 127,000 to 1.9 million bbls for these wells. Porosity and permeability in the more productive wells (Permit #1678) average 16 percent and 11.5 md, respectively, and porosity and permeability in the less productive wells (Permit #2327) average 12 percent and 3 md, respectively (Fig. 51A). The mudstone/wackestone associated with this cycle has the potential to be a barrier to vertical flow in the field. Cycle B and Cycle C also occur across the field (Fig. 10). Cycle B thickness ranges from 8 to 101 feet with an average thickness of 47 feet (Fig. 18), and the thickness of Cycle C ranges from 11 to 86 feet with an average thickness of 40 feet (Fig. 19). These cycles are part of shoal complexes which include lagoonal deposits. The reservoirs associated with these cycles are a result of depositional and diagenetic processes, particularly dolomitization. Dolomitization (lower dolomitized zone) can be pervasive in the shoal grainstone lithofacies and in the lagoon wackestone lithofacies in these cycles (Fig. 12) and the interval immediately below Cycle C. Hydrocarbons have been produced from Cycle B in 17 wells, and oil and gas have been produced from Cycle C in 5 wells in the field. Three wells (Permit #1847, #2248B and #2263) only have been perforated in Cycle B, and the cumulative oil production is 350,000 to 3.2 million bbls for these wells, respectively, One well (Permit #2109) only has been

perforated in Cycle C, and its cumulative oil production is 1.7 million bbls. Porosity and permeability in well Permit #1847 average 17.5 percent and 9 md, respectively (Fig. 51B). The large scatter of the porosity and permeability data for this well illustrates the heterogeneity in Cycle B. Production from the upper part of the middle Smackover interval immediately above Cycle C is from the only two wells perforated in this interval that are located in the central part of the field. Cumulative oil production for well Permit #2130B is 2.8 million, and cumulative oil production for well Permit #4575B is 2.4 million bbls. Porosity and permeability in well Permit #4575B average 19 percent and 15 md, respectively (Fig. 52A). Permeability shows good correlation (0.87) with porosity in this interval probably due to dolomitization of these carbonates. The best producing well (Permit #1804) is perforated in Cycles A, B and C, and the well production is 3.3 million bbls of oil. Porosity and permeability in Cycle C in this well average 20 percent and 4 md, respectively (Fig. 52B). The variability of the porosity and permeability data for this well and wells (Permit #1732B and #4575B) (Fig. 53) illustrates the heterogeneity within and among Cycles A, B and C.

Although the primary control on reservoir architecture in Smackover reservoirs, including Womack Hill Field, is the fabric of the depositional lithofacies, diagenesis plays a significant role in modifying reservoir quality (Benson, 1985). Of the diagenetic events, the multiple dolomitization and dissolution events probably had the greatest influence on the quality in Smackover reservoirs. While the dolomitization created only minor amounts of intercrystalline porosity, it significantly enhanced permeability; it also stabilized the lithology which reduced the potential for later porosity loss due to compaction (Benson, 1985). The dissolution events enlarged primary (interparticle) and early secondary (moldic and intercrystalline) pores (McKee, 1990). Although the dissolution did not create large amounts of new porosity, it did expand existing pore throats and enhanced permeability (Benson, 1985).

Porosity in the shoal grainstone reservoirs at Womack Hill Field is chiefly secondary. The main pore types in the Smackover reservoirs, including the Womack Hill Field area, are solution-enlarged interparticle, intercrystalline dolomite, and grain moldic. Primary interparticle porosity has been reduced in the field due to compaction and cementation. Solution-enlarged interparticle and

grain moldic porosity is produced by early leaching in the vadose zone that dissolved aragonite in the Smackover carbonates (McKee, 1990). Moldic porosity is produced by early, fabric selective dissolution of aragonitic grains and is associated with areas of subaerial exposure (Benson, 1985). Intercrystalline porosity is chiefly a result of mixed-water dolomitization resulting from the mixing of marine and meteoric waters or from the mixing of evaporitic brines with meteoric waters (McKee, 1990). Several phases of dolomitization have been identified in the Smackover carbonates at Womack Hill Field. The upper zone of dolomitization is fabric-destructive and is a result of an early stage diagenetic event that involves downward-moving, evaporitically-concentrated brine, and the lower zone of dolomitization is, in part, fabric-destructive creating large amounts of intercrystalline porosity and permeability and is a result of mixing zone processes. Vuggy porosity of Choquette and Pray (1970), which is common in the field area, is the product of late, non-fabric selective dissolution of calcite or dolomite and is produced by solution enlargement of earlier formed interparticle or intercrystalline pores (Benson, 1985; Benson and Mancini, 1999). Reservoirs characterized by vuggy porosity have good porosity and permeability (Benson and Mancini, 1984). Shelter, intraparticle, and fracture pores are also present in the Smackover reservoirs in the Womack Field area (McKee, 1990).

Pore systems are the building blocks of reservoir architecture. Pore origin, geometry, and spatial distribution determine the amount and kind of reservoir heterogeneity. Pore systems affect not only hydrocarbon storage and flow but also reservoir producibility and flow unit quality and comparative rank within a field. Hydrocarbon recovery efficiency and total recovery volume are determined by the 3-D shape and size of the pores and pore throats (Kopaska-Merkel and Hall, 1993; Ahr and Hammel, 1999). Therefore, the pore systems (pore topology and geometry and pore throat size distribution) of the Womack Hill Field reservoirs are extremely important. Pore throat size distribution is one of the important factors determining permeability because the smallest pore throats are the bottlenecks that determine the rate of which fluids pass through a rock. Permeability has been shown to be directly related to the inherent pore system and degree of heterogeneity in Smackover reservoirs (Carlson *et al.*, 1998; Mancini *et al.*, 2000). Generally, the more

homogeneous (little variability in architecture and pore systems) the reservoir, the greater the hydrocarbon recovery from that reservoir. However, heterogeneity at one scale is not necessarily paralleled by heterogeneity at other scales. For example, the shoal grainstone reservoirs at Womack Hill Field can be dominated by a moldic or intercrystalline pore system and have low mesoscopic-scale heterogeneity but low to high microscopic-scale heterogeneity, depending upon the pore system. The heterogeneity is a function of both depositional and diagenetic processes. The grainstones accumulated in linear shoal environments, which tend to have uniformity of paleoenvironmental condition within a given shoal, but these carbonates can be later subjected to dissolution and dolomitization, such as at Womack Hill Field, to produce dolograins and large crystalline dolostones. The moldic pore system is characterized by multi-sized pores that are poorly connected by narrow pore throats. Pore size is dependent on the size of the carbonate grain that was leached. The intercrystalline pore system is characterized by moderate-sized pores that are well-connected by uniform pore throats. The size of the pores is dependent upon the dolomite crystal size. Interparticle porosity of Lucia (1998), which includes intergrain and intercrystal pore types in grainstones, dolograins and large crystalline dolostones, provides for high connectivity in carbonate reservoirs and results in high permeability (Lucia, 1998; Jennings and Lucia, 2001).

### **Petrophysical and Engineering Characterization**

Petrophysical and Engineering Characterization is on schedule except for a delay in well downhole pressure testing. Extensive efforts have been made to integrate and correlate the core and well log data for the field. Reservoir permeability has been correlated with core porosity, gamma ray well log response, and resistivity well log response. The petrophysical data have been segregated into flow units prescribed by the geological data, and for the data in these flow units a histogram of core porosity and the logarithm of core permeability. These histograms yield statistical measures, such as the mean and median values, which will be used to develop spatial distributions and to provide data for the numerical simulation model. Evaluation of production, injection and shut-in bottomhole pressure data for the field have been interpreted and analyzed using appropriate

mechanisms, such as decline type curve analysis and estimated ultimate recovery analysis. The volumetric results are relevant as virtually every well yielded an appropriate signature for decline type curve analysis. However, a discrepancy in the estimate of total compressibility for this system has arisen, and the absolute volumetric results will need to be revised. The estimation of flow properties, such as permeability and skin factor has emerged as a problematic issue because little early time data, which are required for this analysis, are available. Therefore, the results of these analyses should be considered qualitative. The correlation of estimated ultimate recovery and the  $N_{c+}$  product is consistent suggesting that a strong relationship exists between contacted oil-in-place and recovery.

### **Microbial Characterization**

Microbial Characterization is on schedule with the recent acquisition of Smackover core material from south Alabama. Initially water samples and core samples taken from wells in the Womack Hill Field yielded no micro-organisms capable of growing at 90°C. This result was due to a combination of factors, including the fact that the core samples were exposed to air for decades and the equipment necessary to maintain an anaerobic environment was inadequate. Well cuttings from the Smackover Formation acquired from a field near Womack Hill Field were analyzed for micro-organisms. Growth of micro-organisms was evident in the samples prepared from these well cuttings in association with oil from the Womack Hill Field. These organisms consumed ethanol and are presumed to produce carbon dioxide or the gas was derived from organic acids produced from the oil reacting with carbonate. These findings suggest that micro-organisms capable of producing acetic acid from ethanol have a high probability of being present in Womack Hill Field and of being induced to grow and be metabolically active at the subsurface temperature in the reservoir.

### **3-D Geologic Model**

The 3-D geologic model (Fig. 105), shows that the petroleum trap at Womack Hill Field is more complex than originally interpreted. The 2-D seismic data assists with the location of the major fault to the south of the field (Fig. 13). However, the seismic data are not adequate to

determine if the petroleum trap is a fault trap (bounded on three sides by dip closure and on a fourth side by a fault) or a faulted anticline trap (four-way dip closure). The geologic modeling shows that the trap in the western part of the field is a fault trap with closure to the south against the fault, and that the trap in the central and eastern parts of the field is a faulted anticline trap with four-way dip closure. In addition, the fault salt anticline trap appears to consist of two distinct highs separated by a structural low in the central part of the field (Fig. 105). The 2-D seismic data (west-east line P2635-136, Figs. 20), which is along the northern margin of the field, shows a north-south trending fault in the vicinity of the Choctaw-Clarke County line. If the fault trace is projected south to intersect with the major west-east fault (Fig. 13), the offset in the two structural highs along the southern margin of the field may be attributed to the effects of this north-south trending fault. Also, the pressure difference and well Permit #4575B between wells (Permit #4575B) in the western and central parts of the field (unitized area) and wells (Permit #1804) in the eastern part of the field may be attributed to the flow barrier in the field due to this fault.

The 3-D geologic modeling also shows that the Smackover reservoirs at Womack Hill Field is heterogeneous (Fig. 106). Four reservoir intervals are identified in the field area (Fig. 10). These include Cycle A, Cycle B, Cycle C, and the interval immediately below Cycle C (Fig. 9). Although the Cycle A reservoir is the most productive areally (has been productive in 21 wells), the production from this reservoir is highly variable with cumulative oil production ranging from 127,000 to 1.9 million bbls for wells only perforated in Cycle A. The thickness and lateral and vertical reservoir quality are also variable for the Cycle A reservoir interval. The Cycle B reservoir interval also is heterogeneous in thickness and lateral and vertical reservoir quality; however, the overall porosity as indicated by density log analysis is higher in this interval than the other reservoir intervals. The Cycle C reservoir interval also is heterogeneous in thickness and reservoir quality. Although the total oil production from this interval is not as high as the Cycle A and Cycle B reservoir intervals, production from well Permit #2109, the only well solely perforated in this interval and located in the western part of the field has had a cumulative oil production of 1.7 million bbls. The reservoir interval immediately below Cycle C has only been perforated in two

wells (well Permit #2130B and well Permit #4575B) in the central part of the field. Reservoir quality is high and production is high. The geologic modeling indicates this reservoir interval has the potential for high reservoir quality in the western part of the field in the vicinity of well Permit #1667 and well Permit #2109. The high reservoir quality and productivity in this interval in well Permit #2130B and well Permit #4575B is attributed to mixing zone dolomitization (fresh water lens development in structurally higher areas of the field). The area around well Permit #2109 is in a structurally higher area in the field (Figs. 13 and 105).

A permeability barrier to flow, especially in the Cycle A reservoir interval is present potentially between the western (well Permit #4575B) and eastern (well Permit #1804) parts of the field (Figs. 53 and 106). Communication in the field through the Cycle B reservoir interval appears likely, in comparing the porosity and permeability data between well Permit #1732B and well Permit #1804 (Fig. 53) and in comparing the area of well Permit #2130B with the area of well Permit #1804 (Fig. 106). The improved reservoir communication in the Cycle B interval is probably due to dolomitization. Porosity and permeability data are insufficient in the field to assess the potential of a permeability barrier to flow in the Cycle C reservoir interval and the reservoir interval immediately below Cycle C. Communication between the western part of the field and the area of well Permit #1804 appears likely, but communication between the wells in the western part and the other wells in the eastern part of the field probably is limited.

## **CONCLUSIONS**

Pruet Production Co. and the Center for Sedimentary Basin Studies at the University of Alabama, in cooperation with Texas A&M University, Mississippi State University, University of Mississippi, and Wayne Stafford and Associates are undertaking a focused, comprehensive, integrated and multidisciplinary study of Upper Jurassic Smackover carbonates (Class II Reservoir), involving reservoir characterization and 3-D modeling and an integrated field demonstration project at Womack Hill Oil Field Unit, Choctaw and Clarke Counties, Alabama, Eastern Gulf Coastal Plain.

Phase I (3.0 years) of the proposed research involves characterization of the shoal reservoir at Womack Hill Field to determine reservoir architecture, heterogeneity and producibility in order to increase field productivity and profitability. This work includes core and well log analysis; sequence stratigraphic, depositional history and structure study; petrographic and diagenetic study; and pore system analysis. This information will be integrated with 2-D seismic data and probably 3-D seismic data to produce an integrated 3-D stratigraphic and structural model of the reservoir at Womack Hill Field. The results of the reservoir characterization and modeling will be integrated with petrophysical and engineering data and pressure communication analysis to perform a 3-D reservoir simulation of the field reservoir. The results from the reservoir characterization and modeling will also be used in determining whether undrained oil remains at the crest of the Womack Hill structure (attic oil), in assessing whether it would be economical to conduct strategic infill drilling in the field, and in determining whether the acquisition of 3-D seismic data for the field area would improve recovery from the field and is justified by the financial investment. Parallel to this work, engineers are characterizing the petrophysical and engineering properties of the reservoir, analyzing the drive mechanism and pressure communication (through well performance data), and developing a 3-D reservoir simulation model. Further, the engineering team members will determine what, if any, modifications should be made to the current pressure maintenance program, as well as assess what, if any, other potential advanced oil recovery technologies are applicable to this reservoir to extend the life of the field by increasing and maintaining productivity and profitability. Also, in this phase, researchers are studying the ability of *in-situ* micro-organisms to produce a single by-product (acid) in the laboratory to determine the feasibility of initiating an immobilized enzyme technology project at Womack Hill Field Unit.

The principal problem at Womack Hill Field is productivity and profitability. With time, there has been a decrease in oil production from the field, while operating costs in the field continue to increase. In order to maintain pressure in the reservoir, increasing amounts of water must be injected annually. These problems are related to cost-effective, field-scale reservoir management, to reservoir connectivity due to carbonate rock architecture and heterogeneity, to pressure

communication due to carbonate petrophysical and engineering properties, and to cost-effective operations associated with the oil recovery process.

Improved reservoir producibility will lead to an increase in productivity and profitability. To increase reservoir producibility, a field-scale reservoir management strategy based on a better understanding of reservoir architecture and heterogeneity, of reservoir drive and communication and of the geological, geophysical, petrophysical and engineering properties of the reservoir is required. Also, an increased understanding of these reservoir properties should provide insight into operational problems, such as why the reservoir is requiring increasing amounts of freshwater to maintain the desired reservoir pressure, why the reservoir drive and oil-water contact vary across the field, how the multiple pay zones in the field are vertically and laterally connected and the nature of the communication within a pay zone.

The principal research efforts for Year 2 of the project have been reservoir characterization, which has included three (3) primary tasks: geoscientific reservoir characterization, petrophysical and engineering property characterization, and microbial characterization and recovery technology analysis, which has included 3-D geologic modeling. In the second year, the research focus has primarily been on completion of the geoscientific reservoir characterization and 3-D geologic modeling tasks. This work was scheduled for completion in Year 2.

Geoscientific Reservoir Characterization has been completed. The upper part of the Smackover Formation is productive from carbonate shoal complex reservoirs that occur in vertically stacked heterogeneous porosity cycles (A, B, and C). The cycles typically consist of carbonate mudstone/wackestone at the base and ooid and oncoidal grainstone at the top. The carbonate mudstone/wackestone lithofacies has been interpreted as restricted bay and lagoon sediments, and the grainstone lithofacies has been described as beach shoreface and shoal deposits. Porosity has been enhanced through dissolution and dolomitization. The grainstone associated with Cycle A is dolomitized (upper dolomitized zone) in much of the field area. Although Cycle A is present across the field, its reservoir quality varies laterally. Dolomitization (lower dolomitized zone) can be pervasive in Cycle B, Cycle C and the interval immediately below Cycle C. Cycle B and Cycle C

occur across the field, but they are heterogeneous in depositional texture and diagenetic fabric laterally. Porosity is chiefly solution-enlarged interparticle, grain moldic and dolomite intercrystalline pores with some intraparticle and vuggy pores. Pore systems dominated by intercrystalline pores have the highest porosities. Median pore throat aperture tends to increase with increasing porosity. Probe permeability strongly correlates with median pore throat aperture, and tortuosity increases with increasing median pore throat aperture. Larger tortuosity and median pore throat aperture values are associated with pore systems dominated by intercrystalline pores.

Petrophysical and Engineering Characterization is on schedule except for a delay in well downhole pressure testing. Extensive efforts have been made to integrate and correlate the core and well log data for the field. Reservoir permeability has been correlated with core porosity, gamma ray well log response, and resistivity well log response. The petrophysical data have been segregated into flow units prescribed by the geological data, and for the data in these flow units a histogram of core porosity and the logarithm of core permeability. These histograms yield statistical measures, such as the mean and median values, which will be used to develop spatial distributions and to provide data for the numerical simulation model. Evaluation of production, injection and shut-in bottomhole pressure data for the field have been interpreted and analyzed using appropriate mechanisms, such as decline type curve analysis and estimated ultimate recovery analysis. The volumetric results are relevant as virtually every well yielded an appropriate signature for decline type curve analysis. However, a discrepancy in the estimate of total compressibility for this system has arisen, and the absolute volumetric results will need to be revised. The estimation of flow properties, such as permeability and skin factor has emerged as a problematic issue because little early time data, which are required for this analysis, are available. Therefore, the results of these analyses should be considered qualitative. The correlation of estimated ultimate recovery and the  $N_{c+}$ - product is consistent suggesting that a strong relationship exists between contacted oil-in-place and recovery.

Microbial Characterization is on schedule with the recent acquisition of Smackover core material from south Alabama. Initially water samples and core samples taken from wells in the

Womack Hill Field yielded no micro-organisms capable of growing at 90°C. This result was due to a combination of factors, including the fact that the core samples were exposed to air for decades and the equipment necessary to maintain an anaerobic environment was inadequate. Well cuttings from the Smackover Formation acquired from a field near Womack Hill Field were analyzed for micro-organisms. Growth of micro-organisms was evident in the samples prepared from these well cuttings in association with oil from the Womack Hill Field. These organisms consumed ethanol and are presumed to produce carbon dioxide or the gas was derived from organic acids produced from the oil reacting with carbonate. These findings suggest that micro-organisms capable of producing acetic acid from ethanol have a high probability of being present in Womack Hill Field and of being induced to grow and be metabolically active at the subsurface temperature in the reservoir.

A 3-D Geologic Model has been constructed for the Womack Hill Field structure and reservoir(s). The 3-D geologic modeling shows that the petroleum trap is more complex than originally interpreted. The geologic modeling indicates that the trap in the western part of the field is a fault trap with closure to the south against the fault, and that the trap in the central and eastern parts of the field is a faulted anticline trap with four-way dip closure. The pressure difference between wells in the western and central parts of the field and wells in the eastern part of the field may be attributed to a flow barrier due to the presence of a north-south trending fault in the field area. The modeling shows that the Smackover reservoirs are heterogeneous. Four reservoir intervals are identified in the field area: Cycle A, Cycle B, Cycle C, and the interval immediately below Cycle C. A permeability barrier to flow is present potentially between the western and eastern parts of the field.

## **REFERENCES**

Ahr, W.M., and Hammel, B., 1999, Identification and mapping flow units in carbonate reservoirs: an example from Spraberry (Permian) field, Garza County, Texas, USA: Energy Exploration and Exploitation, v. 17, p. 311-334.

- Bebout, D.G., and Loucks, R.G., 1984, Handbook for logging carbonate rocks: Handbook 5, The University of Texas at Austin, Bureau of Economic Geology, Austin, Texas, 43 p.
- Benson, D.J., 1985, Diagenetic controls on reservoir development and quality, Smackover Formation of southwest Alabama: Gulf Coast Association of Geological Societies Transactions, v. 35, p. 317-326.
- Benson, D.J., 1988, Depositional history of the Smackover Formation in southwest Alabama: Gulf Coast Association of Geological Societies Transactions, v. 38, p. 197-205.
- Benson, D.J., and Mancini, E.A., 1984, Porosity development and reservoir characteristics of the Smackover Formation in southwest Alabama, in Jurassic of the Gulf Rim, Proceedings GCS-SEPMF 3<sup>rd</sup> Research, p. 1-17.
- Benson, D.J., and Mancini, E.A., 1999, Diagenetic influence on reservoir development and quality in the Smackover updip basement ridge play, southwest Alabama: Gulf Coast Association of Geological Society Transactions, v. 99, p. 95-101.
- Blasingame, T.A. *et al.*, 1998, "Well Performance Analysis (WPA) (software) Vers. 1.8b, Texas A&M U., College Station, Texas (1998).
- Breiman, L. and Friedman, J., 1985, Estimating Optimal Transformations for Multiple Regression and Correlation, Journal of the American Statistical Association (September 1985) 80, No. 391, 590.
- Carlson, E.C., Benson, D.J., Groshong, R.H., and Mancini, E.A., 1998, Improved oil recovery from heterogeneous carbonate reservoirs associated with paleotopographic basement structures: Appleton Field, Alabama: SPE/DOE Eleventh Symposium on Improved Oil Recovery, p. 99-105.
- Carozzi, A.V., 1958, Micro-mechanisms of sedimentation in the epicontinental environment: Journal of Sedimentary Petrology, v. 28, p. 133 – 150.
- Choquette, P.W., and Pray, L.C., 1970, Geologic nomenclature and classification of porosity in sedimentary carbonates: American Association of Petroleum Geologists Bulletin, v. 54, p. 207-250.

- Dake, L.P., 1977, *Fundamentals of Reservoir Engineering*, Elsevier, Amsterdam.
- Doublet, L.E., and Blasingame, T.A., 1996, Evaluation of injection well performance using decline type curves: paper SPE 35205 presented at the 1996 SPE Permian Basin Oil and Gas Recovery Conference, Midland, TX, March 27-29.
- Doublet, L.E., Pande, P.K., McCollum, T.J., and Blasingame, T.A., 1994, Decline curve analysis using type curves—analysis of oil well production data using material balance time: application to field cases: paper SPE 28688 presented at the 1994 Petroleum Conference and Exhibition of Mexico held in Veracruz, Mexico, October 10-13.
- Erwin, C.R., Eby, D.E., and Whitesides Jr., V.S., 1979, Clasticity index: a key to correlating depositional and diagenetic environments of Smackover reservoirs, Oaks field, Claiborne Parish, Louisiana: *Gulf Coast Association of Geological Societies Transactions*, v. 29, p. 52–62.
- Fetkovich, M.J., 1980, "Decline Curve Analysis Using Type Curves," *JPT* (June 1980) 1065.
- Folk, R.L., 1993, SEM imaging of bacteria and nannobacteria in carbonate sediments and rocks: *Journal of Sedimentary Petrology*, v. 63, p. 990-999.
- Folk, R.L., and Lynch, F.L., 1997, Nannobacteria are alive on Earth as well as Mars: *Proceedings of the International Symposium on Optical Science, Engineering, and Instrumentation (SPIE)*, v. 3111, p. 406-419.
- Folk, R.L., and Lynch, F.L., 1998, Morphology of nannobacterial cells in the Allende carbonaceous chondrite, *in* Hoover, R.B., ed., *Instruments, methods, and missions for astrobiology: Proceedings of the Society of Photo-optical Instrumentation Engineers*, v. 3441, p. 112-122.
- Folk, R.L., and Lynch, F.L., 2001, Organic matter, putative nannobacteria, and the formation of ooids and hardgrounds: *Sedimentology*, v. 48, p. 215-229.
- Folk, R.L., Kirkland, B.L., Rodgers, J.C., Rodgers, G.P., Rasmussen, T.E., Lieske, C., Charlesworth, J.E., Severson, S.R., and Miller, V.M., 2001, Precipitation of minerals in human arterial plaque: the potential role of nannobacteria: *Geological Society of America annual meeting, abstracts with programs*, p. A-189.

- Fratesi, S.E., and Lynch, F.L., 2001, Comparison of organic matter preservation techniques for SEM study of geologic samples: Geological Society of America annual meeting, abstracts with programs, p. A-296
- Gregg, J.M., and Sibley, D.F., 1984, Epigenetic dolomitization and the origin of xenotopic dolomite texture: *Journal of Sedimentary Petrology*, v. 54, n. 3, p. 908–931.
- Hopkins, T.L., 2002, Integrated petrographic and petrophysical study of the Smackover Formation, Womack Hill Field, Clarke and Choctaw Counties, Alabama: Texas A&M University, unpublished Masters thesis, 156 p.
- Humphrey, J.D., Ransom, K.L., and Matthews, R.K., 1986, Early meteoric control of Upper Smackover production, Oaks field, Louisiana: *American Association of Petroleum Geologists Bulletin*, v. 70, n. 1, p. 70 – 85.
- Jennings, J.W., and Lucia, F.J., 2001, Predicting permeability from well logs in carbonates with a link to geology for interwell permeability mapping: *Society of Petroleum Engineers Paper* 71336, p. 1-16.
- Kerans, C., and Tinker, S.W., 1997, Sequence stratigraphy and characterization of carbonate reservoirs: *SEPM Short Course No. 40*, 13 p.
- Kirkland, B.L., Lynch, F.L., Rahnis, M.A., Folk, R.L., Molineux, I.J., and McLean, R.J.C., 1999, Alternative origins for nanobacteria-like objects in calcite: *Geology*, v. 27, pp. 347-350.
- Kopaska-Merkel, D.C., and Hall, D.R., 1993, Reservoir characterization of the Smackover Formation in southwest Alabama: *Geological Survey of Alabama Bulletin* 153, 111 p.
- Lucia, F.J., 1999, *Carbonate reservoir characterization*: Springer, New York, 226 p.
- Mancini, E.A., Benson, D.J., Hart, B.S., Balch, R.S., Parcell, W.C., and Panetta, B.J., 2000, Appleton field case study (eastern Gulf Coastal Plain): field development model for Upper Jurassic microbial reef reservoirs associated with paleotopographic basement structures: *American Association of Petroleum Geologists Bulletin*, v. 84, p. 1699-1717.

- McKay, D.S., Gibson, E.K., Thomas-Keprta, K.L., Vali, L.H., Romanek, C.S., Clemmett, S.J., Chillier, Z.D.F., Maechling, C.R., and Zare, R.N., 1996, Search for past life on Mars: Possible relic biogenic activity in Martian meteorite ALH84001: *Science*, v. 273, p. 924.
- McKee, D.A., 1990, Structural controls on lithofacies and petroleum geology of the Smackover Formation: eastern Mississippi Interior Salt Basin, Alabama: University of Alabama, unpublished master's thesis, 254 p.
- Spark, I., Patey, I., Duncan, B., Hamilton, A., Devine, C., and McGovern-Traa, C., 2000, The effects of indigenous and introduced microbes and deeply buried hydrocarbon reservoirs, North Sea: *Clay Minerals*, v. 35, p. 5-12.



